Appendix B

PRELIMINARY DRAFT

EFFICIENT PROBABILISTIC HAZARD ANALYSIS FOR NON-LINEAR SOIL SITES WITH UNCERTAIN PROPERTIES

C. A. CORNELL and PAOLO BAZZURRO
STANFORD UNIVERSITY
1/1997

OBJECTIVE:

Find $S_A^S(f)$ versus annual frequency of excedance (i.e., the hazard curve for $S_A(f)$) at the top of a nonlinear soil column. Or, at a minimum, find $S_A^S(f)$ at a given mean return period (MRP = 1/annual hazard; e.g., 5 x 10^{-4}/yr or 2000 years), usually that of the spectral acceleration given at rock, $S_A^R(f)$, i.e., find the that has the same MRP as that of the given value of $S_A^R(f)$. In either case we want results versus f (oscillator frequency) implying, in the second case, that a Uniform Hazard Spectrum (UHS) of $S_A^R(f)$ is given and we want a UHS of $S_A^S(f)$ (at the same return period).

METHOD 1 - Amplification Function (AF) Oriented

<u>Simplifield Level:</u>

In this case we ignore dependence of AF on ground motion amplitude and magnitude to show as clearly as possible the nature of the probability mechanics ("convolution"); later we'll add that dependence, but we'll <u>then</u> argue that, provided that we base the results on "local" estimates (in the probability/amplitude/magnitude range of prime interest, i.e., where the major contribution to the integral arises), the simplified level may be sufficiently accurate. Therefore this approximation is most likely to work when we ask for only a UHS of $S_A^S(f)$ at one MRP level, and not on an entire hazard curve for a wide range of $S_A^S(f)$ levels.

We assume[1] that we can represent the problem as (for <u>given</u> value f_1) :

---

[1] Some difficulties with this assumption are that we know that physically $S_A^S(f_1)$ depends to some degree on $S_A^R(f)$ at <u>all</u> frequencies, f. We'll capture this later by introducing magnitude dependence which will carry with it a different fixed <u>shape</u> for $S_A^R(f)$ for each magnitude (which is also an approximation, of course).

$$S_A^S\,(f) = S_A^R\,(f_l) \bullet AF\,(f_l) \qquad (1)$$

.e., is an "amplification factor" (or "function," when considered vs. f) format. For simplicity of notation below replace this by

$$Z = X \bullet Y \qquad (2)$$

where $X = S_A^R\,(f_l)$, etc. Both X and Y are random variables (RV) and we want to deduce the distribution of the RVZ from the given distributions of X and Y. (This is referred to as a problem in "functions of random variables" - see Benjamin and Cornell [1970], Section 2.3)

Assuming probabilistic independence between X and Y (an assumption that we'll drop later), it is "easy" to show that [2]

$$G_Z(z) = P[\,Z>z] = \int P[X>\frac{z}{y}]\, f_Y\,(y)dy = \int G_X\,(z/y)\, f_Y(y)dy \qquad (3)$$

or by symmetry:

$$= \int f_X\,(x)\, P[Y>\frac{z}{x}\,]\, dx = \int f_X\,(x)\, G_Y\,(z/x)\, dx \qquad (4)$$

[2] The easy way to think of this is in a "discrete" form, e.g.,

$$P[Z = z_k] = \sum_{all\ y_j} P[X = \frac{z_k}{y_j}]\, P[Y = y_j]$$

which says $R.V.Z$ will equal value z_k if and only if Y takes on some value y_j and X takes on value z_k / y_j (implying $Y \cdot X = y_j \cdot (z_k/y_j) = z_k$). We consider the probability of this event by the product $P[\,] \cdot P[\,]$ and then consider (i.e., sum over) all possibilites for y_j. Eq. 3 considers this the $Z>z$ case rather than the $Z = z$ case.

where f_W is the probability density function (PDF) of any random variable, W, (e.g., a lognormal PDF for Y, the amplification factor, due to random soil property variables), and G_W is the complementary cumulative distribution function (CCDF) of any random variable, W (e.g., G_X is the hazard curve for $S_A^R(f_1)$, i.e., the annual probability of exceeding level x). Note that two forms (1) and (2) (in Eq. 3 and Eq. 4, respectively) are given. The first one (Eq. 3) avoids "differentiating" the hazard curve and with some approximations leads to a clean analytical result for G_Z given in Equation 5 below.

Note, especially clearly in Form 2 (Eq. 4), that this integration recognizes that values of z (or $S_A^S(f_1)$) near, for example, 2000 years (MRP)) may "come from" values of x (or $S_A^R(f_1)$) above or below the 2000 year value.

Implementation of Eq. 3 (Form 1) requires therefore an integration of the hazard curve at rock with the (lognormal, say) PDF of the amplification factor. Under certain assumptions (see Cornell [1996], for example) the result of the integration is:

$$G_Z(z) \cong G_X(z/\hat{Y})\, e^{\frac{1}{2}k_1^2 \sigma_{\ln Y}^2} \cong G_X(z/\hat{Y})\bullet(1 \ \ to \ \ 2) \qquad (5)$$

where $\hat{Y}$ and σ_{lnY}^2 are the median of Y (i.e., $\hat{AF}(f_1)$) and the variance of its log (roughly its squared COV), and k_1 is the slope (on log-log paper) of G_X near $\frac{z}{\hat{Y}}$. Recall X stands for spectral acceleration at a rock outcrop and Z for that at the soil surface.

A problem is that this simple result seems to imply an amplification factor (described by its distribution, median, coefficient of variation (COV), etc.) that is "fixed", i.e., is associated with (a) a given spectral shape at rock (e.g., the UHS shape) <u>and</u> (b) a given amplitude (e.g., the amplitude of the UHS or, more specifically, of $S_A^R(f_1)$) -- or, <u>alternatively</u>, the assumption that the $AF(f_1)$ is independent of amplitude (i.e., the soil column is linear) and independent of the spectral <u>shape</u> at rock (e.g., the soil column is a very, lightly damped, narrow band, linear system). Practically we might decide to use "local" values. The magnitude-dependent spectral shape and ground motion level from which $\hat{AF}(f_1)$ is derived might be the UHS at rock, or other specific, appropriate values of magnitude and spectral level (see below), or, finally any reasonable value of $\hat{AF}(f_1)$ believed to be associated with the correct level of ground motion and causative spectral shape (i.e., magnitude).

<u>Not-so-Simplified level</u> (Magnitude and Amplitude Dependence):

The uneasiness we had with "independence" of various kinds in the example above can be relaxed by building in magnitude and amplitude dependence explicitly. So a more general version of Form 2 (Eq. 4) in the order of dependence as we normally consider it - i.e., AF depends on S_A^R, or Y depends on X (and magnitude as well) is:

$$G_Z(z) = \int_{all\ x} \left[\sum_{all\ m_i} G_Y(\frac{z}{x} \mid M = m_i\ and\ X = x) \bullet P[M = m_i \mid \tilde{X} = x] \right] \bullet f_X(x)\,dx \qquad (6)$$

The three factors inside the integral and sum represent:

probabilty distribution on amplification factor - due to soil properties - given rock level amplitude $X = x$ and a specific magnitude (i.e. spectral shape).	•	likelihoods of different magnitudes being the "cause" of $X = x$ (Source: PSHA de-aggregation).	•	probability rock input level is x (Source differentiation of rock rock hazard curve, i.e., $P[X = x_j]$ in "discrete" or numerical form)

In CCDF form (i.e., $G_Z(z) = \int_z^{\infty} f_Z(u)\,du$) and discretized:

$$G_Z(z) = \sum_{x_j} \sum_{m_i} G_{Y|M,X}(\frac{z}{x} \mid m_i and x_j) \bullet p_{M|X}(m_i \mid x_j) \bullet P[X = x_j] \qquad (7)$$

in which $P[X = x_j]$ is the discrete probability mass function (PMF) of the rock level spectral acceleration or $p_X(x)$; and $p_{M|X}(m_i|x_j)$ is the conditional distribution of M given X (from de-aggregation), and their product is just $p_{M,X}(m_i, x_j)$, the joint PMF of M and X, i.e , $P[M = m_i\ and\ X = x_j]$ Further $G_{Y|M,X}$ is the conditional (e.g., lognomal) CCDF of the amplification factor, which has a <u>median</u> (at f_1) that depends on (1) the magnitude level, m_i, and (2) the intensity at rock as measured by $S_A^R(f_1) = x_j$. (The standard deviation $\sigma_{\ln Y}$ may also depend on M or X.) Call this median $\hat{m}_Y(m,x)$. Then, assuming (conditional) lognormality of the amplification factor, Y.

$$G_{Y|M,X}(z/x \mid m_i\ and\ x_j) = \hat{\Phi}\left(\frac{\ln[z/x] - \ln[\hat{m}_Y(m,x)]}{\sigma_{\ln Y}} \right) \qquad (8)$$

in which $\hat{\Phi}(\cdot)$ is the standard Gaussian CDF.

Although we shall provide simplifications below, implementation of Eq. 7 is basically straightforward. In principle one should select a representative sample of rock records from each of several magnitude intervals, m_j and scale them successively to each of several amplitude levels, $x_j = S_A^R(f_1)$ In each case the records should be run through a sample of soil column representations. For each magnitude-amplitude pair, one needs to estimate the median and standard deviation of the amplification factor, and hence its distribution (Eq. 8). To obtain the entire spectrum at the soil surface this process would have to be repeated for each frequency, f_1, of interest. If one is limited by a lack of empirical records, he might use empirical or semi-theoretical spectral acceleration attenuation laws to estimate the rock spectrum for each magnitude interval, and then use either simulated records or frequency domain analysis (in an "equivalent-linear" soil amplification procedure) to predict the corresponding surface spectra for a suite of soil column samples. In each case the simulated records (or the rock spectrum in the frequency-domain approach) should be scaled first each of the selected amplitude levels. Needless to say, one would want to chose the magnitude levels, amplitude levels, and number of frequencies carefully to minimize their numbers. It is recommended to select rock amplitude levels near that associated with the mean return period(s) of primary interest, and magnitudes levels near those with significant (conditional) probability mass $P_{M|X}(m, x^*)$, where x^* is defined to be the rock amplitude with a MRP near that of primary interest).

Simplification of Not-so-Simplified Method

If we assume, which is reasonable, that the relative contributions to the hazard from different M's are not sensitive to rock amplitude in the range of interest (i.e., in the range of major contributions to the integration, which is, say, a factor of σ_{lnY} either side of the x of interest - e.g. S_A^R near 2000 yrs MRP), then we can replace $P_M(m_i \mid x_j)$ by $P_M^*(m_i)$, *i.e.*, $P_M(m_i \mid x_j)$ evaluated at $x_j = x_{MRP}$ or, call it, in general x^*. This removes a level of dependence and the need to "de-aggregate" the PSHA at multiple x levels. Similarly we might well assume that the Y dependence on X can be replaced by the "local" level of X. In different words we evaluate the median (and COV) of AF only at $x_j = x_{MRP}$ or x^*, e.g., at the $S_A^R(f_i)$ set equal to the 2000 year level. Thus we get (making both these simplifications[3]):

$$G_Z(z) = \sum_{x_j}\sum_{m_i} G_{Y|M,X}\left(\frac{z}{x_j} \mid m_i \text{ and } x^*\right) \cdot P_M^*(m_i) \cdot P_X[x_j] \qquad (9)$$

Note that this notation, which is non-standard, is intended to imply that we use rock input level x^* (only) to establish the median amplification (over multiple soil profiles), but we keep the randomness in input level when coupling it with the random amplification factor (Y) to get the

[3]It is of course possible, if accuracy dictates it, to make only one or the other of the two simplifications

CCDF of the surface level (Z). So we see the median amplification as being in the integral a fixed level $\hat{m}_Y(m_i,x^*)$ even though it depends on the "local" level of x, i.e., x^*_i, and, of course, on each magnitude level in the sum.

With this simplification, we can again introduce an analytical approximation that may be very helpful. We re-write Eq. 9 and make a change of variables (analogous to the difference between Eq. 3 and Eq. 4) getting

$$G_Z(z) = \sum_{m_i} P_M^*(m_i) \cdot \int G_{Y|M,X}\left(\frac{z}{x} \mid m_i, x^*\right) \cdot f_X(x)dx \qquad (10)$$

$$= \sum_{m_i} P_M^*(m_i) \cdot \int G_X\left(\frac{z}{y}\right) \cdot f_{Y|M,X}\,(y|m_i,x^*) \qquad (11)$$

$$\cong \sum_{m_i} P_M^*(m_i) \cdot G_X\left(\frac{z}{\hat{m}_Y(m_i,x^*)}\right) \cdot e^{\frac{1}{2}k_1^2\sigma^2_{\ln Y}(m_i,x^*)} \qquad (12)$$

In Eq. 11 $f_{Y|M,X}\,(y|m_i, x^*)$ is the PDF of the amplification factor $AF(f_1)$ for a given magnitude (spectral shape) in the sum and a given level of the input (rock) intensity as measured by $S_A^R(f_1)$ being set equal to the MRP value, e.g., to 5 x 10^{-4} level. We assume in Eq. 12 that Y is (conditionally) lognormally distributed with median equal to $\hat{m}_Y(m_i,x^*)$ (i.e., the median $AF(f_1)$ depends on m_i and x^*). In implementation this approach requires, for each m_i scaling the input to x^* and finding the median (and $\sigma_{\ln Y}(m_i,x^*)$) amplification over the soil profiles.

This result can be seen to be a "magnitude-weighted" version of Eq. 5. Note that what happens here is that the hazard of exceeding level z at the surface is calculated for each magnitude level and this hazard is average over $P_M^*(m_i)$ the (approximate) conditional distribution of magnitude given the "local" intensity level.

The factor $e^{\frac{1}{2}k_1^2\sigma^2}$ in Eq. 12 inflates the hazard G_X to a degree dependent on the variability in amplification caused by soil variability (and on the slope of the hazard curve, which reflects the relative likelihood of levels of intensity above and below x^*).

We have developed a similar approach for structures (e.g., Cornell [1996]) where, in contrast, we use in effect $X = S_A^R(f_{sc})$, i.e., the spectral amplitude at the soil column natural frequency, f_{sc}, for all outputs (here these are the surface-level $S_A^S(f_1)$ for different f_1 values) or Z's. In this case Y corresponds to the factor by which one multiplies input $S_A^R(f_{sc})$ to get the output $S_A^S(f_1)$. Thus Y contains in effect not only the ratio $S_A^S(f_1)/S_A^R(f_1)$ but also the (spectral shape) ratio $S_A^R(f_1) / S_A^R(f_{sc})$, which in our method here is fixed for a given $M = m_i$ in Eq. 12. The two

methods could be put into close correspondence. (We capture any variability in the spectral shape and its impact through Y and its statistics.) Finally, in the structural method we manipulate the counterpart of Eq. 12 to put it in terms of the worst value of m_i (i.e., that producing the highest median Y). Then we collect "corrections" to it for other magnitudes and their weights into a single "magnitude" factor, less than one, something like the k_m in liquefaction analysis. One therefore gets a benefit for considering magnitude more carefully. We could easily do that here as well.

METHOD 2 - A More Direct Approach

This method by-passes the amplification function notion and goes immediately to the (soil surface) output $Z = S_A^S(f_1)$ In the same notation as above we get

$$G_Z(z) = \sum_{x_j} \sum_{m_i} G_{Z|M,X}(z|m_i \, and \, x_j) \cdot P[M=m_i and \, X=x_j] \tag{13}$$

The last factor, $P[M=m_i and \, X=x_j] = p_{M|X}[m_i \mid x_j] \cdot p_x[x_j]$ appears in Equation 7 also. In Eq. 7 $G_{Y|M,X}(z/x|m_i,x_j)$ is in fact just the conditional probability that $Z>z$, or in effect $G_{Z|M,X}(z|m_i,x_j)$ as in Eq. 13) because it is the (conditional) probability that the amplification Y is larger than z/x, i.e. larger than the ratio of the specified values of $S_A^S(f_1)$ and $S_A^R(f_1)$. If the amplification is greater than z/x then the soil spectral acceleration Z is greater than z.

So the bases of the two methods are the equivalent. The difference is that in this method we need for each m_i and x_j (i.e., for each magnitude level and each $S_A^R(f_1)$) the CCDF of $S_A^S(f_1)$. In practice this requires, for example, running n records from a given M (and R if necessary) that have been scaled to $S_A^R(f_1) = x_i$, through, say, s samples of the soil column and plotting the CCDF of the output $S_A^S(f_1)$. Notice that in principle this should be repeated for every amplitude level x_i and every magnitude level.

This method too can be simplified by replacing $P[M = m_i \, and \, X = x_j] = p_{M|X}[m_i|x_j] \cdot p_X[x_j]$ by $p[m_i|x^*] \cdot p_X(x_j)$. We have called the first factor $p_M^*(m_i)$ in Eq. 9. Secondly we could replace $G_{Z|M,X}(z|m_i \, and \, x_j)$ by what we shall call $G_{Z|M,X}(z|m_i x_j; x^*)$ which is analogous to the first factor in the sum in Eq. 9. $G_{Z|M,X}(z|m_i,x_j;x^*)$ denotes here an approximation based on analyses made only at rock amplitude x^*. This implies (for each f_1) scaling the records to only one level, x^*, and using these results to create an approximation such as the median surface amplitude is proportional to the rock amplitude, the proportionality factor being based on the results of the single-level analyses. This would be repeated for different rock spectral shapes associated with different magnitudes.

Then we get in place of Eq. 13; if we do only the first step of simplification (but not the second)

$$G_Z(z) \approx \sum_{x_j} \sum_{m_i} G_{Z|M,X}(z \mid x_j, m_i) \bullet P_M^*(m_i) \bullet p_X(x_j) \qquad (14)$$

$$G_Z(z) \approx \sum_{m_i} \left[\int G_{Z|M,X}(z \mid m_i, x) \bullet f_X(x)\, dx \right] \bullet P_M^*(m_i) \qquad (15)$$

which, under suitable assumptions, can be reduced to a "magnitude-weighted" analytical result analogous to that in Eq. 12. (See Eq. 19).

Introducing the second approximation also, we obtain:

$$G_Z(z) \approx \sum_{m_i} \left[\int G_{Z|M,X}(z \mid m_i, x; x^*) \bullet f_X(x)\, dx \right] \bullet P_M^*(m_i) \qquad (16)$$

in which $G_{Z|M,X}(z \mid m_i, x; x^*)$ is the local approximatation discussed above. For example, if we assume that for given $M = m_i$ the median of Z is simply a constant c_i times x and that $\sigma_{\ln Z|M,X}$ is a constant σ_i(the two constants being determined from the analyses of records input at rock at amplitude x^*), and that $G_{Z|M,X}$ is approximately lognormal, then we get

$$G_Z(z) \approx \sum_{m_i} \left[\int \hat{\Phi}\left(\frac{\ln(z/c_i x)}{\sigma_i} \right) \bullet f_X(x)\, dx \right] \bullet P_M^*(m_i) \qquad (17)$$

which, after integration by parts becomes:

$$G(z) \approx \sum_{m_i} G_X\left(\frac{z}{c_i} \right) e^{\frac{1}{2} k_1^2 \sigma_i^2} \bullet P_M^*(m_i) \qquad (18)$$

A more accurate result, and one that will be accurate over a wider range of values of z, can be obtained by capturing (locally) the non-linearity of the median of Z with respect to X through analyses at *two* levels of input amplitude near x^*. If a function of the form $c_i x^{b_i}$ is fit to these two

median values (for each mgnitude level), then an analytical result is still possible:

$$G(z) \approx \sum_{m_i} G_X\left[\left(\frac{z}{c_i}\right)^{1/b_i}\right] e^{\frac{1}{2}(k_i^2 \sigma_i^2/b_i^2)} \bullet P_M^*(m_i) \qquad (19)$$

Note that $\left(\frac{z}{c_i}\right)^{1/b_i}$ is just the value of X one "expects" to cause level z at magnitude level m_i.

Feb. 11, 1997 Addendum: The first method, as defined by Eq. 6, i.e, with no "local approximations" has been implemented by Richard Lee of Westinghouse/Savannah River Site using equivalent-linear amplification analyses conducted by Walt Silva and EPRI hazard results. The results, which are available for a wide hazard range, seem reasonable but require some further verification. At Stanford we shall use these results to test the simplifications proposed. In a later version of this document we shall amplify the exposition of the proposal that we scale the input to the soil column frequency only (for all surface frequencies). This approach is also undergoing testing by Walt Silva. Our next steps at Stanford will be to use real or simulated records and full non-linear analysis of the soil column. In the interim please consult us before referencing this document-in-progress.

REFERENCES:

1. Benjamin, J.R., and Cornell, C.A., "*Probability, Statistics, and Decision for Civil Engineers*", McGraw Hill Co., N.Y., 1970

2. Cornell, C.A., "Calculating Building Seismic Performance Reliability: A Basis for Multi-level Design Norms", *Proc. Eleventh World Conf. On Earthquake Engineering*, Acapulco, Mexico, June, 1996.

ACKNOWLEDGMENTS:

This work was supported by the U.S. Nuclear Regulatory Commission under Grant No. NRC-04-95-075 to Stanford University.

[wppapers\soilsite2-7]

SOIL SURFACE SEISMIC HAZARD AND DESIGN BASIS GUIDELINES FOR PERFORMANCE CATEGORY 1 & 2 SRS FACILITIES

Disclaimer

SOIL SURFACE SEISMIC HAZARD AND DESIGN BASIS GUIDELINES FOR PERFORMANCE CATEGORY 1 & 2 SRS FACILITIES

by

R.C. Lee

Approved by: Lawrence A. Salomone
Lawrence A. Salomone
SRS Chief Geotechnical Engineer

TABLE OF CONTENTS

LIST OF ACRONYMS

BLWN/RVT	band limited white noise/random vibration theory
CCDF	Complementary Cumulative Distribution Function
D-bar	average earthquake distance
DBE	design basis earthquake
DOE	United States Department of Energy
EPRI	Electric Power Research Institute
EUS	Eastern United States
LLNL	Lawrence Livermore National Laboratory
M-bar	average earthquake magnitude
mb	body wave magnitude
MH	high magnitude
ML	low magnitude
MM	median magnitude
Mw	moment magnitude
NEHRP	National Earthquake Hazards Reduction Program
NEI	Nuclear Energy Institute
NRC	United States Nuclear Regulatory Commission
PC1	Performance Category 1
PC2	Performance Category 2
PC3	Performance Category 3
PC4	Performance Category 4
PGA	peak ground acceleration
POE	probability of exceedance
PSHA	probabilistic seismic hazard assessment
RVT	random vibration theory
Sa	5% damped spectral acceleration
SAF	soil amplification function (frequency dependent)
SEUS	South-eastern United States
SGS	Site Geotechnical Services
SRS	Savannah River Site
SSCs	structures, systems and components
STD	Standard
Sv	5% damped spectral velocity
UBC	Uniform Building Code
UHS	uniform hazard spectrum
USGS	United States Geological Survey
UTA	University of Texas at Austin
Vs	shear-wave velocity
WSRC	Westinghouse Savannah River Company

LIST OF TABLES

LIST OF FIGURES

Figure 5.3 (c) - Logarithmic standard deviation of 5 % damped amplification function for disaggregated mean-magnitude (M-bar) soil category 2 on crystalline rock. Corresponding bedrock peak ground acceleration (PGA) ranging from 0.05g (G005MM) to 0.75g (G075MM).

Figure 5.4 (a) - 5 % damped response spectra of disaggregated low-magnitude (ML) crystalline bedrock control motions used to generate soil response for soil category 2. Bedrock peak ground acceleration (PGA) ranges from 0.05g (G005ML.R00) to 0.75g (G075ML.R00).

Figure 5.4 (b) - Mean 5 % damped response spectral amplification functions for disaggregated low-magnitude soil category 2 on crystalline rock. Corresponding bedrock peak ground acceleration (PGA) ranges from 0.05g (G005ML) to 0.75g (G075ML).

Figure 5.4 (c) - Logarithmic standard deviation of 5 % damped amplification functions for disaggregated low-magnitude soil category 2 on crystalline rock. Corresponding bedrock peak ground acceleration (PGA) ranges from 0.05g (G005ML) to 0.75g (G075ML).

Figure 5.5 (a) - 5 % damped response spectra of disaggregated high-magnitude (MH) crystalline bedrock control motions used to generate soil response for soil category 2. Bedrock peak ground acceleration (PGA) ranges from 0.05g (G005MH.R00) to 0.75g (G075MH.R00).

Figure 5.5 (b) - Mean 5 % damped response spectral amplification functions for disaggregated high- magnitude soil category 2 on crystalline rock. Corresponding bedrock peak ground acceleration (PGA) ranges from 0.05g (G005MH) to 0.75g (G075MH).

Figure 5.5 (c) - Logarithmic standard deviation of 5 % damped amplification functions for disaggregated high-magnitude soil category 2 on crystalline rock. Corresponding bedrock peak ground acceleration (PGA) ranges from 0.05g (G005MH) to 0.75g (G075MH).

Figure 6.1 - Soil surface hazard curves (solid lines) for 1-Hz oscillator frequency computed from EPRI bedrock hazard curves (dashed lines). Hazard curves are for six soil and bedrock conditions (see text for explanation of legend). EPRI 1-Hz bedrock hazard (dashed line) is shown for interpolated segments (solid symbols) and extrapolated segments (open symbols).

Figure 6.2 - Soil surface hazard curves (solid lines) for 2.5-Hz oscillator frequency computed from EPRI bedrock hazard curves (dashed lines). Hazard curves are for six soil and bedrock conditions (see text for explanation of legend). EPRI 2.5-Hz bedrock hazard (dashed line) is shown for interpolated segments (solid symbols) and extrapolated segments (open symbols).

Figure 6.3 - Soil surface hazard curves (solid lines) for 5-Hz oscillator frequency computed from EPRI bedrock hazard curves (dashed lines). Hazard curves are for six soil and bedrock conditions (see text for explanation of legend). EPRI 5-Hz bedrock hazard (dashed line) is shown for interpolated segments (solid symbols) and extrapolated segments (open symbols).

Figure 6.4 - Soil surface hazard curves (solid lines) for 10-Hz oscillator frequency computed from EPRI bedrock hazard curves (dashed lines). Hazard curves are for six soil and bedrock conditions (see text for explanation of legend). EPRI 10-Hz bedrock hazard (dashed line) is shown for interpolated segments (solid symbols) and extrapolated segments (open symbols).

Figure 6.5 - Soil surface hazard curves (solid lines) for 1-Hz oscillator frequency computed from LLNL bedrock hazard curves (dashed lines). Hazard curves are for six soil and bedrock conditions (see text for explanation of legend). LLNL 1-Hz bedrock hazard (dashed line) is shown for interpolated segments (solid symbols) and extrapolated segments (open symbols).

Figure 6.6 - Soil surface hazard curves (solid lines) for 2.5-Hz oscillator frequency computed from LLNL bedrock hazard curves (dashed lines). Hazard curves are for six soil and bedrock conditions (see text for explanation of legend). LLNL 2.5-Hz bedrock hazard (dashed line) is shown for interpolated segments (solid symbols) and extrapolated segments (open symbols).

Figure 6.7 - Soil surface hazard curves (solid lines) for 5-Hz oscillator frequency computed from LLNL bedrock hazard curves (dashed lines). Hazard curves are for six soil and bedrock conditions (see text for explanation of legend). LLNL 5-Hz bedrock hazard (dashed line) is shown for interpolated segments (solid symbols) and extrapolated segments (open symbols).

Figure 6.8 - Soil surface hazard curves (solid lines) for 10-Hz oscillator frequency computed from LLNL bedrock hazard curves (dashed lines). Hazard curves are for six soil and bedrock conditions (see text for explanation of legend). LLNL 10-Hz bedrock hazard (dashed line) is shown for interpolated segments (solid symbols) and extrapolated segments (open symbols).

Figure 6.9 - Combined EPRI and LLNL soil surface hazard envelope for oscillator frequencies of 1, 2.5, 5, and 10 Hz. Probability of exceedance vs. spectral velocity.

Figure B.1 (c) - Computed 1-Hz soil surface hazard curves with disaggregation constrained to MH. EPRI/LLNL bedrock hazard continued to soil surface (solid lines). Hazard curves reflect six soil and bedrock conditions (see Section 6 for explanation of legend). EPRI/LLNL 1-Hz bedrock hazard (dashed line) is shown for interpolated segments (solid symbols) and extrapolated segments (open symbols).

Figure B.2 (a) - Computed 2.5-Hz soil surface hazard curves with disaggregation constrained to ML. EPRI/LLNL bedrock hazard continued to soil surface (solid lines). Hazard curves reflect six soil and bedrock conditions (see Section 6 for explanation of legend). EPRI/LLNL 2.5-Hz bedrock hazard (dashed line) is shown for interpolated segments (solid symbols) and extrapolated segments (open symbols).

Figure B.2 (b) - Computed 2.5-Hz soil surface hazard curves with disaggregation constrained to MM. EPRI/LLNL bedrock hazard continued to soil surface (solid lines). Hazard curves reflect six soil and bedrock conditions (see Section 6 for explanation of legend). EPRI/LLNL 2.5-Hz bedrock hazard (dashed line) is shown for interpolated segments (solid symbols) and extrapolated segments (open symbols).

Figure B.2 (c) - Computed 2.5-Hz soil surface hazard curves with disaggregation constrained to MH. EPRI/LLNL bedrock hazard continued to soil surface (solid lines). Hazard curves reflect six soil and bedrock conditions (see Section 6 for explanation of legend). EPRI/LLNL 2.5-Hz bedrock hazard (dashed line) is shown for interpolated segments (solid symbols) and extrapolated segments (open symbols).

Figure B.3 (a) - Computed 5-Hz soil surface hazard curves with disaggregation constrained to ML. EPRI/LLNL bedrock hazard continued to soil surface (solid lines). Hazard curves reflect six soil and bedrock conditions (see Section 6 for explanation of legend). EPRI/LLNL 5-Hz bedrock hazard (dashed line) is shown for interpolated segments (solid symbols) and extrapolated segments (open symbols).

Figure B.3 (b) - Computed 5-Hz soil surface hazard curves with disaggregation constrained to MM. EPRI/LLNL bedrock hazard continued to soil surface (solid lines). Hazard curves reflect six soil and bedrock conditions (see Section 6 for explanation of legend). EPRI/LLNL 5-Hz bedrock hazard (dashed line) is shown for interpolated segments (solid symbols) and extrapolated segments (open symbols).

Figure B.3 (c) - Computed 5-Hz soil surface hazard curves with disaggregation constrained to MM. EPRI/LLNL bedrock hazard continued to soil surface (solid lines). Hazard curves reflect six soil and bedrock conditions (see Section 6 for explanation of legend). EPRI/LLNL 5-Hz bedrock hazard (dashed line) is shown for interpolated segments (solid symbols) and extrapolated segments (open symbols).

Figure B.4 (a) - Computed 10-Hz soil surface hazard curves with disaggregation constrained to ML. EPRI/LLNL bedrock hazard continued to soil surface (solid lines). Hazard curves reflect six soil and bedrock conditions (see Section 6 for explanation of legend). EPRI/LLNL 10-Hz bedrock hazard (dashed line) is shown for interpolated segments (solid symbols) and extrapolated segments (open symbols).

Figure B.4 (b) - Computed 10-Hz soil surface hazard curves with disaggregation constrained to MM. EPRI/LLNL bedrock hazard continued to soil surface (solid lines). Hazard curves reflect six soil and bedrock conditions (see Section 6 for explanation of legend). EPRI/LLNL 10-Hz bedrock hazard (dashed line) is shown for interpolated segments (solid symbols) and extrapolated segments (open symbols).

Figure B.4 (c) - Computed 10-Hz soil surface hazard curves with disaggregation constrained to MH. EPRI/LLNL bedrock hazard continued to soil surface (solid lines). Hazard curves reflect six soil and bedrock conditions (see Section 6 for explanation of legend). EPRI/LLNL 10-Hz bedrock hazard (dashed line) is shown for interpolated segments (solid symbols) and extrapolated segments (open symbols).

Figure C.1 - Computed 1-Hz soil surface hazard curves derived from combined EPRI/LLNL bedrock hazard (solid lines). Hazard curves are for six soil and bedrock conditions (see Section 6 for explanation of legend). EPRI/LLNL 1-Hz bedrock hazard (dashed line) is shown for interpolated segments (solid symbols) and extrapolated segments (open symbols).

Figure C.2 - Computed 2.5-Hz soil surface hazard curves derived from combined EPRI/LLNL bedrock hazard (solid lines). Hazard curves are for six soil and bedrock conditions (see Section 6 for explanation of legend). EPRI/LLNL 2.5-Hz bedrock hazard (dashed line) is shown for interpolated segments (solid symbols) and extrapolated segments (open symbols).

Figure C.3 - Computed 5-Hz soil surface hazard curves derived from combined EPRI/LLNL bedrock hazard (solid lines). Hazard curves are for six soil and bedrock conditions (see Section 6 for explanation of legend). EPRI/LLNL 5-Hz bedrock hazard (dashed line) is shown for interpolated segments (solid symbols) and extrapolated segments (open symbols).

Figure F.7 - LLNL rock hazard disaggregation element 2,2 (Mw 5.75, 20.4 km) for the 1, 2.5, 5, and 10 Hz oscillator. Values less than 1% were identically 0 and not plotted.

Figure F.8 - LLNL rock hazard disaggregation element 2,3 (Mw 6.25, 20.4 km) for the 1, 2.5, 5, and 10 Hz oscillator. Values less than 1% were identically 0 and not plotted.

Figure F.9 - LLNL rock hazard disaggregation element 2,4 (Mw 6.75, 20.4 km) for the 1, 2.5, 5, and 10 Hz oscillator. Values less than 1% were identically 0 and not plotted.

Figure F.10 - LLNL rock hazard disaggregation element 2,5 (Mw 7.5, 20.4 km) for the 1, 2.5, 5, and 10 Hz oscillator. Values less than 1% were identically 0 and not plotted.

Figure F.11 - LLNL rock hazard disaggregation element 3,1 (Mw 5.25, 38.9 km) for the 1, 2.5, 5, and 10 Hz oscillator. Values less than 1% were identically 0 and not plotted.

Figure F.12 - LLNL rock hazard disaggregation element 3,2 (Mw 5.75, 38.9 km) for the 1, 2.5, 5, and 10 Hz oscillator. Values less than 1% were identically 0 and not plotted.

Figure F.13 - LLNL rock hazard disaggregation element 3,3 (Mw 6.25, 38.9 km) for the 1, 2.5, 5, and 10 Hz oscillator. Values less than 1% were identically 0 and not plotted.

Figure F.14 - LLNL rock hazard disaggregation element 3,4 (Mw 6.75, 38.9 km) for the 1, 2.5, 5, and 10 Hz oscillator. Values less than 1% were identically 0 and not plotted.

Figure F.15 - LLNL rock hazard disaggregation element 3,5 (Mw 7.5, 38.9 km) for the 1, 2.5, 5, and 10 Hz oscillator. Values less than 1% were identically 0 and not plotted.

Figure F.16 - LLNL rock hazard disaggregation element 4,1 (Mw 5.25, 77.8 km) for the 1, 2.5, 5, and 10 Hz oscillator. Values less than 1% were identically 0 and not plotted.

Figure F.17 - LLNL rock hazard disaggregation element 4,2 (Mw 5.75, 77.8 km) for the 1, 2.5, 5, and 10 Hz oscillator. Values less than 1% were identically 0 and not plotted.

Figure F.29 - LLNL rock hazard disaggregation element 6,4 (Mw 6.75, 253. km) for the 1, 2.5, 5, and 10 Hz oscillator. Values less than 1% were identically 0 and not plotted.

Figure F.30 - LLNL rock hazard disaggregation element 6,5 (Mw 7.5, 253. km) for the 1, 2.5, 5, and 10 Hz oscillator. Values less than 1% were identically 0 and not plotted.

Figure F.31 - LLNL rock hazard disaggregation element 7,1 (Mw 5.25, 350. km) for the 1, 2.5, 5, and 10 Hz oscillator. Values less than 1% were identically 0 and not plotted.

Figure F.32 - LLNL rock hazard disaggregation element 7,2 (Mw 5.75, 350. km) for the 1, 2.5, 5, and 10 Hz oscillator. Values less than 1% were identically 0 and not plotted.

Figure F.33 - LLNL rock hazard disaggregation element 7,3 (Mw 6.25, 350. km) for the 1, 2.5, 5, and 10 Hz oscillator. Values less than 1% were identically 0 and not plotted.

Figure F.34 - LLNL rock hazard disaggregation element 7,4 (Mw 6.75, 350. km) for the 1, 2.5, 5, and 10 Hz oscillator. Values less than 1% were identically 0 and not plotted.

Figure F.35 - LLNL rock hazard disaggregation element 7,5 (Mw 7.5, 350. km) for the 1, 2.5, 5, and 10 Hz oscillator. Values less than 1% were identically 0 and not plotted.

SOIL SURFACE SEISMIC HAZARD AND DESIGN BASIS GUIDELINES FOR PERFORMANCE CATEGORY 1 & 2 SRS FACILITIES

EXECUTIVE SUMMARY

This report describes the development of Savannah River Site (SRS) soil seismic hazard for oscillator frequencies of 1, 2.5, 5 and 10 Hz. This soil surface hazard supersedes all previous soil hazard analyses conducted for the SRS. In addition, Performance Category 1 and 2 (PC1 and PC2) design basis spectra are developed in accordance with Department of Energy (DOE)-Standard (STD)-1023 and building code criteria from the 1997 NEHRP Recommended Provisions (NEHRP, 1997). These spectra complement the PC3 and PC4 design basis spectra contained in the March, 1997 report (Lee et al., 1997). The design basis spectra contained in this report are for the design of new or evaluation of existing PC1 and PC2 structures, systems and components (SSCs) within the SRS boundary. These spectra should be used in conjunction with building code requirements only.

Existing probabilistic seismic hazard evaluations conducted by the Lawrence Livermore National Laboratory (LLNL) (Savy, 1996) and the Electric Power Research Institute (EPRI) (NEI, 1994) were adopted (as the bedrock seismic hazard) in this analysis as required by DOE STD-1023. The soil amplification functions (SAFs) used to develop soil surface hazard incorporate the available SRS velocity and dynamic property database available to about mid-1996. The spectra are based on soil properties and stratigraphy from various locations at the SRS (Lee et al., 1997).

Ground motions associated with annual probabilities for PC1-PC4 structures (having target annual probabilities of exceedance of $2x10^{-3}$ to $1x10^{-4}$) are considered "high-confidence". This means that we associate a comparable confidence level for the soil surface hazard (computed in this analysis) as we do the LLNL and EPRI bedrock hazard (applied in this analysis).

For risk assessment purposes, the soil surface hazard was computed for annual probabilities as low as 10^{-7}, a probability range in excess of the available SRS bedrock hazard disaggregation probabilities. In addition, this probability range results in computed strains that are beyond the range that have been measured in SRS laboratory soil samples. These "lower-confidence" ground motions (identified parenthetically in Tables 6.6-6.9) are based on the best data available and are judged to be conservative for ground motion hazard. PC3 and PC4 uniform hazard spectra computed from this analytical method show that the previously computed PC3 and PC4 design basis spectra (Lee et al., 1997) are conservative.

Figures 6.9 and 6.10 illustrate the soil surface hazard for annual probabilities ranging from about 10^{-2} to 10^{-7}. The hazard is tabulated in Tables 6.6-6.9. The design basis spectra for PC1 and PC2 SSCs are given in Table 7.5 (Figure 7.4). These design spectra meet the DOE-STD-1023 requirements by accepting the criteria of the 1997 NEHRP Recommended Provisions and envelope the soil surface uniform hazard spectra derived using DOE-STD-1020 target return periods. PC1 and PC2 spectral shapes were taken from the broadened PC3 shape derived in by Lee et al., 1997. These design basis spectra are for incorporation into the SRS engineering guide 01060 and can be used as the basis for evaluation of PC1 and PC2 SSCs in conjunction with building code requirements.

Probabilistic risk assessments incorporating these soil surface hazards should also account for SSCs at risk due to soil deformation in the form of liquefaction and settlement, as the overall risk may be different because of site-specific soil conditions.

1.0 INTRODUCTION

An SRS-specific probabilistic seismic hazard assessment (PSHA) and associated seismic design basis is critically dependent upon the local geological and geotechnical properties at the site or facility location. Past PSHAs did not incorporate these detailed site properties; consequently, those hazard results should not be used for SRS-specific applications. Methodologies have been developed for generating SRS-specific mean response spectra on soil from mean bedrock response spectra. The implementation of DOE-STD-1023 requirements at the SRS for PC3 and PC4 facilities was developed in Lee et al., (1997) (hereafter referred to as Report 1). In Report 1, Lawrence Livermore National Laboratory (LLNL) (Savy, 1996) and Electric Power Research Institute (EPRI) (NEI, 1994) bedrock spectra were combined and then scaled by the mean soil/bedrock response to derive the ground motion spectrum at the soil surface. The SRS-specific soil response (soil amplification function) was based on soil properties obtained using an extensive database of geological, geophysical, geotechnical and seismic data representing the SRS. A methodology was developed to demonstrate that the mean scaling approach to obtain spectra at the ground surface from input bedrock spectra met or exceeded the DOE-STD-1023 criteria. This methodology was described in Report 1 and also presented in Lee et al. (1998). Further refinements of the hazard-based methodology to obtain fully probabilistic seismic hazard for the soil surface are described in this report. SRS soil

surface hazard is computed and used to develop uniform hazard spectra (UHS), and hazard based design basis spectra in conjunction with building code requirements for PC1 and PC2 facilities on soil sites.

Note that by SRS-specific spectra (or SRS-specific soil amplification function) we mean spectra that are representative of site properties measured at the SRS. The SRS-specific results contain the range of SRS site properties including soil column thickness, soil and bedrock shear-wave velocity, and dynamic properties. As discussed in Report 1, PC3 and PC4 facilities require additional site-specific data to validate that the facilities properties are well represented by the SRS-specific properties.

Seismic hazard evaluations used in this study are the EPRI and LLNL results for bedrock for the SRS and vicinity. This study does not revise or confirm in any way the experts' evaluations of activity rates, seismic source zonation, or the decay of ground motion with distance used in the LLNL or EPRI seismic hazard assessments. This analysis results in a SRS-specific hazard evaluation for soil sites by continuing the hazard from bedrock to the soil surface using detailed soil response functions. Earthquake magnitude and ground motion level dependence of the site response is accommodated by developing site response functions consistent with the distribution of earthquake magnitude and ground motion levels obtained from dissaggregating the bedrock unifom hazard spectrum.

The ground motion attenuation and seismic source evaluations input to the LLNL and EPRI PSHAs were provided by individuals and organizations with broad expertise and knowledge of the seismotectonic regime and ground motion models in the southeastern U.S. The subject of this investigation is not the LLNL and EPRI hazard studies, but the careful application of those results to obtain a ground motion design basis on soils for the SRS. Significant differences exist between both the EPRI and LLNL hazard analyses and also between these results and the recent national hazards map produced by the United States Geological Survey (USGS) (Frankel et al., 1996). As the understanding of seismotectonics and ground motion attenuation in the southeastern United States evolve, critical assessments of any potential design basis impact will be required.

Frequency and ground motion level dependent soil amplification functions (SAFs) developed in Report 1 accounted for the observed variations in properties throughout the SRS including: soil column thickness, stratigraphy, shear-wave velocity, and material dynamic properties, as well as basement properties. Detailed discussion of these data and the sensitivity of site response to the various parameters are described in Report 1. SAFs (frequency dependent ratio of soil response to bedrock input) were derived in Report 1 by performing a statistical analysis of the response of bedrock spectra through 30 realizable soil columns bounded by the observed variations in soil-column properties over the SRS. Ground motion level dependent distributions of SAFs were derived for each of 6 soil categories: three on crystalline basement and three on Triassic basement. Those SAF distributions are used in this study to compute soil surface hazard. The soil categories are described in Section 5.

The hazard on soil at the ground surface is the envelope of the hazard computed for each of the six soil/bedrock categories. This procedure to compute mean soil surface hazard is more accurate and simplified than the mean scaling approach developed in Report 1. The approach used here defines a mean response rather than a scaling value that approximates a mean response. PC1 and PC2 design basis spectra are computed from the hazard results following DOE-STD-1023 and building code criteria from the 1997 NEHRP Recommended Provisions (NEHRP, 1997). The design basis spectra in conjunction with building code requirements may be used for both new and existing PC1 and PC2 SSCs within the SRS boundary. The design basis spectra and hazard curves contained herein are considered confirmed in accordance with the E7 Manual (WSRC, 1998). As required by DOE, comparison is made of the PC1 and PC2 design motions to the building code.

2.0 SUMMARY OF DESIGN BASIS CRITERIA AND APPROACH TO MEETING ACCEPTANCE CRITERIA

DOE-STD-1023

DOE-STD-1023 provides guidelines for developing site-specific PSHA and criteria for determining ground motion parameters for design earthquakes. It also provides criteria for determination of design response spectra. Five performance categories are specified for facility SSCs (see also DOE-STD-1020): Performance Category (PC0) applies to SSCs that require no hazard evaluation; PC1 requires performance "preventing major structural collapse that would endanger personnel"; PC2 requires performance to "maintain capacity to function and occupant safety"; PC3 and PC4 facilities contain toxic or radioactive materials and so a level of performance is required such that "hazardous materials can be controlled and confined, occcupants protected, and functioning of the SSC is not interrupted"; PC4 requires performance comparable to commercial nuclear power plants. The development herein of PC1 and PC2 site spectra are in accordance with DOE-STD-1023-96 and building code criteria (NEHRP, 1997). PC3 and PC4 design spectra were developed in Report 1 and are not impacted by this report. The targeted annual probabilities for each performance category are shown in Table 2.1.

Acceptable approaches to meet the criteria for PC1 and PC2 facilities are (DOE-STD-1023-96):

1) Hazard obtained from seismic hazard maps used by current building codes or from national consensus standards are acceptable if no site-specific PSHA has been conducted.
2) For sites with a site-specific PSHA, SSCs shall be evaluated or designed for the greater of the site-specific hazard values or the code hazard values, unless DOE approves lower site-specific values.

hazard at the target mean annual probability of exceedance and range of oscillator frequencies of interest. The methodology is the same as that described in Report 1. Using the disaggregated EPRI bedrock hazard, Report 1 showed that the mean-based scaling of the bedrock UHS gives results equivalent to or more conservative than the exact methodology of continuing the hazard to the soil surface.

As discussed in Report 1 hazard at the surface of a non-linear soil column (soil surface hazard) can be derived using bedrock hazard disaggregation together with a set of frequency, magnitude and ground motion dependent soil amplification functions (SAFs). A thorough discussion of this procedure is contained in Report 1. As discussed in Report 1, Cornell and Bazzurro (1997) formalized the methodology and we follow that formalism here. Using the notation of Cornell and Bazzurro, the discrete form of the soil surface hazard curve is given by:

$$G_Z(z) = \sum_{x_j} \sum_{m_i} G_{Y|M,X}(z/x|m_i, x_j) * p_{M|X}(m_i|x_j) * P[X = x_j] \qquad (3.1)$$

where the sums are over magnitudes (m_i) and bedrock motion amplitude levels (x_j) contained in the hazard disaggregation; $p_{M|X}(m_i|x_j)*P[X=x_j]$ is the probability mass function, and $G_{Y|M,X}$ is the conditional complementary cumulative distribution function (CCDF) on the amplification factor. The three products in equation 3.1 represent:

(1) the conditional CCDF on the amplification of motion caused by the soil, given rock motion of amplitude X=x associated with earthquake of magnitude M=m,
(2) the conditional probability of magnitude M=m, given rock motion X=x,
(3) the probability of rock motion X=x

The methodology requires disaggregation of bedrock hazard for a suite of bedrock motions. The hazard disaggregation represents the composition of the hazard by earthquake magnitude and distance. For each (bedrock) level of motion, the disaggregated hazard is represented by a table of numbers, where rows represent source distance bins and columns represent source magnitude bins. The sum of all elements of the table is the total probability of exceedance Thus, for a given oscillator frequency and level of bedrock ground motion ($X=x_i$), each element of the hazard disaggregation corresponds to the probability of exceedance of rock ground motion for a specific earthquake distance and magnitude range (see Appendices E and F). For each oscillator frequency, the first differences are taken of the disaggregation elements between adjacent levels of bedrock motion. This results in tables of disaggregations for the probability of occurrence of the mean bedrock control motions. These probability of occurrence disaggregations determine the products of the probability mass function of equation 3.1:

$$p_{M|X}(m_i|x_j)*P[X=x_j]$$

develop soil column thickness for the SRS (Figure 5.1). An SRS generic shear-wave velocity profile was developed from the location-specific data and randomized for both stratigraphic layer thickness and variation in velocity (Toro, 1996) (Figures 5.2 a, b). Normalized shear modulus and damping ratio versus shear-strain relationships were developed for specific soil layers using dynamic properties obtained from laboratory testing by Stokoe et al. (1995).

Development of SAFs

Wave propagation within the soil column is accounted for by using a one-dimensional equivalent linear analysis (Silva 1989). Magnitude dependence of the SAF was accounted for by using three magnitude and distance dependent earthquake spectra for each control motion level as shown in Table 5.1. We call the 5th fractile magnitude and distance pair the low magnitude (ML), the 50th fractile the median or M-bar magnitude (MM), and the 95th fractile the high magnitude (MH) associated with a given control motion amplitude expressed as PGA (Table 5.1). For each control motion PGA level (ranging from 0.05g to 0.75g), the three spectra generated are then convolved through 30 simulated soil columns for each basement type and soil depth range. Thirty SAFs are calculated for each magnitude, distance and PGA level combination. Calculations were made for crystalline rock velocity and depth ranges of 600-800, 800-1000, 1000-1200 ft and the Triassic rock with depth ranges of 900-1100, 1100-1300, 1300-1500 ft. Figure 5.3 (a) illustrates the mean magnitude (M-bar) and distance (D-bar) bedrock control motion spectra for eight levels of bedrock PGA (ranging from 0.05 to 0.75g). The corresponding mean SAF (statistical log-mean for 30 velocity profiles) for basement depth-range 2 (800-1000 ft soil column thickness) over crystalline rock are illustrated in Figure 5.3 (b). The standard deviations are shown in Figure 5.3 (c). Figure sets 5.4 and 5.5 illustrate bedrock control motions and corresponding SAF statistics (mean and standard deviation) for the 5% and 95% magnitude-distance pairs respectively.

6.0 COMPUTATION of SRS SOIL SURFACE HAZARD

The EPRI and LLNL mean magnitude and frequency dependent disaggregated bedrock seismic hazard results are used to develop the EPRI and LLNL soil surface hazard, and then combined to obtain the SRS soil surface hazard. For each of the four ground motion frequencies (1.0, 2.5, 5.0, and 10.0 Hz), the hazard disaggregation is defined for a suite of bedrock spectral ground motions (Table 6.1 for EPRI and Table 6.2 for LLNL). The EPRI hazard disaggregation magnitude and distance intervals are:

mb:	5.0-5.5, 5.5-6.0, 6.0-6.5, 6.5-7.0, >7.0
r (km):	0-25, 25-50, 50-100, 100-150, 150-200, >200

The LLNL hazard disaggregation magnitude and distance intervals are:

Mw:	5.0-5.5, 5.5-6.0, 6.0-6.5, 6.5-7.0, >7.0
r (km):	0-15, 15-25, 25-50, 50-100, 100-200, 200-300, >300

Assumptions and Approximations Used In Soil Surface Hazard Development:

1. A polynomial interpolation of bedrock hazard curves appears to be a good approximation for both LLNL and EPRI for all frequencies based on the goodness of fit of a cubic polynomial to the log POE vs. log Sv.
2. The fitted polynomial is used to extrapolate the bedrock hazard curve to lower and higher annual POE in order to achieve the desired ranges in the POE, but with cautions noted below. The extrapolation of the bedrock hazard curve is unconstrained and leads to potentially large sources of uncertainty in the soil surface hazard.
3. The hazard disaggregation, between bedrock levels of motion, is linearly interpolated on a log-log scale (Appendix ~~E and~~ F). ~~Magnitude sensitivity to the~~ soil surface hazard is considered in Appendix B. Based on the results of Appendix B, the magnitude sensitivity of the soil hazard is significant and cannot be neglected in the hazard analysis.
4. Distance dependence of the SAF is not considered. It is expected that the effect of distance on the computed SAF is second-order except at the lowest POE's (largest ground motions). At these lowest POE's, the mean source distance is reduced to the extent that the point source approximation may no longer be valid and the resulting SAF may differ significantly from a point-source evaluation.
5. The three-point magnitude dependence contained in the SAFs (ML, MM, MH) is linearly interpolated to account for the magnitude dependence contained in the bedrock disaggregation.
6. The SAFs and corresponding control motions of Report 1 are assumed to cover the necessary ranges of bedrock hazard motions described in Tables 6.1 and 6.2. In addition, the SAFs are assumed to be log-normally distributed and linear interpolation of the log-normal distribution is assumed to be adequate for developing soil surface hazard.
7. Where rock hazard values exceeded the range defined by the SAFs, SAF median and standard deviations were conservatively fixed at the limiting values.
8. A lower bound on the SAF of 0.5 is also applied for all frequencies to limit the non-linearity of the soil column.
9. Truncation of the probability of exceedance at $\pm 2\sigma$ was used to avoid accumulation of extremely low POE's.

SRS Soil Surface Hazard by Soil Column Classification

The computed SRS soil surface hazard curves for all combinations of bedrock and soil classifications derived from the EPRI bedrock hazard curve, are shown in Figures 6.1 through 6.4. The curves represent hazard at the top of the soil column for oscillator frequencies of 1, 2.5, 5 and 10 Hz respectively. The corresponding soil surface hazard derived from LLNL bedrock hazard is shown in Figures 6.5 through 6.8. The soil surface hazard curves were computed using the methodology described in Section 3. The dashed lines in the figures are the EPRI or LLNL bedrock hazard curves. The appropriate

disaggregation was used in each case. Open symbols on the dashed lines indicate extrapolation beyond either the LLNL or EPRI bedrock hazard values. Solid lines are computed soil surface hazard derived from the bedrock hazard disaggregations and distributions on soil transfer functions. The legends are read as follows: the first number (1, 2p5, 5, 10) is oscillator frequency; the first letter (e or l) is either e for EPRI or l for LLNL bedrock hazard disaggregation; the second letter is c to t for crystalline or Triassic bedrock; and the last number is 1, 2, or 3, for soil depth range. Thus, the hazard corresponding to "2p5et3" corresponds to the 2.5 Hz EPRI bedrock hazard for soil depth range 3 (1300-1500 ft) overlying Triassic bedrock.

High and low probability extrapolations of bedrock hazard curves were made to meet the ranges of probability required for engineering risk assessments. Soil surface hazard results computed in the range of bedrock hazard extrapolations are considered more uncertain. Consequently, computed ground surface hazard curves for annual probabilities greater than about 10^{-2} or less than about 10^{-6} should be used with caution. These results were computed using a 2-σ truncation on the ground motion probability of exceedance and a lower bound of 0.5 on the SAF. Sensitivity of these parameters is reviewed in Appendix A.

There are general features in common among all the soil surface hazard curves. At higher annual probabilities, the soil surface hazard curves approximately parallel the rock hazard curve (i.e., nearly the same slope) until ground motions are sufficiently large that non-linear soil effects begin. For larger ground motions, frequency dependent nonlinear soil response increasingly reduces the probability of exceedance as compared to the bedrock hazard curve (soil surface hazard increasing slope). Significant nonlinear behavior of the soil, manifest in the soil surface hazard curves for the four frequencies, do not become clearly evident until annual probabilities of exceedance are less than about 10^{-4} ($< 10^{-5}$ for 1.0 Hz). At much lower POEs ($\cong 10^{-6}$), the soil surface hazard curves again begin to parallel the bedrock hazard curve. This behavior occurs at lower annual probabilities because of the constraint placed on reduction of motion due to non-linear soil response. This is partially an artifact of the limited range of SAFs; however, the calculation of site response for the upper range control motion is approaching the limits of the reliability of the equivalent linear method and the reliable range of measured strain-dependent damping for some soil layers used in the analysis. For computation of very low probability ($<10^{-6}$) soil surface hazard, limiting the upper range of control motions (or equivalently limiting the peak soil strains) adds added conservatism to those segments of the soil surface hazard curve that would otherwise be based on tenuous extrapolations of laboratory testing data. In addition, the added conservatism obtained by limiting the degree of soil degradation may compensate for the additional uncertainty in the equivalent linear approximation at these strain levels.

Envelopes of the computed soil surface hazard curves plotted as spectral velocity and spectral acceleration, are shown in Figures 6.9 and 6.10 respectively. These curves form the basis for development of UHS at the top of the soil column. Ground motions

corresponding to annual probabilities from about $2x10^{-3}$ to $2x10^{-5}$ are classified as high-confidence regions on the hazard curves. This means that we associate a comparable confidence level for the computed soil surface hazard as we do the LLNL and EPRI bedrock hazard. Tables 6.3-6.5 identify the higher confidence ranges in the soil surface hazard. Portions of the soil surface hazard used at much lower POEs are estimated for risk assessment purposes only. The SRS hazard is tabulated in Tables 6.6-6.9. Although portions of the hazard curve are classified as lower-confidence probabilities (identified parenthetically in Tables 6.6-6.9), they are based on the best available data and are judged to be conservative. Polynomials were fit to the hazard curves shown in Figure 6.10, and those coefficients are given in Table 6.10.

SRS Soil Surface UHS

Figures 6.11 and 6.12 illustrate comparisons of the computed PC3 and PC4 (annual probabilities of exceedance of $5x10^{-4}$ and $1x10^{-4}$ respectively) soil UHS to the PC3 and PC4 DBE spectra derived using the mean scaling methodology of Report 1. The mean based scaling results are seen to be slightly higher than the more exact soil UHS. This was the conclusion reached in Report 1 based on the computed EPRI-based soil surface hazard.

The mean soil response approach of Report 1 used 1-2.5 and 5-10 Hz spectral averages as a basis for scaling. The scaled 5-10 Hz average spectra were higher than the 1-2.5 Hz scaled spectra at nearly all frequencies. The scaling process was repeated in Report 1 for the low (ML), medium (MM), and high magnitude (MH) spectra. We note that the results of the two methodologies, illustrated in Figures 6.11 and 6.12, are in better agreement in the 5-10 Hz range than the 1-2.5 Hz range. This is an expected result because the mean scaling approach of Report 1 used the envelope of the 5-10 Hz and 1-2.5 Hz scaled results. In every case, the 5-10 Hz scaled results enveloped the 1-2.5 Hz scaling.

The effects of non-linearity are also evident in Figures 6.11 and 6.12. Illustrated soil UHS are: (1) the soil surface hazard derived from combining the independently computed EPRI soil and LLNL soil surface hazards; and (2) the soil surface hazard derived from the EPRI and LLNL combined bedrock hazard (Appendix C). Combining the EPRI and LLNL soil surface hazard at the surface results in a reduced surface hazard at 10 Hz for PC3 (5 and 10 Hz for PC4) as compared to the soil surface hazard derived from the EPRI and LLNL combined bedrock hazard. This reduction is a consequence of the greater soil degradation occurring in the LLNL soil surface hazard. We note better agreement with the results of Report 1 in this case because the EPRI and LLNL hazards were combined at bedrock in that analysis. The hazard results should properly be combined at the soil surface.

Figure 6.13 illustrates the PC1-PC4 soil UHS derived from the linear interpolation of soil surface hazard curve envelope shown in Figure 6.10 (the combined EPRI and LLNL soil surface hazard). For comparison, the PC3 and PC4 DBE spectra from Report 1 are

shown. As noted above, the PC3 and PC4 DBE spectra conservatively envelope the soil UHS.

7.0 DEVELOPMENT OF PC1 AND PC2 DESIGN BASIS IN CONJUNCTION WITH NEHRP BUILDING CODE REQUIREMENTS

As discussed in Section 2, DOE-STD-1023 allows significant latitude for development of PC1 and PC2 design basis spectra. As discussed below, there are significant technical issues with the current codes (UBC-97) and guidelines (NEHRP, 1997) that inhibit their being fully adopted at the SRS. The recent NEHRP (1997) guidelines suggest that key design basis criteria are evolving towards greater margin in seismic design. Because of wide acceptance of this new criteria, a mutual agreement between the DOE and Site Geotechnical Services was reached that the seismic design criteria defined by NEHRP (1997) would be adopted for the seismic design basis at the SRS. As discussed below, the EPRI and LLNL soil surface hazard, derived using SRS-specific site response functions, are used together with the NEHRP (1997) design criteria to derive PC1 and PC2 design basis spectra. These spectra meet minimum requirements in DOE-STD-1020.

DOE-STD-1020 Requirements

Minimum requirements for PC1 and PC2 SSCs are spectra having annual probability of exceedence of $2x10^{-3}$ and $1x10^{-3}$ respectively (return periods of 500 and 1000 years). Figure 7.1 illustrates the 1, 2.5, 5 and 10 Hz spectral values having return periods of 500 and 1000 years. These spectra were derived from the combined EPRI and LLNL soil surface hazard (Section 6).

NEHRP-97 Recommended Building Code Requirements

Although the 1997 NEHRP Recommended Provisions for Seismic Regulations for New Buildings (NEHRP-97) spectrum does not become effective until the year 2000, it is important to consider the implication of the standard to the SRS. The NEHRP-97 design spectrum is defined as 2/3 of the maximum considered earthquake ground motion, i.e., 2/3 of the 2500 year UHS. NEHRP-97 uses a discretized hazard map, which in principle, properly accounts for geographic distance of the site from seismic sources. However, NEHRP-97 is based on hazard maps prepared by the USGS (Frankel et al., 1996), which are based on different source and ground motion attenuation models than that used by either EPRI or LLNL.

Figure 7.2 compares the SRS 500 and 1000 year return period earthquake UHS to the spectrum derived following the NEHRP-97 guidelines (Chapter 4). The NEHRP-97 spectrum uses the USGS seismic hazard map for soft-rock site category (2,500 < Vs < 5,000 ft/sec) (Frankel et al., 1996). Thus, the spectral values shown on Figure 7.2 were adjusted for site class "D" which is characterized by soils having shear wave speeds of 600< Vs <1,200 ft/sec and standard penetration test resistance values (N-values) of 15-50

in the upper 100 ft. In addition, as recommended in NEHRP-97, the design spectral response was taken as 2/3 of the maximum considered ground motions and further reduced by 20% (as allowed by NEHRP) to make the spectrum more consistent with the SRS-specific assessment. The NEHRP-97 seismic coefficients derived for the SRS are listed in Table 7.1.

The NEHRP-97 spectrum (Figure 7.2) may appear to be generally consistent with the spectral shape derived from the detailed site specific assessments (Report 1). However, the NEHRP-97 spectrum is considered inappropriate for the SRS for several reasons:

(1) direct measurements of shear-wave velocity in the SRS-specific soil and bedrock assessments invalidates the soft-rock assumption made in the USGS hazard model. Measured bedrock shear-wave speeds at the SRS range from about 7,000-12,000 ft/sec. These bedrock wave-speeds define a hard-rock site condition.

(2) hard-rock to hard-rock comparison for EPRI/LLNL and the USGS hazard by making proper adjustments to remove the soft-rock response. Table 7.2 shows a comparison of corrected USGS hard-rock spectral values to soft-rock values (the soft-rock hazard always entails a significant amplification as compared to hard-rock results). Table 7.3 shows the comparison of corrected USGS hard-rock values to the average of the LLNL/EPRI bedrock values taken from Report 1. The hard-rock comparisons are favorable at 5-Hz.

(3) the USGS 1-Hz bedrock spectral acceleration is significantly higher by about a factor of two as compared to the average of EPRI/LLNL. Atkinson and Boore (1998) have shown that the 1-Hz USGS attenuation model is biased-high as compared to other Eastern U.S. attenuation models.

(4) the USGS may not fully constrain the fault rupture to occur within the Charleston special source zone (personal conversation between R. Lee and A. Frankel). This problem with the hazard algorithm results in higher computed hazard at sites outside the source zone, such as the SRS.

PC1 and PC2 Design Basis Recommendations

From the discussion of the NEHRP-97 spectrum comparison, we conclude that there is not an adequate technical basis at this time to reject the EPRI and LLNL hazard evaluations and the SRS-specific response in favor of the USGS hazard evaluation and the NEHRP-97 soil amplification factors. When the technical issues with the USGS regional hazard maps have been resolved, a relatively straightforward procedure can be used to incorporate the USGS bedrock hazard into the SRS design basis.

The NEHRP-97 design basis criteria indicate a trend towards additional margin in the earthquake design of new structures. To be consistent with design basis guidance for low-hazard facilities, we adopt the NEHRP-97 design criteria for PC1 and PC2 structures. We also recommend that at this time the NEHRP-97 criteria be applied with the LLNL/EPRI soil hazard for PC1 and PC2 facilities. Figure 7.3 illustrates the EPRI/LLNL soil UHS for a return period of 2500 years. The PC3 design basis spectral shape (Report 1) was scaled to envelope the 2500 year UHS. The recommended PC1

spectrum is shown as 2/3 of the 2500 year return period spectrum. Following NEHRP-97 guidance, PC2 design basis is an importance factor of 1.5 times PC1 (Table 7.5).

Figure 7.4 more clearly shows the recommended PC1 design basis spectrum as compared to the NEHRP-97 spectrum. Although the absolute level of the PC1 spectrum is lower than the NEHRP spectrum for reasons discussed above, it is apparent that the NEHRP shape does not capture the longer period deep soil response of a site such as the SRS. For example, by scaling the spectral shapes to the same 100 Hz level, the NEHRP-97 spectrum falls below the SRS design spectrum between about 0.4 to 2 Hz.

UBC-97 Building Code Requirements

The UBC-97 requires a design response spectrum in accordance with the UBC hazard maps or a site-specific hazard assessment having a 10% probability of exceedance in 50 years (POE of about 2 x 10^{-3} yr^{-1}). Development of a UBC spectrum requires use of a seismic zone map which dates from the 1980s. The UBC seismic zone map has the SRS contained in the same seismic zone as Charleston and eastern Tennessee, two zones with much higher rates of seismicity than the SRS. Thus, the use of broad zones tends to penalize the SRS. UBC-97 also uses updated site response factors from NEHRP-94 but not NEHRP-94 maps and that introduces an inconsistency that results in over-conservative surface motions at sites like the SRS.

8.0 DISCUSSION

Assumptions and Limitations on SRS-Specific Hazard

The soil hazard at the ground surface is derived using a methodology which directly incorporates SRS-specific site response functions, derived from the large SRS geotechnical and geological database, to continue the EPRI and LLNL bedrock hazard to the soil surface. The computed mean soil surface hazard for 1, 2.5, 5 and 10 Hz oscillator frequencies are judged to be as reliable as the mean EPRI and LLNL bedrock hazard assessments at the annual exceedance rates required for PC1-PC4 design basis.

Lower probability segments of the hazard curve (< 10^{-5} yr^{-1}), derived for the purpose of application to PRAs, required a number of assumptions and special qualifications. At low POEs (< 10^{-5} for 1, 2.5 and 5 Hz and < 10^{-6} for 10 Hz) the soil surface hazard is computed using extrapolations of the LLNL and EPRI bedrock hazard curves. At these exceedances, the bedrock hazard curve is extrapolated and is not otherwise constrained. While the bedrock hazard curve becomes increasingly uncertain below these low POEs, the site response model becomes increasingly more conservative because the SAFs, for greater soil deformations, have a lower bound on the median and fixed standard deviation. For these reasons, ground motions for these probabilities are qualified. Table 6.5 lists the high-confidence ranges for annual probability of exceedances where high-confidence simply indicates a judgement that the confidence level is nearly equivalent to the confidence in bedrock hazard reported by either EPRI or LLNL. Users of the SRS

soil surface hazard should be aware of these assumptions when using the soil surface hazard results beyond the high-confidence ranges identified in Table 6.5. Unless the EPRI or LLNL bedrock hazard slope changes significantly from the trend defined by the fitting polynomial at low POEs, the soil surface hazard for exceedances lower than these low values will be conservative in ground motion. The low-POE hazard is judged to be conservative because the SAFs, corresponding to the low-POE hazard, have a constrained distribution (fixed median and standard deviation) that limits the amount of soil non-linearity and reduction of the ground motion amplitude by the soil column.

If higher confidence is needed on the low-POE range of soil surface hazard (high spectral velocities), significant additional work would be required to refine and improve the reliability of the site response analyses. Tasks to improve the reliability of the soil surface hazard include incorporating laboratory tests for higher peak strain levels to better model strain-dependent shear-modulus and damping at greater ranges of deformation. Also, a non-linear soil response model may be required. Higher confidence in the low-POE bedrock hazard may also entail additional effort. This effort would require a rerun of the PSHA and possibly additional expert evaluations.

While the ground motion hazard at low-POEs is considered conservative for ground motion PRAs, the results may be entirely inappropriate and possibly unconservative for PRAs where liquefaction and settlement are considered. For ground motion probabilities less than about 10^{-4}, significant soil deformation may occur and at lower probabilities ($< 10^{-6}$) permanent soil deformation (including liquefaction and settlement) is likely. At these annual exceedance rates, soil deformation phenomena likely would be occurring despite the hazard result showing a nearly consistent slope of the soil surface hazard relative to the bedrock hazard. Thus, the user is cautioned that if a ground motion PRA is conducted for a facility, site-specific liquefaction and settlement issues may in fact be more important and should be included in any PRA assessment.

The importance of earthquake distance dependence in the soil SAFs has not been explored. At lower POEs ($< 10^{-5}$) the average contributing earthquake distance (D-bar) will be significantly reduced. This distance effect is accounted for to a degree in the procedure for generating SAF control motions. However, as the bedrock hazard probabilities decrease, controlling magnitudes increase and corresponding source distances decrease making the point source and vertical wave incidence assumptions questionable. These factors may significantly modify the SAF and correspondingly modify computed soil surface hazard. For more reliable PRAs, the sensitivity of the computed hazard to the effects of the finite source should be conducted.

Mean Soil Surface Hazard

In this evaluation, the mean bedrock hazard of EPRI and LLNL were used together with SRS-specific SAFs to continue the hazard and compute a "mean" soil surface hazard. Soil response so conditions the soil surface hazard, that a question remains as to whether this result is really a mean result. It is generally observed that ground

motion variability in rock exceeds that of soil. This is a result of the non-linear soil behavior effectively filtering out the higher-motions that can skew the mean. Consequently, we expect that if each hazard curve from the family of bedrock curves generated in the original PSHA were continued to the surface, using a process as defined in Section 3, the statistical mean, computed at the soil surface, would be somewhat lower than the soil "mean" that is estimated in Section 6. A quantitative assessment of the degree of conservatism could only be derived from laborious, SRS-specific soil analyses using the large number of bedrock evaluations.

Comparison to Mean Based Scaling Approach Used In Report 1

The soil surface hazard methodology to compute or continue the hazard from bedrock to the soil surface (described in Section 3), is an exact and straight-forward procedure. Excellent comparisons were observed between the PC3 and PC4 design basis spectra derived from the mean based scaling methodology described in Report 1, and the UHS values derived in this study using the exact methodology. The comparison indicates that the PC3 and PC4 design basis spectra, derived using the mean-based scaling methodology, slightly exceed the DOE criteria. This comparison suggests that for stiff soil sites, the mean-based scaling methodology achieves at least a mean hazard so long as the magnitude and frequency dependence in the SAF is enveloped as was done in Report 1. For softer soil sites and/or more stringent criteria, the spectra derived from the mean-based scaling methodology would be expected to underestimate the UHS as compared to the exact methodology described in Section 3. In general, it is recommended that the methodology described in Section 3 be used for the process of developing a site-specific mean soil surface spectrum from mean bedrock hazard.

Use of Prior Probabilistic Seismic Hazard Assessments

PSHAs developed for the SRS prior to the LLNL and EPRI studies (i.e., Coats and Murray, 1984, URS/Blume, 1982) as well as the hazard derived from the combination of the original EPRI and LLNL soil surface hazard (Wingo, 1994), were derived for PGA only and were not SRS-specific. Historically, engineering applications and earthquake design used PSHAs that were PGA-based, a practice that has diminished for the last 20 years because of improved interpretations from broader-band seismic recording and the better understanding of the broad-band nature of seismic hazard. Although development of an approximate PGA hazard curve is discussed below, use and development of PGA PSHAs is not recommended nor consistent with DOE-STD-1023.

General Comments on Future Development of Site-Specific PSHAs

The approach developed for deriving site-specific soil surface hazard from bedrock hazard curves introduces a number of opportunities for future site-specific hazard evaluations, most of which should be cost-effective in the normally long interval between development or renewal of design basis seismic hazards for critical DOE facilities.

1. Because site response is a critical factor in the total hazard model for soil sites such as the SRS, the methodology discussed in Section 3 lends itself to important uses to illustrate and model important soil factors that control seismic hazard. For example, the contributions to the POE of magnitude and strain-dependence of the site response can be easily followed with this approach. Also, the effects of soil non-linearity has a pronounced effect on the soil surface hazard and can be easily observed. Such effects can be otherwise easily obscured in the conduct of a soil surface PSHA.

2. PSHAs should always be designed to evaluate hazard for both rock outcrop and soil-surface horizons. There are several reasons for this. First, soil-structure-interaction and soil stability/liquefaction analyses commonly apply convolution techniques to model the phenomena and consequently, a detailed UHS at bedrock can be essential for this task to avoid the use of de-convolution techniques. Second, bedrock outcrop hazard analyses are better suited to compare hazard results to regional studies as was done for the comparison of the SRS hazard to NEHRP recommended motions. Third, introduction of generic site response into the uniform hazard evaluation may not as efficiently capture the site response as the methodology employed here, unless the ground motion attenuation functions have been specifically prepared for that site. Finally, the understanding of site response for a site such as the SRS tends to evolve over time more rapidly than the hazard model (i.e., earthquake zones, seismic source models, crustal structure and hard-rock ground motion attenuation models). This evolution is a result of new construction and a continuous improvement in state-of-practice for evaluation and measurement of soil and bedrock velocity structure and strain-dependent material properties. Consequently, improvements in knowledge of soil velocity, laboratory measurements of dynamic properties, approach to convolution analyses, or seismic measurements of site response can be incorporated into the site hazard in an efficient manner without regenerating the complete hazard evaluation.

3. A full hazard disaggregation at each target design basis annual probability level should always be done for any critical facility. The POE ranges (at least for bedrock) should be taken to the largest extremes allowed by the analysts. Careful attention to these requirements can result in future cost savings for the reasons described above.

4. The uniform hazard should be completed for as many oscillator frequencies as possible (>10). A larger number of frequencies is of particular value in developing a design basis spectral shape from a soil UHS.

Future Developmental Work

1. With resolution of DOE concerns on recent USGS regional hazard maps (Frankel et al., 1996), SRS soil hazard can be modified to incorporate the USGS bedrock hazard results. A new analysis would require USGS hazard evaluations for SRS bedrock conditions with the associated disaggregation for at least the four frequencies used in the

EPRI and LLNL analysis (1, 2.5, 5 and 10 Hz). A weighting scheme for the EPRI, LLNL and USGS soil surface hazard would also be incorporated in consultation with the DOE.

2. The soil surface hazard methodology (Section 3) lends itself to additional analyses related to seismic induced failure of SRS soils. It is a straightforward task to track peak shear-strains and cyclic stress ratios (τ/σ) for each soil layer in a hazard analysis. By doing so, probabilities of exceedance and probabilities of occurrence of the cyclic stress ratios can be estimated for each soil layer. Such an analysis could be used to develop a probabilistic analysis of liquefaction or soil settlement. This would provide an alternative approach to assessments using deterministic assessments.

3. Soil surface PGA hazard was not developed in this report because of the issues attendant with LLNL and EPRI bedrock PGA hazard. A rough approximation to the soil surface PGA hazard can be made using available ground motion level dependent M-bar soil spectral shapes together with the four soil surface hazard curves.

4. To increase confidence and reduce unnecessary conservatism in the SRS soil surface hazard evaluations at low POEs typically required for PRAs, we suggest the following tasks:

a) Incorporate distance dependence in the SAFs, at least for the very near distances. This task would consider finite fault sources (as opposed to point seismic sources) and account for appropriate incidence angles.

b) For improved PRAs, incorporate non-linear soil response analysis to effectively extend the peak strain range of the SAFs and obtain more reliable (and less overly conservative) hazard at the low POEs. The non-linear analysis may require additional laboratory analysis of SRS soils.

9.0 CONCLUSIONS AND RECOMMENDATIONS

Soil Surface Hazard for the SRS

DOE recommended bedrock PSHAs previously completed for the SRS and vicinity were used to develop SRS-specific mean soil surface hazard for four oscillator frequencies. This hazard is the first SRS-specific study that incorporates a fully integrated set of geologic and geophysical soil measurements. The soil surface hazard methodology, to compute or continue hazard from bedrock to soil surface, is exact, straight-forward and economical. Subtle or significant changes in the soil model can be easily integrated into the approach to test the sensitivity of new data to the soil surface hazard or to make a refinement to the soil surface hazard.

Figures 6.9 and 6.10 show the recommended SRS soil surface hazard for oscillator frequencies of 1, 2.5, 5, and 10 Hz. These values are tabulated in Tables 6.6-6.9. The target annual POEs range from 10^{-2} to 10^{-7}, sufficient for all DOE performance categories

and risk assessments. However, significant assumptions are required to derive soil surface hazard at the lower probabilities. For annual probabilities less than about 10^{-5}, we approach the limit of the state-of-practice for both measuring soil deformation in the laboratory and modeling inelastic wave propagation in the soil. Assumptions were made to limit the soil deformation and consequently provide a conservative result. PRAs should account for SSCs potentially at risk to soil deformation in the form of liquefaction and settlement.

PC1 and PC2 Design Spectra for the SRS

The PC1 and PC2 design spectra (Figure 7.4, Table 7.5) are derived using the new site hazard, DOE-STD-1023 guidelines and building code (NEHRP-97) criteria and account for the wide range in SRS material properties and geometries including soil shear-wave velocities, uncertainty or range in soil column thickness, and type of basement material. This methodology is more exact than that used in Report 1, however, the results of this investigation support the conclusion that the mean-based scaling results of Report 1 provide at least a mean response. The site response analyses described herein are intended to provide design basis guidance for PC1 and PC2 SSCs.

10.0 ACKNOWLEDGEMENTS

Technical discussions with Allin Cornell and Walt Silva improved the approach. Document reviews by Jeff Kimball, Brent Gutierrez, Carl Stepp, and Carl Costantino significantly improved the text.

11.0 REFERENCES

Atkinson, G.M., and D.M. Boore, 1998. Evaluation of Models for Earthquake Source Spectra in Eastern North America, Bull. Seis. Soc. Am., Vol. 88, 917-934.

Bernreuter, D.L., 1997. Letter report from Don Bernreuter to Jeff Kimball. Lawrence Livermore National Laboratory, Fission Energy and Systems Safety Program, May 15, 1997, NTFS97-123.

Boore, D.M., 1983. Stochastic simulation of high-frequency ground motions based on seismological models of the radiated spectra, Bull. Seis. Soc. Am., Vol. 73, 1865-1894.

Coats, D.W., and R.C. Murray, 1984. Natural Phenomena Hazards Modeling Project: Seismic Hazard Models for Department of Energy Sites, Lawrence Livermore National Laboratory, UCRL-53582, Rev. 1.

Cornell, C.A., and P. Bazzurro, 1997. Efficient Probabilistic Hazard Analysis for Non-Linear Soil Sites with Uncertain Properties.

Frankel, A., C. Mueller, T. Barnhard, D. Perkins, E.V. Leyendecker, N. Dickman, S. Hanson, and M. Hopper, 1996. National Seismic Hazard Maps, June 1996: Documentation, U.S. Geological Survey, Denver, CO, 73pp

Hanks, T.C., and R.K. McGuire, 1981. The character of High-Frequency Strong Ground Motion, Bull. Seism. Soc. Am., Vol. 71, 2071-2095.

Herrmann, R.B., 1986. Surface-wave studies of some South Carolina earthquakes, Bull. Seis. Soc. Am., Vol. 76, 111-121.

Kimball, J., 1998. Supplemental Response to Issues 3, 4, and 9. Seismic Action Items for Defense Nuclear Facilities Safety Board, WSRC letter from L.A. Salomone to A.H. Hadjian, PECD-SGS-98-0124, July 6, 1998.

Lee, R.C., 1994. H-Area Seismology Summary and General Discussion, WSRC-TR-94-0529.

Lee, R. C., 1996. Investigations of Nonlinear Dynamic Soil Properties at the Savannah River Site, WSRC-TR-96-0062, Rev. 0, March 1996.

Lee, R.C., M.E. Maryak, and M.D. McHood, 1997. SRS Seismic Response Analysis and Design Basis Guidelines, WSRC-TR-97-0085, Rev. 0.

Lee, R.C., W. Silva, and A. Cornell 1998. Alternatives in Evaluating Soil and Rock-Site Seismic Hazard, Seismological Research Letters, Vol. 69, no. 1, pp 81.

NEHRP (1997), National Earthquake Hazards Reduction Program (NEHRP) Recommended Provisions. For Seismic Regulations For New Buildings And Other Structures, Building Seismic Safety Council, Part 1 Provisions (FEMA 302).

NEI, 1994. Nuclear Energy Institute, Washington, D.C., Seismic Siting Decision Process, May 24, 1994.

Ou, G.B. and R.B. Herrmann, 1990. A statistical model for ground motion produced by earthquakes at local and regional distances, Bull. Seis. Soc. Am., Vol. 80, 1397-1417.

Savy, J.B., 1996. Fission Energy and Systems Safety Program, April 24, 1996, SANT96-147JBS, letter from J.B. Savy, Deputy Associate Program Leader Natural Phenomena Hazards to Jeff Kimball, DOE.

Silva, W., 1989. Site dependent specification of strong ground motion; in Dynamic Soil Property and Site Characterization, Proceedings of the Workshop sponsored by the National Science Foundation and the Electric Power Research Institute, Palo Alto, California.

State of South Carolina, Department of Health and Environmental Control (SCDHEC). Final Regulation, Department of Health and Enviromental Control, Chapter 61, 61-104, Hazardous Waste Management Location Standards, Statutory Authority: 1976 Code Section 44-56-30, -35.

Stokoe, Kenneth H., II, Hwang, Seon-Keun, Darendeli, Mehment, and N. K. James Lee, 1995. *Correlation Study of Nonlinear Dynamic Soil Properties: Savannah River Site, Aiken, South Carolina*, Rev. 0, File No. SRS-FR-CDP-95, University of Texas at Austin, Department of Civil Engineering, September 13, 1995.

Toro, G.R., 1996. Probabilistic Models of Site Velocity Profiles at the Savannah River Site, Aiken, South Carolina, Final Report to WSRC, April 4, 1997.

UBC-Uniform Building Code, 1994.

UBC-Uniform Building Code, 1997.

URS/John A. Blume and Associates, Engineers, 1982. "Update of Seismic Criteria for the Savannah River Plant, Vol. 1 of 2", Geotechnical: URS/JAB 8144, San Francisco, CA, prepared for E.I. du Pont de Nemours and Company, DPE 3699, 293 pp.

U. S. Department of Energy, 1994. *DOE Standard: Natural Phenomena Hazards Design and Evaluation Criteria for Department of Energy Facilities*, DOE-STD-1020-94, Washington, D. C. April 1994.

U. S. Department of Energy, 1995. *DOE Standard: Natural Phenomena Hazards Assessment Criteria,* DOE-STD-1023-95, Change Notice #1, Washington, D. C. January 1996.

Wingo, H.E., 1994. Development of Probabilistic Seismic Hazard Curve for DWPF at SRS, Rev. 1 (U), WSRC-TR-93-317.

WSRC, 1996. Conduct of Engineering and Technical Support Engineering Manual, E7.

WSRC, 1998. Calculation of Soil Surface Hazard at the SRS, WSRC Calculation #K-CLC-G-00062.

12.0 TABLES

Table 2.1. Target Soil Surface Hazard Annual Probabilities of Exceedance (APE) for Seismic Design and Risk Assessment of SRS Facilities.

APE (yr-1)	Safety Category
2×10^{-3}	PC1 & UBC (10% in 50 yrs)
1×10^{-3}	PC2
5×10^{-4}	PC3
4×10^{-4}	UBC (2% in 50 yrs); SCDHEC (10% in 250 yrs)
1×10^{-4}	PC4
1×10^{-7}	Required for PRA

Table 5.1. PGA-Controlling Earthquake Median Magnitude-Distance Pairs with 5% and 95% Confidence Range Determined from Disaggregation of EPRI Bedrock Hazard Curve (Report 1).

	Magnitudes (Mw)			Distance (km)		
PGA(g)	5%	M-bar	95%	5%	D-bar	95%
0.05	4.8	5.7	6.8	36	42	79
0.10	4.8	5.7	6.8	17	36	43
0.20	5.0	5.9	7.2	8	21	36
0.25	5.0	5.9	7.2	4	17	32
0.30	5.0	6.0	7.2	9	19	58
0.40	5.0	6.0	7.2	6	15	43
0.50	5.5	6.2	7.8	7	13	54
0.75	5.5	6.2	7.8	5	9	24

Table 6.1. Bedrock Motions (Sv in cm/sec) for Indicated Ground Motion Frequencies Based on EPRI (NEI, 1994) Hazard Curves.

f (Hz)			
1.0	2.5	5.0	10.0
1.0	1.0	1.0	1.0
5.0	2.0	2.0	2.0
9.31	6.0	5.5	5.5
10.0	8.67	8.13	5.85
20.0	16.0	10.5	8.42
30.0	26.0	15.0	10.5
50.0	40.0	20.5	18.5
90.0	90.0	30.0	30.0

Table 6.2. Bedrock Motions (Sv in cm/sec) for Indicated Ground Motion Frequencies Based on LLNL (Savy, 1996) Hazard Curves.

f (Hz)			
1.0	2.5	5.0	10.0
0.874	1.11	0.556	0.493
1.56	1.97	0.987	0.877
2.78	3.51	1.75	1.56
4.93	6.25	3.12	2.78
8.77	11.1	5.56	4.93
15.6	19.7	9.87	8.77
27.8	35.1	17.5	15.6
49.3	62.5	48.8	27.8
87.7	111.	104.	

Table 6.3. Recommended Minimum Ranges on Soil Surface Hazard Probability (Maximum Ranges of Ground Motion) based on: (1) Interpolated Bedrock Minimum POE Ranges Where LLNL and EPRI Bedrock Hazard Not Extrapolated; and (2) Where Range of SAF Control Motions not Exceeded.

	Interpolated Bedrock Hazard		Max. control mtn./Min SAF	
f (Hz)	POE (yr-1)	GM (cm/sec)	POE (yr-1)	GM (cm/sec)
1	2×10^{-5}	80	6×10^{-6}	200
2.5	6×10^{-6}	100	2×10^{-5}	70
5	2×10^{-5}	30	2×10^{-6}	30
10	1×10^{-7}	30	5×10^{-7}	20

Table 6.4. Recommended Maximum Range of Soil Surface Hazard (Minimum Range of Ground Motion) Based on Maximum POE Range Where LLNL and EPRI Bedrock Hazard Curves are Not Extrapolated.

	Interpolated Bedrock Hazard	
f (Hz)	POE (yr-1)	GM (cm/sec)
1	3×10^{-3}	3
2.5	2×10^{-3}	4
5	2×10^{-3}	3
10	2×10^{-3}	2

Table 6.5. High-Confidence Range of Mean Soil Surface Hazard and Corresponding Range of Ground Motion. High Confidence Range is Based on Soil Surface Hazard That is Not Dependent on Extrapolated Ranges of Bedrock Hazard Curves or Site Amplification.

f (Hz)	POE (yr^{-1})	GM (cm/sec)
1	$3 \times 10^{-3} - 2 \times 10^{-5}$	3-80
2.5	$2 \times 10^{-3} - 2 \times 10^{-5}$	4-70
5	$2 \times 10^{-3} - 2 \times 10^{-5}$	3-30
10	$2 \times 10^{-3} - 5 \times 10^{-7}$	2-20

Table 6.6. SRS 1 Hz Mean Soil Surface Hazard. Values that are Derived from Extrapolation of Bedrock Hazard or that Apply the Extreme Range of SAFs are in Parenthesis.

Sv (cm/sec)	Sa (g's)	APE
(1.87)	(0.0120)	1.00E-02
(3.35)	(0.0215)	5.60E-03
5.53	0.0354	3.20E-03
8.33	0.0534	2.00E-03
14.63	0.0937	1.00E-03
24.14	0.1546	5.00E-04
28.15	0.1803	4.00E-04
42.48	0.2721	2.00E-04
60.17	0.3854	1.00E-04
73.71	0.4721	5.60E-05
89.63	0.5741	3.20E-05
110.09	0.7051	1.80E-05
(136.72)	(0.8757)	9.99E-06
(169.17)	(1.0835)	5.60E-06
(208.94)	(1.3382)	3.20E-06
(259.84)	(1.6642)	1.80E-06
(324.31)	(2.0772)	1.00E-06
(398.9)	(2.5549)	5.60E-07
(487.08)	(3.1197)	3.20E-07
(594.21)	(3.8058)	1.80E-07
(716.33)	(4.5880)	9.99E-08

Table 6.8 - SRS 5 Hz Mean Soil Surface Hazard. Values that are Derived from Extrapolation of Bedrock Hazard or that Apply the Extreme Range of SAFs are in Parenthesis.

Sv (cm/sec)	Sa (g's)	APE
(1.25)	(0.0400)	1.00E-02
(2.21)	(0.0708)	5.60E-03
(3.53)	(0.1130)	3.20E-03
5.03	0.1611	2.00E-03
7.49	0.2399	9.99E-04
10.49	0.3359	5.00E-04
11.29	0.3616	4.00E-04
14.18	0.4541	2.00E-04
17.8	0.5700	1.00E-04
20.19	0.6466	5.60E-05
22.81	0.7305	3.20E-05
25.85	0.8278	1.80E-05
(29.37)	(0.9406)	1.00E-05
(33.73)	(1.0802)	5.61E-06
(39.24)	(1.2566)	3.20E-06
(45.85)	(1.4683)	1.80E-06
(53.77)	(1.7219)	9.99E-07
(64.06)	(2.0515)	5.60E-07
(76.38)	(2.4460)	3.20E-07
(91.51)	(2.9305)	1.80E-07
(109.02)	(3.4913)	1.00E-07

Table 6.9. SRS 10 Hz Mean Soil Surface Hazard. Values that are Derived from Extrapolation of Bedrock Hazard or that Apply the Extreme Range of SAFs are in Parenthesis.

Sv (cm/sec)	Sa (g's)	APE
(0.62)	(0.0397)	1.00E-02
(0.97)	(0.0621)	5.60E-03
(1.42)	(0.0909)	3.20E-03
1.92	0.1230	2.00E-03
2.9	0.1857	1.00E-03
3.87	0.2479	5.00E-04
4.2	0.2690	4.00E-04
5.44	0.3484	2.00E-04
6.39	0.4093	1.00E-04
7.22	0.4624	5.60E-05
8.14	0.5214	3.20E-05
9.2	0.5892	1.80E-05
10.35	0.6629	1.00E-05
11.49	0.7359	5.60E-06
12.73	0.8153	3.20E-06
14.18	0.9082	1.80E-06
15.87	1.0165	1.00E-06
17.78	1.1388	5.60E-07
(20.73)	(1.3277)	3.20E-07
(24.31)	(1.5570)	1.80E-07
(28.6)	(1.8318)	1.00E-07

Table 6.10. Approximate Polynomial Coefficients* for Combined EPRI and LLNL Soil Surface Hazard Envelope (Coefficients are Only Approximate and Should Not Be Used In Lieu of Tabulated Values).

f (Hz)	c1	c2	c3	c4	c5	c6	ERR (%)
1	-5.1213	-2.7627	-0.3714	0.4166	0.1287	-0.0152	15
2.5	-4.7461	-2.9311	0.1006	0.6659	-0.5504	-0.4149	11
5	-5.0527	-4.1374	-0.1382	2.1955	0.5486	-0.273	17
10	-5.949	-5.1818	2.0818	9.3078	7.2228	1.7829	12

*Coefficients are to be used for the following polynomial:

$$\log_{10}(APE)=c1+c2*x+c3*x^2+c4*x^3+c5*x^4+c6*x^5$$

Where APE is the Annual Probability of Exceedance and x is the $\log_{10}$ of spectral acceleration in g's. ERR is the maximum error (in percent) in the Annual Probability of Exceedance (using the polynomial) as compared to tabulated values.

Table 7.1. Coefficients and factors used for Implementation of 1997 Edition of the NEHRP Recommended Provisions.

S_s (short period spectral acceleration) = 0.49g
S_1 (1 second period spectral acceleration) = 0.17g
(Map values represent NEHRP soft rock category (Vs<5,000 ft/sec)

For site class D:
$S_{MS} = Fa*S_s = 1.4*0.49g = 0.69g$
$S_{M1} = Fv*S_1 = 2.1*0.17g = 0.34g$

Design response acceleration paramters are taken as 2/3 the MCE Ground Motion Values:
$S_{DS} = 2/3\ S_{MS} = 0.46g$
$S_{D1} = 2/3\ S_{M1} = 0.24g$

Response spectra corners:
Long corner period: $T_S = S_{D1}/S_{DS} = 0.52$
Short corner period: $T_o = 0.2*(S_{D1}/S_{DS}) = 0.10g$

Response Spectra Computed as Follows:

for T > TS: Sa = SD1/T; @ T =1, Sa = SD1
for T < Ts but > To: Sa = SDS
for $T \leq$ To: $Sa = 0.4*S_{DS} + (0.60*S_{DS}*T)/T_o$

Across the band 20% reduction to correct site-specific assessments
Sa = 0.8*Sa

Table 7.2. Ratio of Hard-Rock to Soft-Rock Used For USGS Hazard Maps (Frankel et al., 1996).

Attenuation Model	Peak Acceleration	5 Hz Sa	1 Hz Sa
Toro	0.66	0.57	0.75
USGS	0.42	0.45	0.67
Average	0.54	0.51	0.71

Table 7.3. Comparison of SRS Hard-Rock Hazard (Using Combined Bedrock EPRI/LLNL) To USGS Hard-Rock Hazard.

Annual Probability	Peak Acceleration*		5 Hz Sa		1 Hz Sa	
	SRS	USGS	SRS	USGS	SRS	USGS
5x10-4	0.10g	0.11g	0.17g	0.21g	0.05g	0.10g
1x10-4	0.27g	0.24g	0.38g	0.45g	0.14g	0.23g

* Taken from the high-frequency end of controlling bedrock design basis spectrum.

Table 7.4. Comparison of Amplification Factors (Relative to Hard-Rock) Between USGS/NEHRP and SRS.

Ground Motion	Peak Acceleration		5 Hz Sa		1 Hz Sa	
Site Conditions	USGS	SRS	USGS	SRS	USGS	SRS
Hard Rock	1.0	1.0	1.0	1.0	1.0	1.0
soft rock	1.85	-	1.96	-	1.41	-
top of soil	2.1	1.6	2.74	1.24	2.96	5.3

Table 7.5. Recommended PC-2 and PC-1 Design Spectral Accelerations (5% damped).

Frequency (Hz)	PC-2 (g's)	PC-1 (g's)
0.1	0.00420	0.00280
0.2	0.0205	0.0136
0.3	0.0355	0.0237
0.4	0.0733	0.0488
0.5	0.128	0.0852
0.6	0.164	0.110
0.7	0.191	0.127
0.8	0.214	0.143
0.9	0.234	0.156
1	0.253	0.168
1.2	0.284	0.189
1.6	0.334	0.222
2	0.339	0.226
3	0.349	0.233
4	0.356	0.237
5	0.362	0.241
6	0.366	0.244
6.5	0.368	0.245
7	0.361	0.241
8	0.348	0.232
9	0.337	0.225
10	0.327	0.218
14	0.294	0.196
20	0.237	0.158
33	0.157	0.105
100	0.157	0.105

13.0 FIGURES

Figure 2.1 Flowchart Showing Steps In a Soil Surface Hazard Evaluation

1. Compute bedrock hazard disaggregation probability of exceedence (POE) for a suite of bedrock ground motions (x^r_i) corresponding target design annual frequencies (F_i) and one or more structural oscillator frequencies (ν_k) (for this example use mean LLNL bedrock outcrop hazard spectra for 5 Hz Sa)

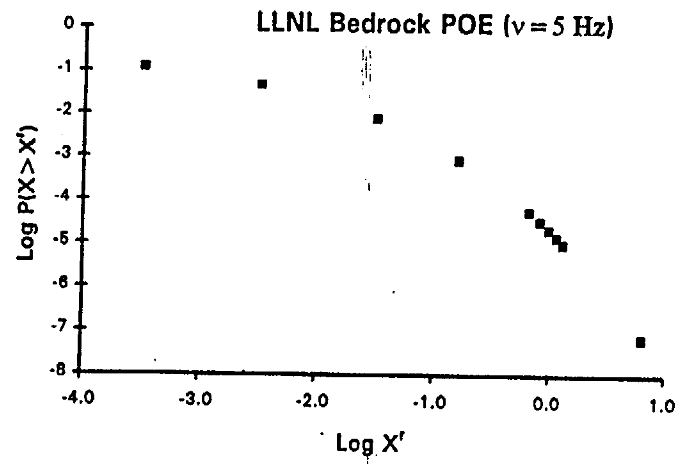

2. Fit polynomials to disaggregated bedrock hazard for each structural frequency

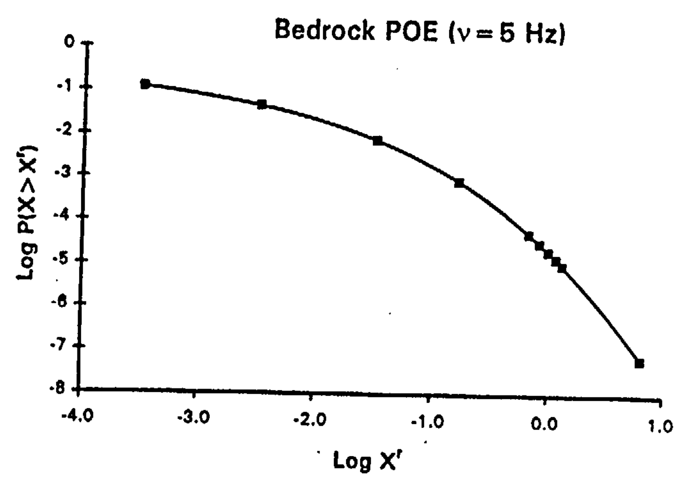

Figure 2.1 - Flow chart and diagrams describing design basis spectra approach.

Figure 2.1 Cont.

3. Compute SAFs (SAFs are dependent on disaggregated magnitude and ground motion level. For this application, SAFs taken from report 1 for each depth range and bedrock type (M-bar shown for illustration)

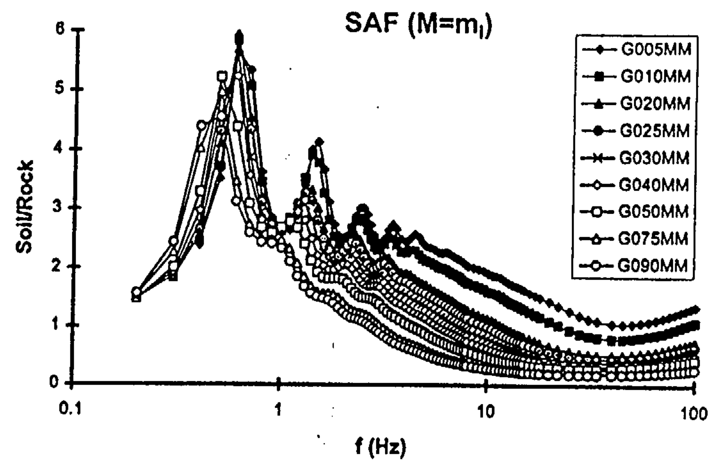

4. Select suite of desired soil surface ground motion values (x') for each structural frequency ν_k (for this example we compute probability of exceeding 10 cm/sec for 5 Hz oscillator).

5. Compute probability of occurrence by differencing the probability of exceedance obtained in steps 1 and 2.

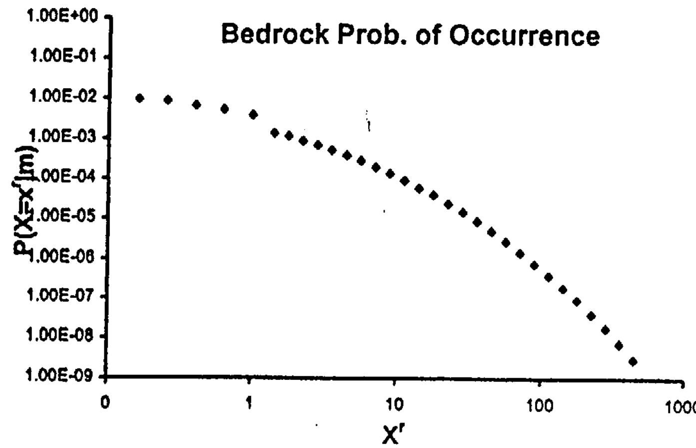

Figure 2.1 - Flow chart and diagrams describing design basis spectra approach.

Figure 2.1 Cont.

6. For each soil-surface ground motion x^s (say x_i^s) compute the complementary cumulative distribution function (CCDF)

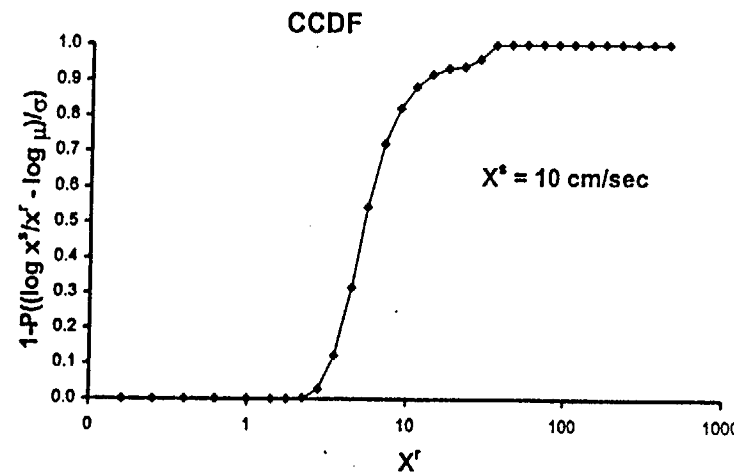

7. For each soil surface ground motion x^s (say x_i^s), compute product of the CCDF and the probability of occurrence

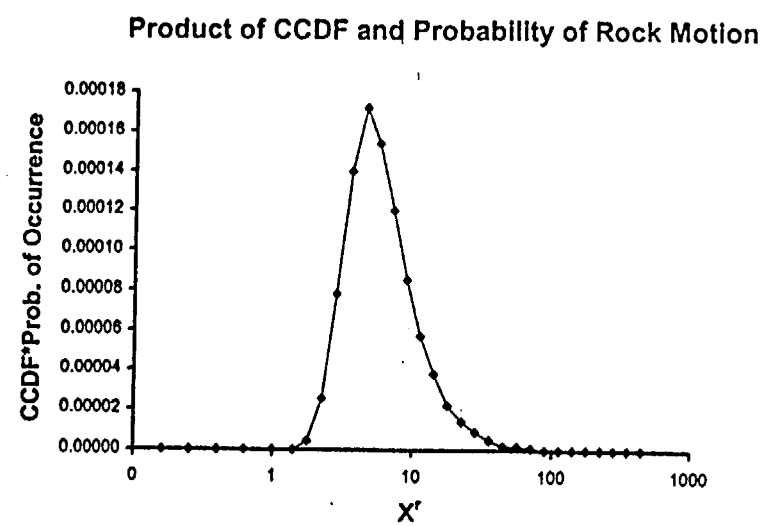

Figure 2.1 - Flow chart and diagrams describing design basis spectra approach.

Figure 2.1 Cont.

8. For each soil surface ground motion x^s (say x_i^s), compute soil surface hazard exceedence ($Gz(x_s)$) as the sum of the products of CCDF*prob. of occurrence

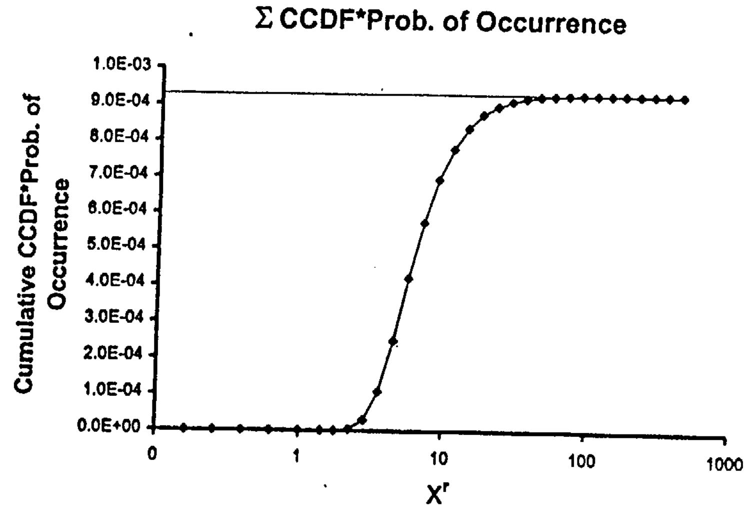

9. Repeat process for suite of soil surface hazard exceedences Gz and oscillator frequencies, ν_k

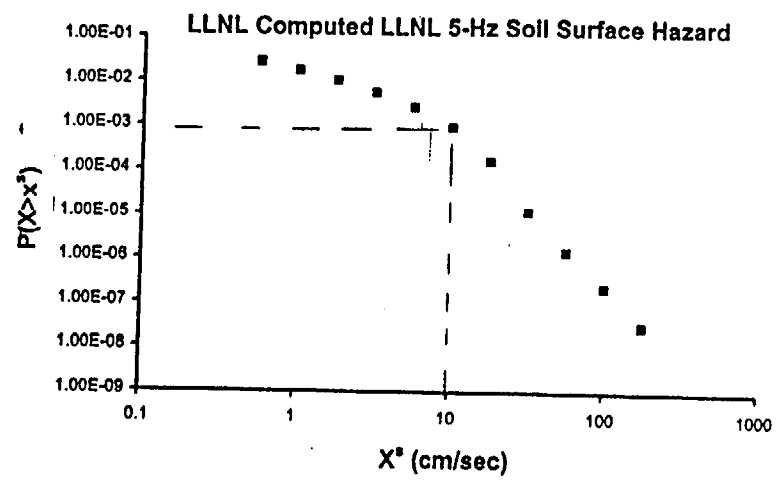

Figure 2.1 - Flow chart and diagrams describing design basis spectra approach.

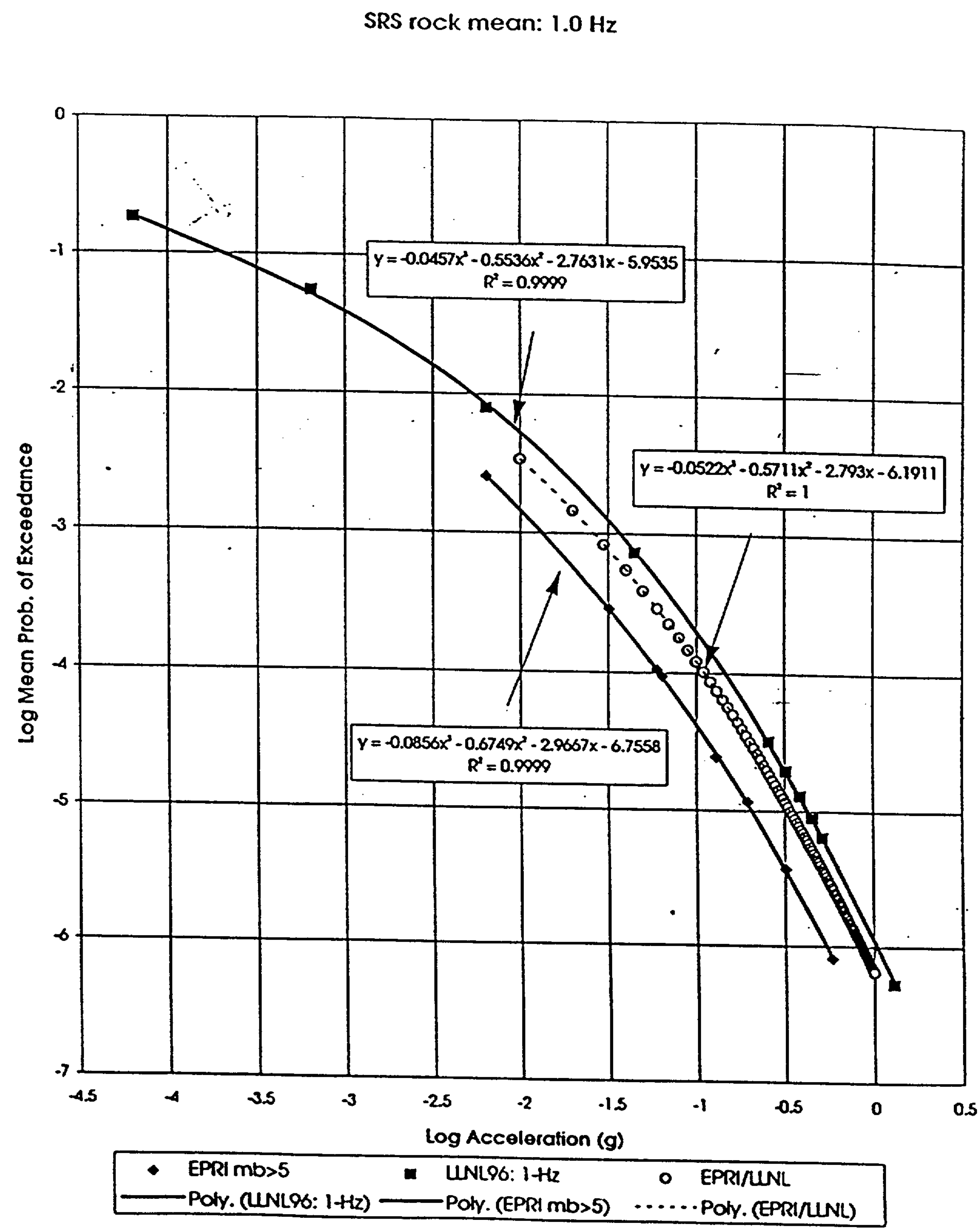

Figure 4.1 - EPRI and LLNL bedrock hazard curves for the SRS (solid symbols) for 1-Hz oscillator frequency. Solid lines illustrate cubic polynomial fits to the hazard values. Dashed line illustrates cubic polynomial fit to the combined EPRI and LLNL bedrock hazard curves.

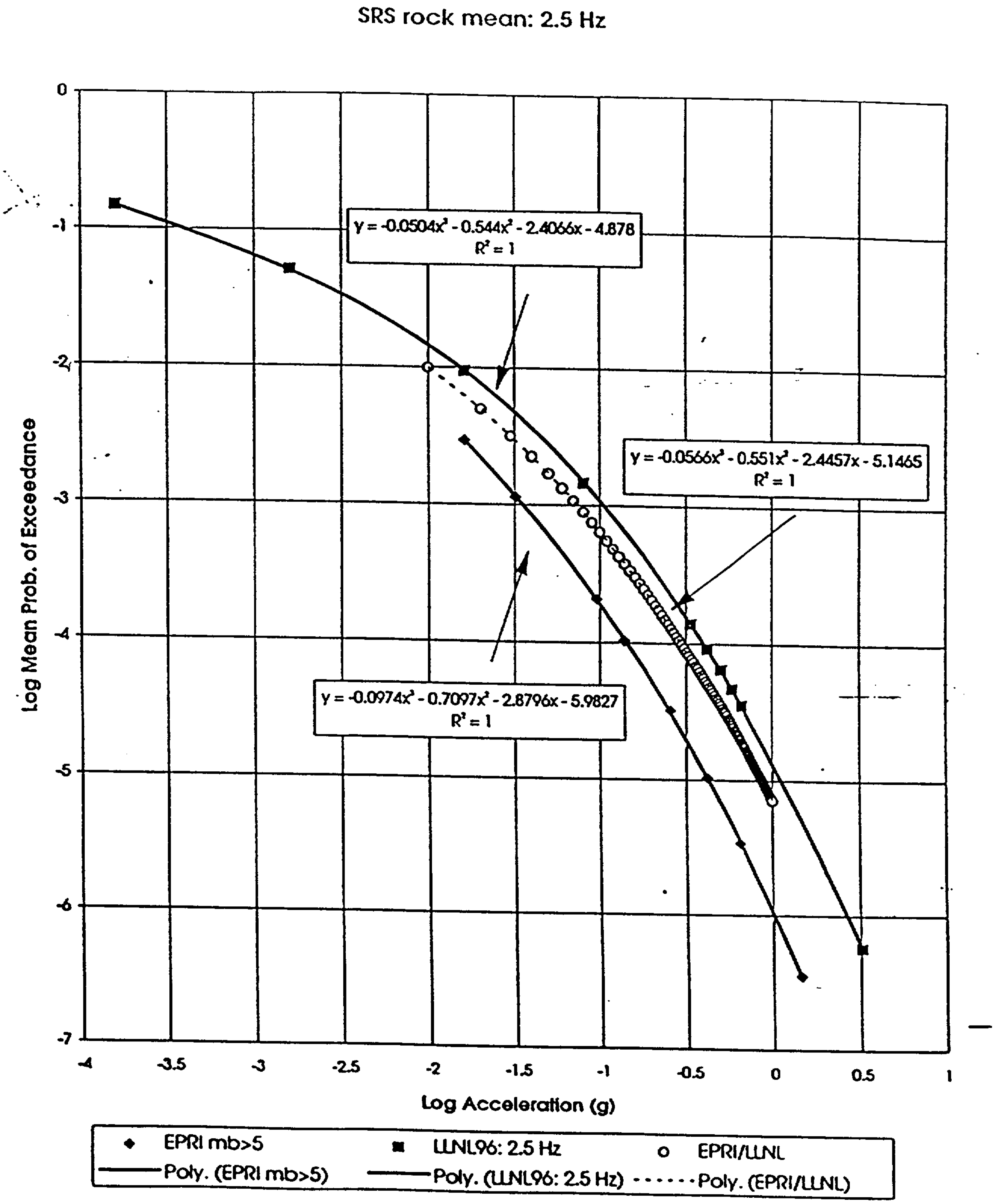

Figure 4.2 - EPRI and LLNL bedrock hazard curves for the SRS (solid symbols) for 2.5-Hz oscillator frequency. Solid lines illustrate cubic polynomial fits to the hazard values. Dashed line illustrates cubic polynomial fit to the combined EPRI and LLNL bedrock hazard curves.

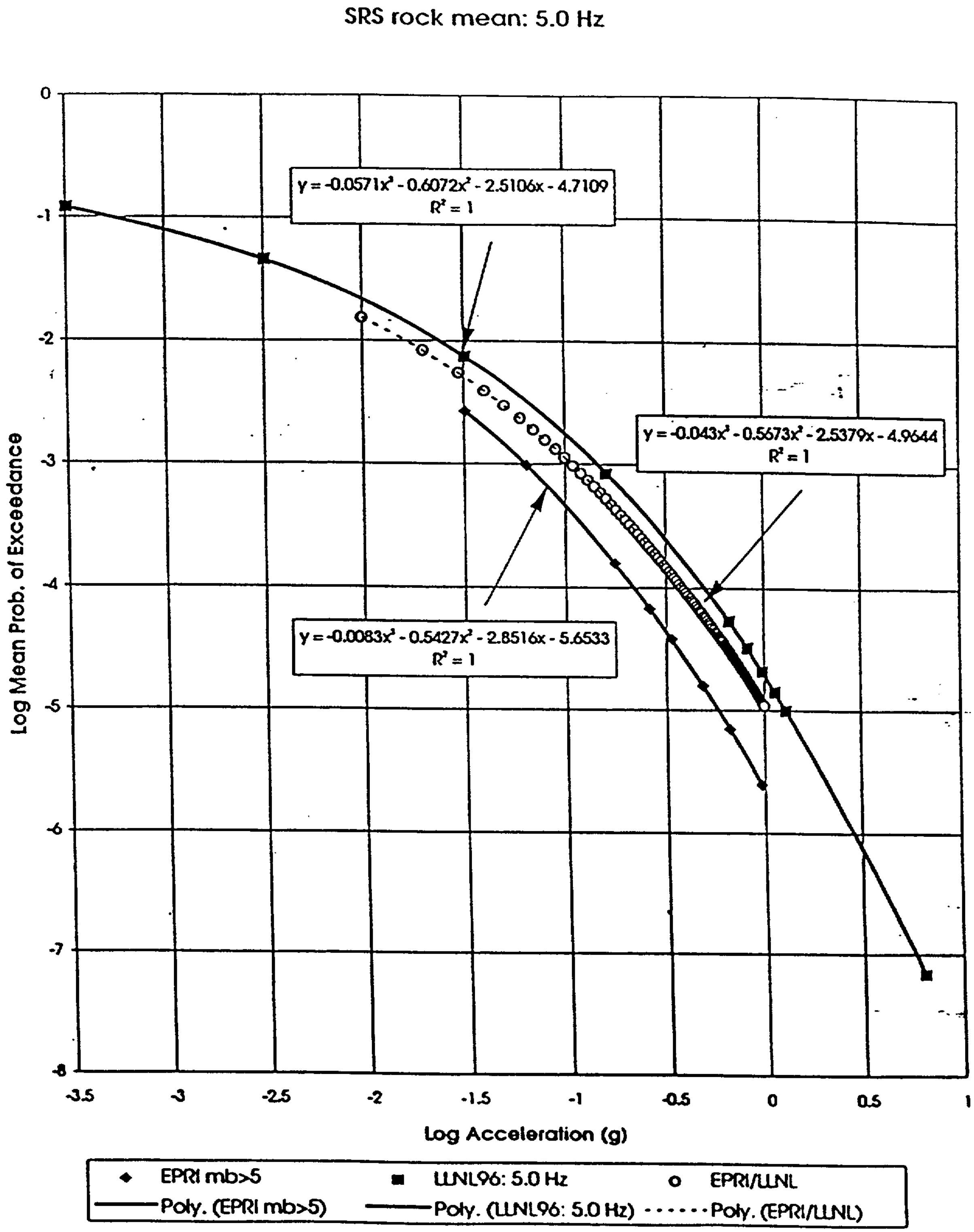

Figure 4.3 - EPRI and LLNL bedrock hazard curves for the SRS (solid symbols) for 5-Hz oscillator frequency. Solid lines illustrate cubic polynomial fits to the hazard values. Dashed line illustrates cubic polynomial fit to the combined EPRI and LLNL bedrock hazard curves.

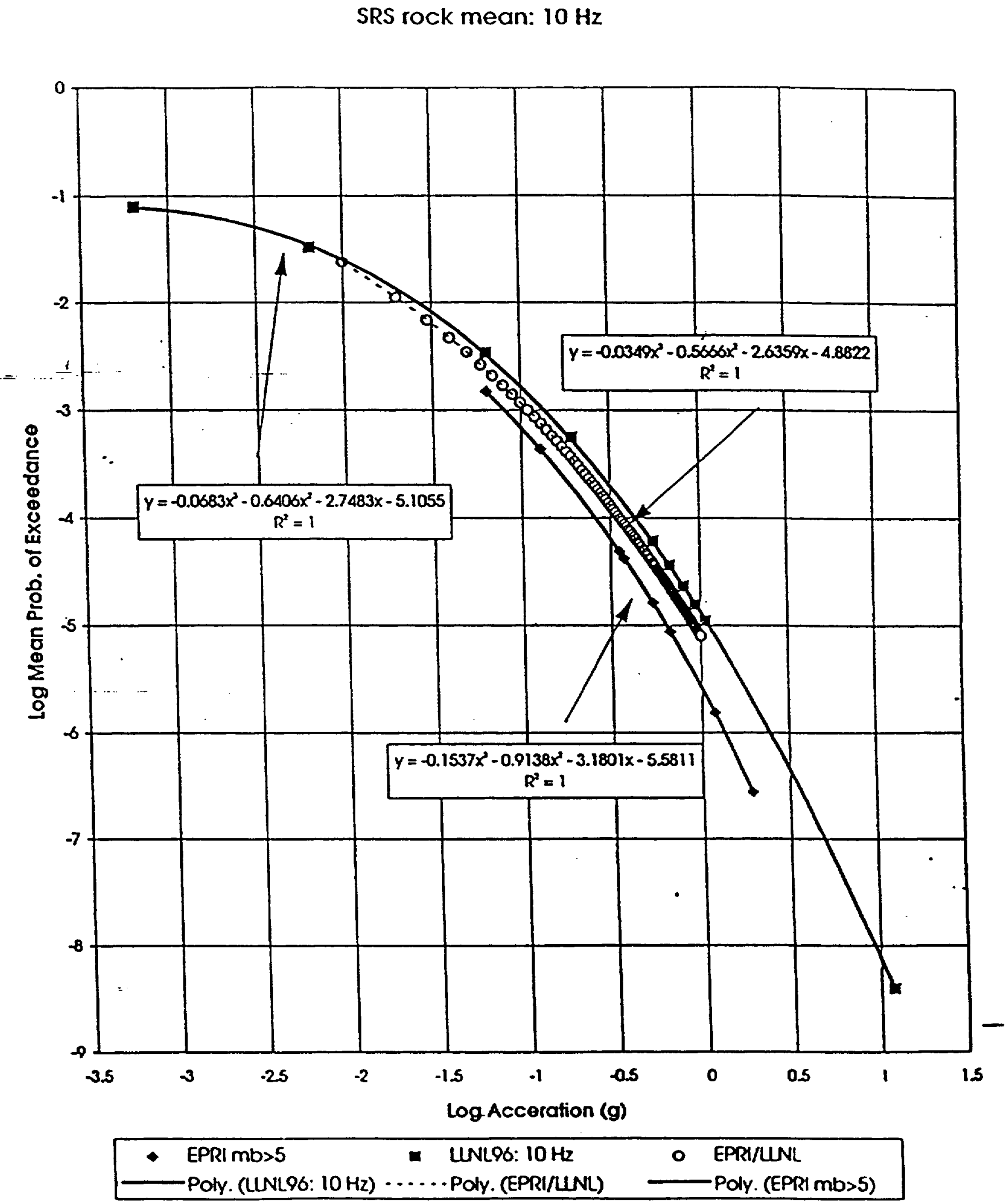

Figure 4.4 - EPRI and LLNL bedrock hazard curves for the SRS (solid symbols) for 10-Hz oscillator frequency. Solid lines illustrate cubic polynomial fits to the hazard values. Dashed line illustrates cubic polynomial fit to the combined EPRI and LLNL bedrock hazard curves.

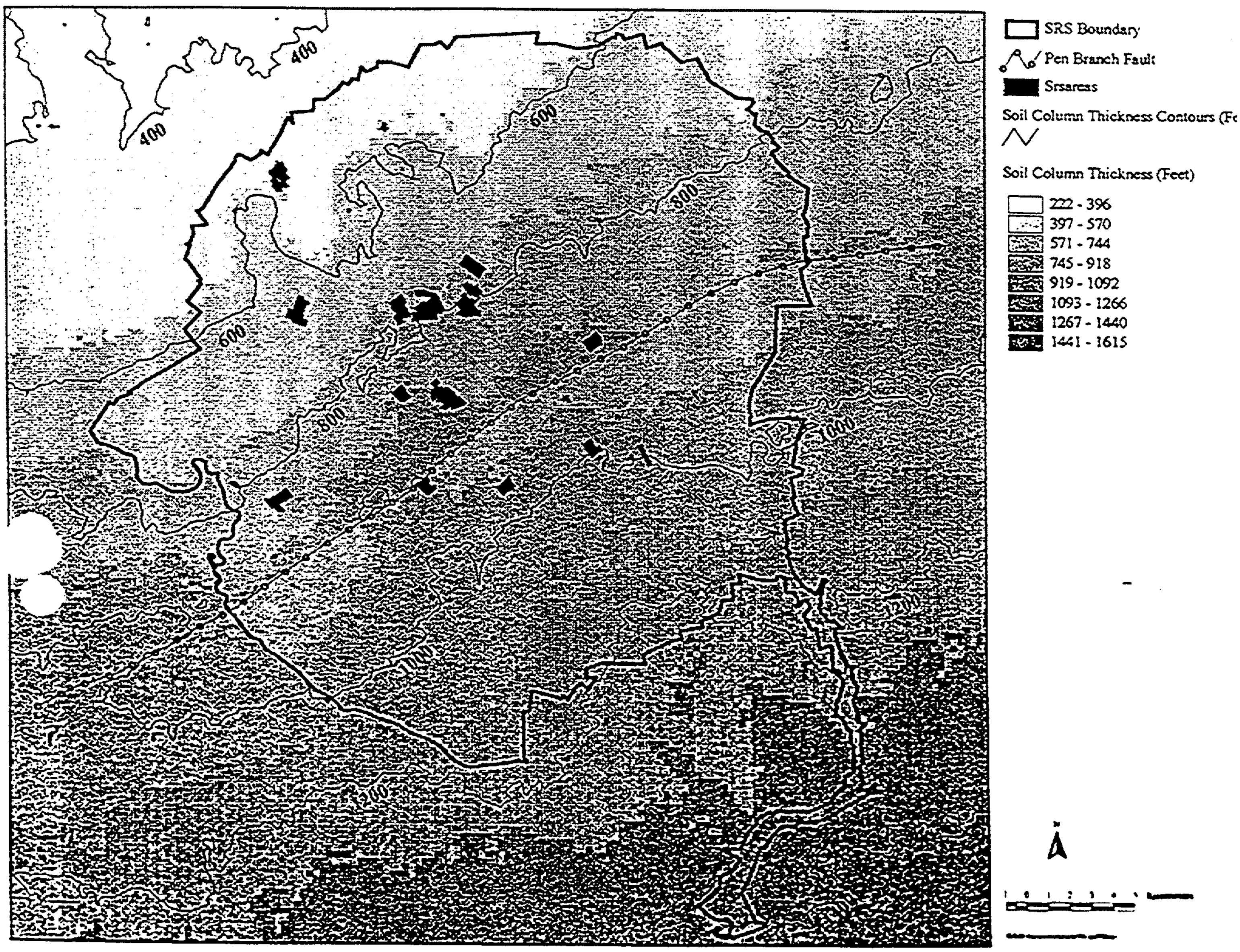

Figure 5.1 - Contours of soil column thickness within the SRS.

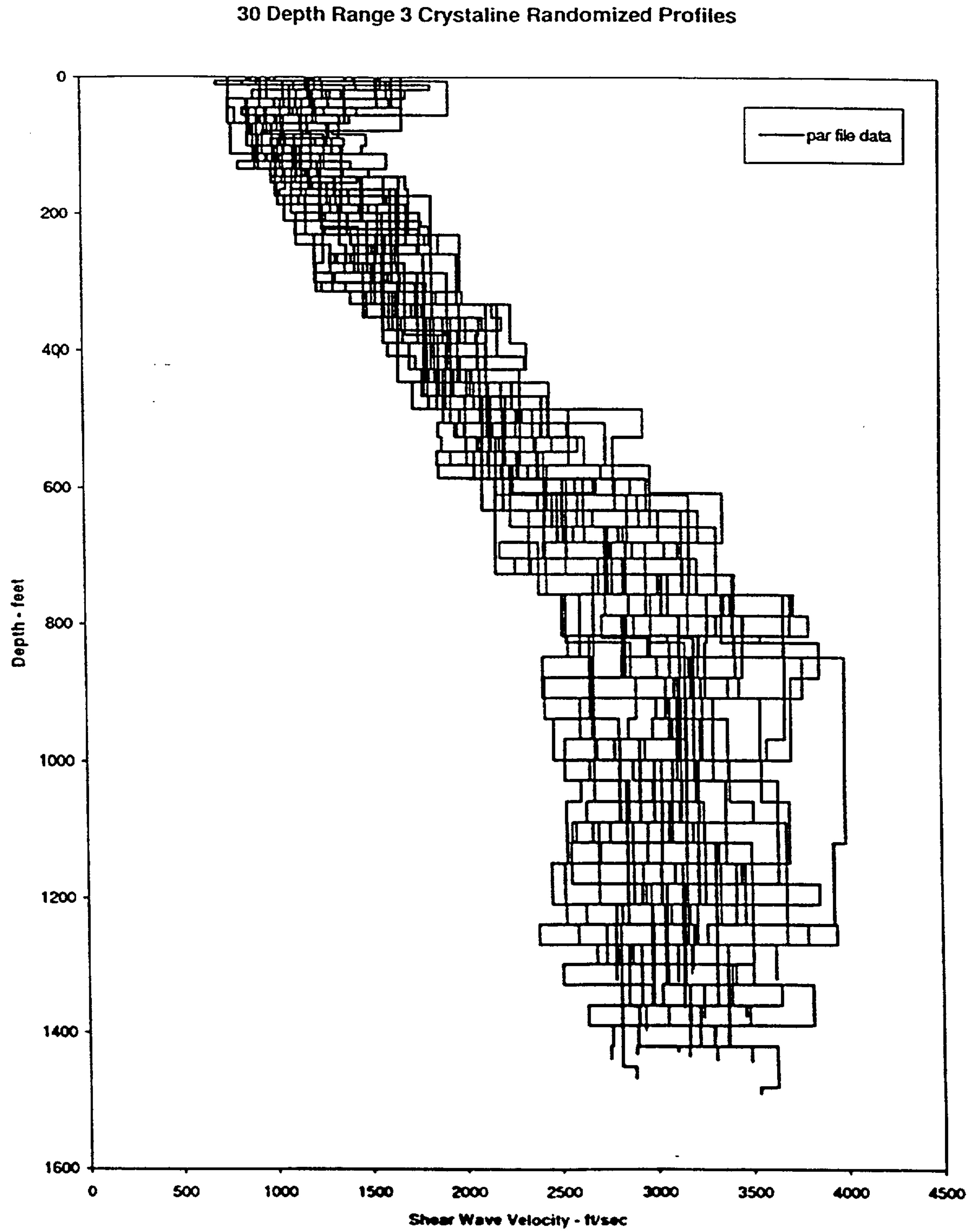

Figure 5.2 (a) - Simulated shear-wave velocity profiles using the SRS generic model and a non-homogeneous Poisson model for layer thickness (Figure taken from Toro (1996)).

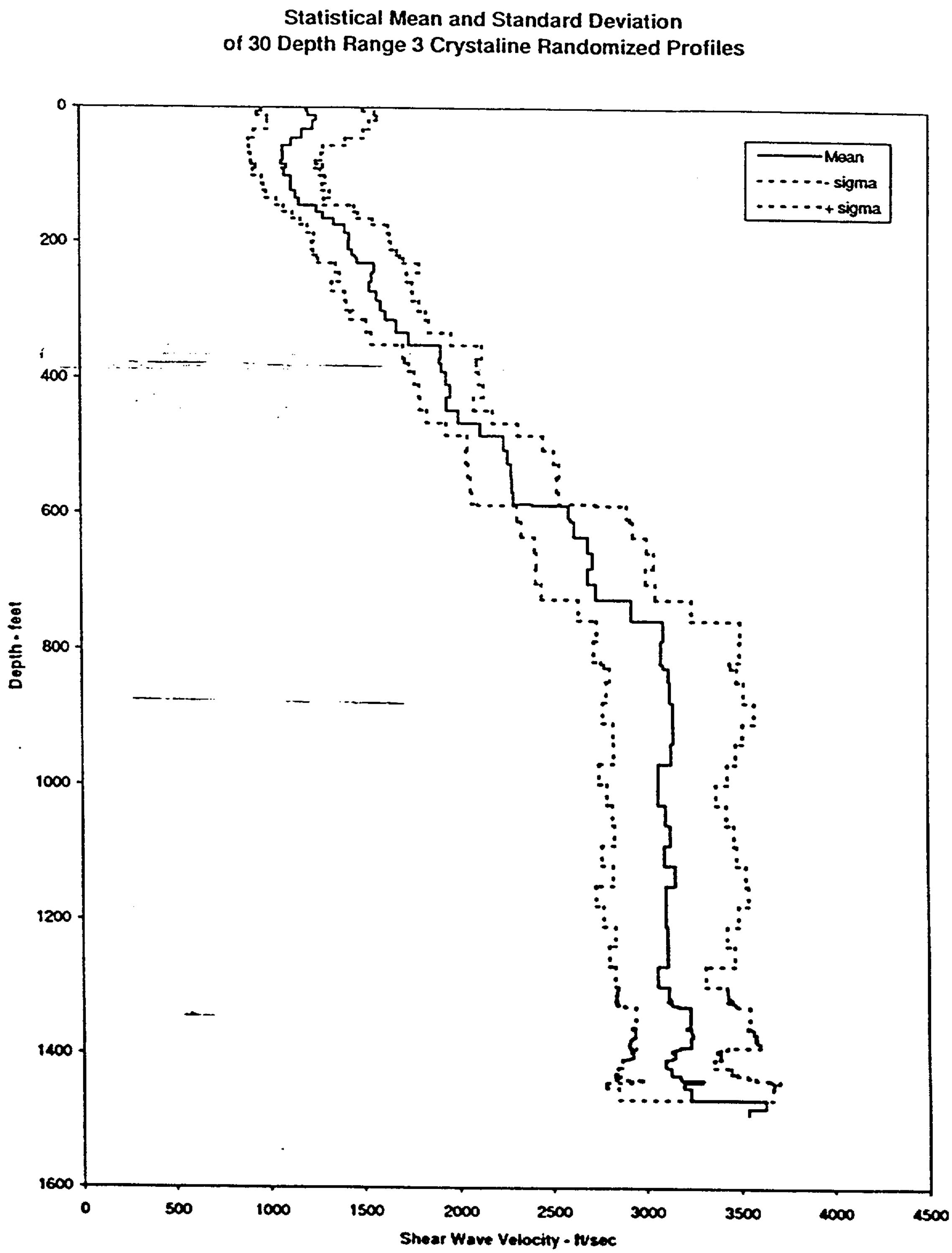

Figure 5.2 (b) - Median shear-wave profile from 30 profiles simulated using the SRS generic velocity model (Figure taken from Toro (1996)).

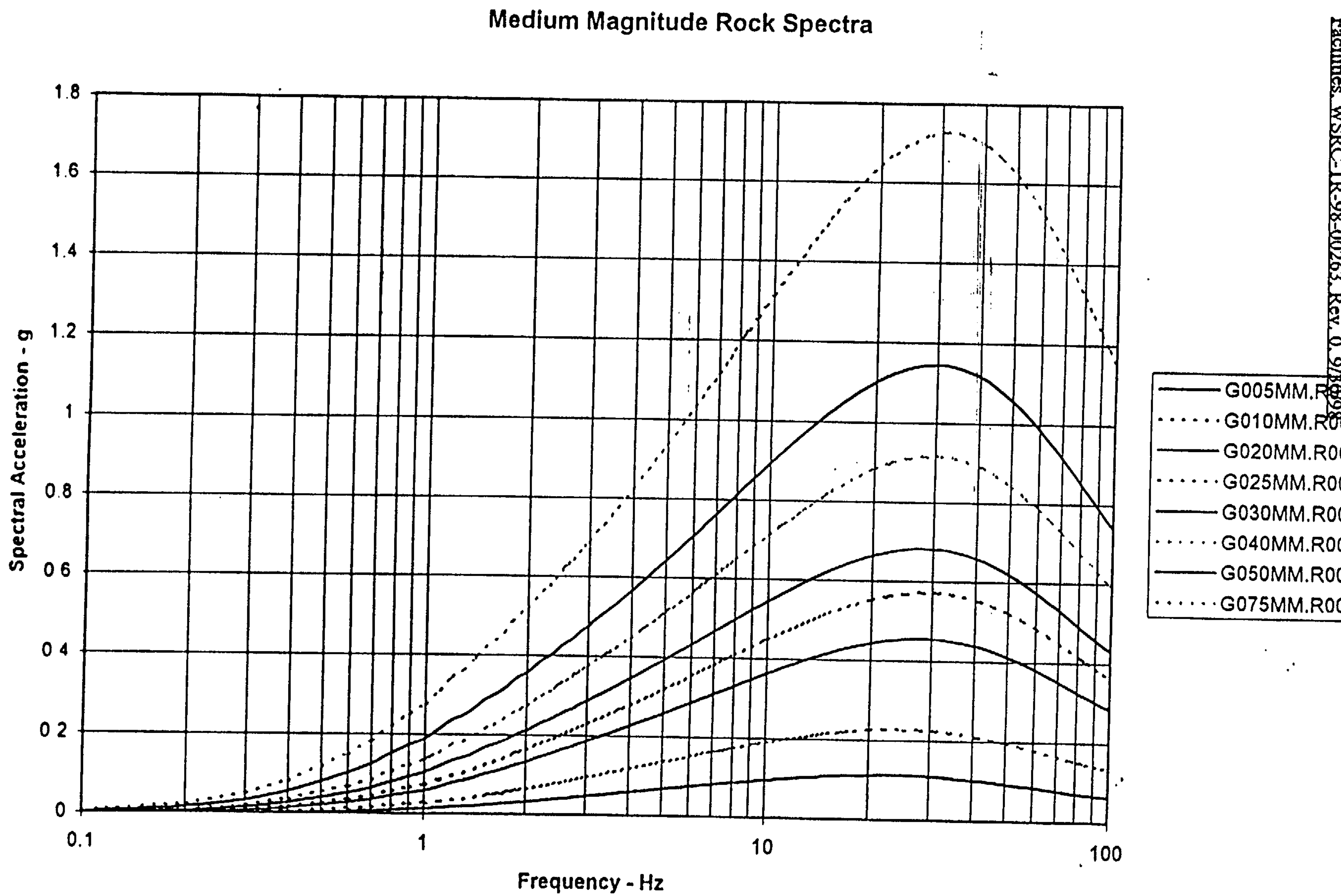

Figure 5.3 (a) - 5 % damped response spectra for disaggregated mean-magnitude (M-bar) crystalline bedrock control motions used to generate soil response for soil category 2. Bedrock peak ground acceleration (PGA) ranges from 0.05g (G005MM.R00) to 0.75g (G075MM.R00).

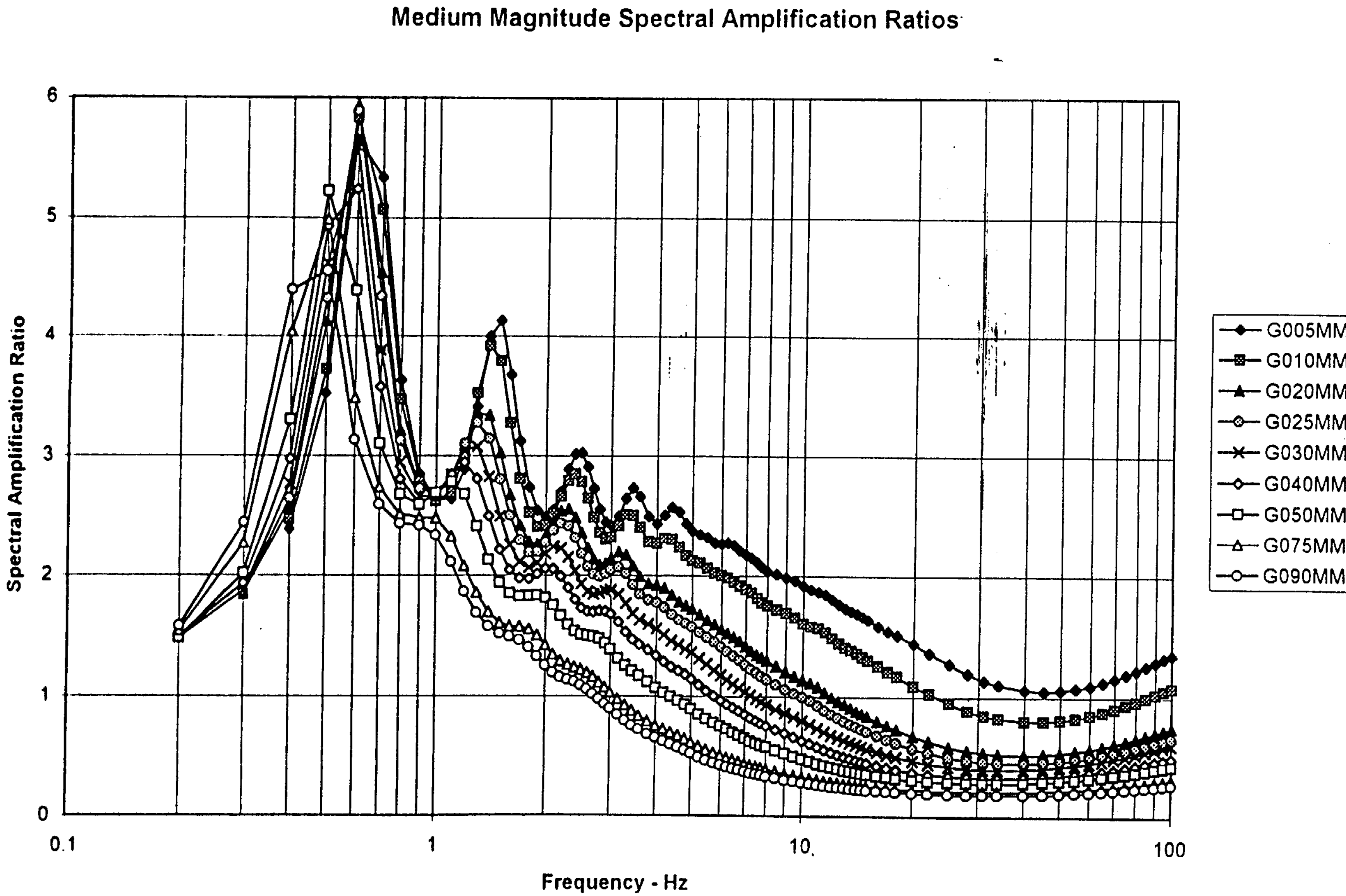

Figure 5.3 (b) - Mean 5 % damped response spectral amplification functions for disaggregated mean-magnitude (M-bar) soil category 2 on crystalline rock. Corresponding bedrock peak ground acceleration (PGA) ranging from 0.05g (G005MM) to 0.75g (G075MM).

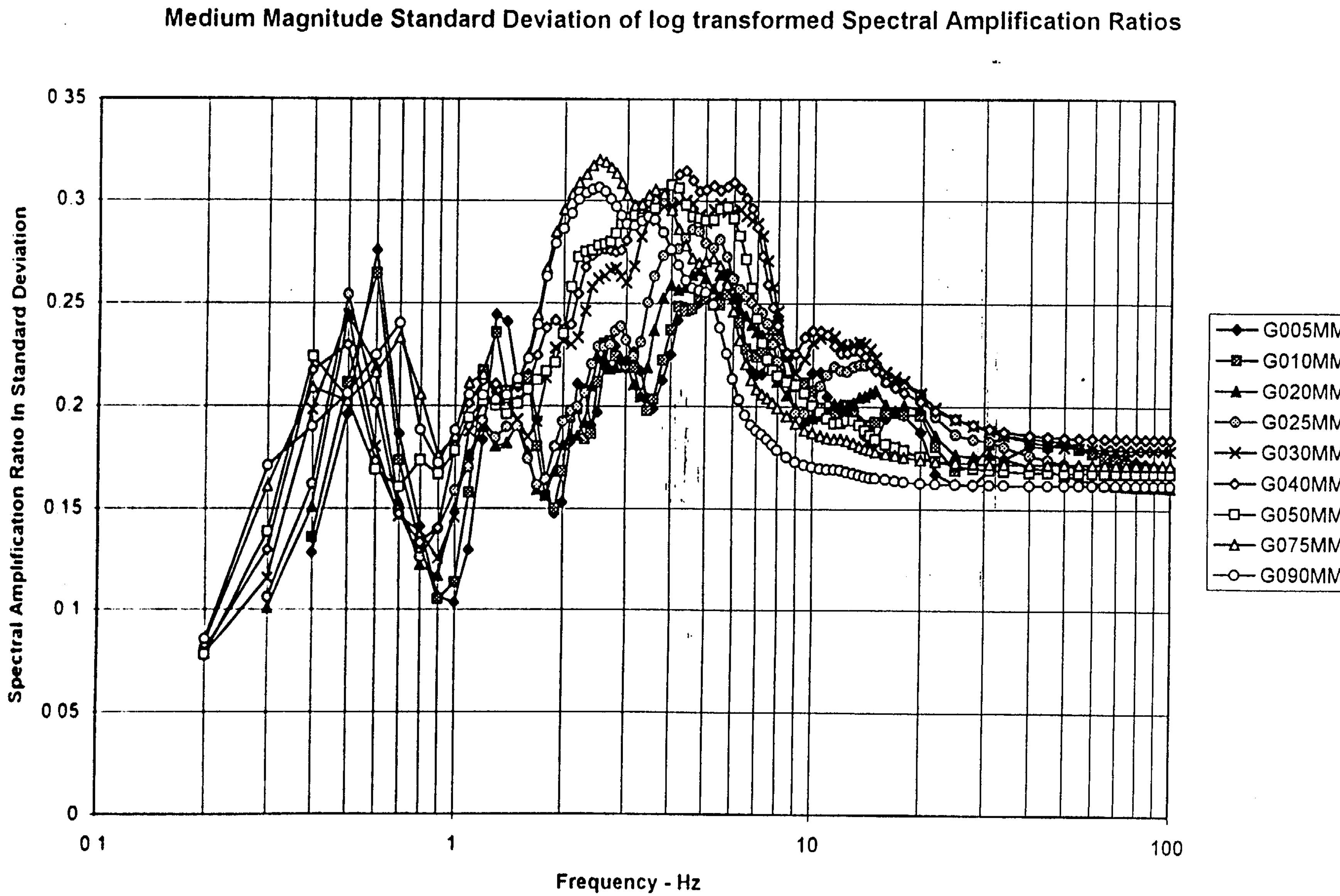

Figure 5.3 (c) - Logarithmic standard deviation of 5 % damped amplification function for disaggregated mean-magnitude (M-bar) soil category 2 on crystalline rock. Corresponding bedrock peak ground acceleration (PGA) ranging from 0.05g (G005MM) to 0.75g (G075MM).

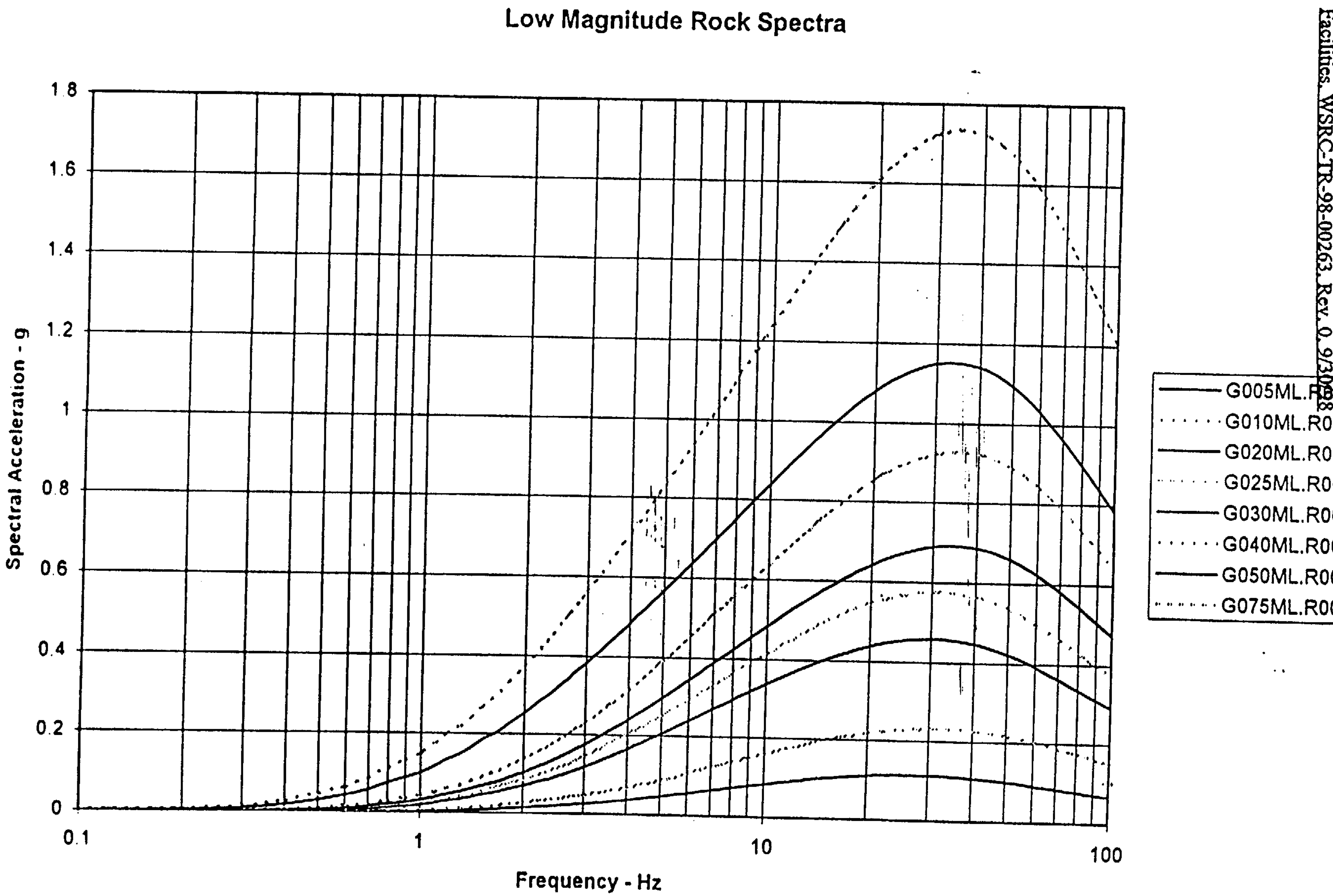

Figure 5.4 (a) - 5 % damped response spectra of disaggregated low-magnitude (ML) crystalline bedrock control motions used to generate soil response for soil category 2. Bedrock peak ground acceleration (PGA) ranges from 0.05g (G005ML.R00) to 0.75g (G075ML.R00).

Low Magnitude Spectral Amplification Ratios

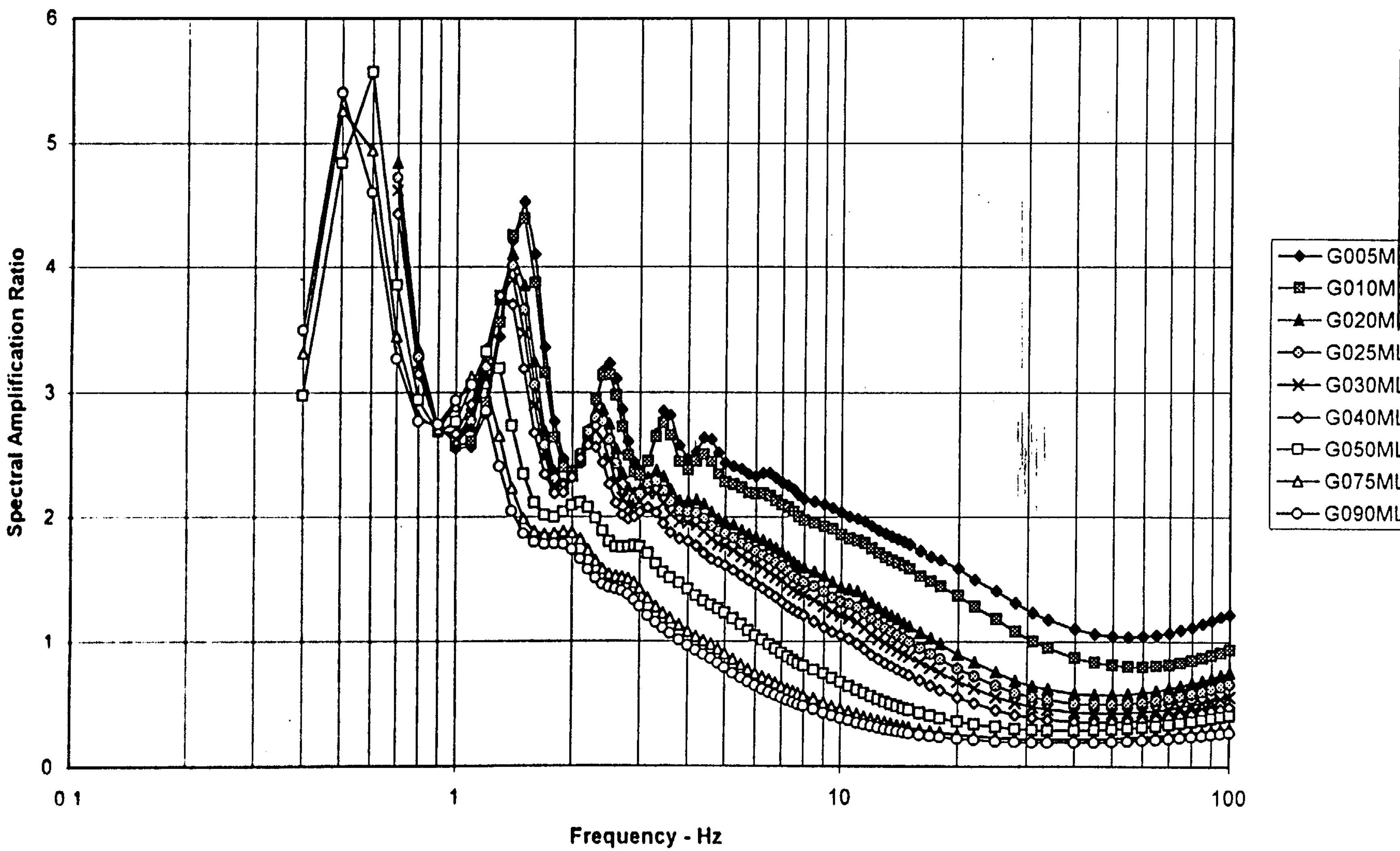

Figure 5.4 (b) - Mean 5 % damped response spectral amplification functions for disaggregated low- magnitude soil category 2 on crystalline rock. Corresponding bedrock peak ground acceleration (PGA) ranges from 0.05g (G005ML) to 0.75g (G075ML).

Westinghouse
Savannah River Company

P.O. Box 616
Aiken, SC 29802

MSD-STI-2000-00369

April 25, 2000

Bruce Cadotte,
WSRC Public Relations Officer
Site Information Programs,
Business Development and Public Affairs Division
Building 705-A

Dear Mr. Cadotte:

REQUEST FOR APPROVAL TO RELEASE SCIENTIFIC/TECHNICAL INFORMATION (U)

The attached document is submitted for classification and technical approvals for the purpose of external release. Please complete the WSRC BD&PAD response section of this letter and return the letter to the undersigned by the date listed below. Patent clearance, if necessary, is requested and received via direct communications between this office and the WSRC Patent Attorney. The document has been reviewed for classification by a WSRC classification staff member. Technical questions pertaining to the contents of this document should be addressed to the author or the manager. Questions concerning the processing of this document should be addressed to the WSRC STI Program office at (803) 725-2765.

Trish Baughman for

Julie M. Bean, Manager
WSRC STI Program

Document No. WSRC-TR-98-00263

Document Title Soil Surface Seismic Hazard and Design Basis Guideline for PC 1 & 2 SRS Facilities

Author A. Poon (Contact)

WSRC BD&PAD response due by May 2, 2000

☑ Approved ☐ Approved with Changes ☐ Not Approved

WSRC BD&PAD Remarks

Bruce Cadotte, Public Relations Officer
WSRC

4/26/00
Date

OSR 25-82-W# (4-89)
Stores. 26-15460.00

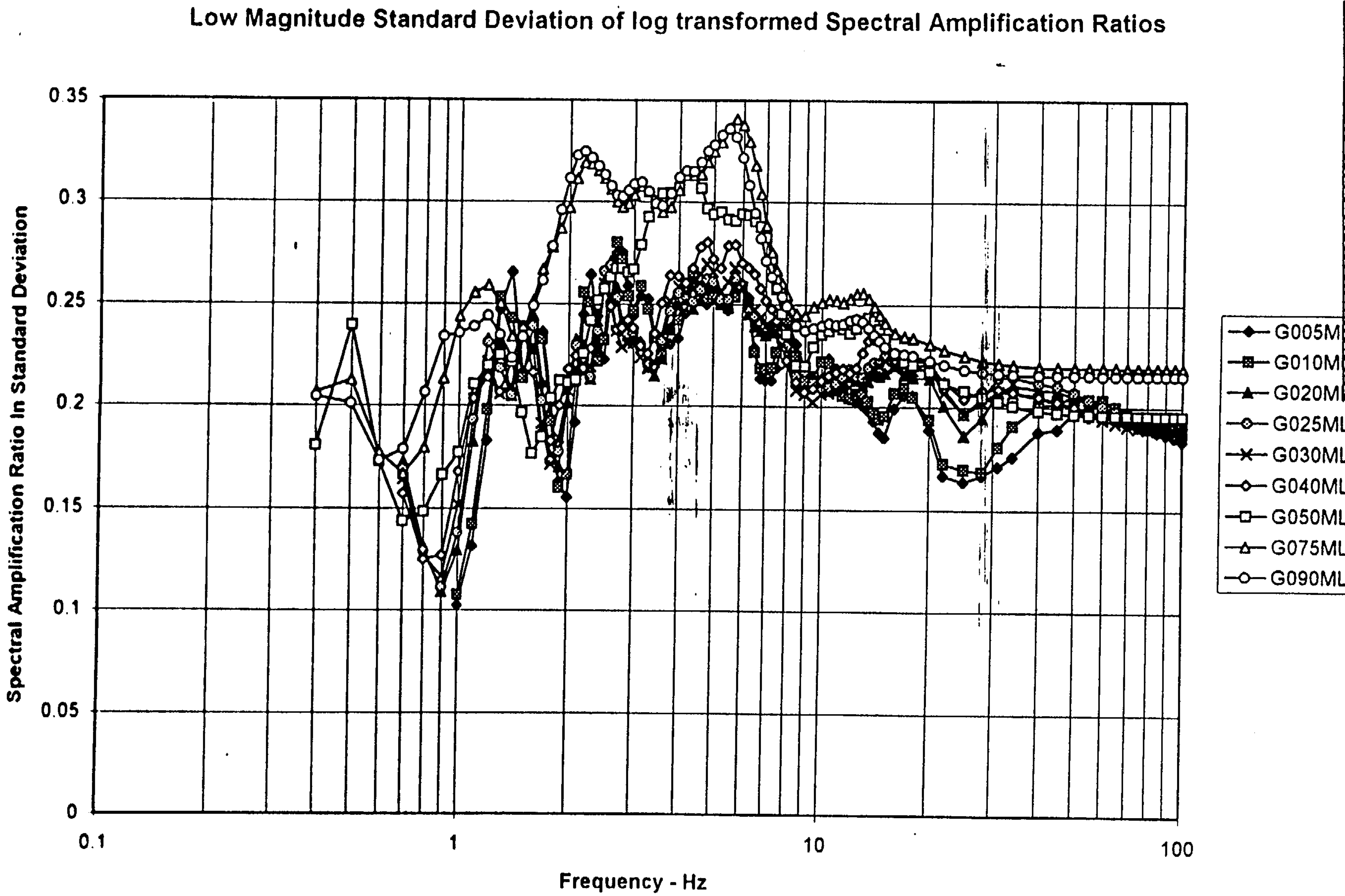

Figure 5.4 (c) - Logarithmic standard deviation of 5 % damped amplification functions for disaggregated low-magnitude soil category 2 on crystalline rock. Corresponding bedrock peak ground acceleration (PGA) ranges from 0.05g (G005ML) to 0.75g (G075ML).

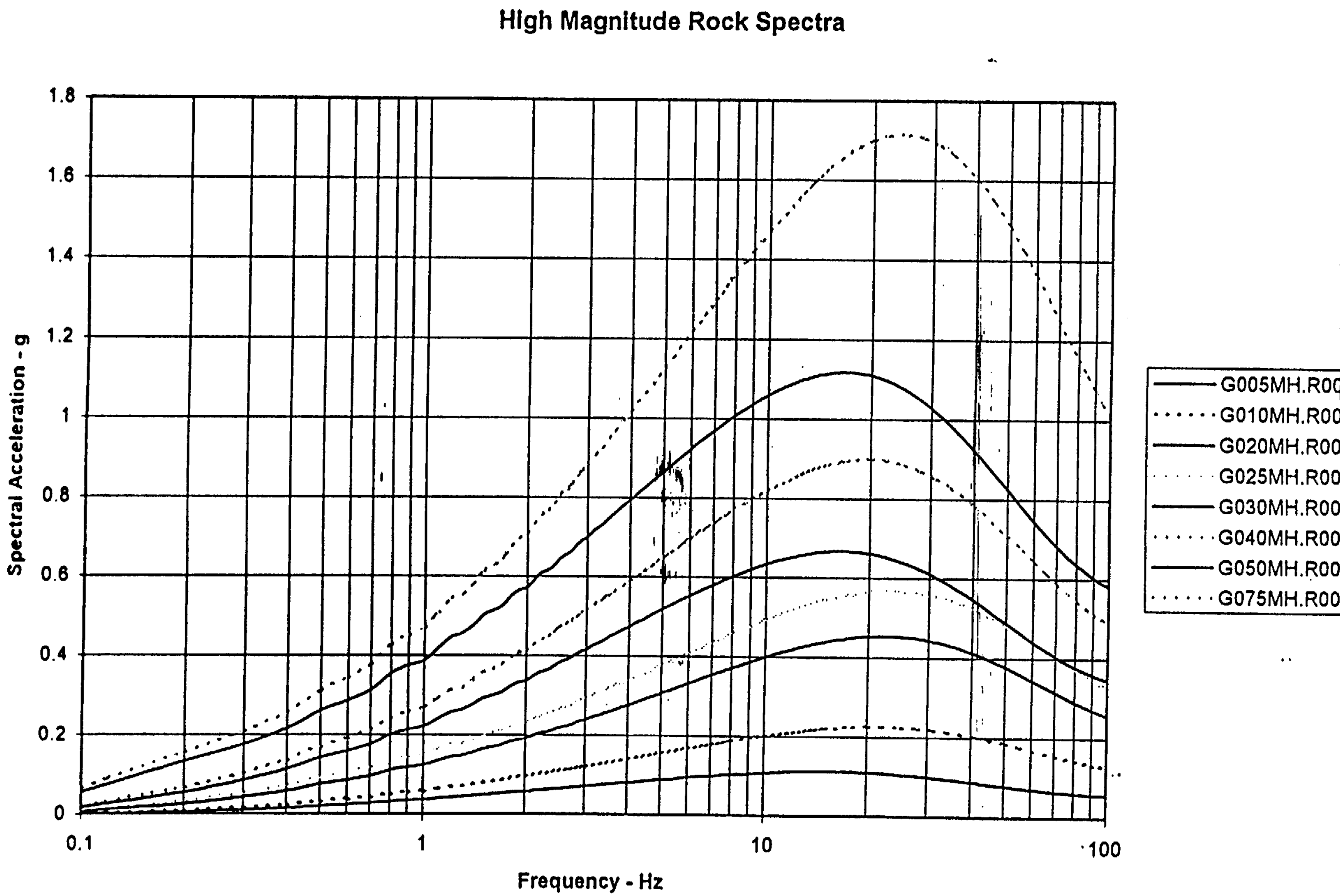

Figure 5.5 (a) - 5 % damped response spectra of disaggregated high-magnitude (MH) crystalline bedrock control motions used to generate soil response for soil category 2. Bedrock peak ground acceleration (PGA) ranges from 0.05g (G005MH.R00) to 0.75g (G075MH.R00).

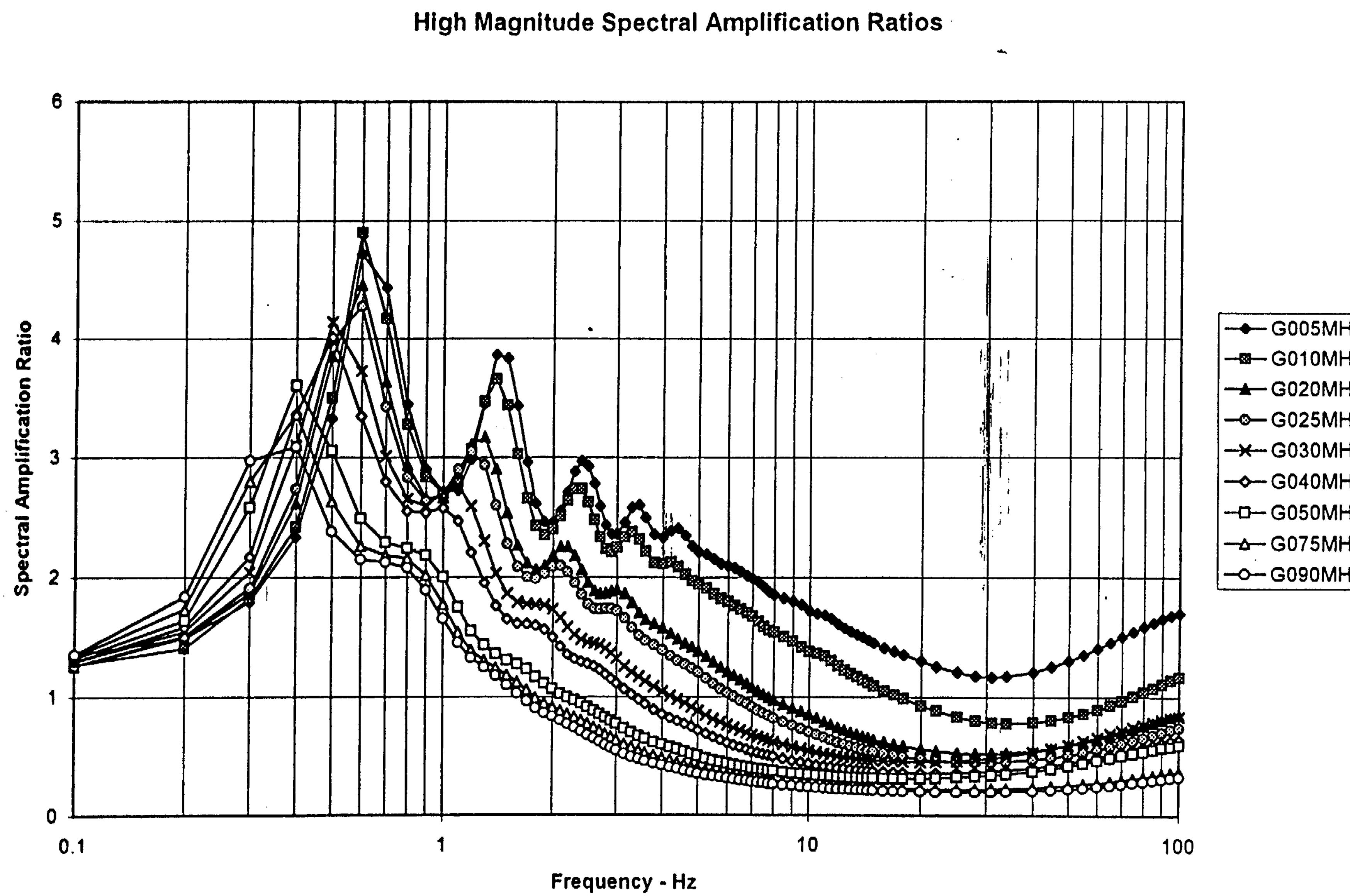

Figure 5.5 (b) - Mean 5 % damped response spectral amplification functions for disaggregated high- magnitude soil category 2 on crystalline rock. Corresponding bedrock peak ground acceleration (PGA) ranges from 0.05g (G005MH) to 0.75g (G075MH).

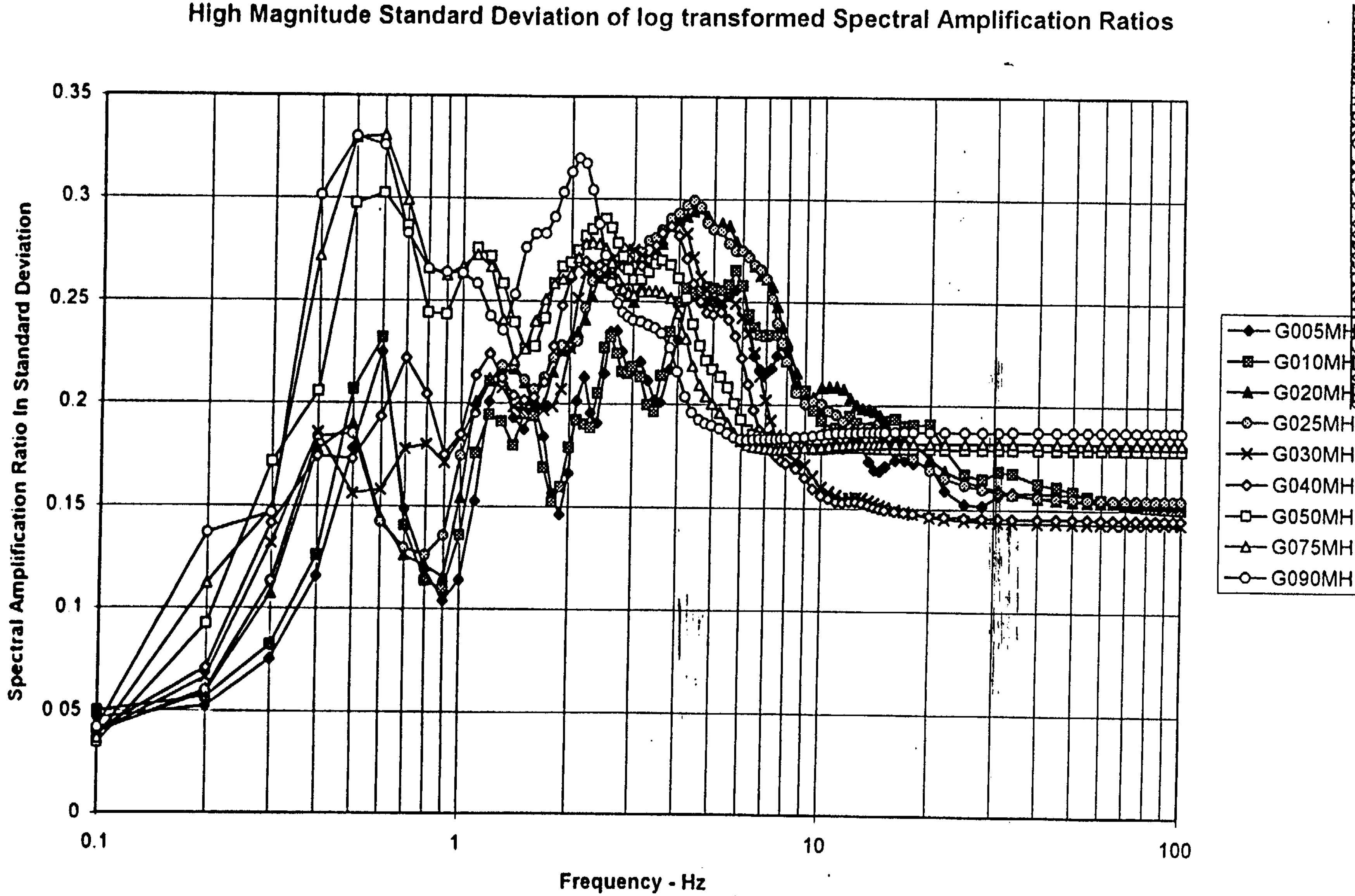

Figure 5.5 (c) - Logarithmic standard deviation of 5 % damped amplification functions for disaggregated high-magnitude soil category 2 on crystalline rock. Corresponding bedrock peak ground acceleration (PGA) ranges from 0.05g (G005MH) to 0.75g (G075MH).

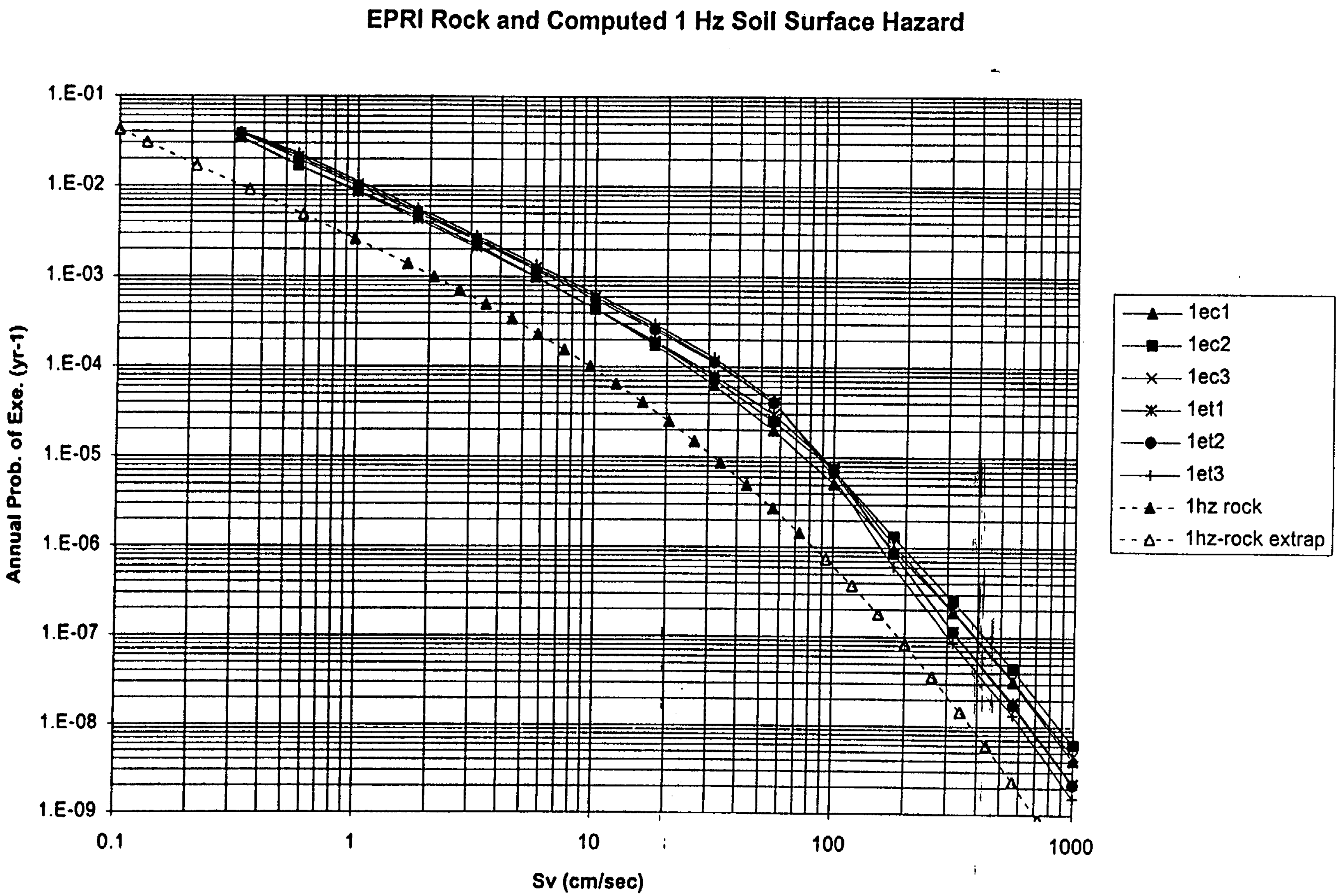

Figure 6.1 - Soil surface hazard curves (solid lines) for 1-Hz oscillator frequency computed from EPRI bedrock hazard curves (dashed lines). Hazard curves are for six soil and bedrock conditions (see text for explanation of legend). EPRI 1-Hz bedrock hazard (dashed line) is shown for interpolated segments (solid symbols) and extrapolated segments (open symbols).

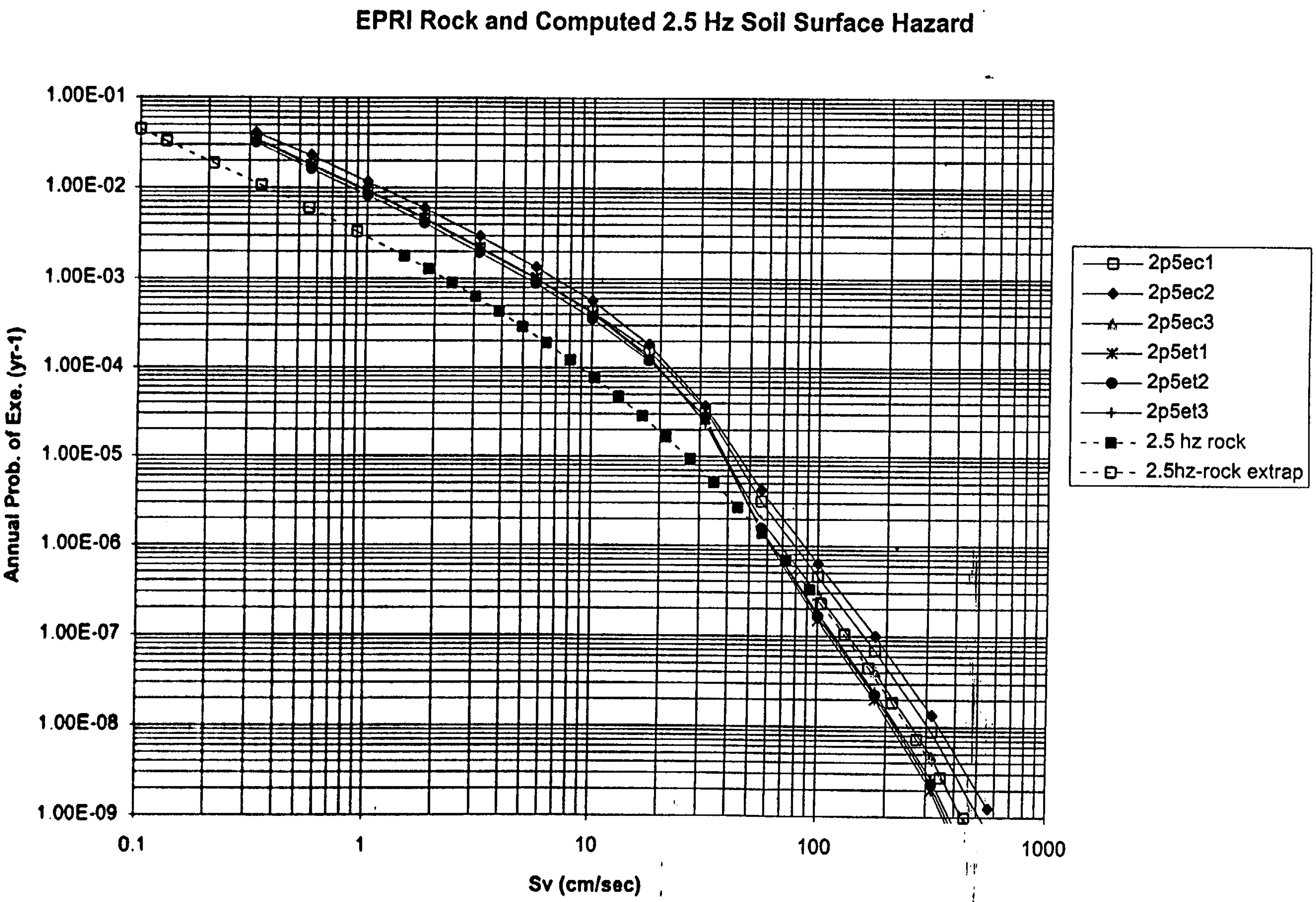

Figure 6.2 - Soil surface hazard curves (solid lines) for 2.5-Hz oscillator frequency computed from EPRI bedrock hazard curves (dashed lines). Hazard curves are for six soil and bedrock conditions (see text for explanation of legend). EPRI 2.5-Hz bedrock hazard (dashed line) is shown for interpolated segments (solid symbols) and extrapolated segments (open symbols).

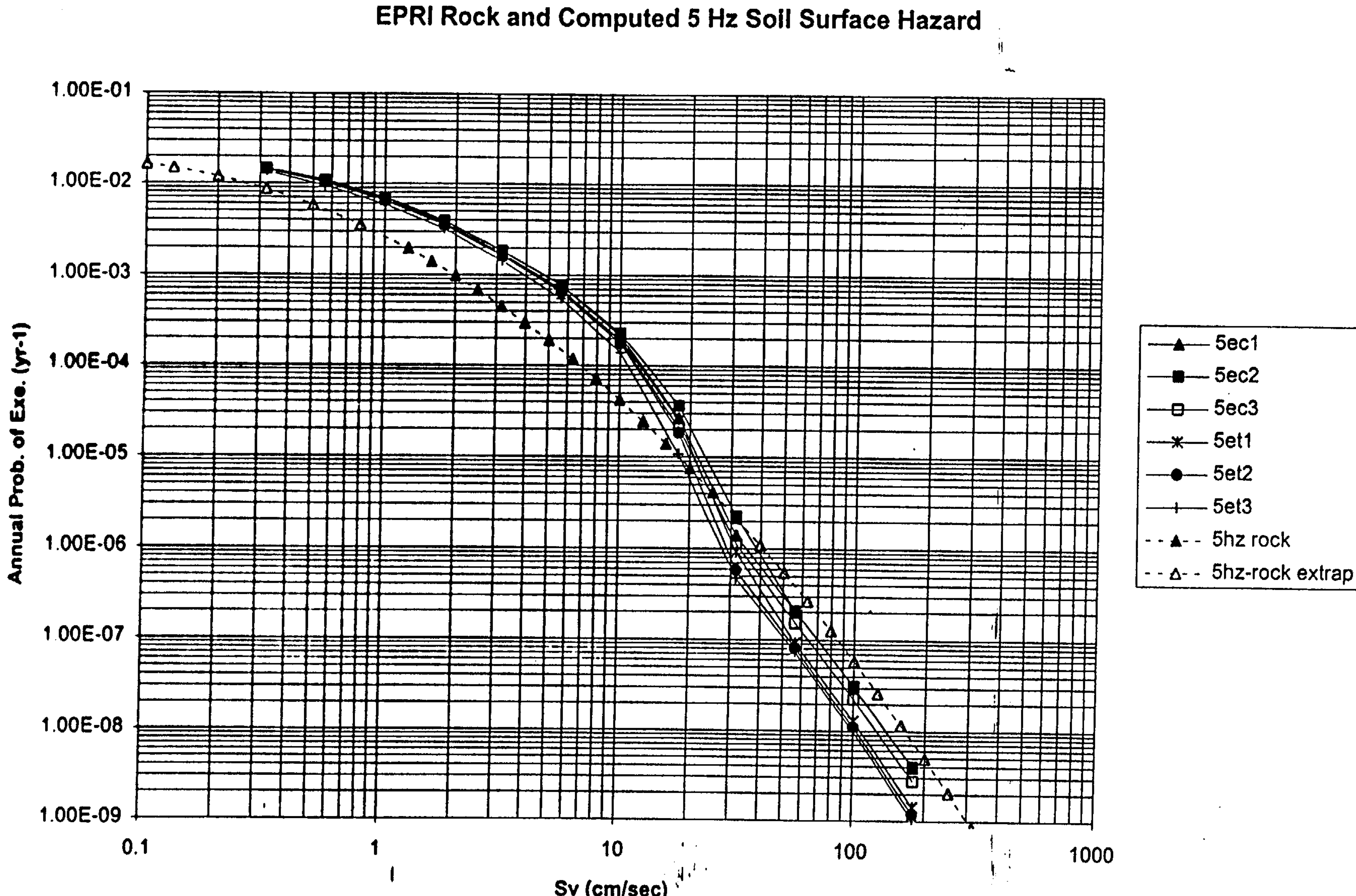

Figure 6.3 - Soil surface hazard curves (solid lines) for 5-Hz oscillator frequency computed from EPRI bedrock hazard curves (dashed lines). Hazard curves are for six soil and bedrock conditions (see text for explanation of legend). EPRI 5-Hz bedrock hazard (dashed line) is shown for interpolated segments (solid symbols) and extrapolated segments (open symbols).

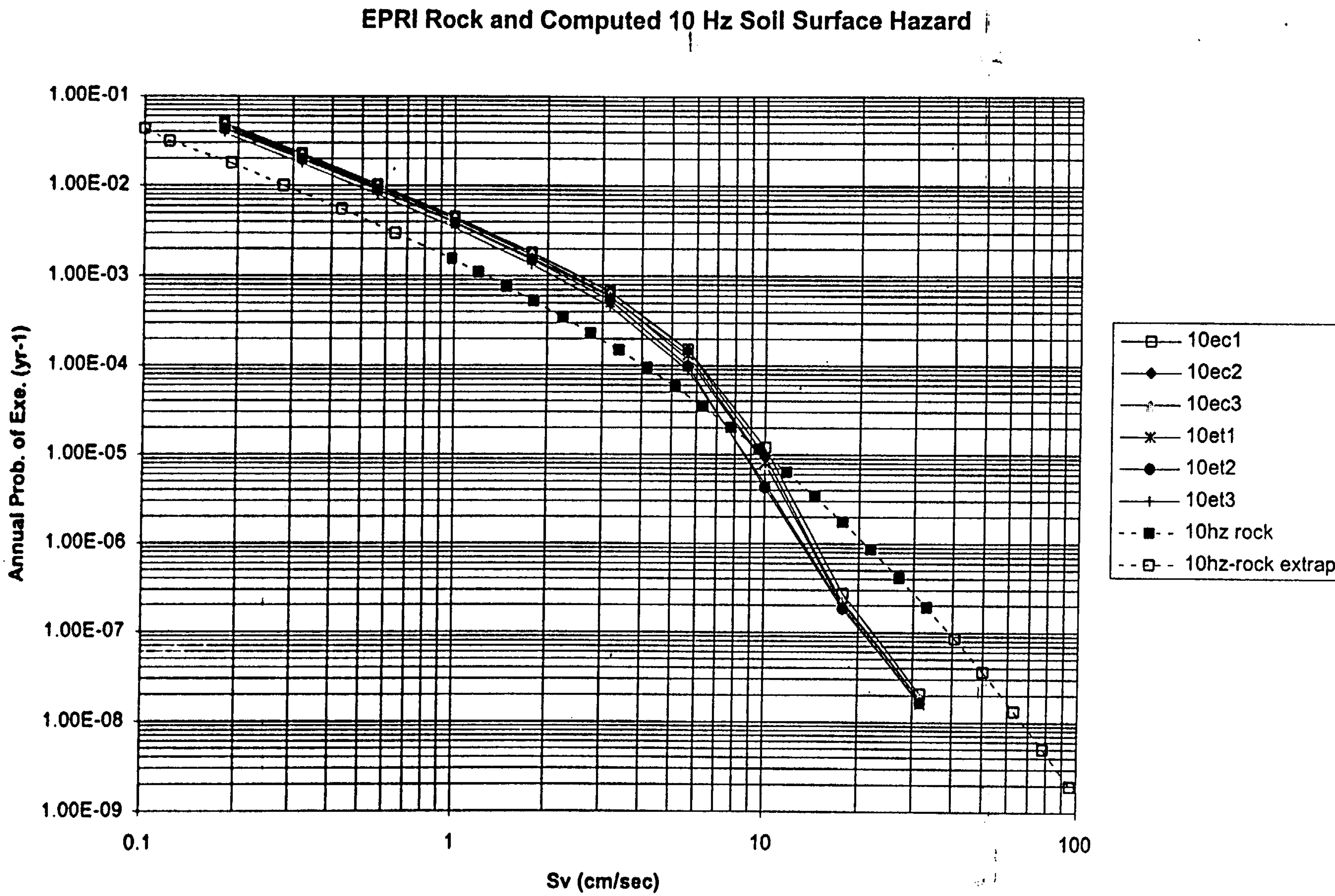

Figure 6.4 - Soil surface hazard curves (solid lines) for 10-Hz oscillator frequency computed from EPRI bedrock hazard curves (dashed lines). Hazard curves are for six soil and bedrock conditions (see text for explanation of legend). EPRI 10-Hz bedrock hazard (dashed line) is shown for interpolated segments (solid symbols) and extrapolated segments (open symbols).

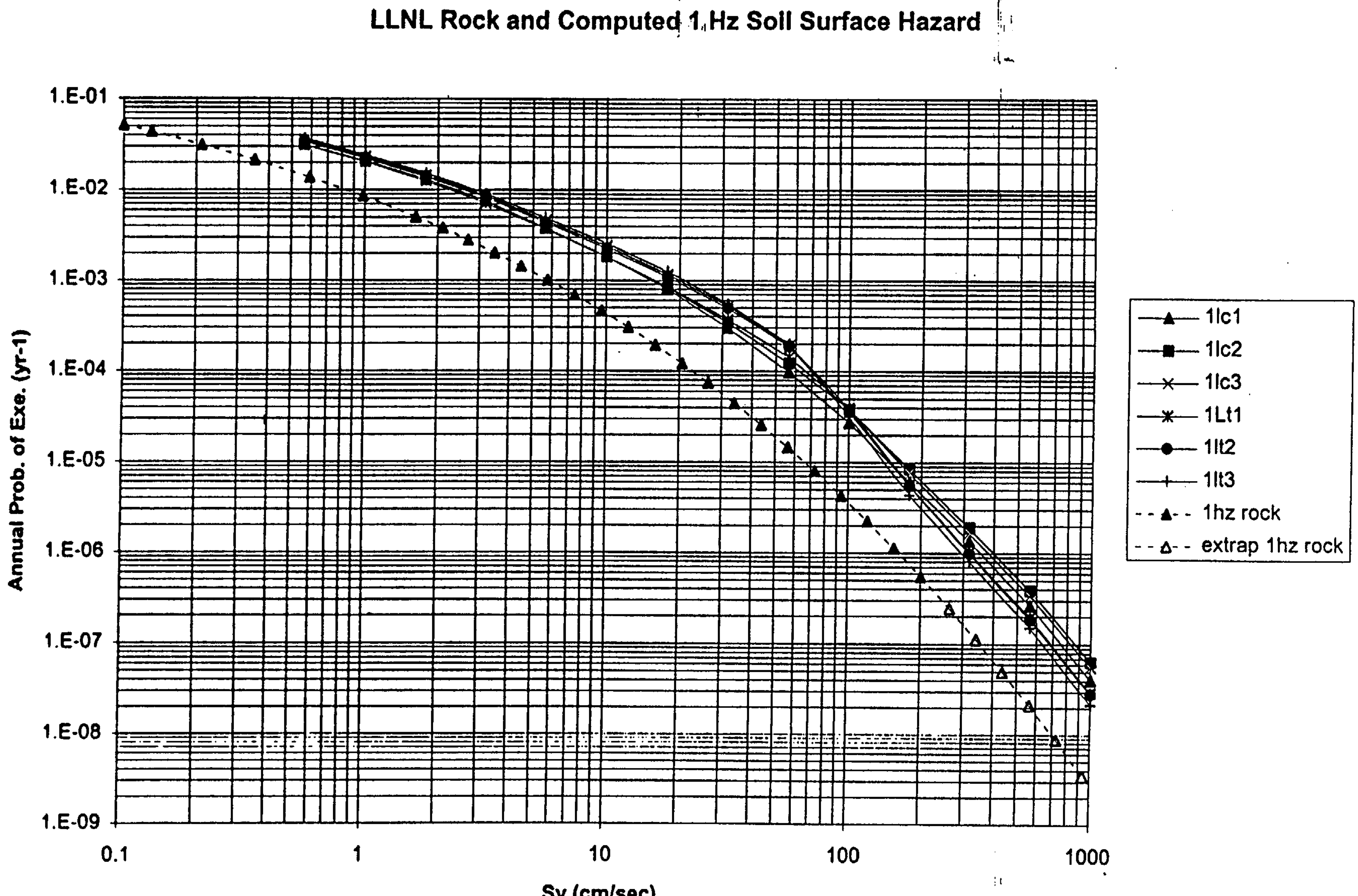

Figure 6.5 - Soil surface hazard curves (solid lines) for 1-Hz oscillator frequency computed from LLNL bedrock hazard curves (dashed lines). Hazard curves are for six soil and bedrock conditions (see text for explanation of legend). LLNL 1-Hz bedrock hazard (dashed line) is shown for interpolated segments (solid symbols) and extrapolated segments (open symbols).

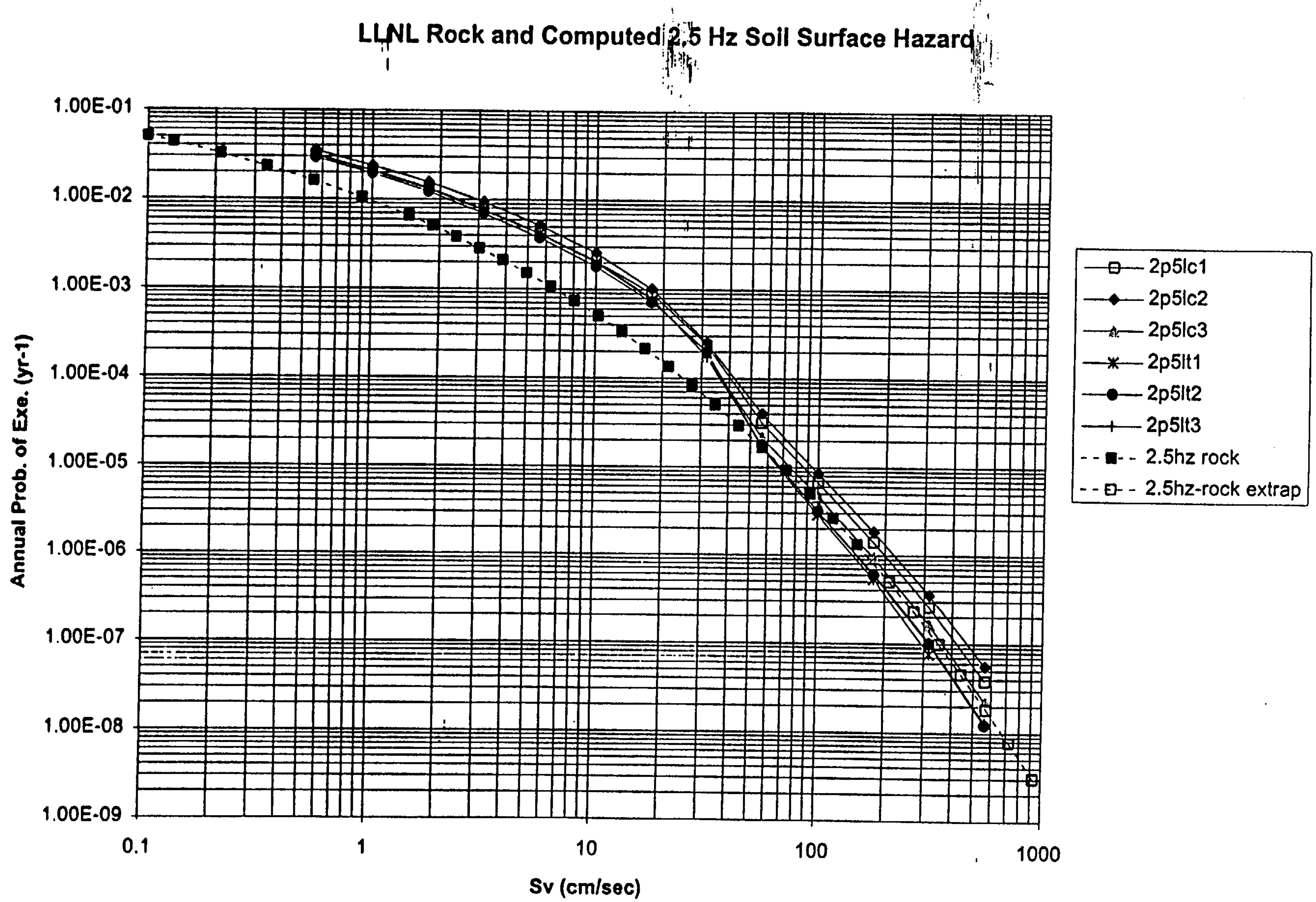

Figure 6.6 - Soil surface hazard curves (solid lines) for 2.5-Hz oscillator frequency computed from LLNL bedrock hazard curves (dashed lines). Hazard curves are for six soil and bedrock conditions (see text for explanation of legend). LLNL 2.5-Hz bedrock hazard (dashed line) is shown for interpolated segments (solid symbols) and extrapolated segments (open symbols).

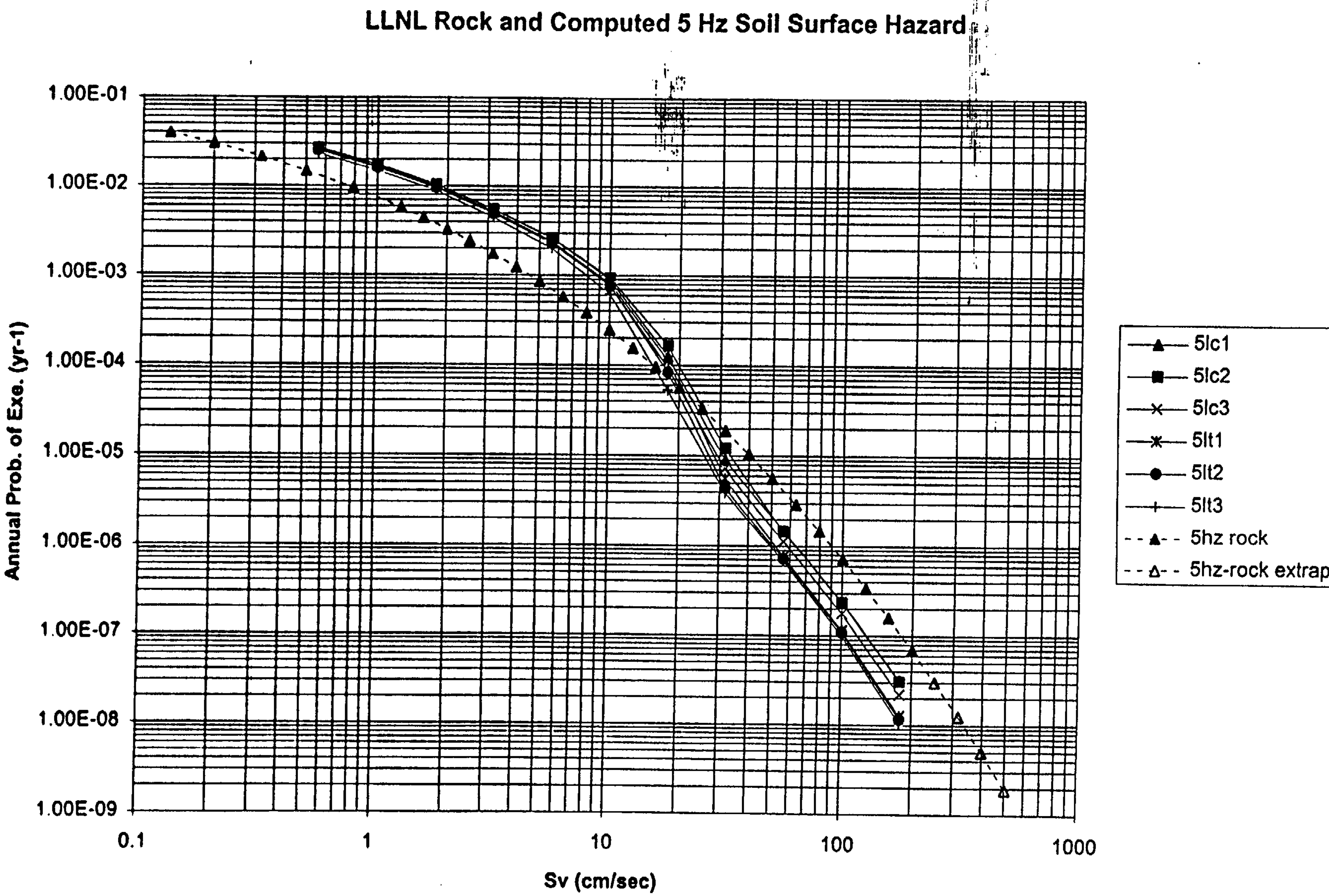

Figure 6.7 - Soil surface hazard curves (solid lines) for 5-Hz oscillator frequency computed from LLNL bedrock hazard curves (dashed lines). Hazard curves are for six soil and bedrock conditions (see text for explanation of legend). LLNL 5-Hz bedrock hazard (dashed line) is shown for interpolated segments (solid symbols) and extrapolated segments (open symbols).

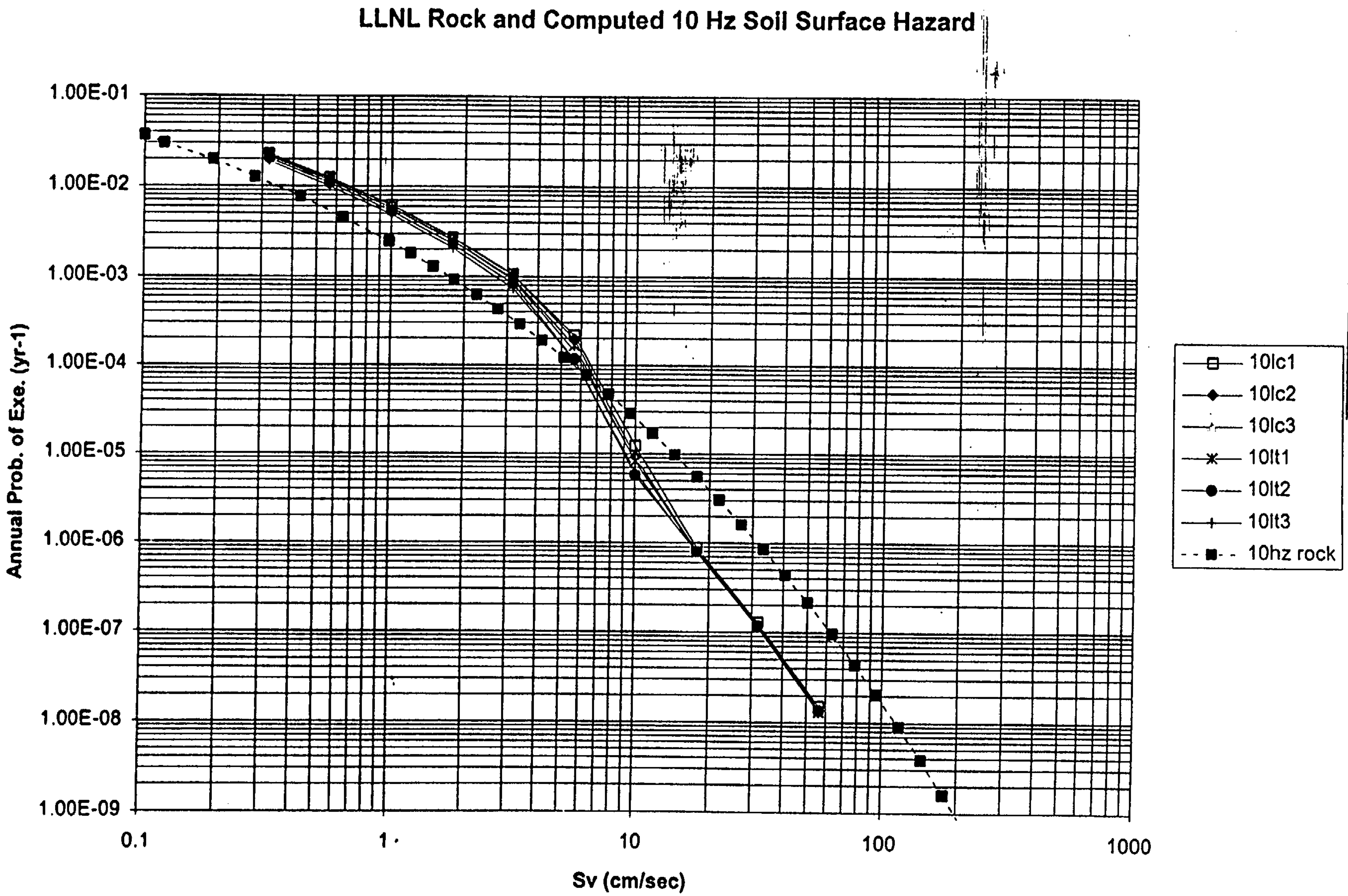

Figure 6.8 - Soil surface hazard curves (solid lines) for 10-Hz oscillator frequency computed from LLNL bedrock hazard curves (dashed lines). Hazard curves are for six soil and bedrock conditions (see text for explanation of legend). LLNL 10-Hz bedrock hazard (dashed line) is shown for interpolated segments (solid symbols) and extrapolated segments (open symbols).

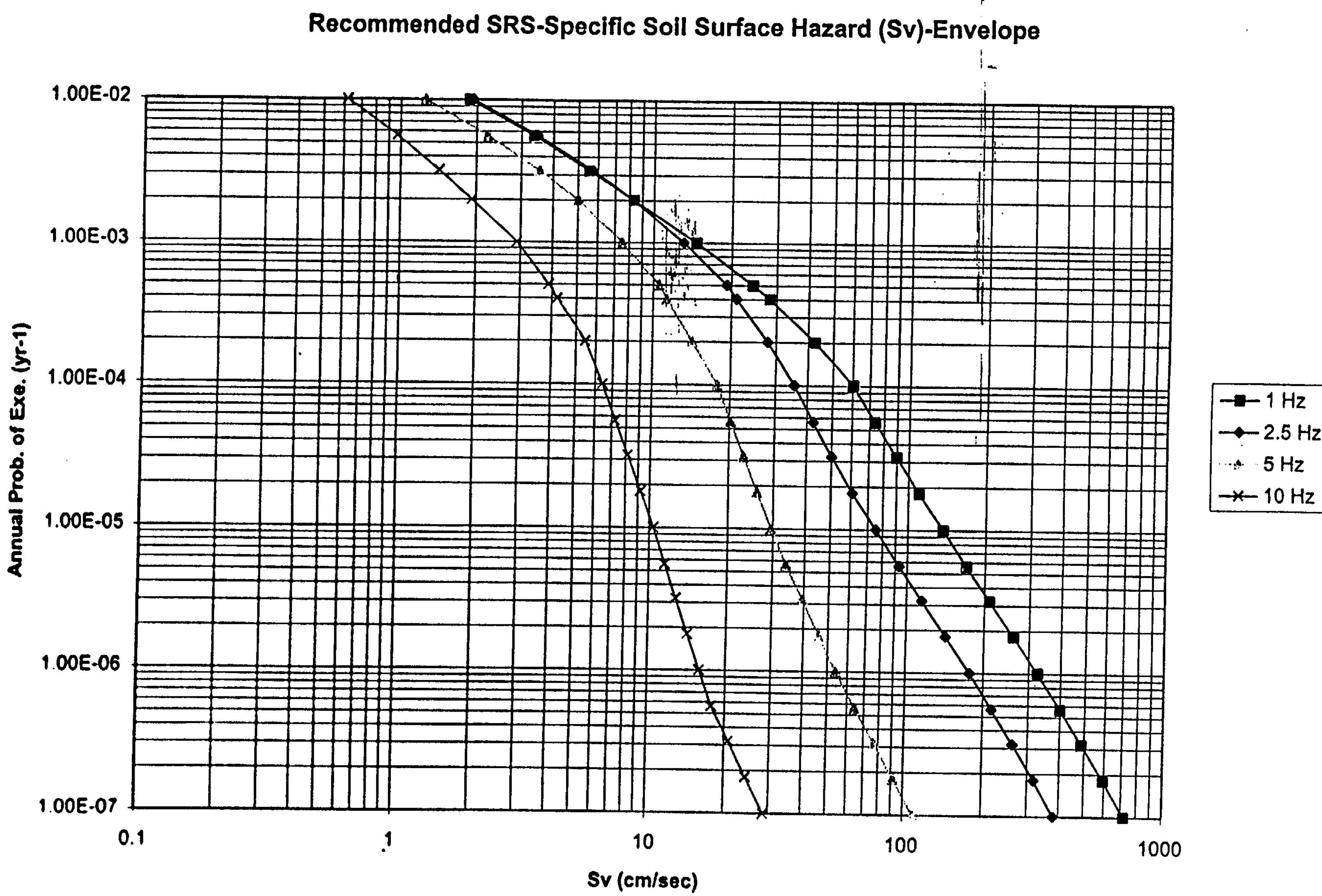

Figure 6.9 - Combined EPRI and LLNL soil surface hazard envelope for oscillator frequencies of 1, 2.5, 5, and 10 Hz. Probability of exceedance vs. spectral velocity.

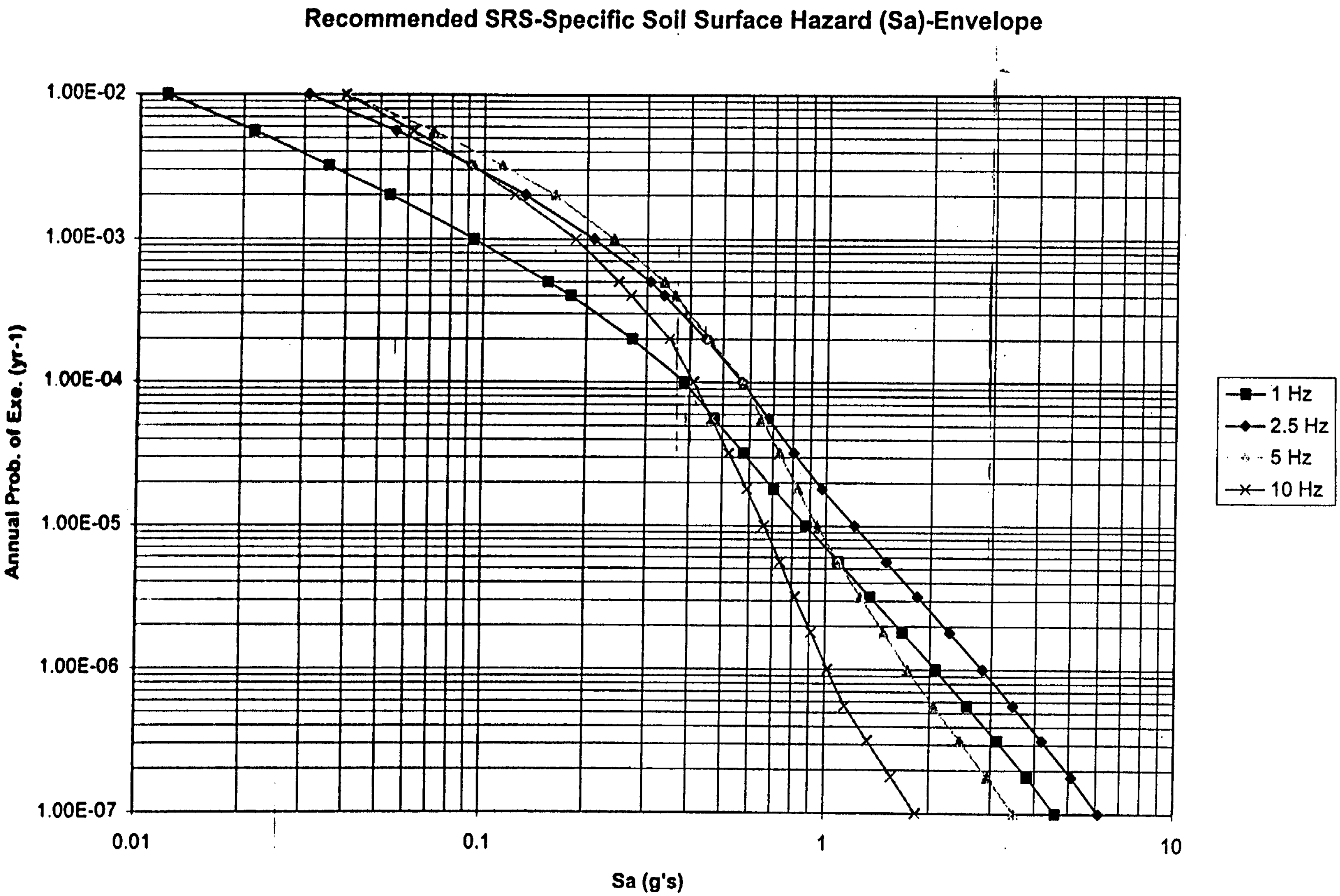

Figure 6.10 - Combined EPRI and LLNL soil surface hazard envelope for oscillator frequencies of 1, 2.5, 5, and 10 Hz. Probability of exceedance vs. spectral acceleration.

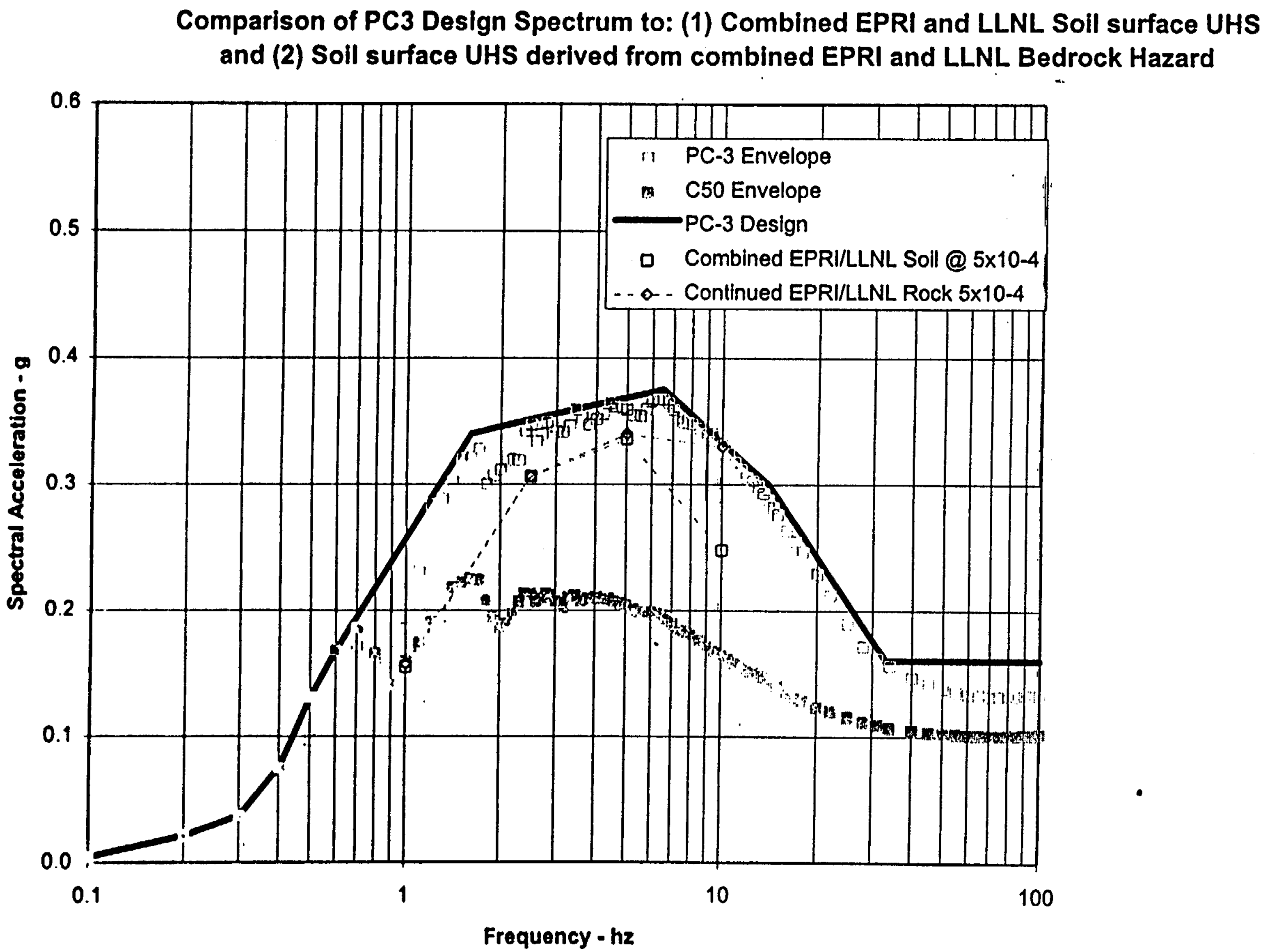

Figure 6.11 - Comparison of PC3 design basis envelope taken from Report 1 (solid line) to: (a) combined EPRI/LLNL soil surface UHS (open squares); and (b) soil surface UHS (open diamonds) based on combined EPRI and LLNL bedrock hazard. Also shown are the Charleston 50th percentile deterministic (C50 Envelope) and the PC3 envelope (PC-3 Envelope) values from Report 1.

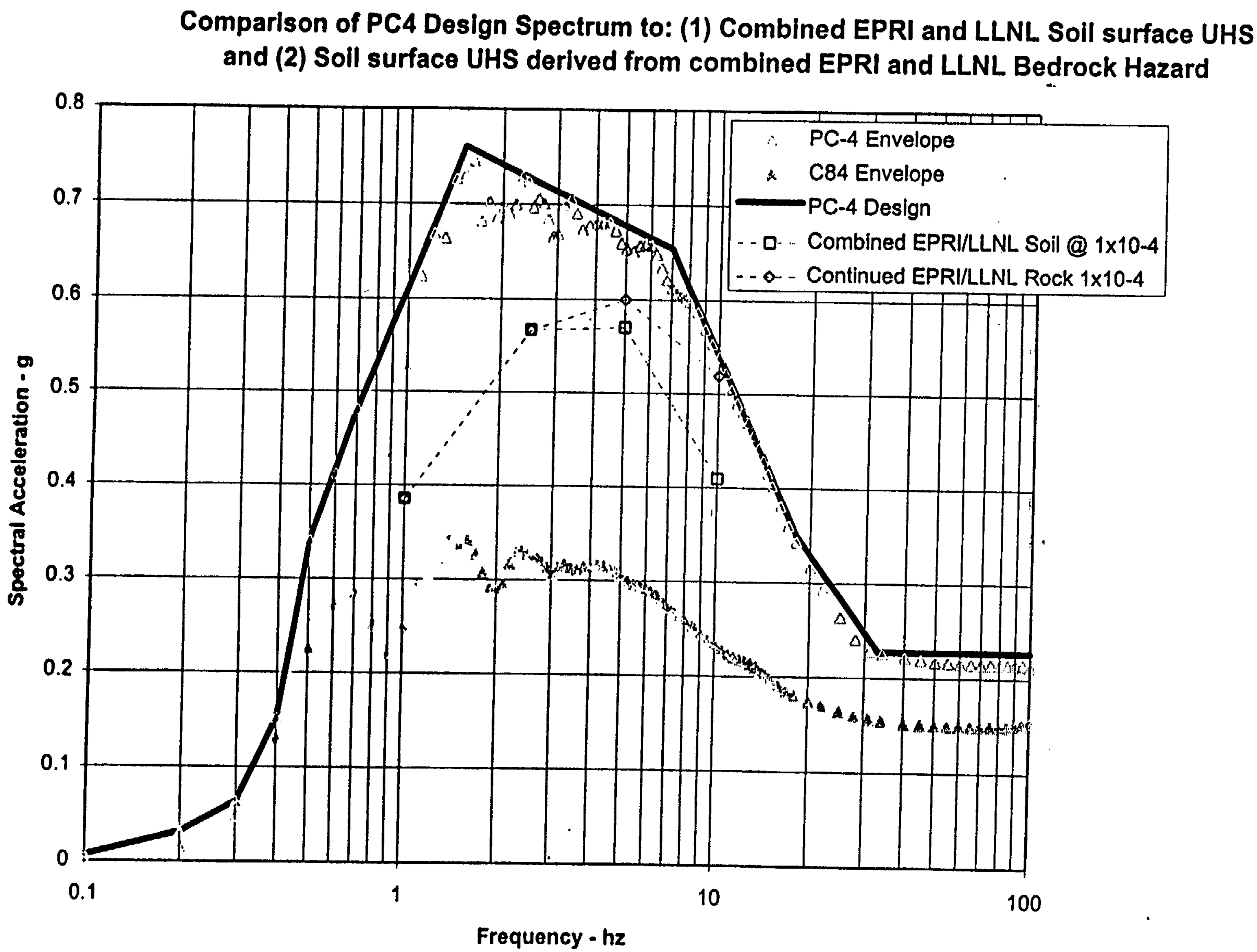

Figure 6.12 - Comparison of PC4 design basis envelope taken from Report 1 (solid line) to: (a) combined EPRI/LLNL soil surface UHS (open squares); and (b) soil surface UHS (open diamonds) based on combined EPRI and LLNL bedrock hazard. Also shown are the Charleston 84th percentile deterministic (C84 Envelope) and the PC4 envelope (PC-4 Envelope) values from Report 1.

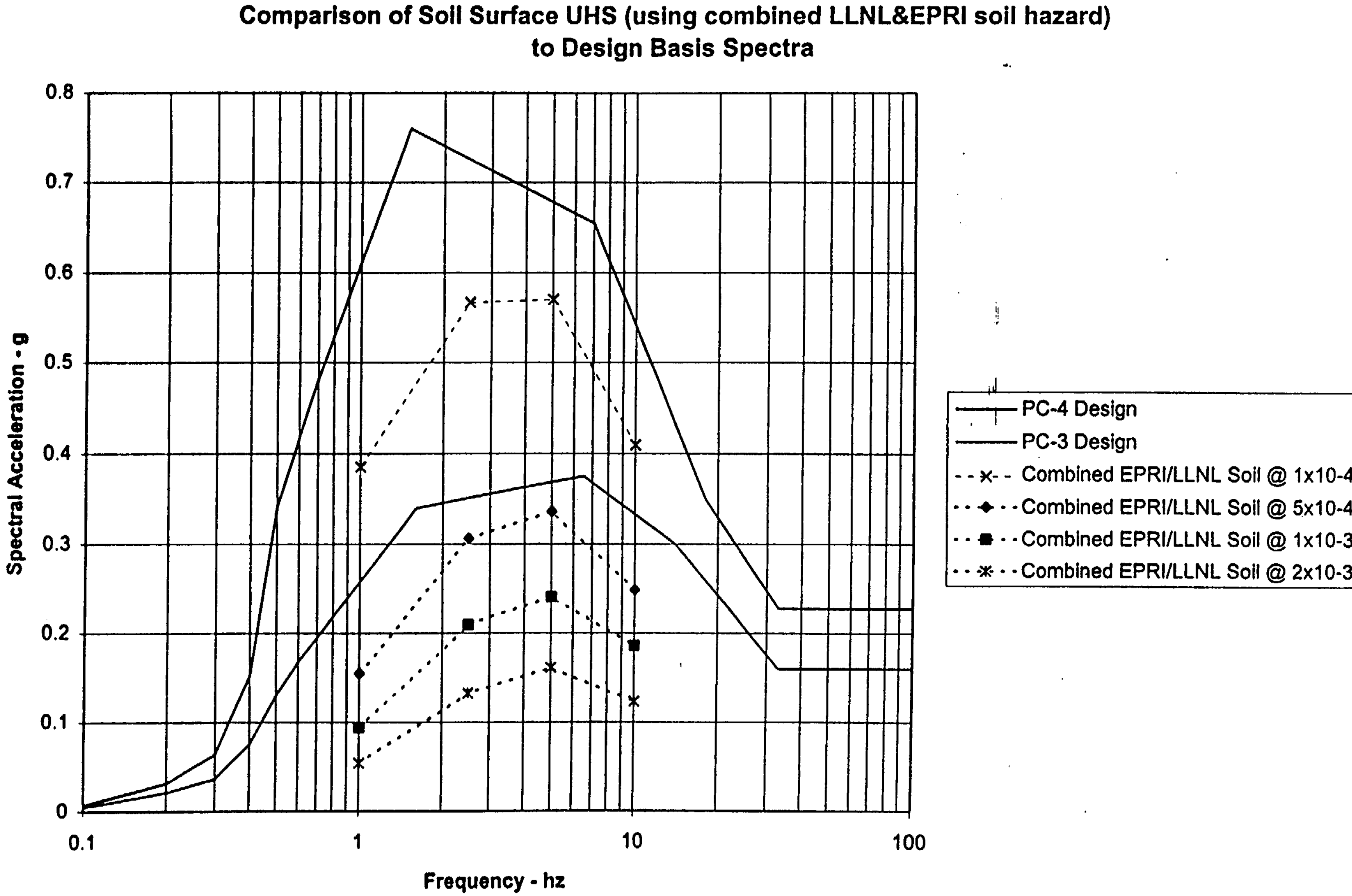

Figure 6.13 - PC3 and PC4 design basis spectra taken from Report 1(solid light lines), and soil surface UHS for the four performance categories of DOE-STD-1020 (dashed lines).

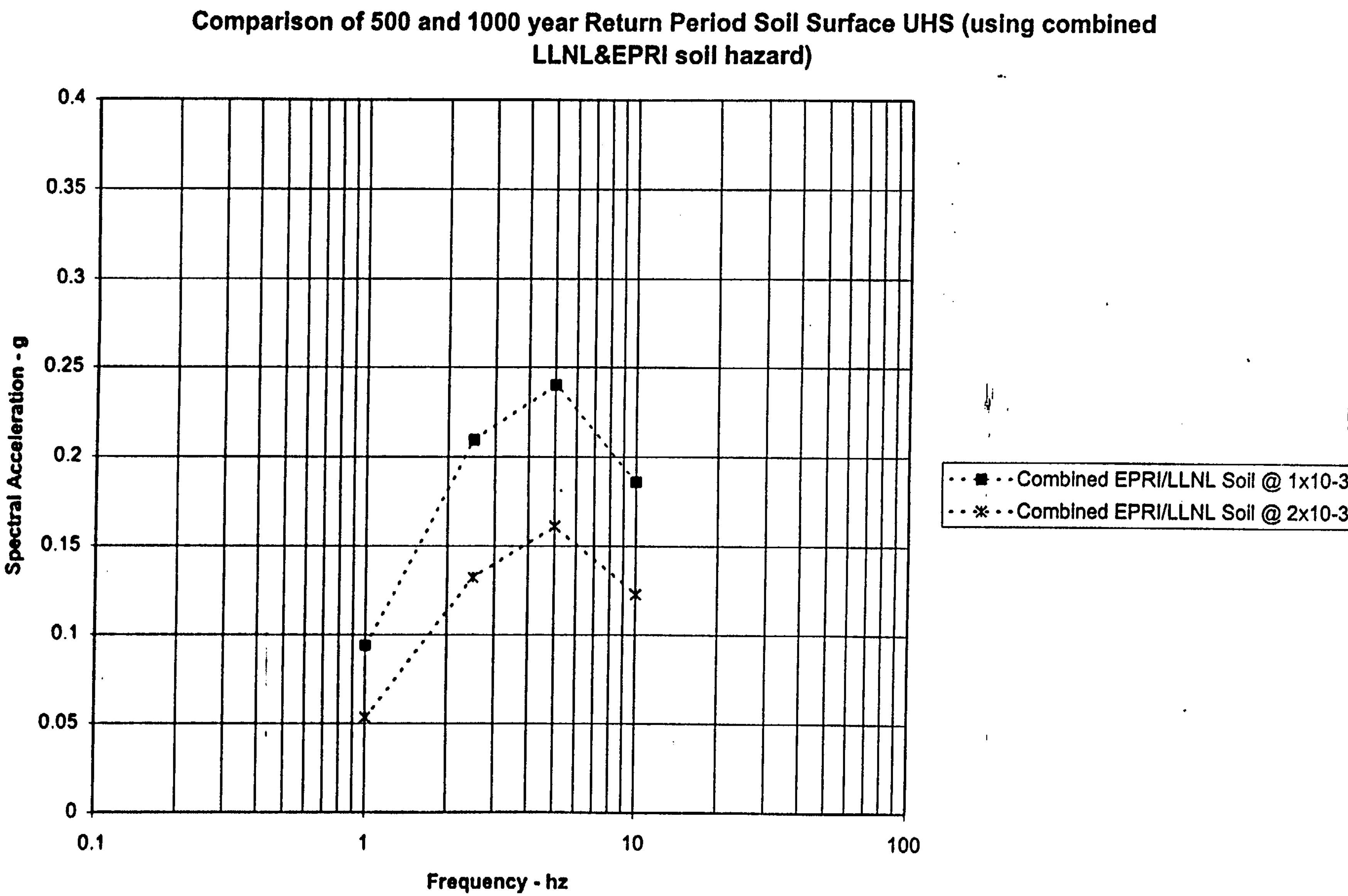

Figure 7.1 - Soil surface UHS (taken from combined EPRI and LLNL soil surface hazard curves) for the PC1 and PC2 performance categories of DOE-STD-1020.

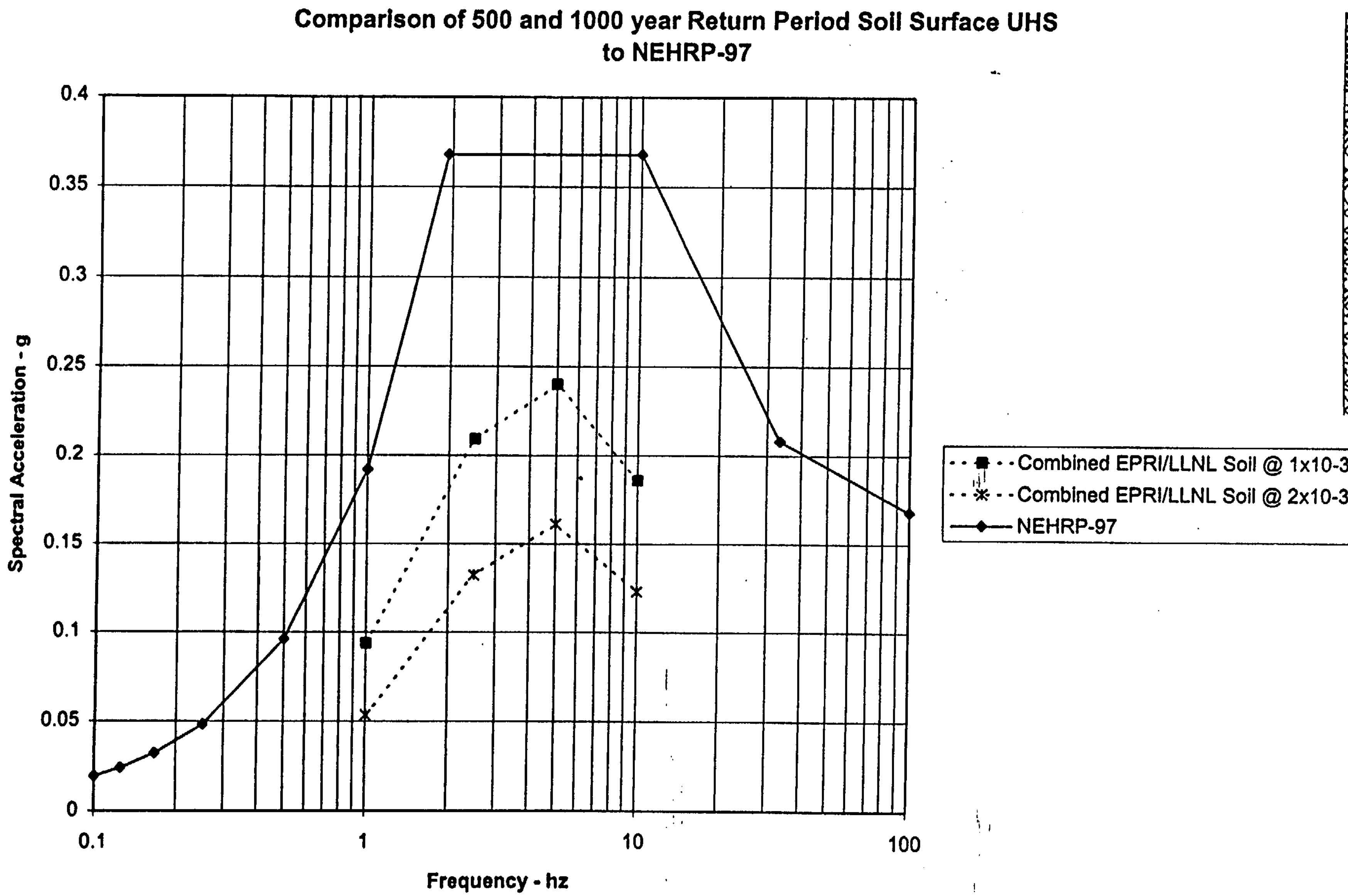

Figure 7.2 - Comparison of the soil surface UHS for the PC1-PC2 performance categories of DOE-STD-1020 (dashed lines) to the NEHRP-97 spectrum for SRS soil conditions. The NEHRP spectrum includes the allowed 20% reduction for adjustment to site-specific studies.

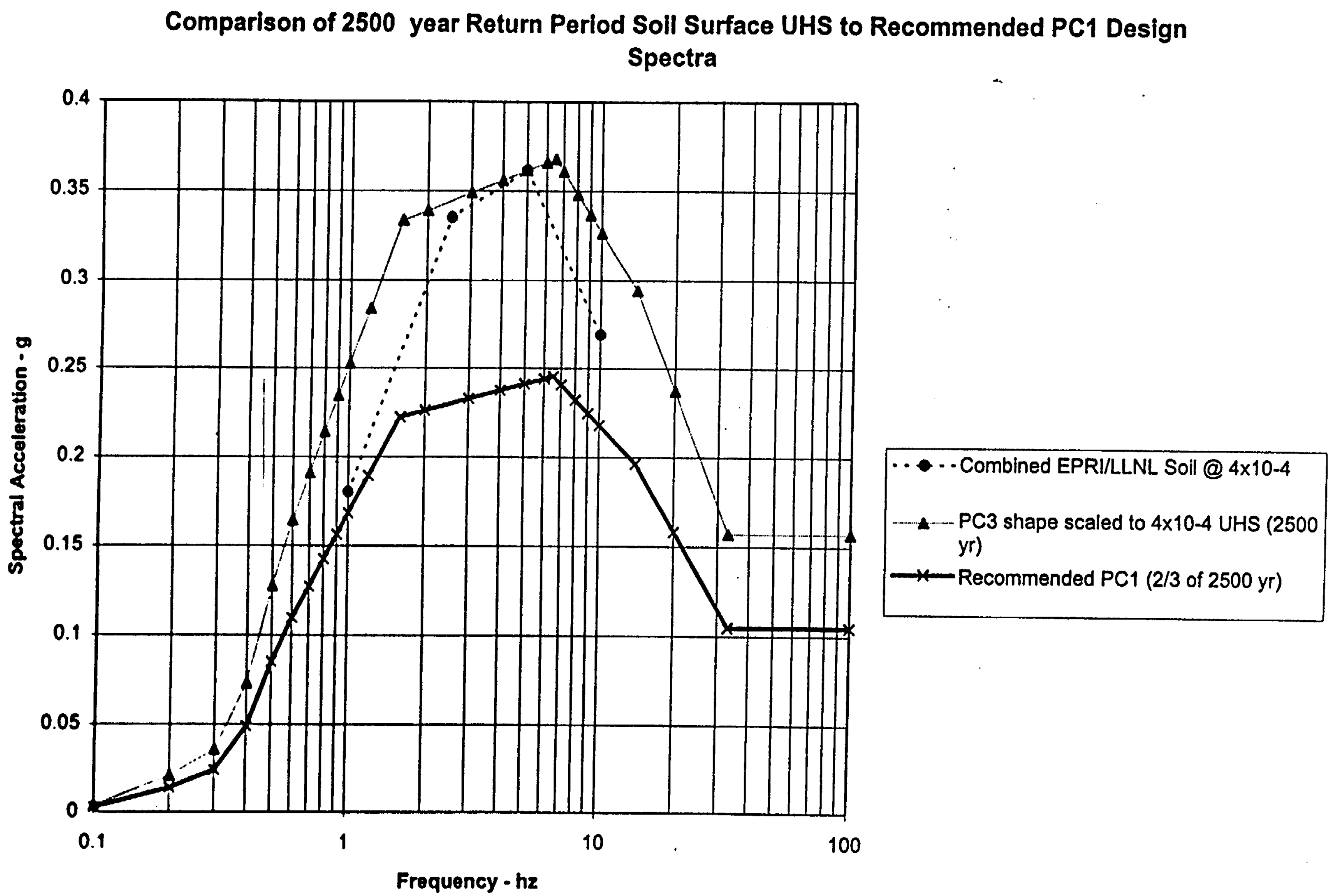

Figure 7.3 - Recommended PC1 design basis spectrum (bold). Also shown are the soil surface UHS for annual probability of 4x10-4 (return period 2500 years (dashed lines)). The recommended PC1 design basis was derived from the NEHRP criteria and the SRS soil surface hazard (PC3 spectral shape of Report 1 was scaled to the 2500 year UHS and reduced by 2/3).

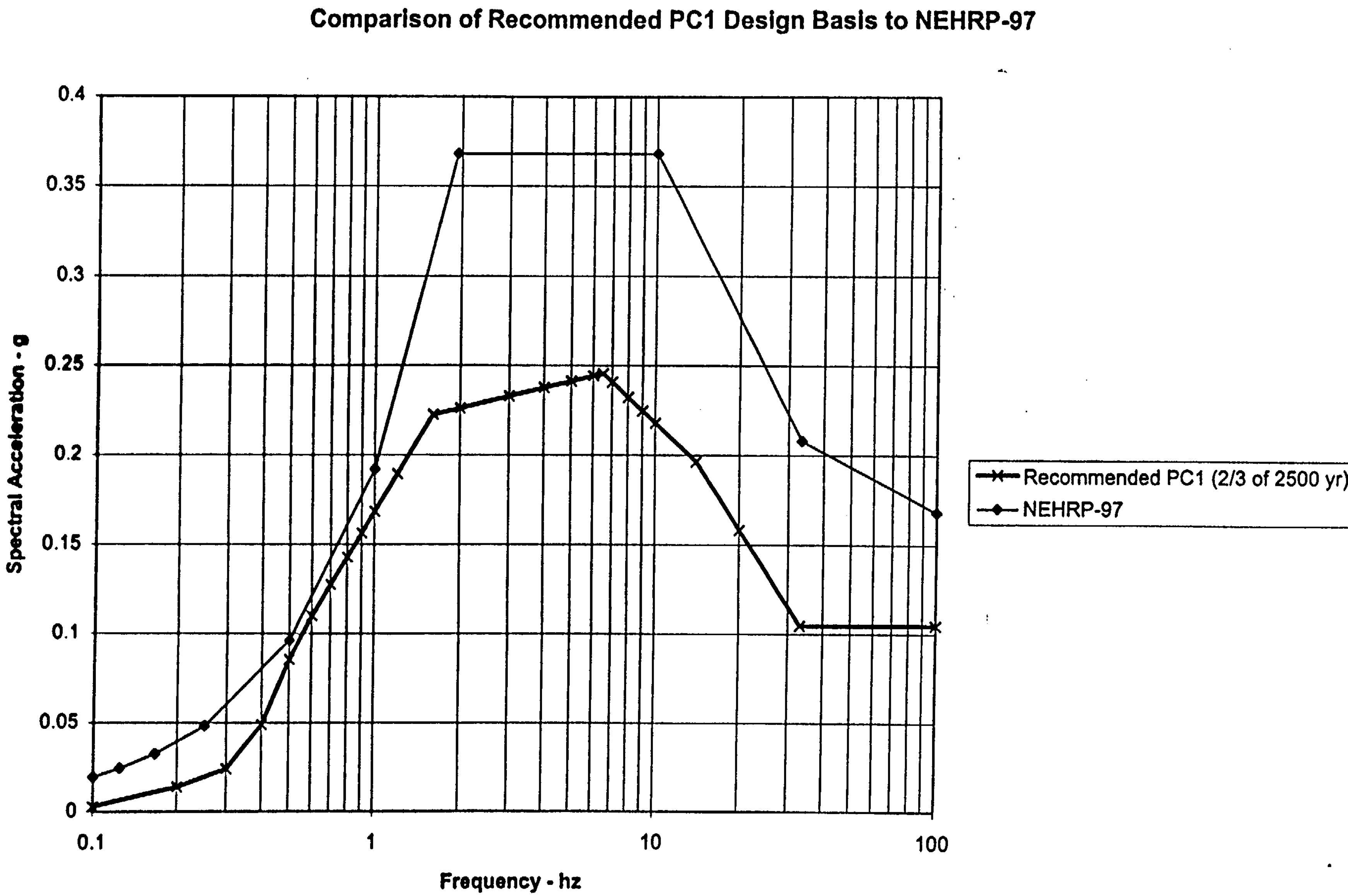

Figure 7.4 - Comparison of the recommended PC1 design basis spectrum (bold) to NEHRP-97.

14.0 APPENDICES

APPENDIX A

INPUT PARAMETER SENSITIVITY STUDIES

Soil surface hazard sensitivity studies were conducted to test the sensitivity of computed soil hazard to: (1) density of input bedrock ground motion values; (2) effect of extrapolating hazard to high and low POEs; (3) effect of truncating the CCDF of the soil surface motion; and (4) effect of applying a lower bound to the SAF.

Density of Input Bedrock Hazard Values

Sensitivity of the soil surface hazard results to density of input bedrock ground motion values was tested. Figure A.1 illustrates the computed 1 Hz soil surface hazard using the EPRI bedrock hazard and soil values of Report 1. As illustrated in the Figure, eight (8) bedrock values and eight (8) soil values were used in the evaluation. The bedrock values and probabilities were as given in the original EPRI hazard evaluation. As noted in Report 1, the computed soil surface hazard curve is not smooth, owing to the large range in bedrock spectral values used in the evaluation; that is, the summation over ground motion used widely spaced and uneven bedrock ground motion values. To test the sensitivity of these values to the analysis, bedrock ground motion intervals were successively subdivided in an effort to smooth the hazard curve (note that this was not possible with the earlier version of the code because there was no utility to interpolate the hazard dissagregation or interpolate the bedrock hazard). As the bedrock intervals are decreased, the soil surface hazard should become increasingly smoother.

Figure A.2 shows an evaluation for 1-Hz soil surface hazard using an approximate factor of two increase in the number of bedrock spectral velocities evaluated at the same soil surface hazard values. Note the significant improvement in the smoothness of the hazard. Figure A.3 illustrates an additional approximate factor of 2 increase in bedrock spectral velocities showing no additional improvement. The three sets of soil surface hazard are shown together in Figure A.4. Based on this limited test, it is judged that bedrock densities of 8-10 values/decade of ground motion would be sufficient to achieve smooth hazard.

Range of Bedrock and Soil Surface Hazard Values

The range of bedrock POE to adequately estimate soil POE was tested. Figure A.5 illustrates the effect on 1 Hz soil surface hazard resulting from two differing ranges of bedrock probability of exceedance. For the test, desired soil surface hazard values ranging from about 2.8 to 240 cm/sec were selected. The first bedrock hazard values selected ranged from about 0.1 to 90 cm/sec (rock1). The computed soil surface hazard curves exhibit a rapid change in slope for soil surface ground motions greater than about 90 cm/sec (soil1). Figure A.5 also shows the low-probability bedrock hazard (values ranging from 1 to 210 cm/sec) used to compute the same desired soil surface values (rock2). The soil surface hazard in this case (soil2) remains nearly parallel to the bedrock

hazard and shows a significant departure from the high-probability case. This illustration shows that the computed soil surface POE is critically dependent on the ground motion range of bedrock hazard used in the probability sum (equation 3.1).

The effect on the high-probability end of the soil surface hazard with two differing bedrock hazard values is shown in Figure A.6. The desired soil surface hazard ranges from about 0.5 cm/sec to 130 cm/sec. One bedrock hazard (1-Hz bedrock1) runs from about 0.6 to 90 cm/sec. The computed soil surface hazard (1Hz soil1) in this case falls to a constant value for probabilities in excess of about $4x10^{-3}$. An alternative bedrock hazard model was selected that spanned the range from 0.1 to 90 cm/sec (1Hz bedrock2). The corresponding soil surface hazard (1Hz soil2) maintained a constant slope with the bedrock hazard.

These observations can be summarized as follows: if the soil amplification is $y = z/x$ where z and x are the soil and bedrock spectral values respectively, and given a desired set of soil spectral velocities z_k, then the set of bedrock spectral velocities x_j should span the range of x_{min} to x_{max} where

$$x_{min} \leq z_{min}/y$$

and

$$x_{max} \geq z_{max}$$

Ground Motion Distribution Truncation and Minimum SAF

The effect of truncating the contributions to the complementary cumulative distribution function (CCDF) for the soil surface motion for the 10 Hz soil surface hazard is shown in Figure A.7. The bedrock hazard values are shown with dashed lines and the soil surface values are shown with the bold line (10hzsoil). Soil surface hazard using 2-σ truncation (10hz-2sigma trunc) on the CCDF of the amplification factor shows slight differences at POEs of about 10^{-5} and slightly increasing differences with decreasing POE. For the production runs made in Section 6, the CCDF was truncated at $\pm 2.5\sigma$.

Figure A.7 also illustrates the effect of limiting the reduction in the SAF on the 10 Hz soil surface hazard. Three SAF limits are shown: 1.5, 1.0, and 0.5. For the 10 Hz oscillator, significant non-linearity is apparent at a ground motion level of about 5 cm/sec corresponding to a POE of about $2x10^{-4}$. In the three cases, the soil surface hazard parallels the bedrock hazard until non-linearity reduces the soil surface hazard to a degree depending on the SAF limit and the soil surface hazard again begins to parallel the bedrock hazard. The SAF cutoff is clearly significant for 10 Hz POE's less than about 10^{-4}. Based on recommendations from Pacific Engineering, an SAF cutoff of 0.5 was used for the analyses completed in Section 6.

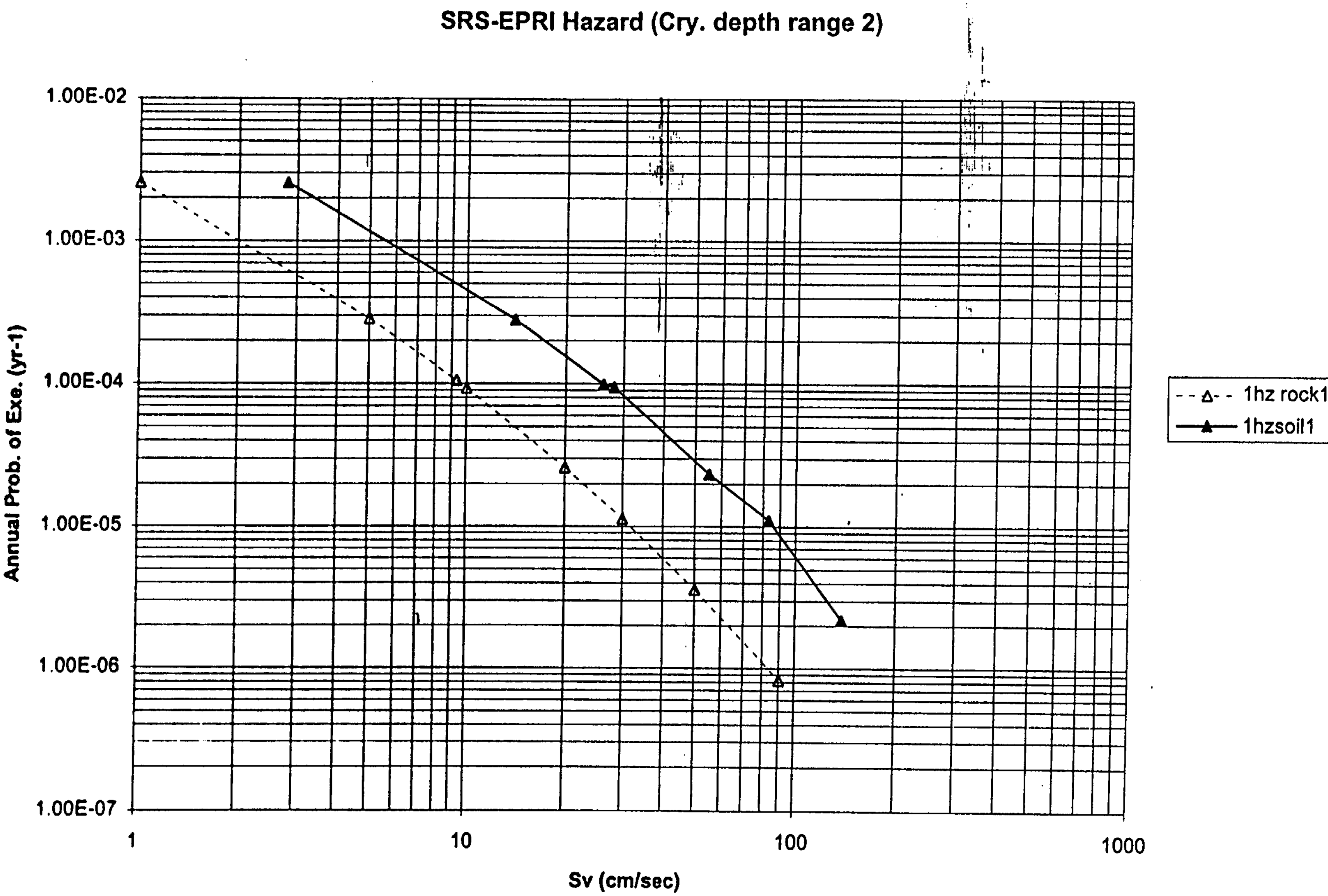

Figure A.1 - EPRI 1-Hz bedrock hazard (dashed) and soil surface hazard (solid) for crystalline depth-range 2 computed using eight (8)-reported values of bedrock hazard disaggregation.

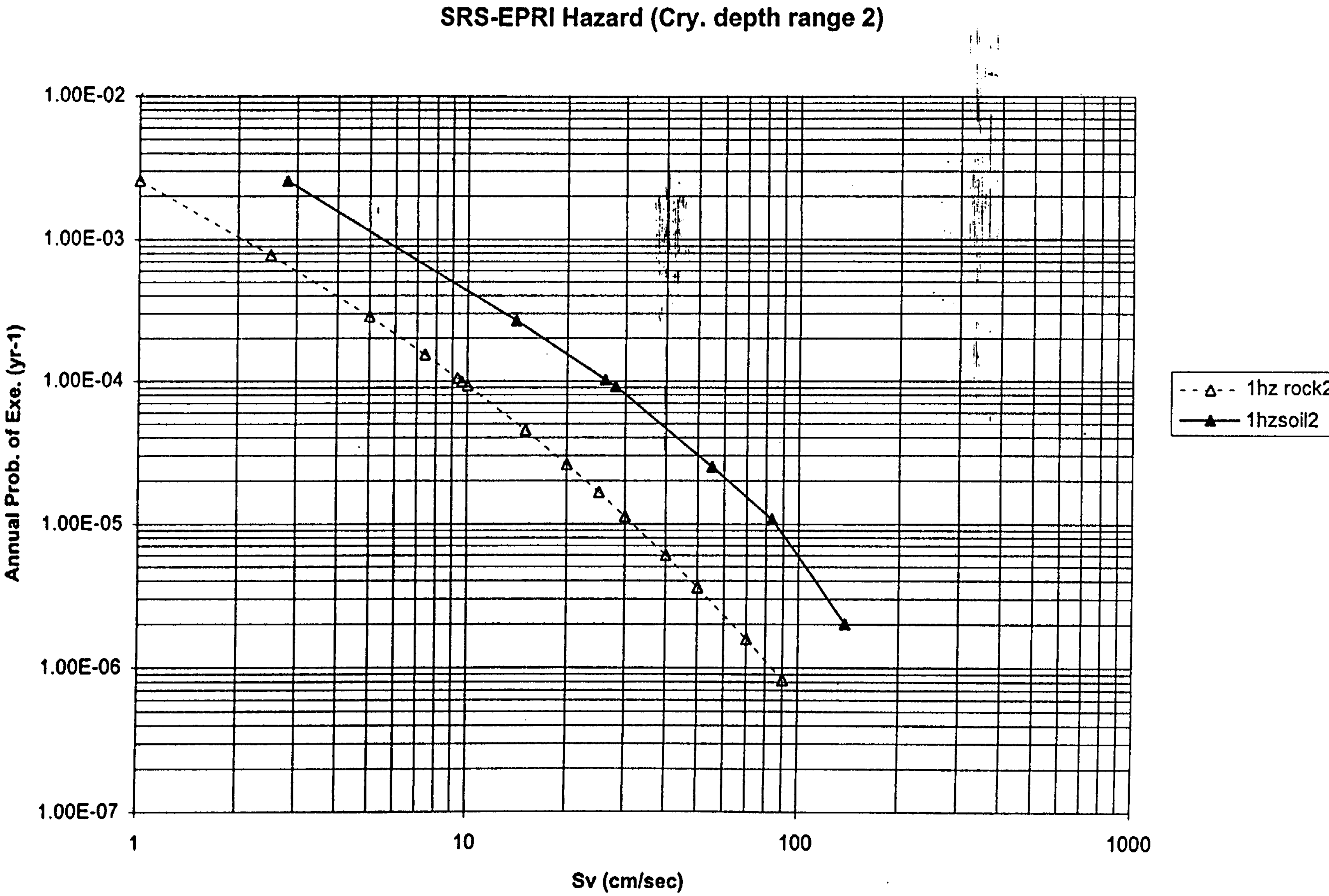

Figure A.2 - EPRI 1-Hz bedrock hazard (dashed) and soil surface hazard (solid) for crystalline depth-range 2 computed using 15 reported and interpolated values of bedrock hazard disaggregation.

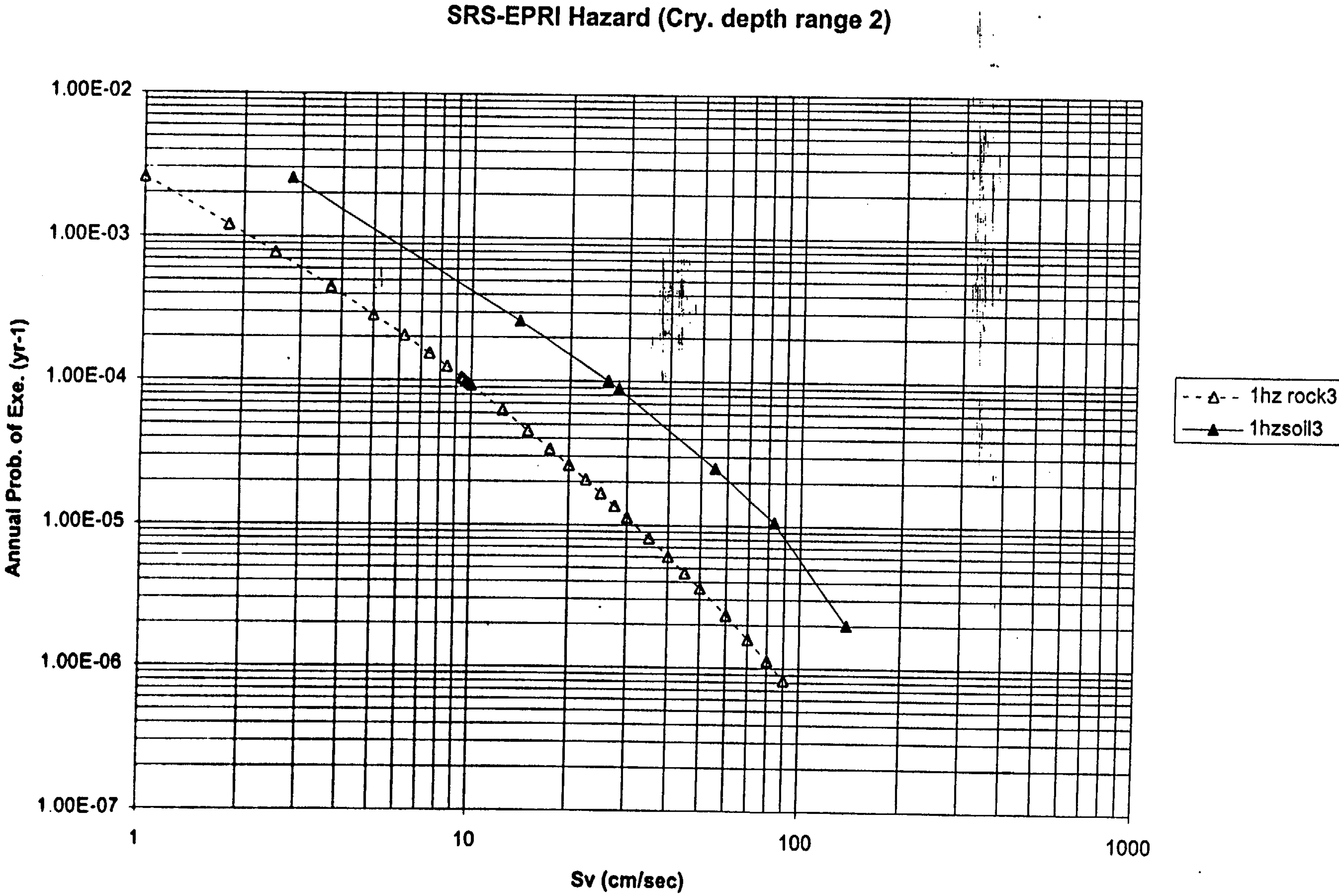

Figure A.3 - EPRI 1-Hz bedrock hazard (dashed) and soil surface hazard (solid) for crystalline depth-range 2 computed using 29 reported and interpolated values of bedrock hazard disaggregation.

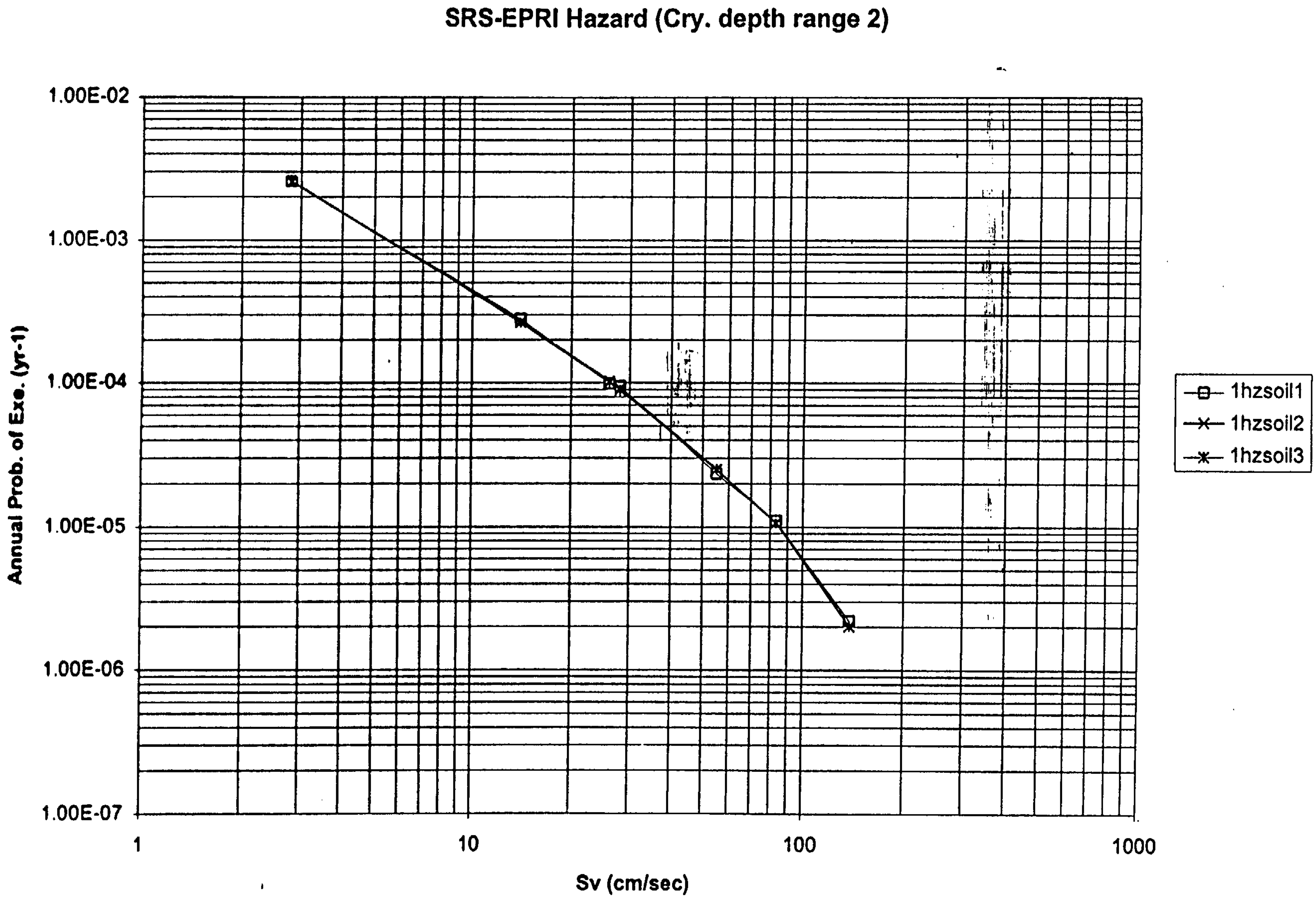

Figure A.4 - Comparison of 1-Hz EPRI soil surface hazard (solid) from Figures A.1-A.3.

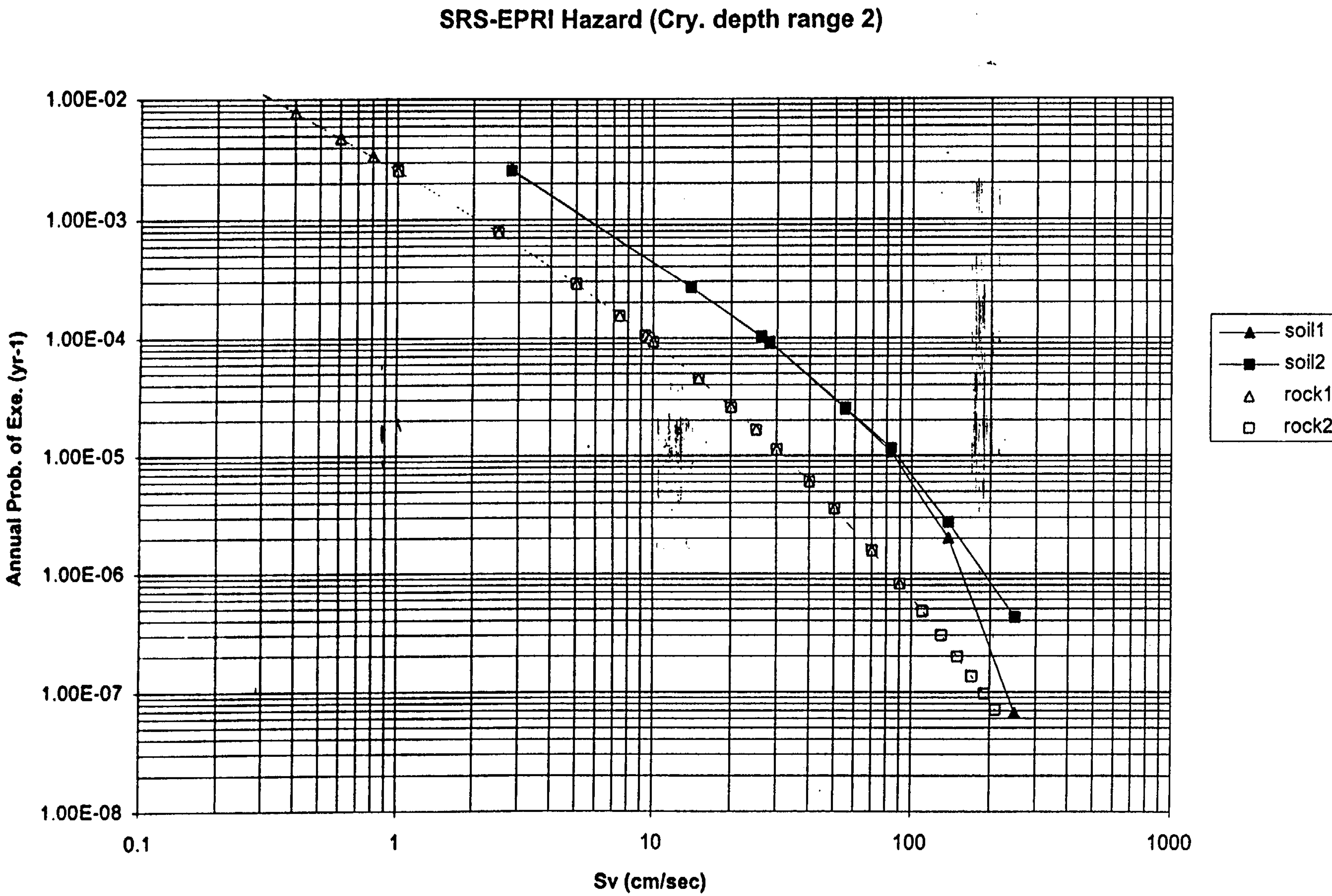

Figure A.5 - Example of sensitivity of computed soil surface hazard to extrapolation of low POE bedrock hazard for 1 Hz oscillator over crystalline bedrock, depth-range 2. Open triangles denote bedrock hazard, and solid triangles are the corresponding computed soil surface hazard. Open squares denote bedrock hazard extrapolated to approximately the same level of motion as the desired soil motion.

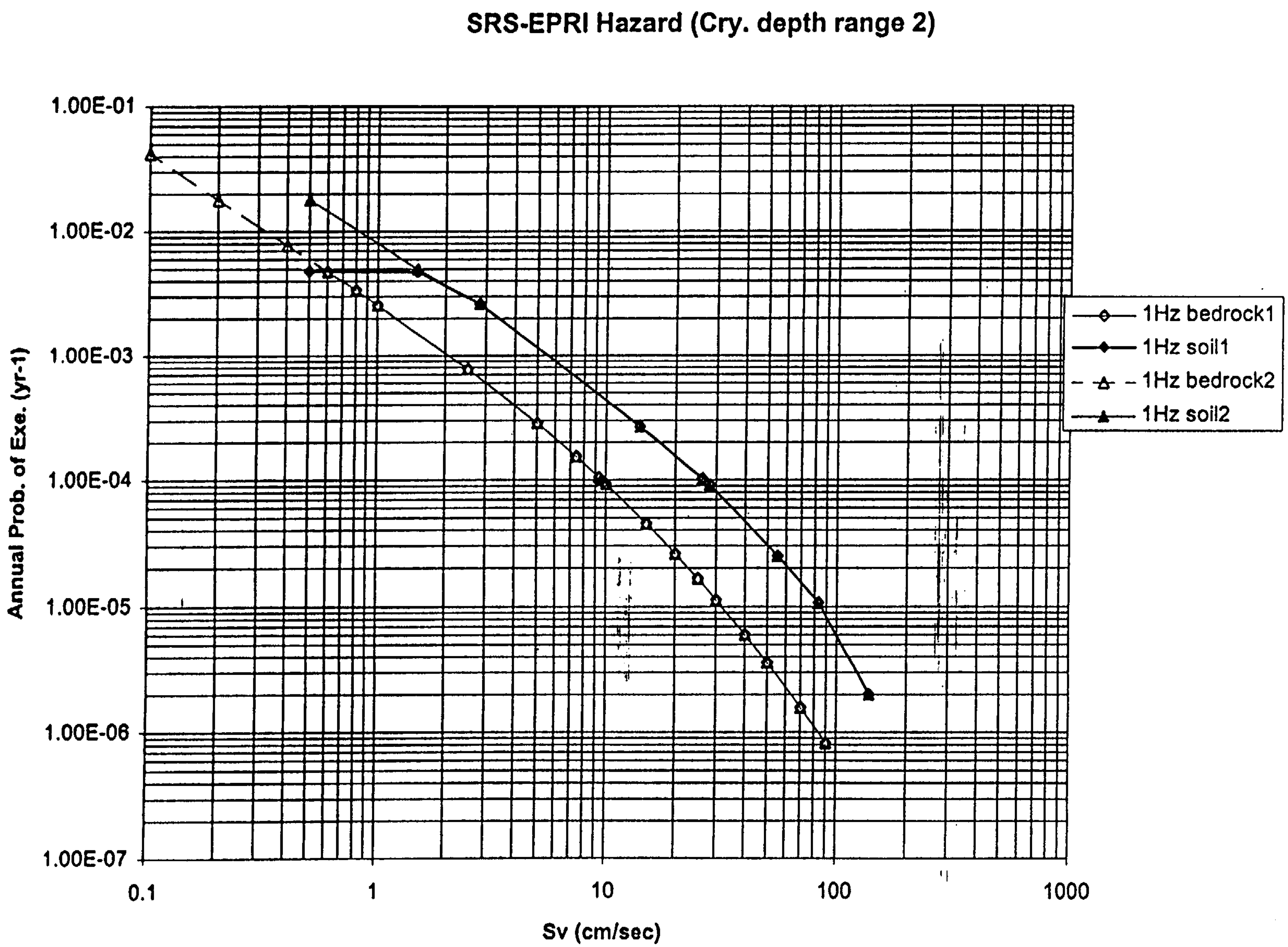

Figure A.6 - Example of sensitivity of computed soil surface hazard to extrapolation of high POE bedrock hazard for 1 Hz oscillator over crystalline bedrock, depth-range 2. Dashed line with diamonds denotes bedrock hazard, and solid line with diamonds is the corresponding computed soil surface hazard computed to the same minimum level of spectral velocity. Dashed line with open triangles denotes bedrock hazard extrapolated to lower levels of motion, and solid line with triangles is the corresponding soil surface hazard.

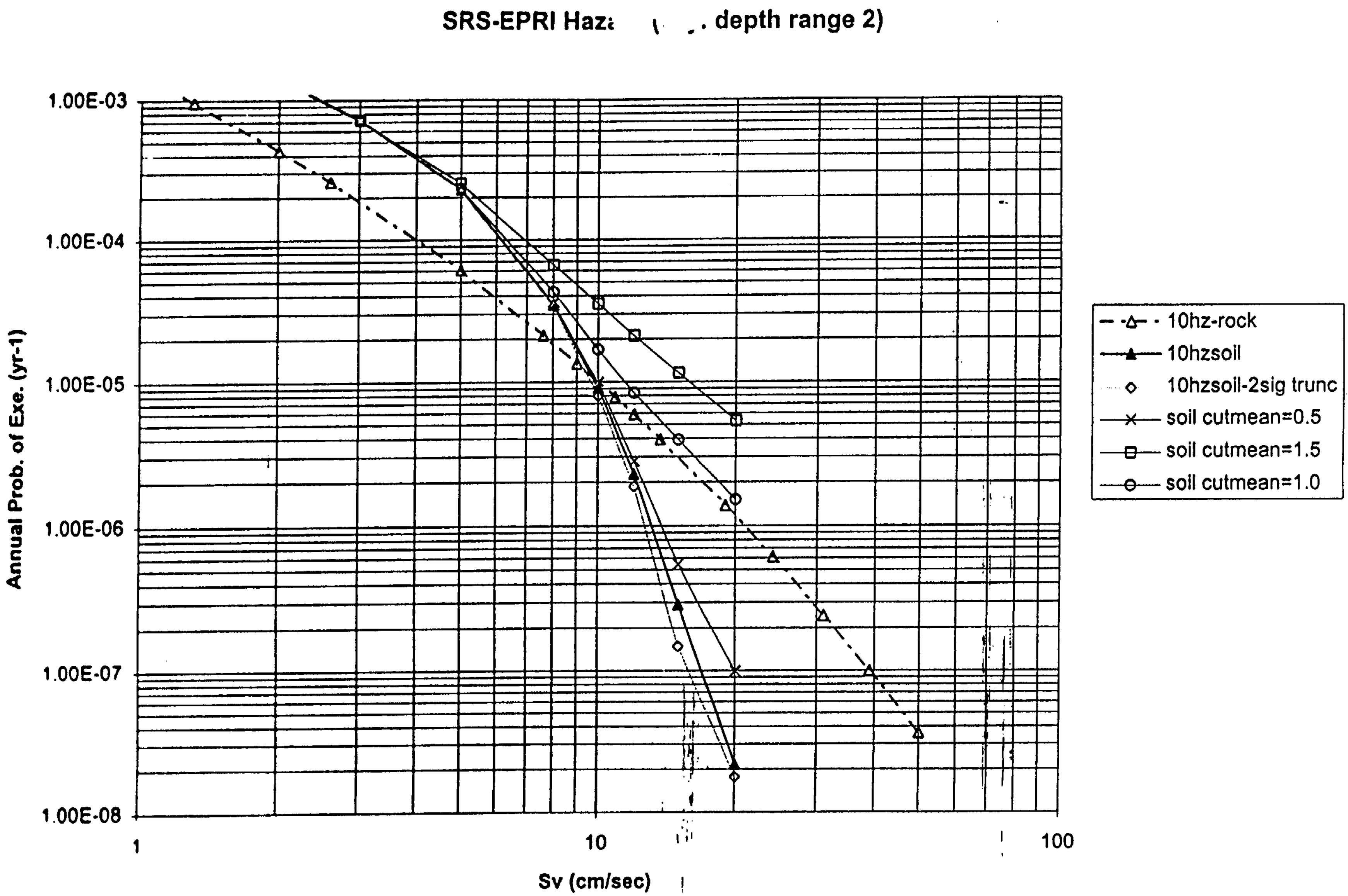

Figure A.7 - Example of sensitivity of computed soil surface hazard to assumptions on cutoffs on the SAF and CCDF for 10 Hz oscillator over crystalline bedrock, depth-range 2. Dashed line with triangles denotes bedrock hazard and the solid line with triangles denotes the soil surface hazard with no minimum on the CCDF or on the SAF. Solid line with squares corresponds to a minimum of 1.5 on the SAF. Solid lines with open circles and x's correspond to SAF minimums of 1.0 and 0.5 respectively. The solid line with diamonds corresponds to no minimum SAF and 1 2-σ truncation of the CCDF.

APPENDIX B

SENSITIVITY STUDIES ON MAGNITUDE DEPENDENCE OF SOIL SURFACE HAZARD

To explore sensitivity of the soil surface hazard results to the bedrock hazard magnitude disaggregation, the combined EPRI/LLNL bedrock hazard was used to compute SRS soil surface hazard at the four oscillator frequencies with the magnitude disaggregation constraining sequentially ML, MM, and MH. Three separate soil surface hazard evaluations were completed for the four frequencies using ML, MM and MH SAFs. Figures B.1(a), B.1(b), and B.1(c) show the low (ML), medium (MM) and high magnitude (MH)-constrained soil surface hazard respectively for the 1 Hz oscillator frequency. Figure sets B.2, B.3, and B.4 are the soil surface hazard curves for 2.5, 5 and 10 Hz oscillator frequencies respectively.

As expected for a given oscillator frequency, comparison of the segments of the hazard curve, where soil motions are primarily in the linear range, show little magnitude dependence. For the 1 Hz soil surface hazard curves shown in Figure set B.1, evidence of non-linearity is apparent for spectral velocities greater than about 50 cm/sec. At higher velocities, the ML and MM magnitudes show only slight changes in slope from soil degradation, primarily in the Triassic sediments. The MH-magnitude shows significant effects of soil degradation. This magnitude dependence is consistent with the SAFs (Figures 5.3, 5.4, 5.5) where at 1 Hz the low- and medium-magnitude SAF ranges from only about 2.6-2.9 and 2.4-2.7 respectively. Natural-log standard deviation ranges from 0.1-0.24 and 0.1-0.18 for low- and medium magnitudes respectively. The high-magnitude SAF exhibits a much higher range from about 1.7-2.7s and has a corresponding natural-log standard deviation ranging from 0.11-0.26.

The low- and medium-magnitude 1 Hz soil surface hazard approximately follows the bedrock hazard at all levels of ground motion (Figures B.1a,b). The high-magnitude soil surface hazard exhibits a rapid change in slope for spectral velocities greater than about 60 cm/sec. Beyond about 200 cm/sec the high-magnitude soil surface hazard (Figure B.1c) returns to the approximate slope of the bedrock hazard as a result of the limit of the range of control motions used to develop the SAFs.

The 2.5 Hz magnitude-constrained soil surface hazard (Figure B.2) exhibits similar behavior, i.e., more linear behavior for spectral velocities less than about 20 cm/sec and then a significant change in slope for velocities between about 20-60 cm/sec, and for velocities greater than about 60 cm/sec a return to the average slope of the bedrock hazard curve.

The 5 Hz and 10 Hz magnitude-constrained soil surface hazard (Figures B.3 and B.4) exhibits similar behavior: at lower motions (high POEs), soil surface hazard curves have approximately the same slope as the bedrock hazard, and at moderately high

motions (> 10 cm/sec for 5 Hz and > 3 cm/sec for 10 Hz oscillator), the soil surface hazard slope increases substantially due to the degradation of the soil column. As the soil motions increase (> 30 cm/sec for 5 Hz and > 18 cm/sec for 10 Hz oscillator) the hazard begins to again parallel the bedrock hazard because at this point, bedrock motions exceed the range in control motions specified for the SAFs.

These results show that the hazard disaggregation is of first order importance for lower POEs. This result emphasizes the need for a detailed hazard disaggregation and for a magnitude dependent SAF.

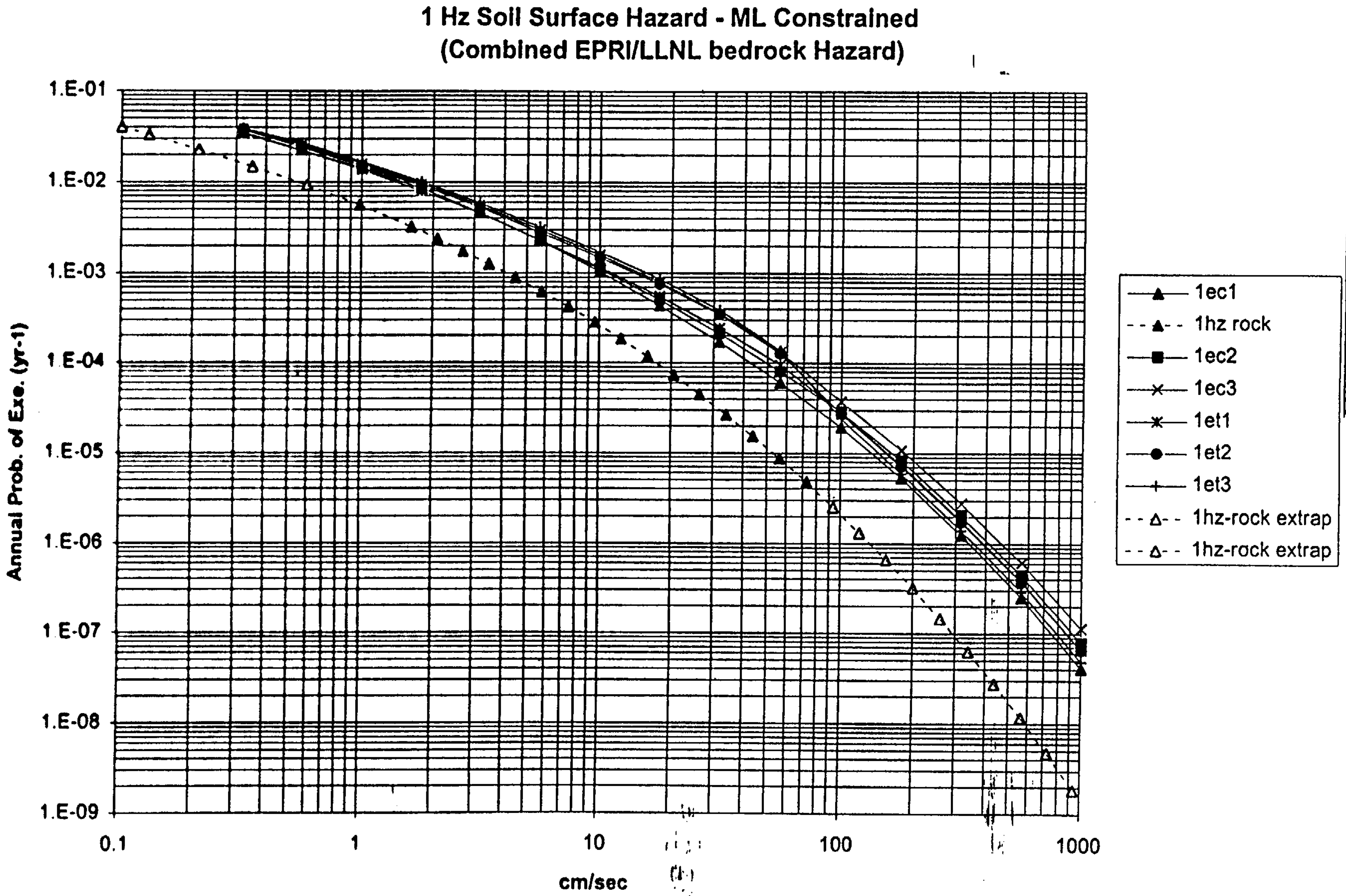

Figure B.1 (a) - Computed 1-Hz soil surface hazard curves with disaggregation constrained to ML. EPRI/LLNL bedrock hazard continued to soil surface (solid lines). Hazard curves reflect six soil and bedrock conditions (see Section 6 for explanation of legend). EPRI/LLNL 1-Hz bedrock hazard (dashed line) is shown for interpolated segments (solid symbols) and extrapolated segments (open symbols).

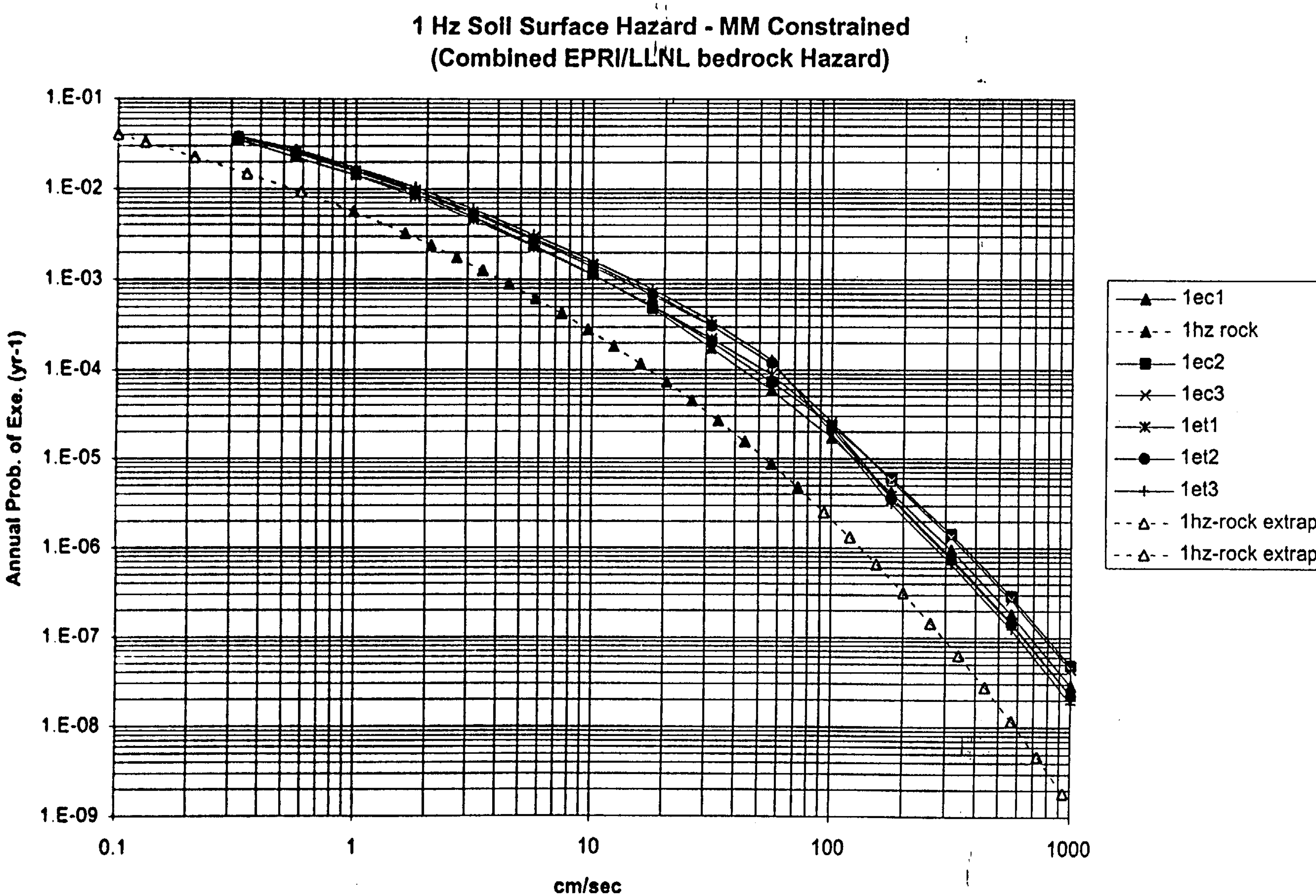

Figure B.1 (b) - Computed 1-Hz soil surface hazard curves with disaggregation constrained to MM. EPRI/LLNL bedrock hazard continued to soil surface (solid lines). Hazard curves reflect six soil and bedrock conditions (see Section 6 for explanation of legend). EPRI/LLNL 1-Hz bedrock hazard (dashed line) is shown for interpolated segments (solid symbols) and extrapolated segments (open symbols).

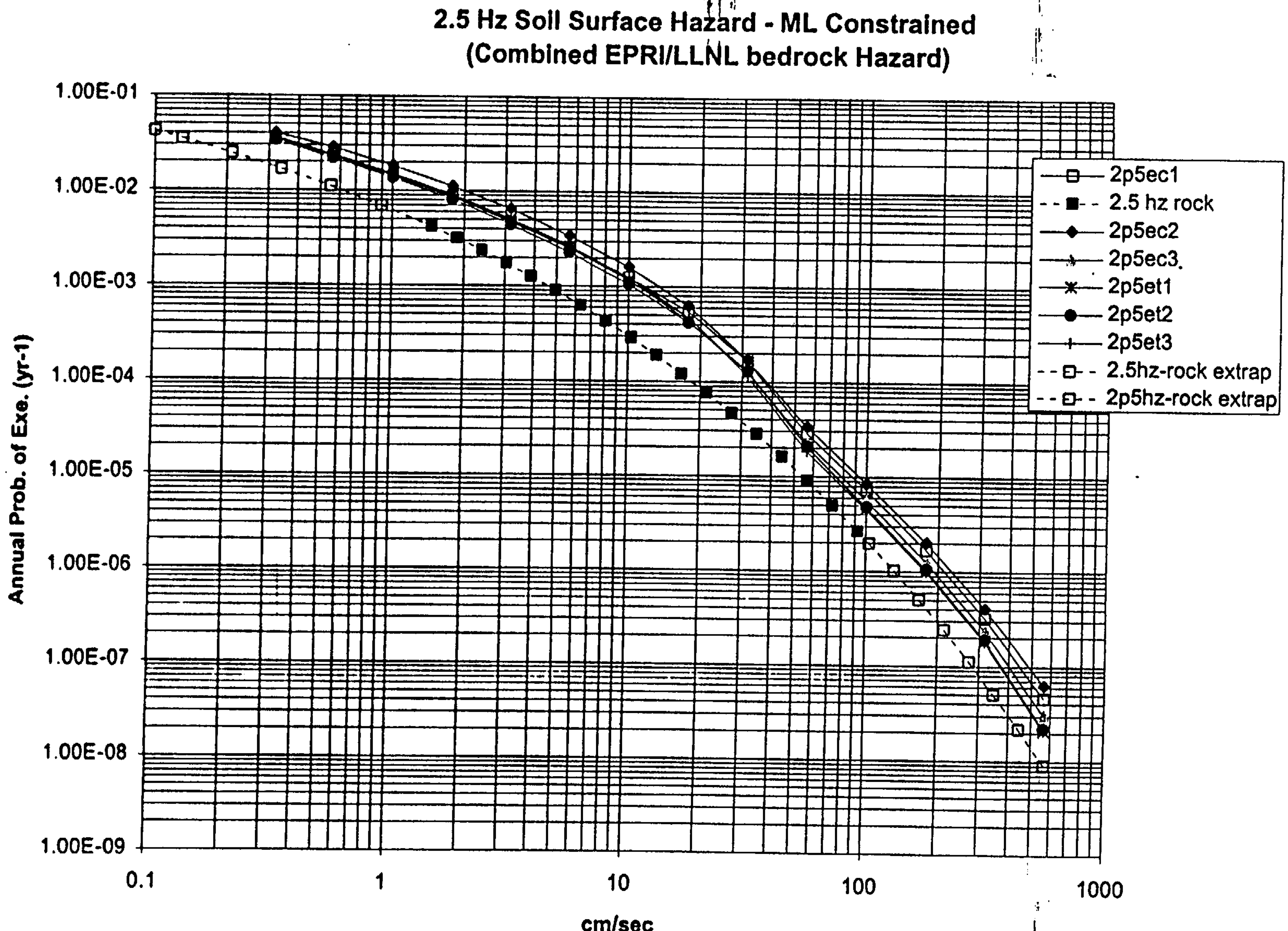

Figure B.2 (a) - Computed 2.5-Hz soil surface hazard curves with disaggregation constrained to ML. EPRI/LLNL bedrock hazard continued to soil surface (solid lines). Hazard curves reflect six soil and bedrock conditions (see Section 6 for explanation of legend). EPRI/LLNL 2.5-Hz bedrock hazard (dashed line) is shown for interpolated segments (solid symbols) and extrapolated segments (open symbols).

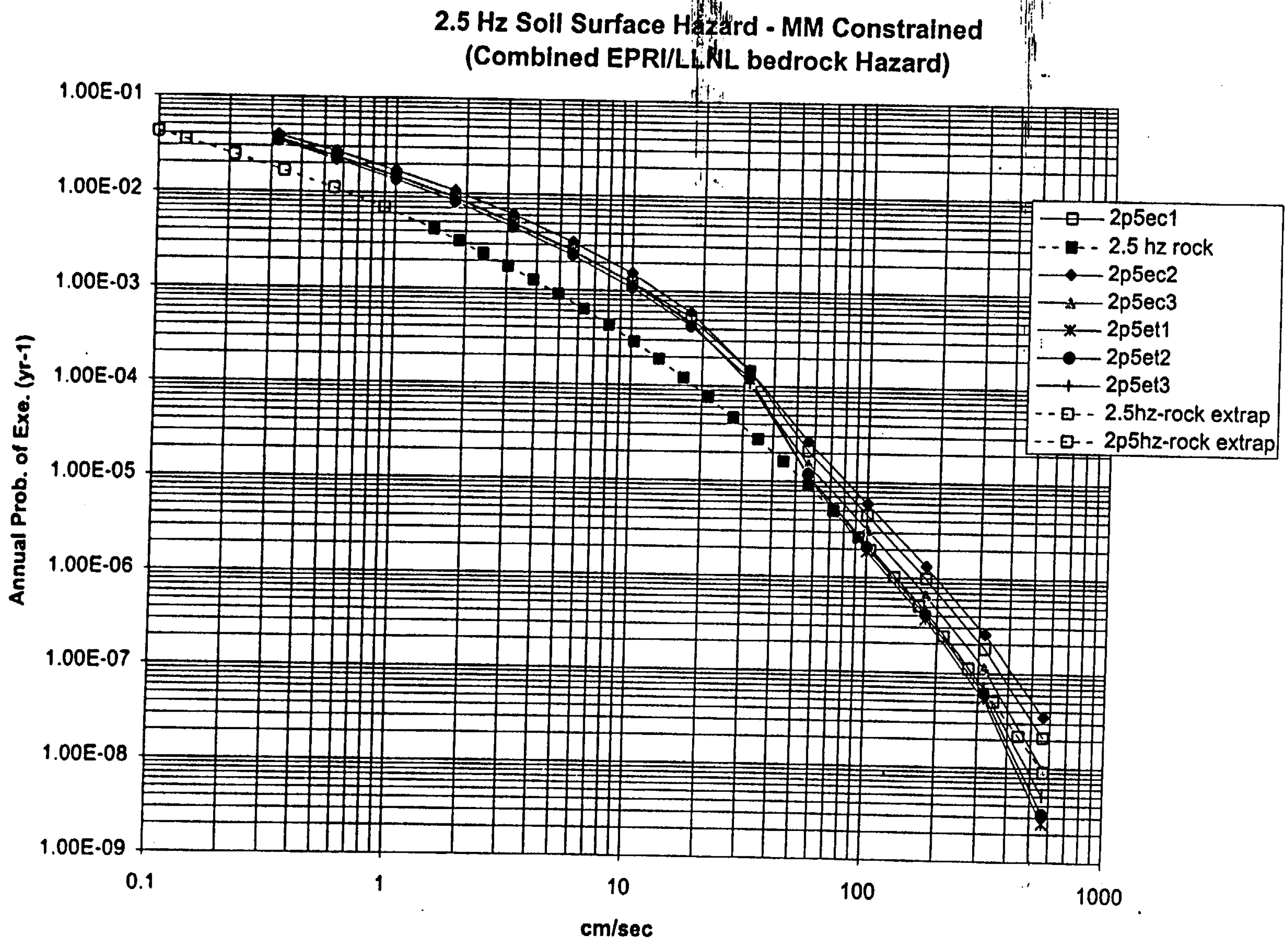

Figure B.2 (b) - Computed 2.5-Hz soil surface hazard curves with disaggregation constrained to MM. EPRI/LLNL bedrock hazard continued to soil surface (solid lines). Hazard curves reflect six soil and bedrock conditions (see Section 6 for explanation of legend). EPRI/LLNL 2.5-Hz bedrock hazard (dashed line) is shown for interpolated segments (solid symbols) and extrapolated segments (open symbols).

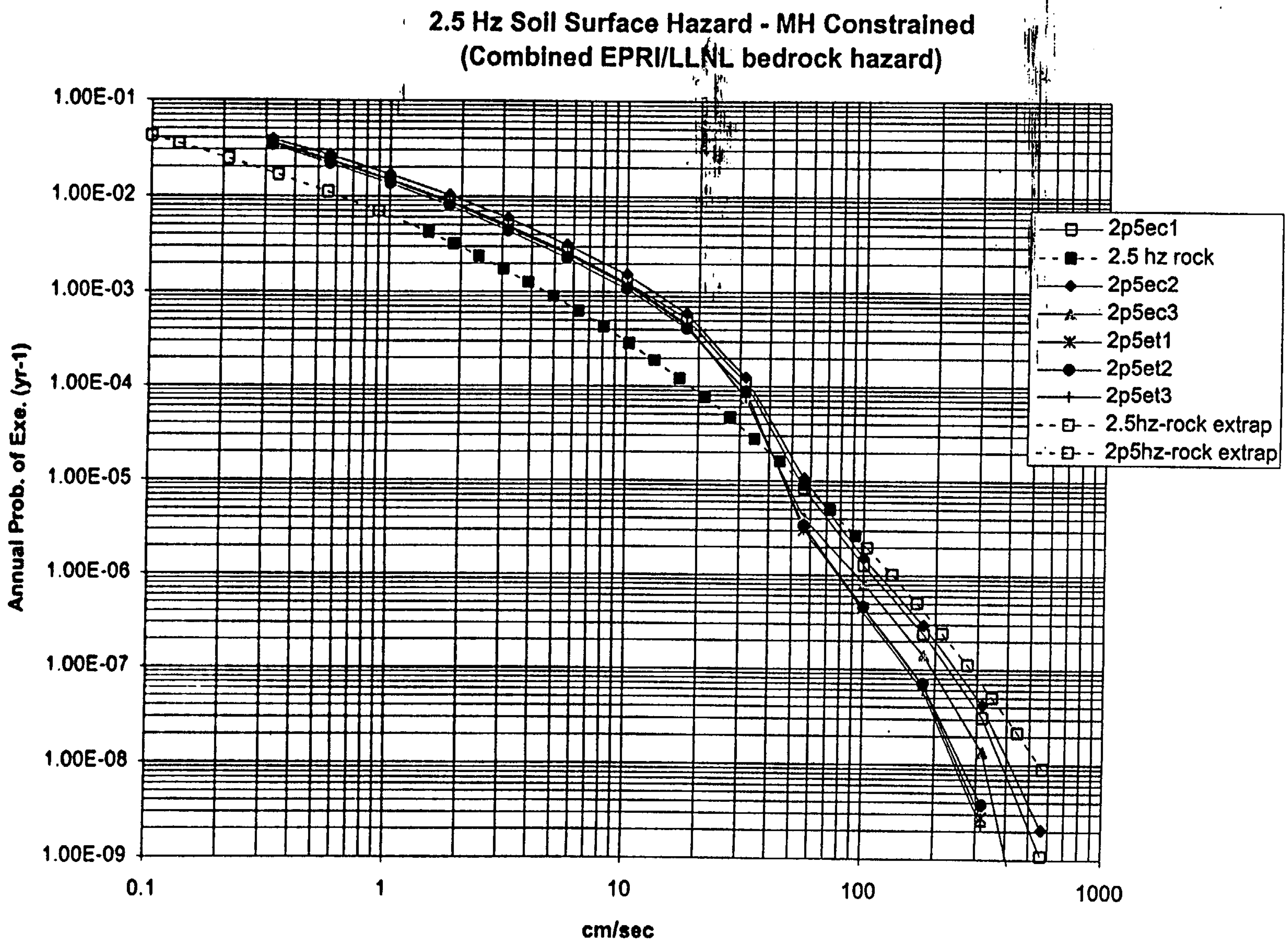

Figure B.2 (c) - Computed 2.5-Hz soil surface hazard curves with disaggregation constrained to MH. EPRI/LLNL bedrock hazard continued to soil surface (solid lines). Hazard curves reflect six soil and bedrock conditions (see Section 6 for explanation of legend). EPRI/LLNL 2.5-Hz bedrock hazard (dashed line) is shown for interpolated segments (solid symbols) and extrapolated segments (open symbols).

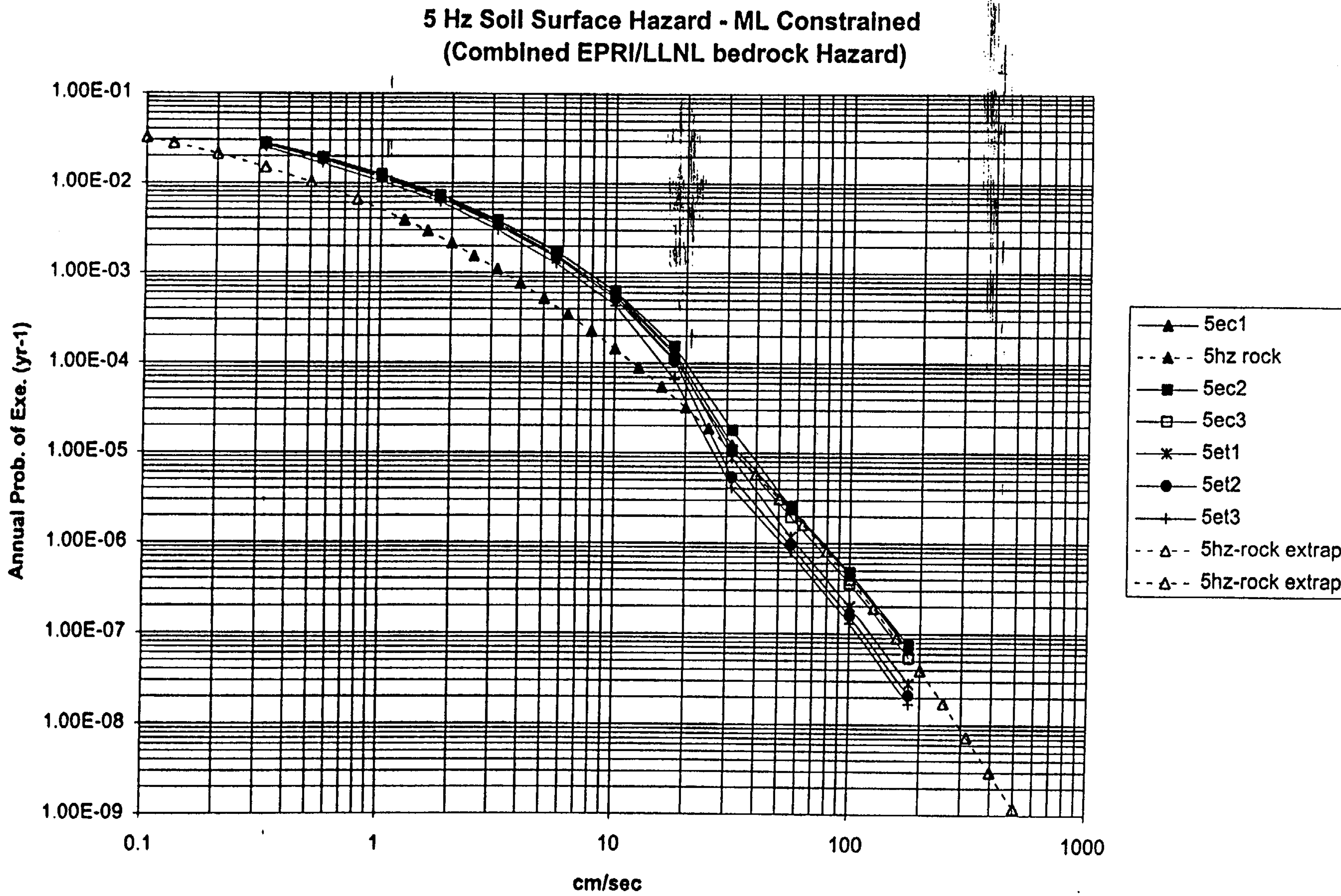

Figure B.3 (a) - Computed 5-Hz soil surface hazard curves with disaggregation constrained to ML. EPRI/LLNL bedrock hazard continued to soil surface (solid lines). Hazard curves reflect six soil and bedrock conditions (see Section 6 for explanation of legend). EPRI/LLNL 5-Hz bedrock hazard (dashed line) is shown for interpolated segments (solid symbols) and extrapolated segments (open symbols).

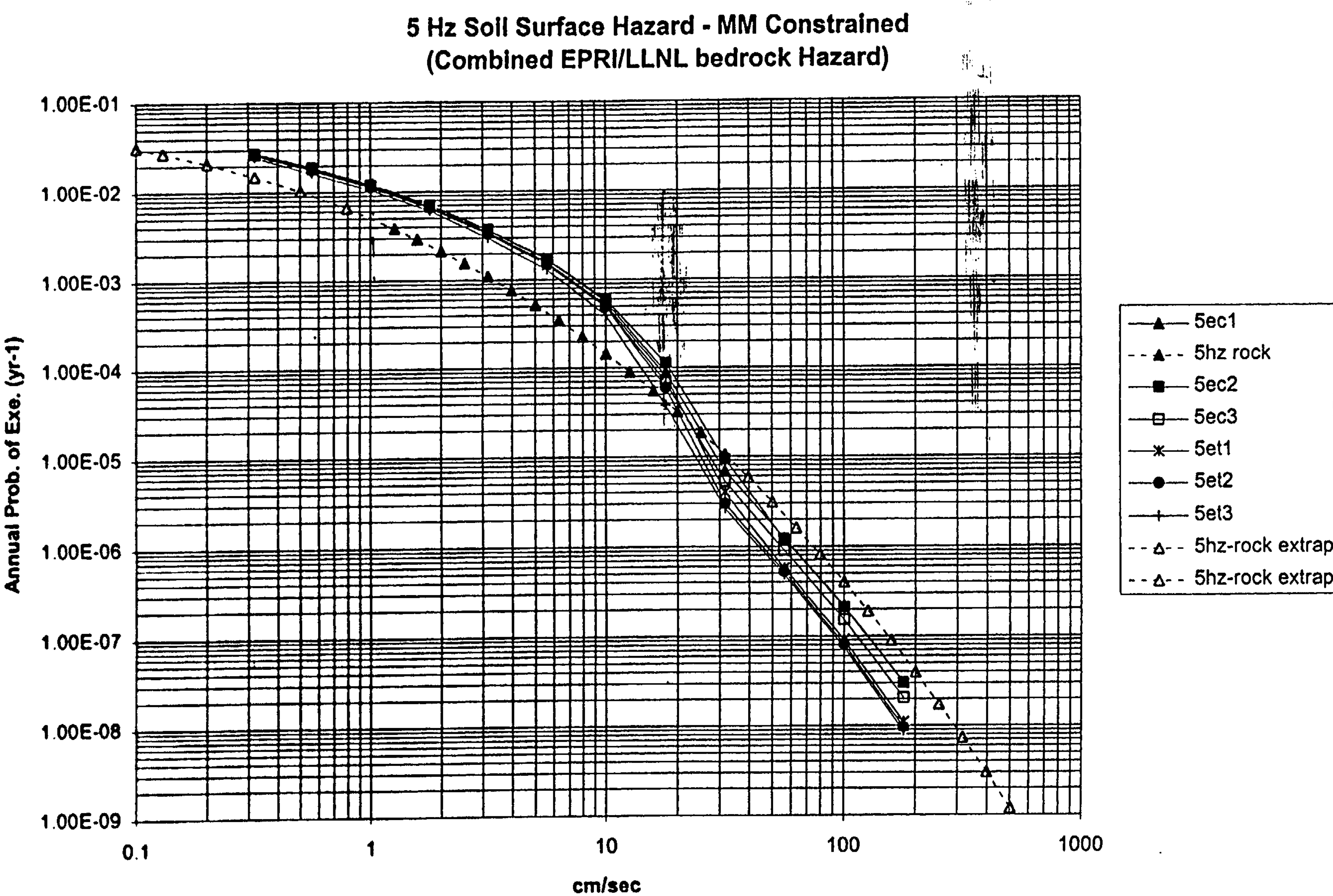

Figure B.3 (b) - Computed 5-Hz soil surface hazard curves with disaggregation constrained to MM. EPRI/LLNL bedrock hazard continued to soil surface (solid lines). Hazard curves reflect six soil and bedrock conditions (see Section 6 for explanation of legend). EPRI/LLNL 5-Hz bedrock hazard (dashed line) is shown for interpolated segments (solid symbols) and extrapolated segments (open symbols).

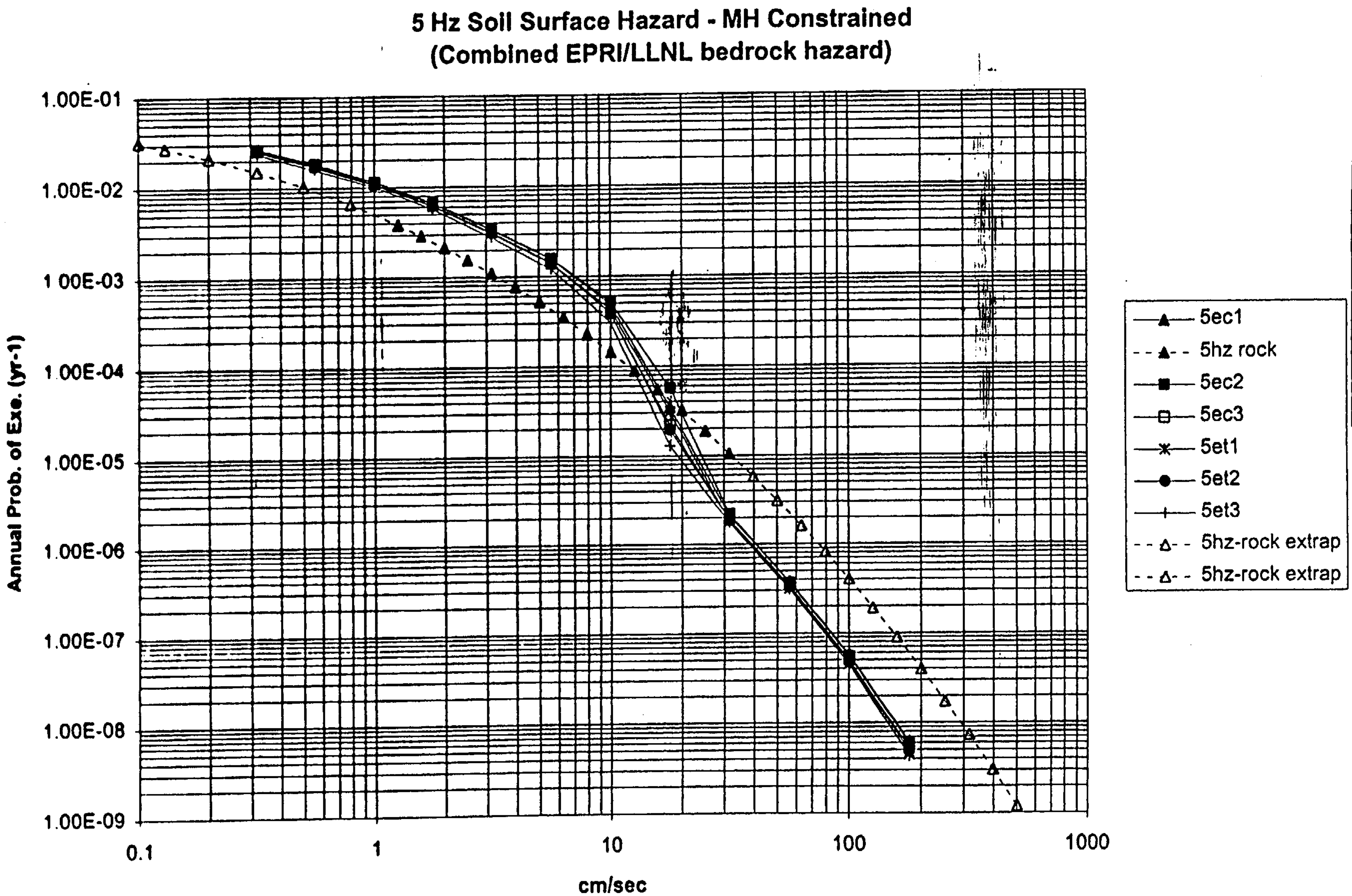

Figure B.3 (c) - Computed 5-Hz soil surface hazard curves with disaggregation constrained to MM. EPRI/LLNL bedrock hazard continued to soil surface (solid lines). Hazard curves reflect six soil and bedrock conditions (see Section 6 for explanation of legend). EPRI/LLNL 5-Hz bedrock hazard (dashed line) is shown for interpolated segments (solid symbols) and extrapolated segments (open symbols).

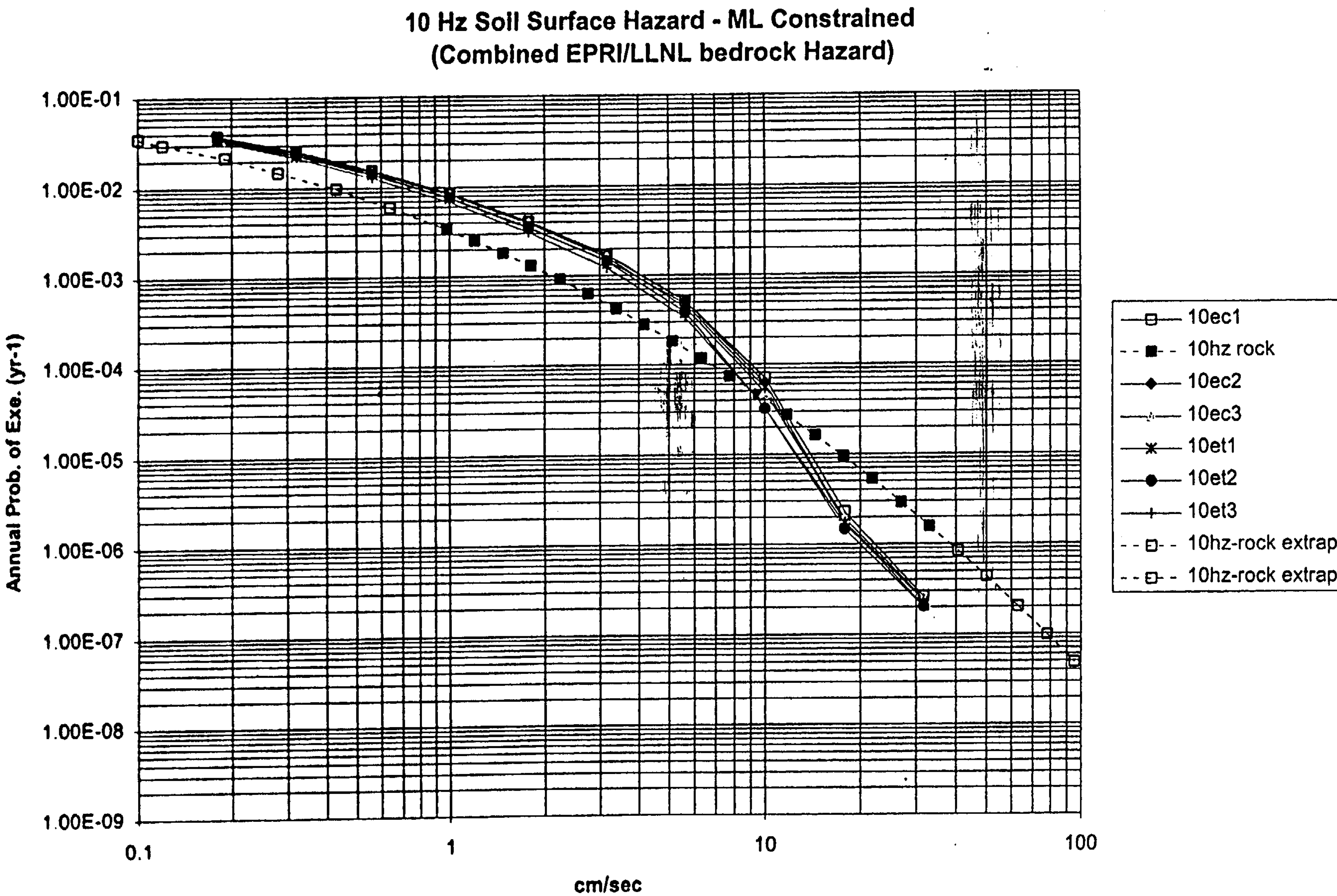

Figure B.4 (a) - Computed 10-Hz soil surface hazard curves with disaggregation constrained to ML. EPRI/LLNL bedrock hazard continued to soil surface (solid lines). Hazard curves reflect six soil and bedrock conditions (see Section 6 for explanation of legend). EPRI/LLNL 10-Hz bedrock hazard (dashed line) is shown for interpolated segments (solid symbols) and extrapolated segments (open symbols).

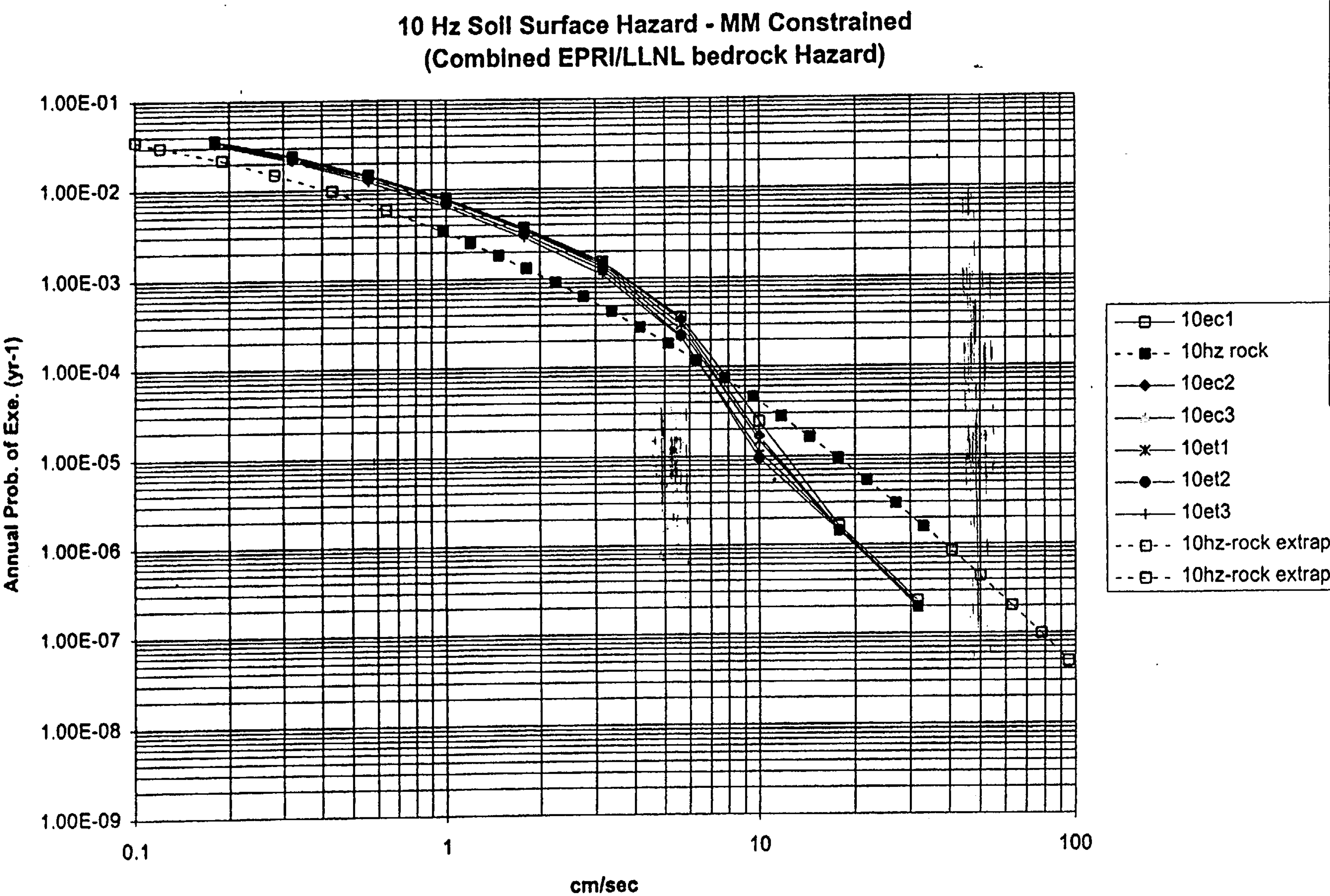

Figure B.4 (b) - Computed 10-Hz soil surface hazard curves with disaggregation constrained to MM. EPRI/LLNL bedrock hazard continued to soil surface (solid lines). Hazard curves reflect six soil and bedrock conditions (see Section 6 for explanation of legend). EPRI/LLNL 10-Hz bedrock hazard (dashed line) is shown for interpolated

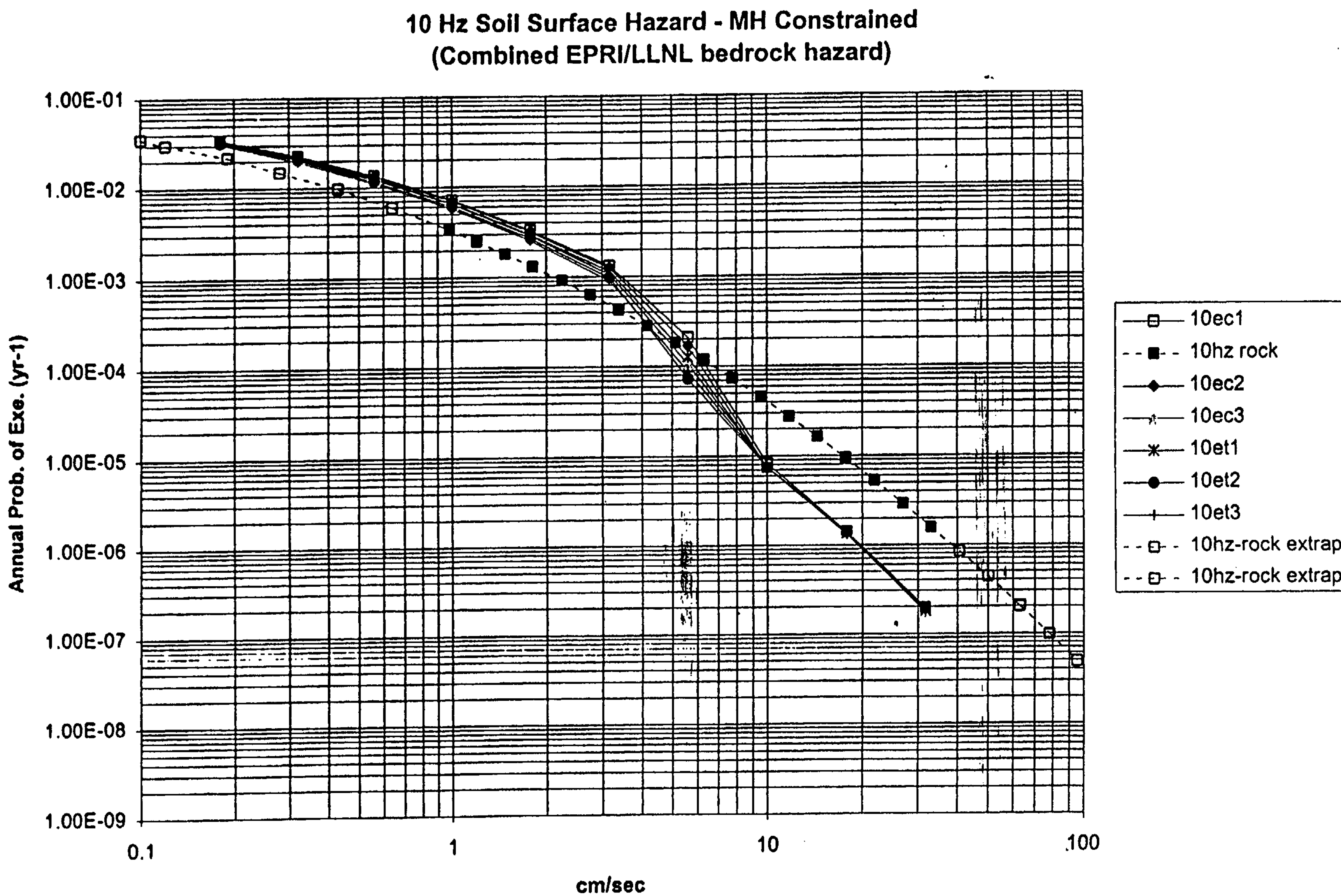

Figure B.4 (c) - Computed 10-Hz soil surface hazard curves with disaggregation constrained to MH. EPRI/LLNL bedrock hazard continued to soil surface (solid lines). Hazard curves reflect six soil and bedrock conditions (see Section 6 for explanation of legend). EPRI/LLNL 10-Hz bedrock hazard (dashed line) is shown for interpolated segments (solid symbols) and extrapolated segments (open symbols).

APPENDIX C

SOIL SURFACE HAZARD BASED ON COMBINED EPRI and LLNL BEDROCK HAZARD

As noted in Section 6, soil surface hazard is evaluated in this report in two ways: (1) evaluate EPRI and LLNL soil surface hazard separately and combine the two hazards at the soil surface; and (2) combine the EPRI and LLNL hazard at bedrock and continue that combined hazard to the soil surface. At higher oscillator frequencies the combined EPRI and LLNL soil surface hazard was lower than the surface hazard derived from the combined EPRI and LLNL bedrock hazard. The combined EPRI and LLNL soil surface hazard curves are included in this Appendix.

Figures C.1 through C.4 are the EPRI/LLNL soil surface hazard curves derived from the combined EPRI and LLNL hazard at bedrock for the 1, 2.5, 5, and 10 Hz oscillators respectively. These evaluations were done using EPRI and LLNL bedrock hazard and the EPRI disaggregation and SRS SAFs.

Figures C.5 and C.6 are the combined EPRI/LLNL soil surface hazard envelopes for spectral velocity and spectral acceleration respectively.

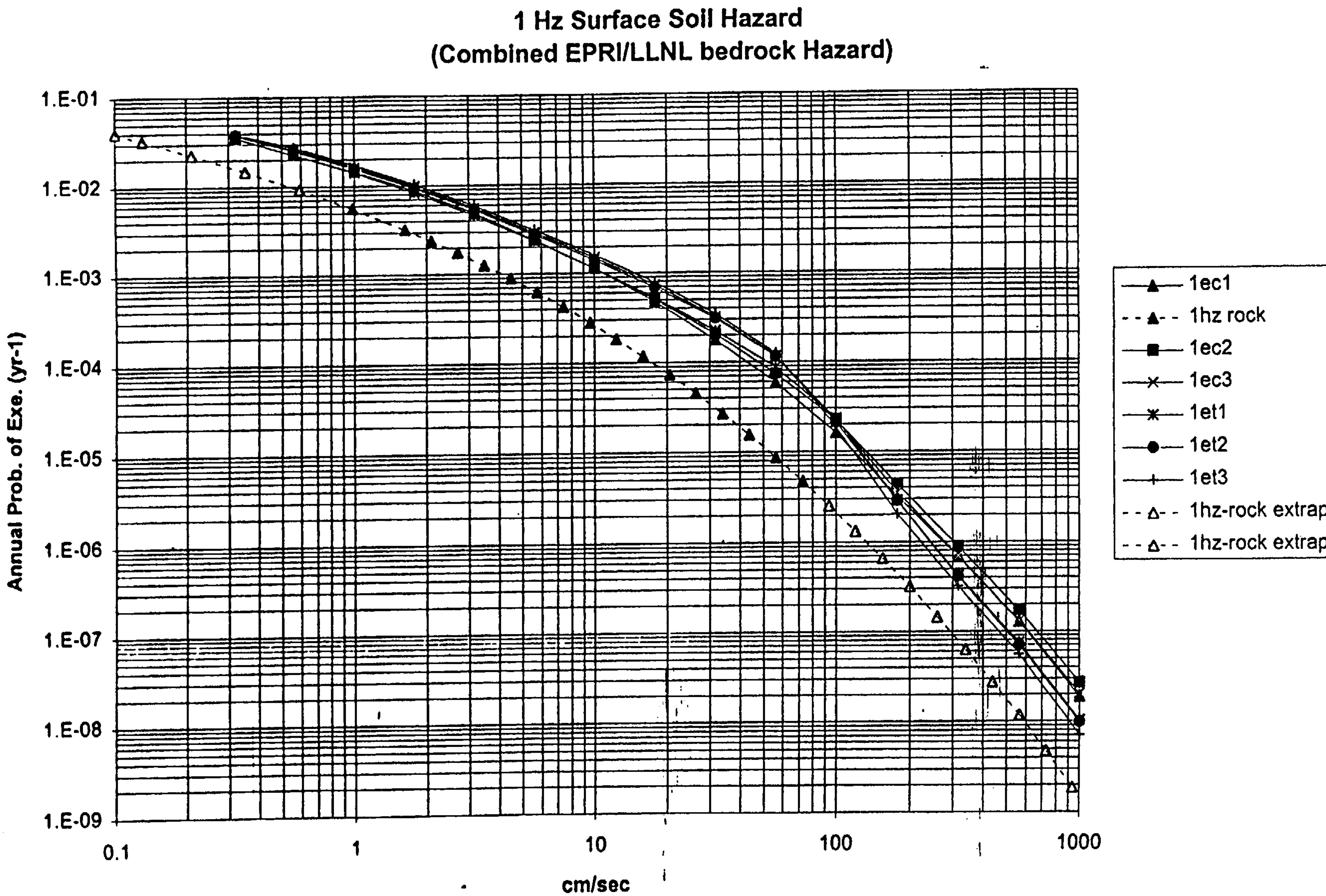

Figure C.1 - Computed 1-Hz soil surface hazard curves derived from combined EPRI/LLNL bedrock hazard (solid lines). Hazard curves are for six soil and bedrock conditions (see Section 6 for explanation of legend). EPRI/LLNL 1-Hz bedrock hazard (dashed line) is shown for interpolated segments (solid symbols) and extrapolated segments (open symbols).

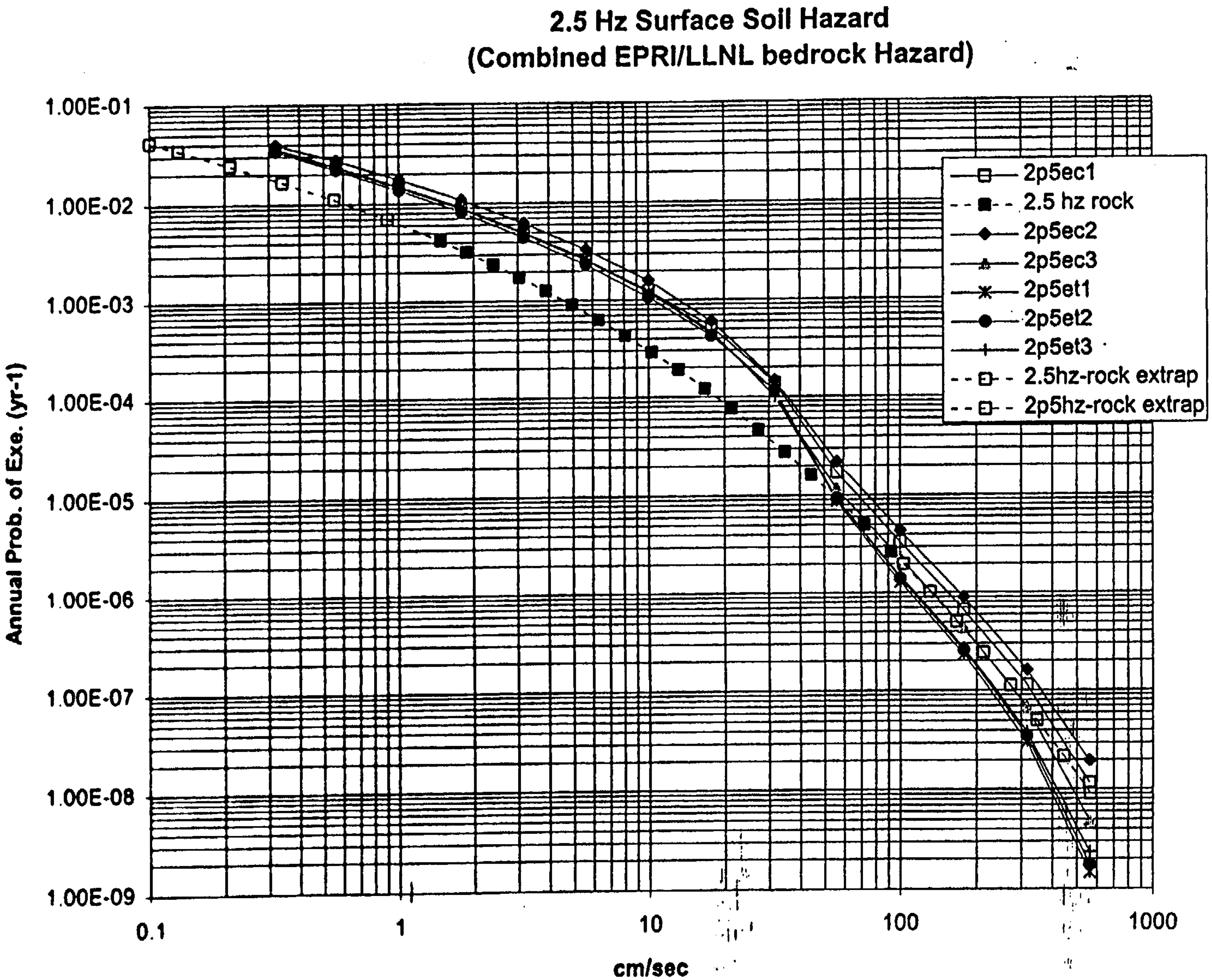

Figure C.2 - Computed 2.5-Hz soil surface hazard curves derived from combined EPRI/LLNL bedrock hazard (solid lines). Hazard curves are for six soil and bedrock conditions (see Section 6 for explanation of legend). EPRI/LLNL 2.5-Hz bedrock hazard (dashed line) is shown for interpolated segments (solid symbols) and extrapolated segments (open symbols).

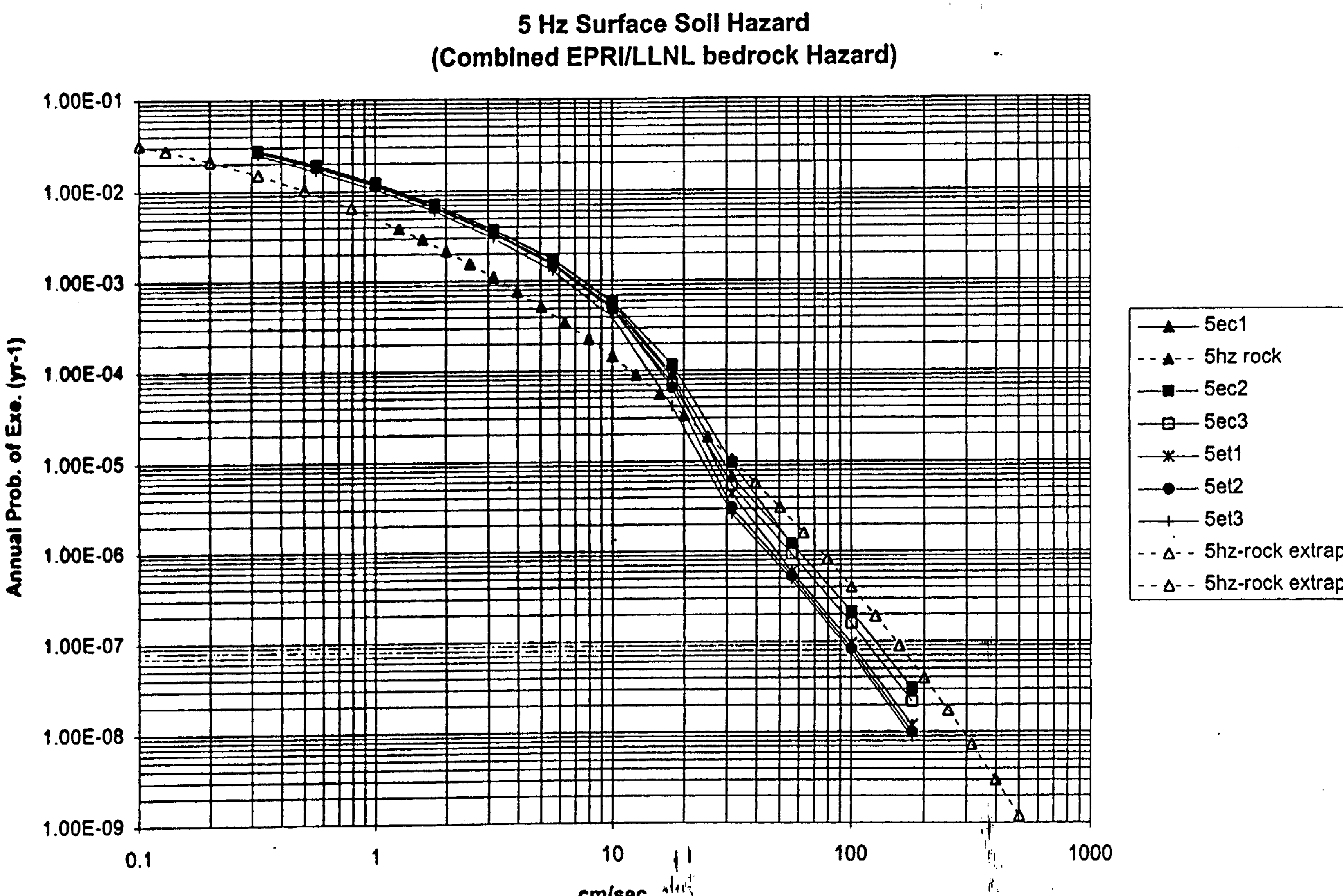

Figure C.3 - Computed 5-Hz soil surface hazard curves derived from combined EPRI/LLNL bedrock hazard (solid lines). Hazard curves are for six soil and bedrock conditions (see Section 6 for explanation of legend). EPRI/LLNL 5-Hz bedrock hazard (dashed line) is shown for interpolated segments (solid symbols) and extrapolated segments (open symbols).

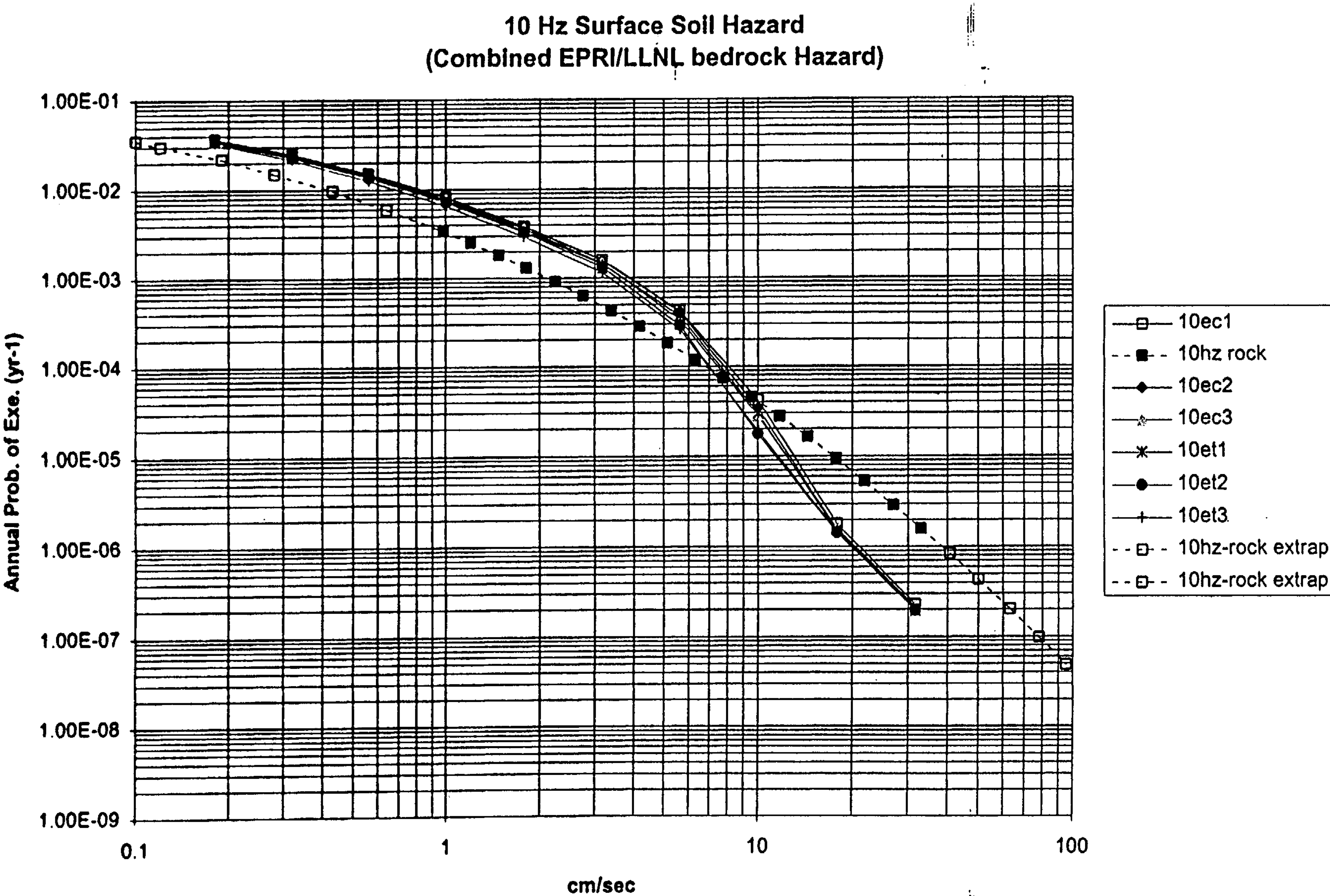

Figure C.4 - Computed 10-Hz soil surface hazard curves derived from combined EPRI/LLNL bedrock hazard (solid lines). Hazard curves are for six soil and bedrock conditions (see Section 6 for explanation of legend). EPRI/LLNL 10-Hz bedrock hazard (dashed line) is shown for interpolated segments (solid symbols) and extrapolated segments (open symbols).

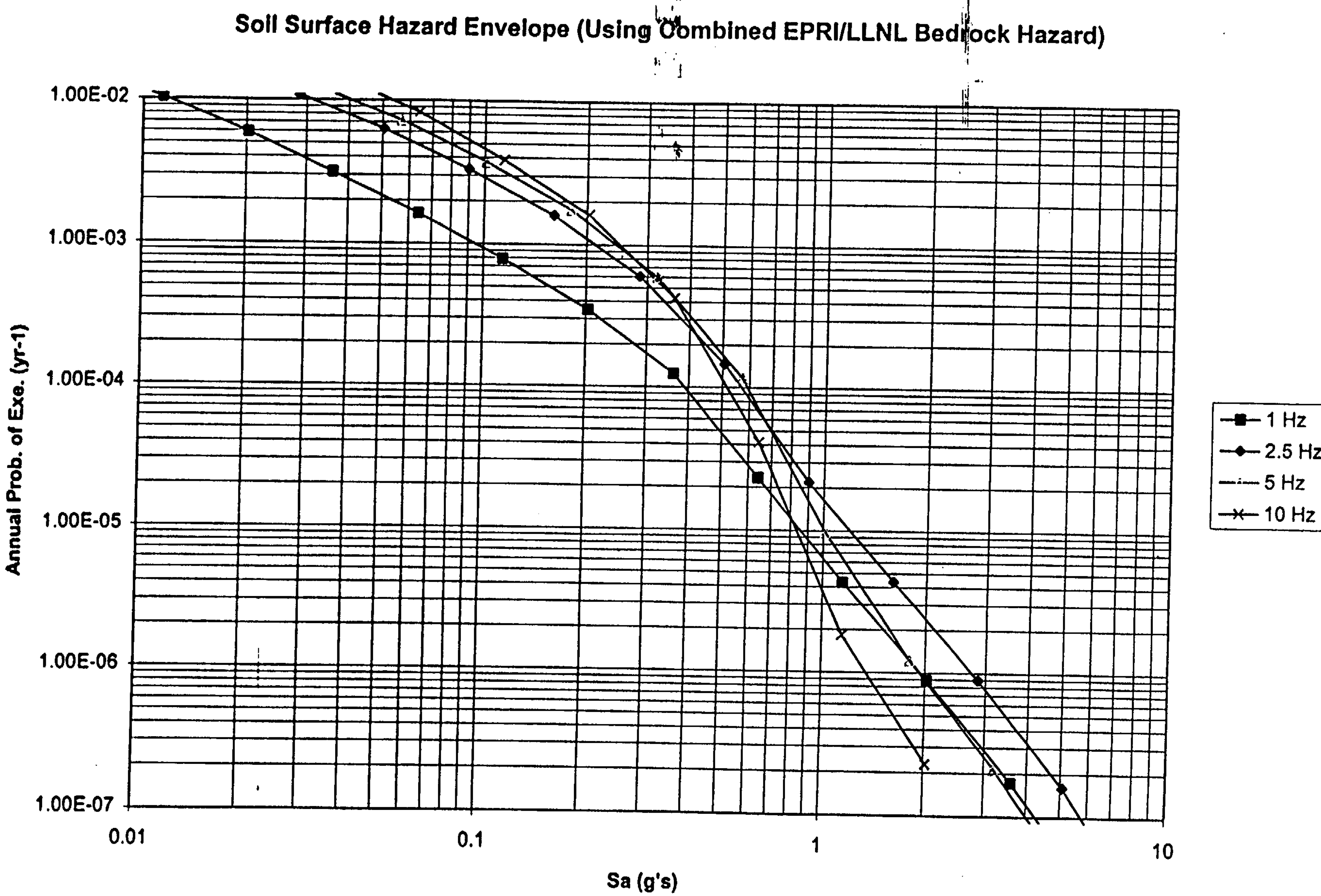

Figure C.5 - Computed soil surface hazard envelope using combined EPRI/LLNL bedrock hazard (solid lines). Hazard curves are for the four oscillator frequencies. POE plotted against spectral acceleration.

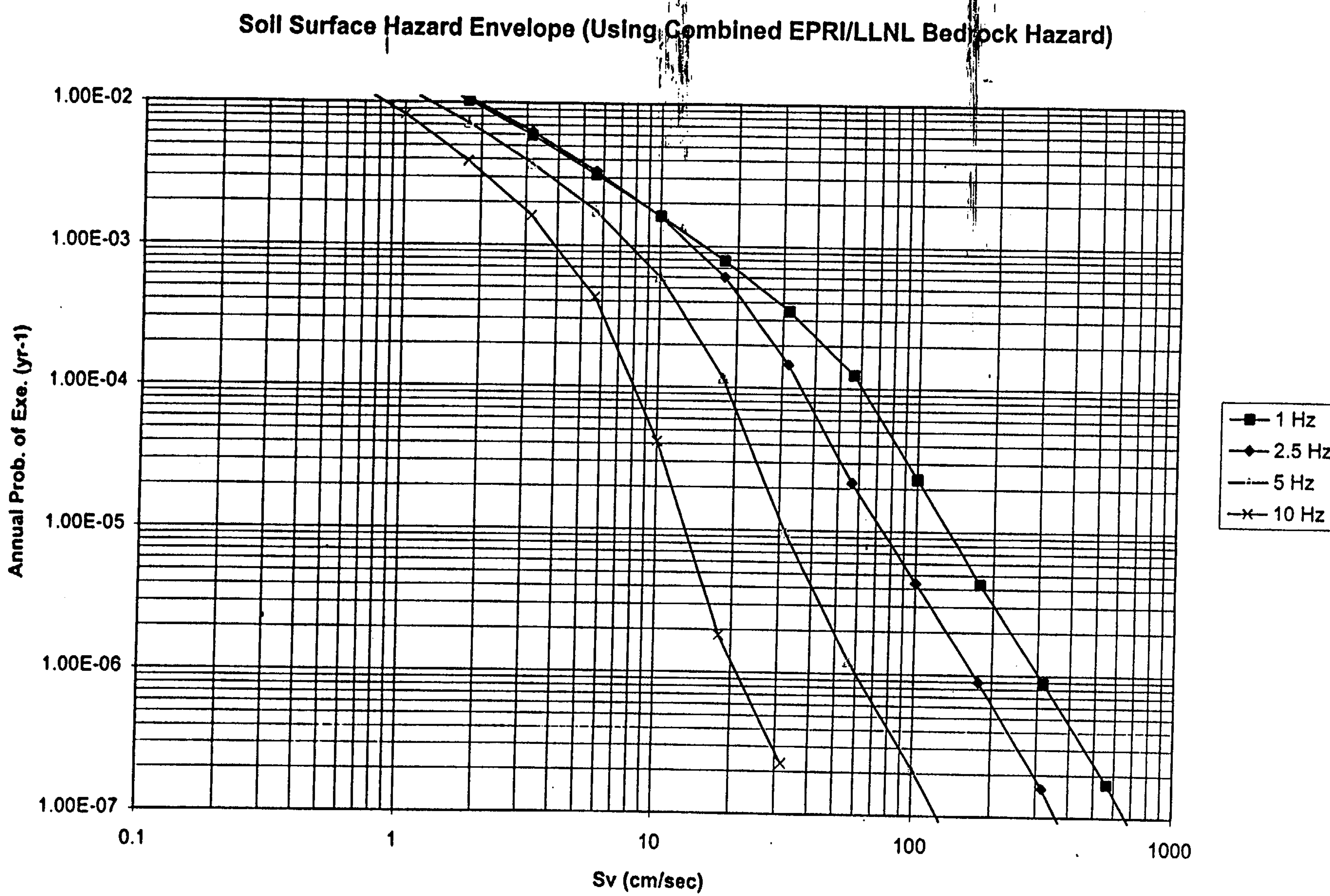

Figure C.6 - Computed soil surface hazard envelope using combined EPRI/LLNL bedrock hazard (solid lines). Hazard curves are for the four oscillator frequencies. POE plotted against spectral velocity.

APPENDIX D

Program SOILHAZF- Features and Simplified Flowchart

The primary features implemented in Program SOILHAZF are:

1. Requires user supplied subroutine of polynomial regressions on the probability of exceedance. Program assumes that the polynomial regression on hazard is a good fit and can be sampled as finely as desired. Note that depending on the input ground motion values, SOILHAZF can extrapolate the input hazard curve.
2. Assumes hazard disaggregation tables are sufficiently dense and span an adequate range of bedrock levels of motion. Disaggregation tables must also be sufficiently dense in earthquake magnitude and distance to allow acceptable approximations of the SAFs. Sensitivity of these parameters to the analysis is explored in Appendix A.
3. Performs linear interpolation of hazard disaggregations. No extrapolations of the disaggregation are done. For ground motion levels above or below the range of the input disaggregations, the disaggregation values are fixed at those extremes.
4. Accepts ground motion level, frequency, magnitude and distance dependent SAFs. The program assumes that the SAFs are log-normally distributed. For a selected earthquake magnitude and distance, the program linearly interpolates between the SAFs. For bedrock motions in excess of the range of SAF control motions, the SAF median and standard deviation is fixed at the highest control motion.
5. Allows for the specification of a lower bound on the SAF.
6. Allows for any number of bedrock and soil ground motion values to be used in the analysis (with modification of program storage, if necessary).
7. Allows user-specified truncation of the ground motion probability of exceedance.

A simplified flow-chart for SOILHAZF is attached.

SOILHAZF Flowchart

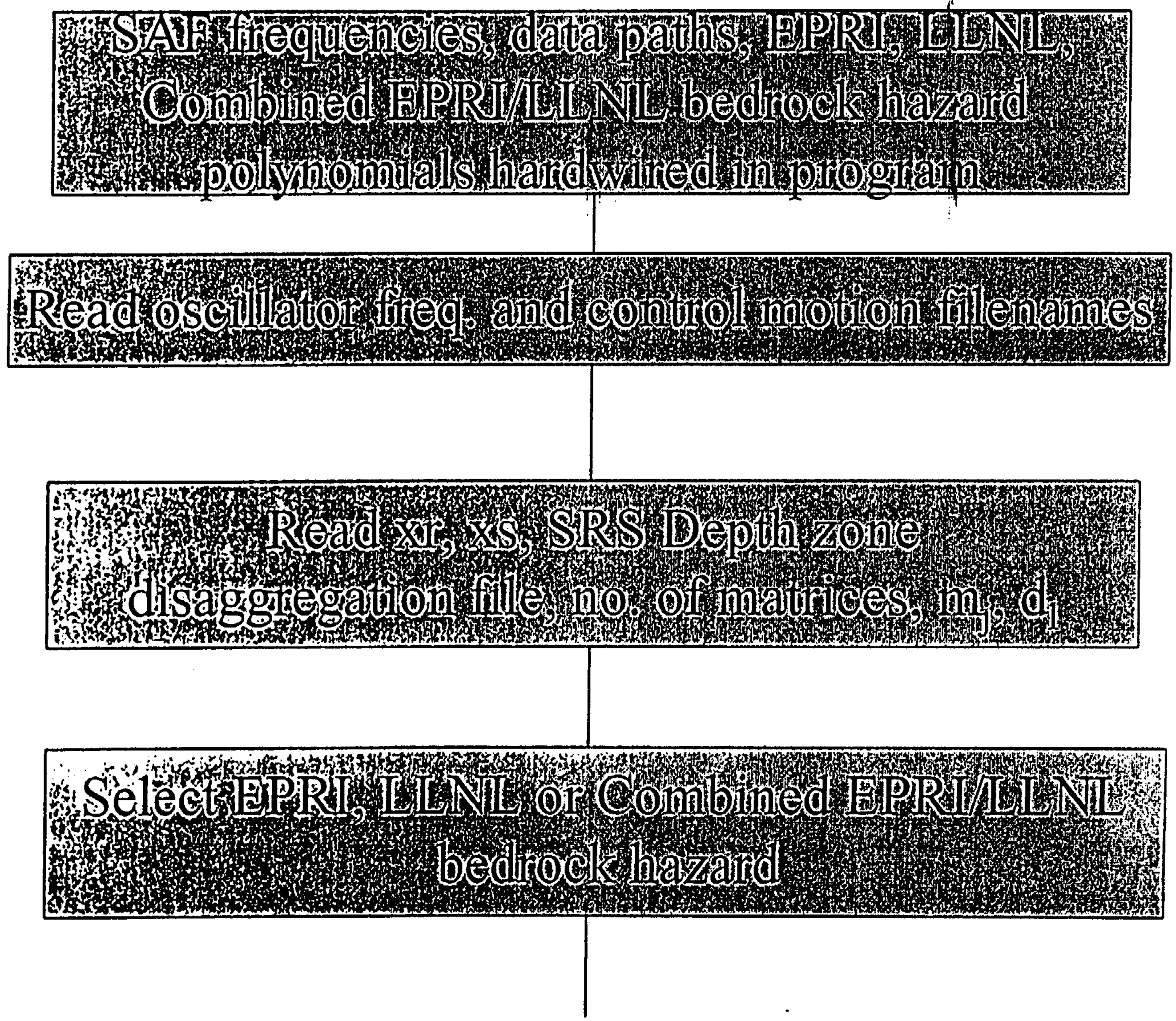

Figure D.1 (a) - Simplified SOILHAZF flowchart.

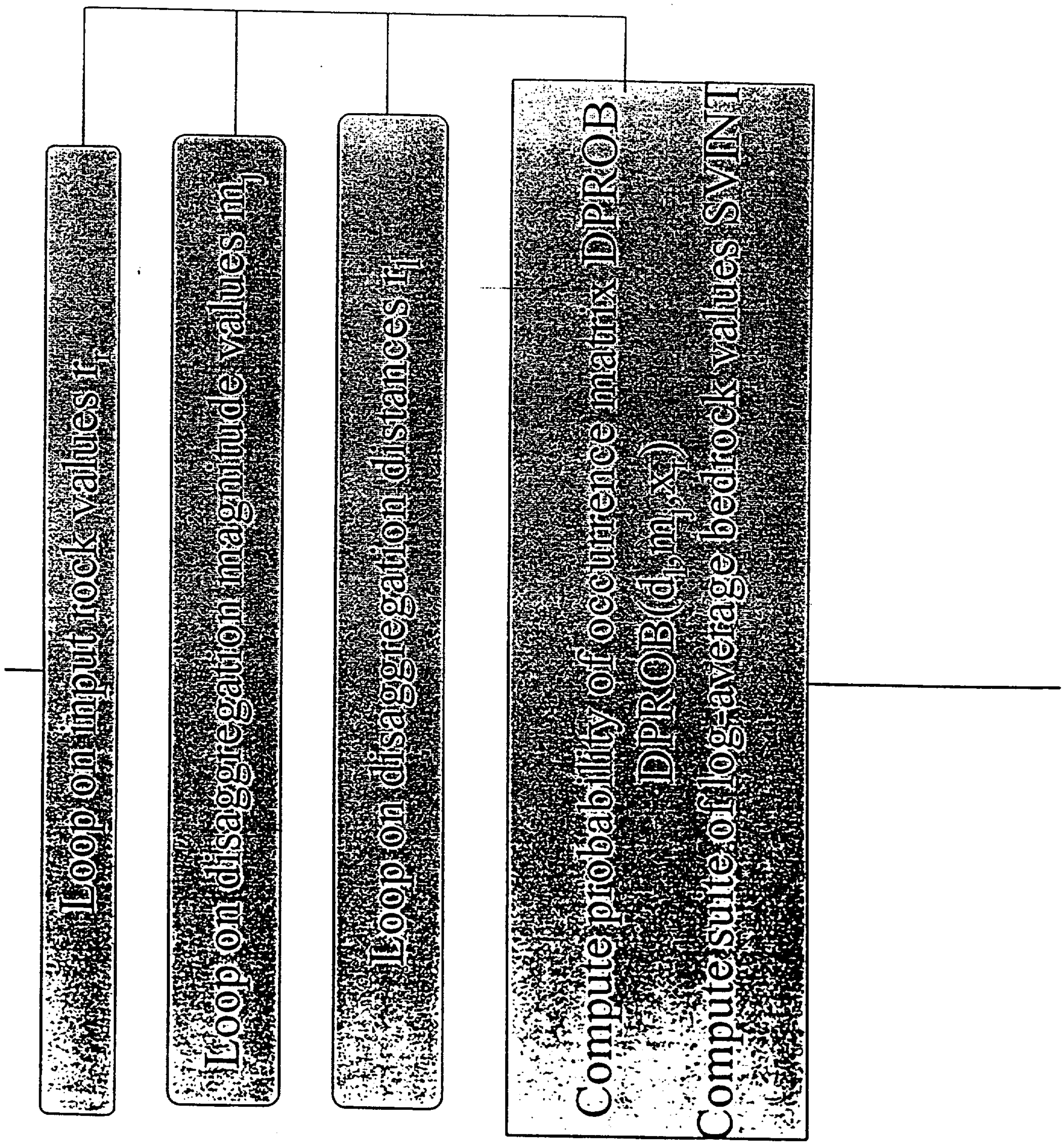

Figure D.1 (b) - Simplified SOILHAZF flowchart.

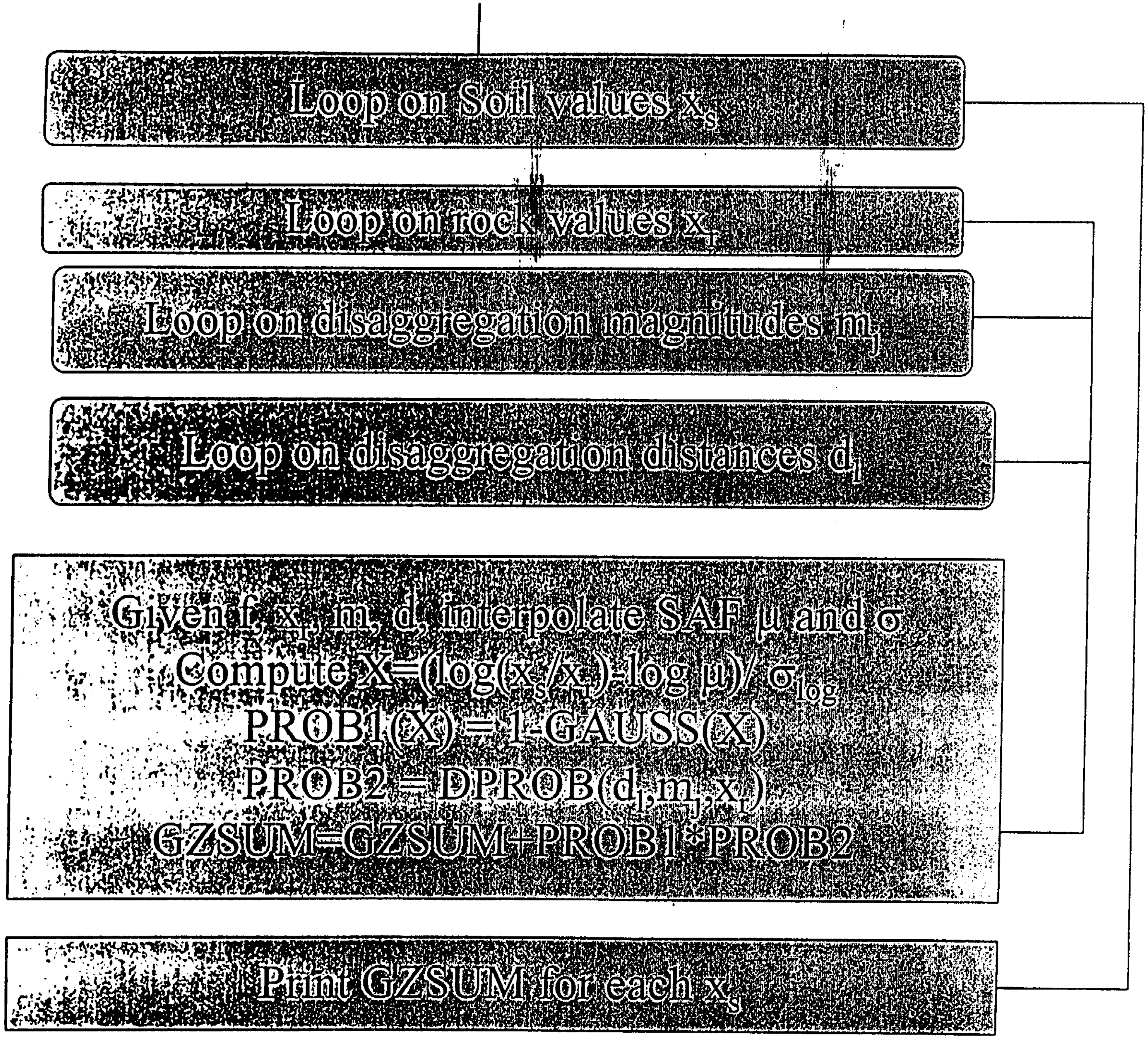

Figure D.1 (c) - Simplified SOILHAZF flowchart.

APPENDIX E

EPRI BEDROCK HAZARD DISAGGREGATION

This Appendix illustrates the EPRI hazard disaggregation.

The EPRI disaggregation magnitude and distance bins are:

Magnitude (m_b): 5.0-5.5, 5.5-6.0, 6.0-6.5, 6.5-7.0, >7.

Distance (km): 0-25, 25-50, 50-100, 100-150, 150-200, >200.

The EPRI disaggregation is comprised of eight (8) tables for each of the four frequencies 1, 2.5, 5, and 10 Hz having dimensions of 6(distance) x 5(magnitude)..

Figures E.1 to E.30 illustrate the 30 elements of the EPRI hazard disaggregation. The element index defines the row and column. For each element of the disaggregation, the percent contribution to the total hazard is shown as a function of response spectral velocity.

Note that disaggregation elements of 2.29 x 10^{-10} or less were not plotted because these were the minimum values stored in the Excel database.

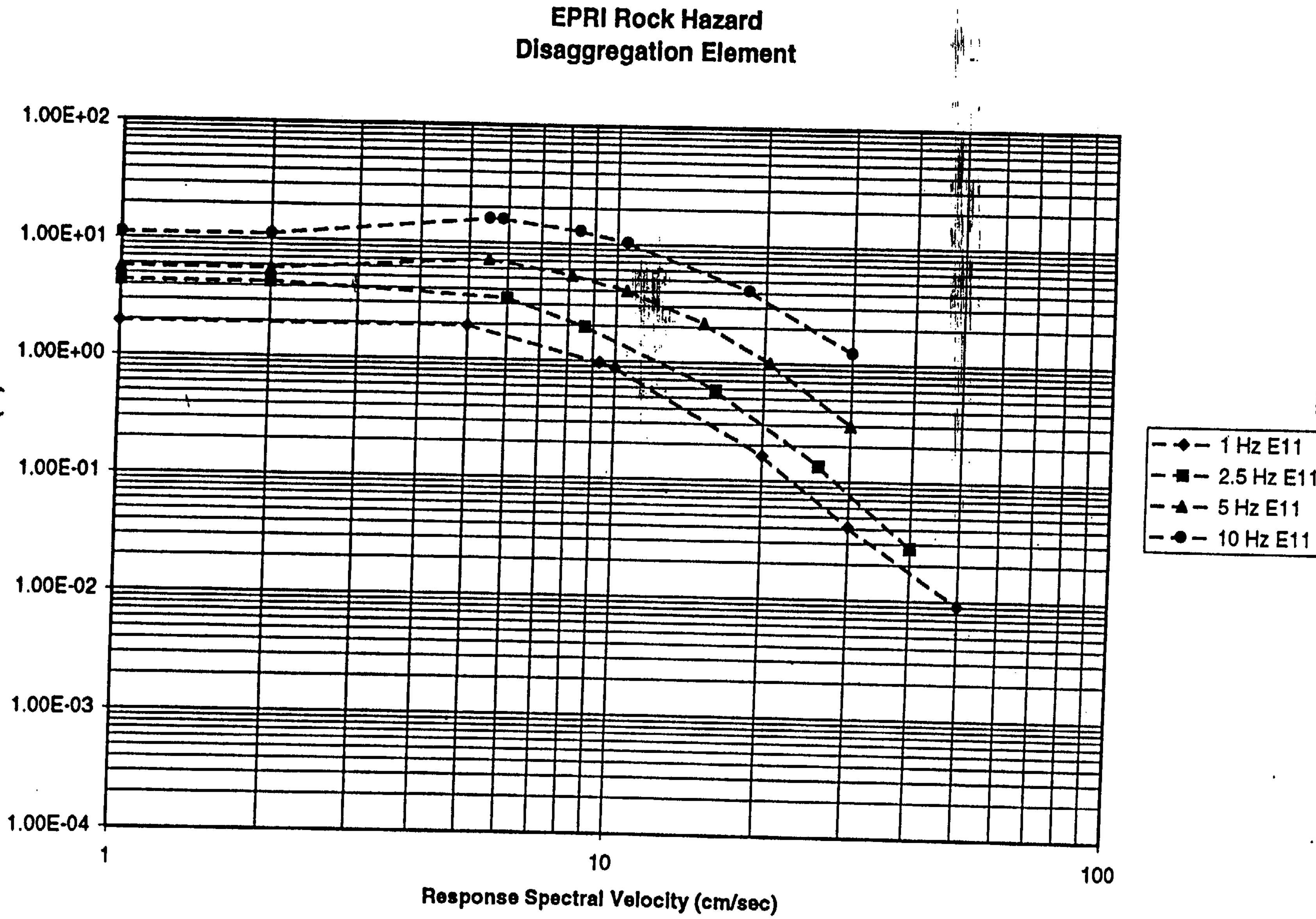

Figure E.1 - EPRI rock hazard disaggregation element 1,1 (Mw 4.75, 12.5 km) for the 1, 2.5, 5, and 10 Hz oscillator.

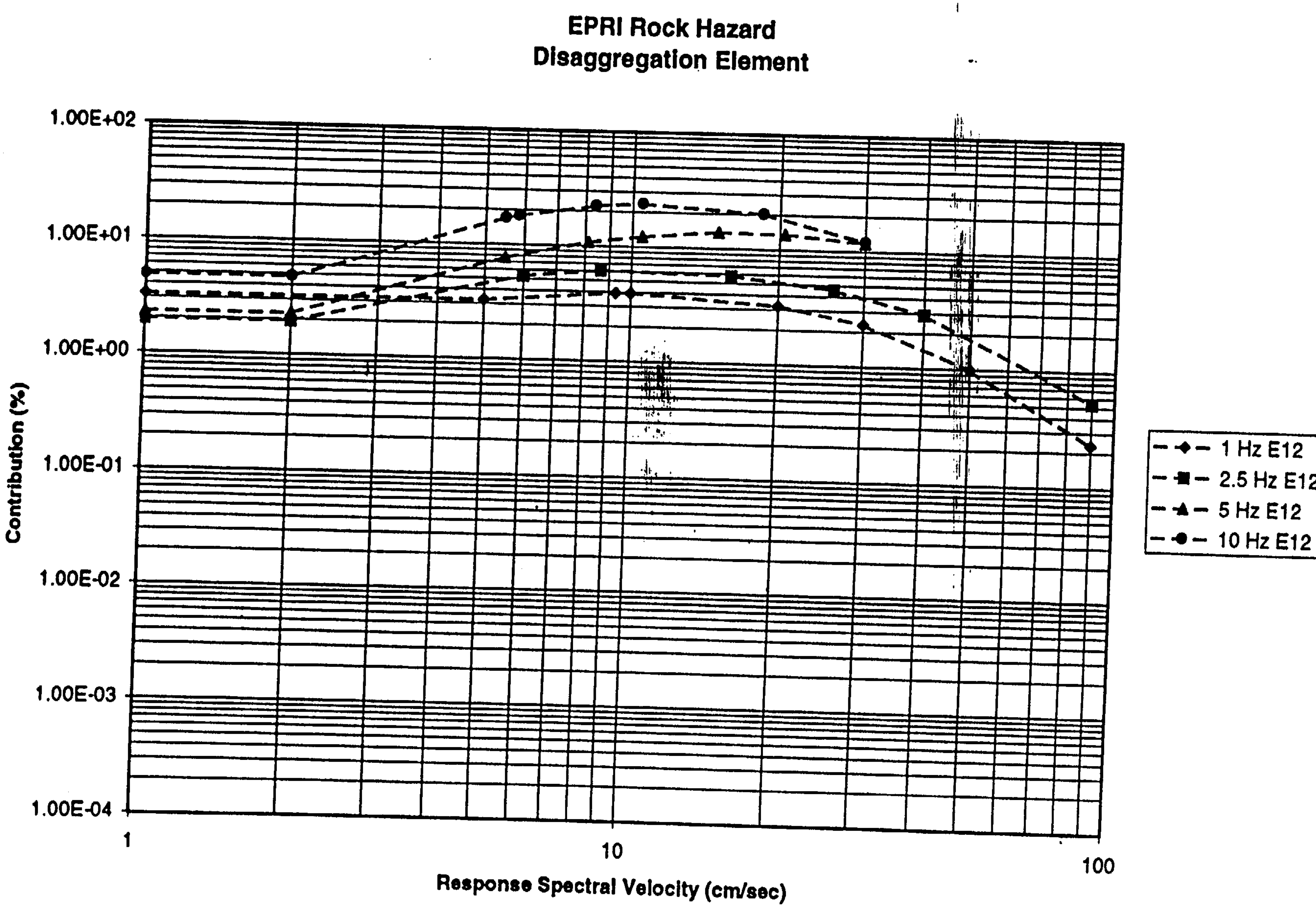

Figure E.2 - EPRI rock hazard disaggregation element 1,2 (Mw 5.25, 12.5 km) for the 1, 2.5, 5, and 10 Hz oscillator

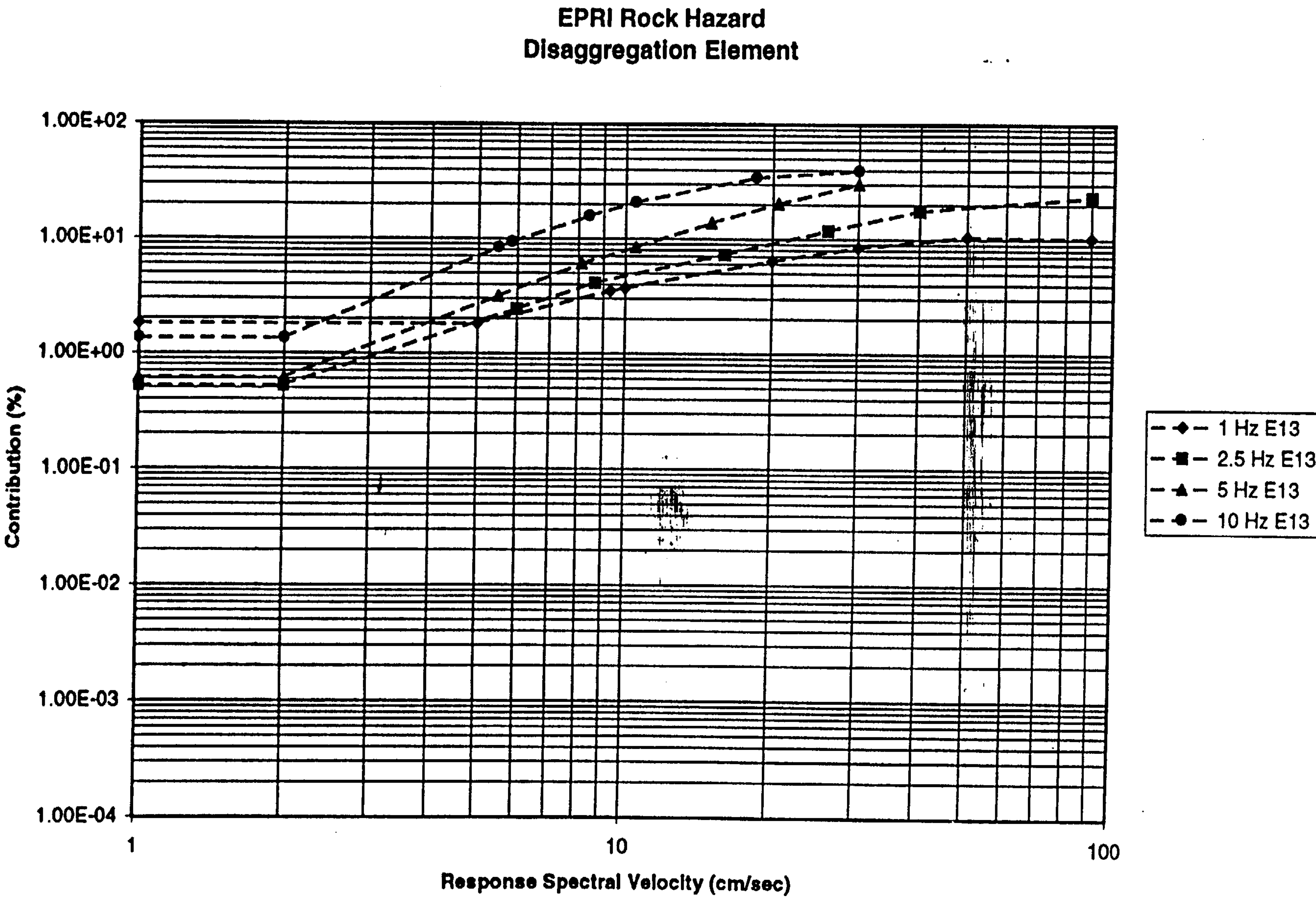

Figure E.3 - EPRI rock hazard disaggregation element 1,3 (Mw 5.9, 12.5 km) for the 1, 2.5, 5, and 10 Hz oscillator.

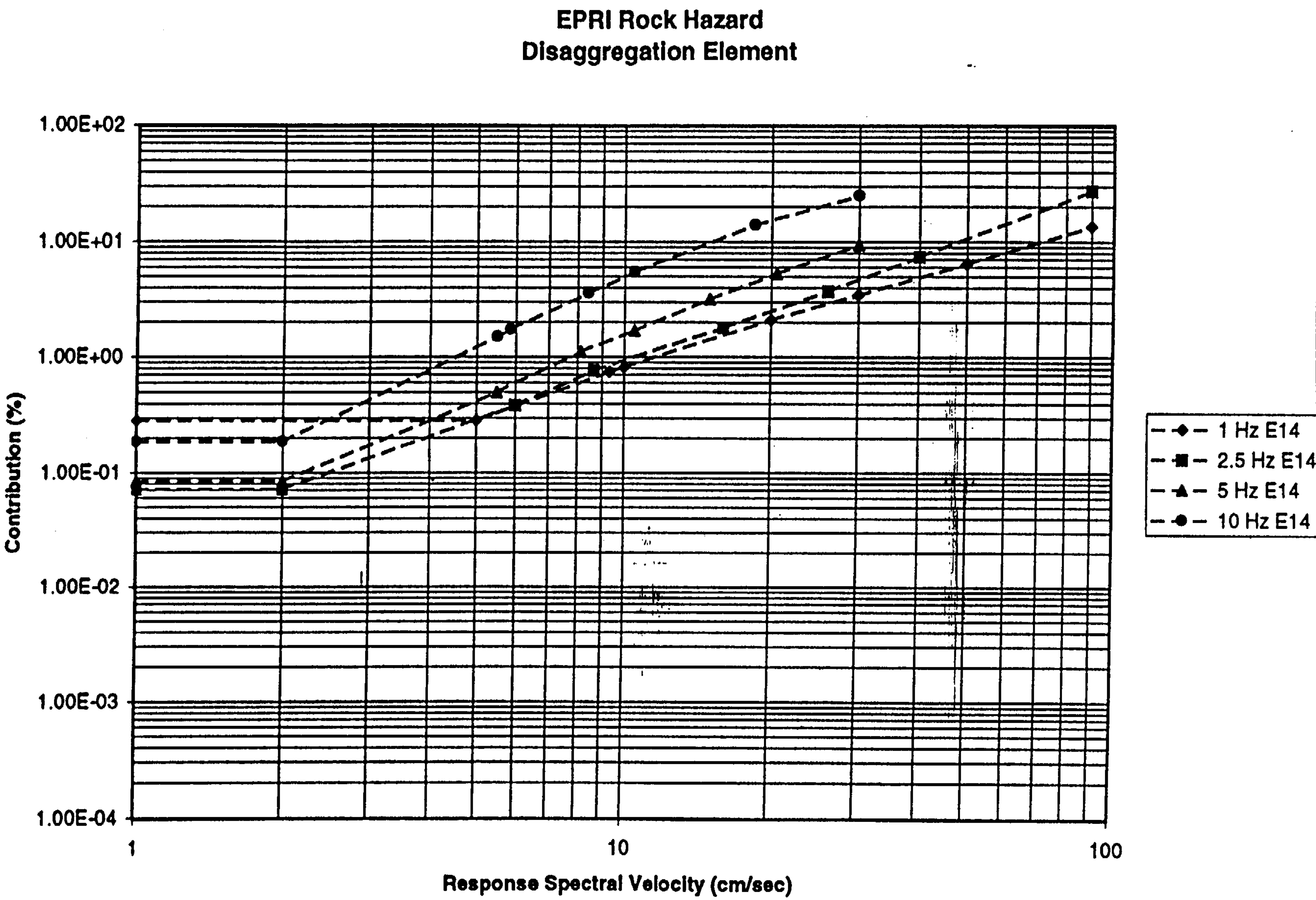

Figure E.4 - EPRI rock hazard disaggregation element 1,4 (Mw 6.7, 12.5 km) for the 1, 2.5, 5, and 10 Hz oscillator.

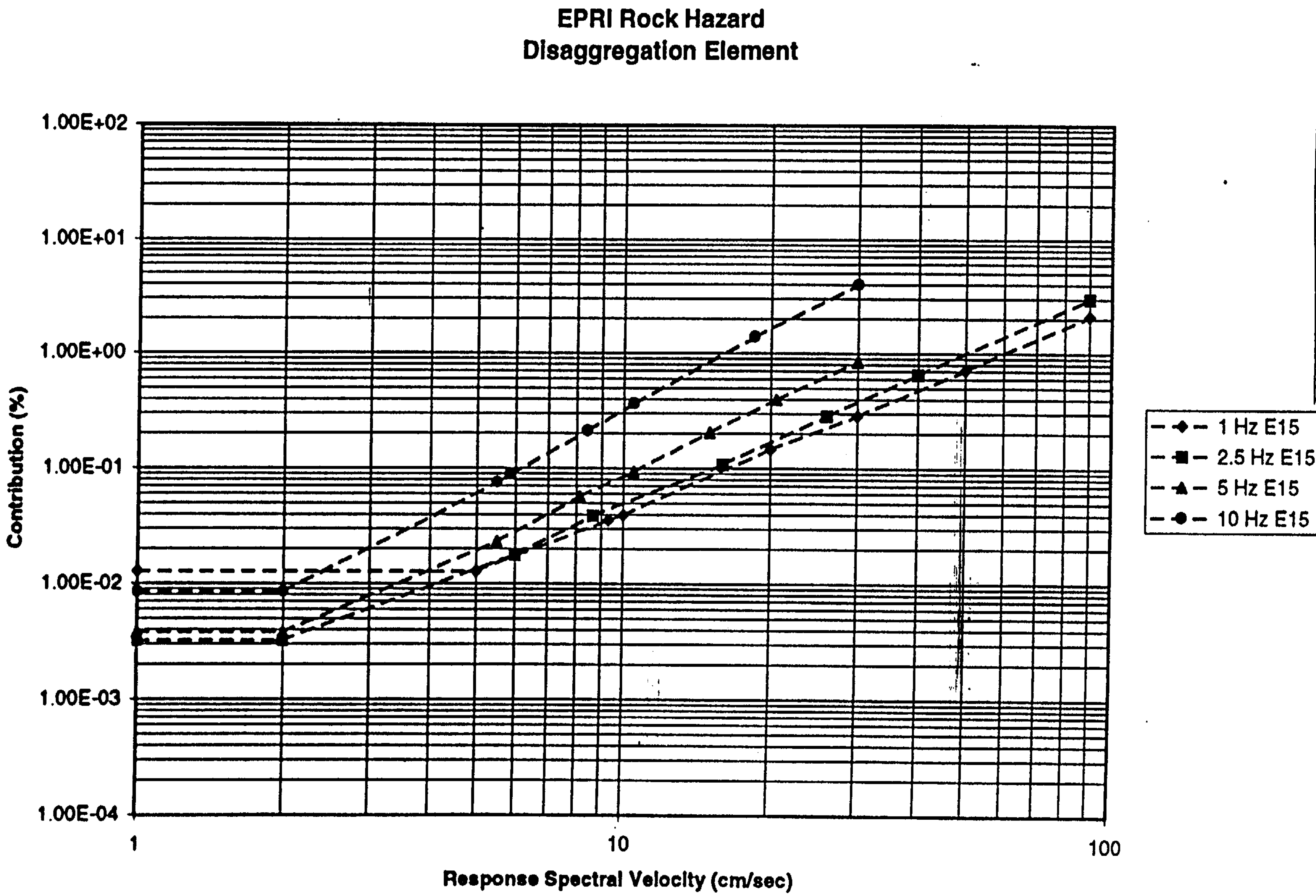

Figure E.5 - EPRI rock hazard disaggregation element 1,5 (Mw 7.8, 12.5 km) for the 1, 2.5, 5, and 10 Hz oscillator.

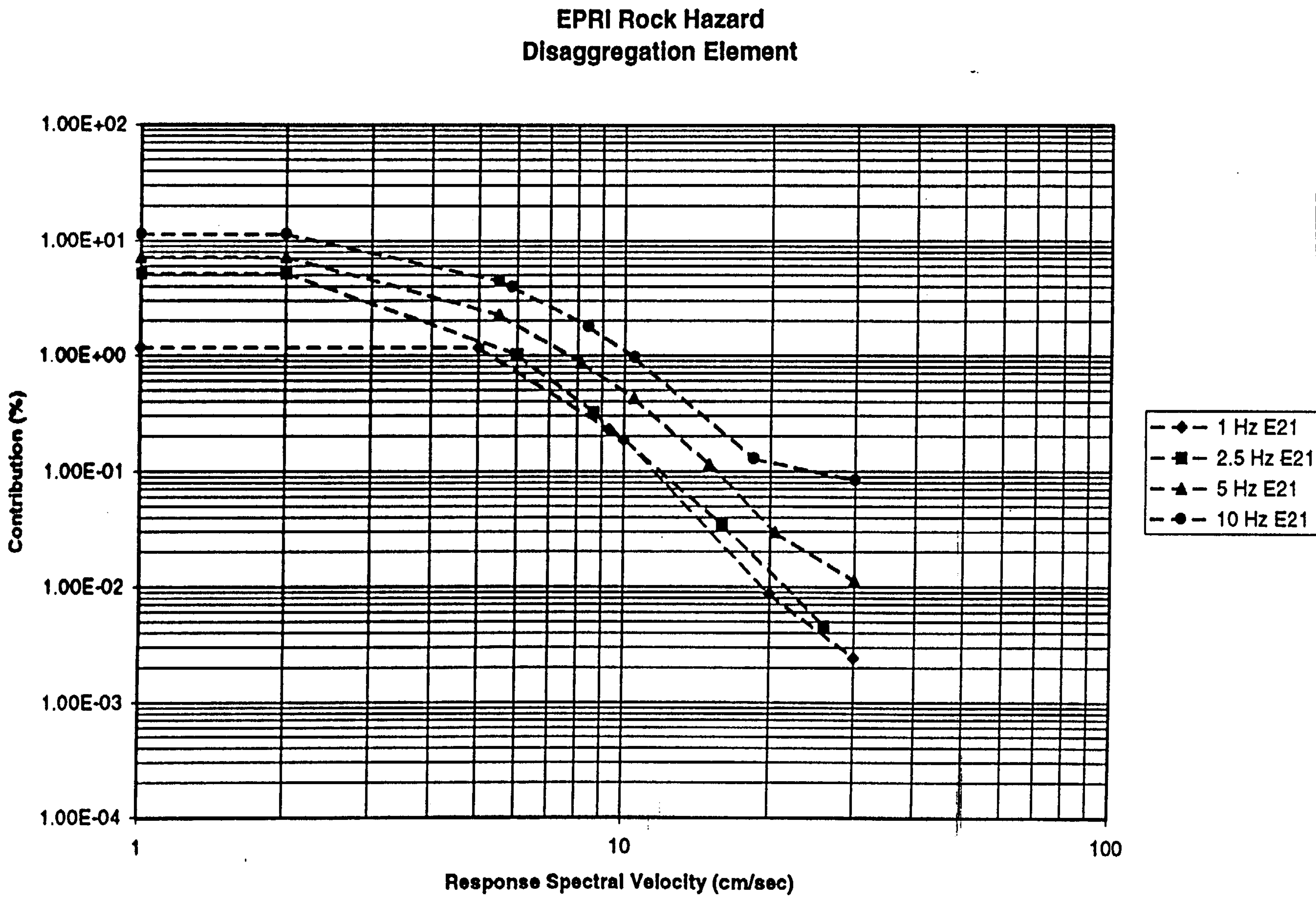

Figure E.6 - EPRI rock hazard disaggregation element 2,1 (Mw 4.75, 37.5 km) for the 1, 2.5, 5, and 10 Hz oscillator.

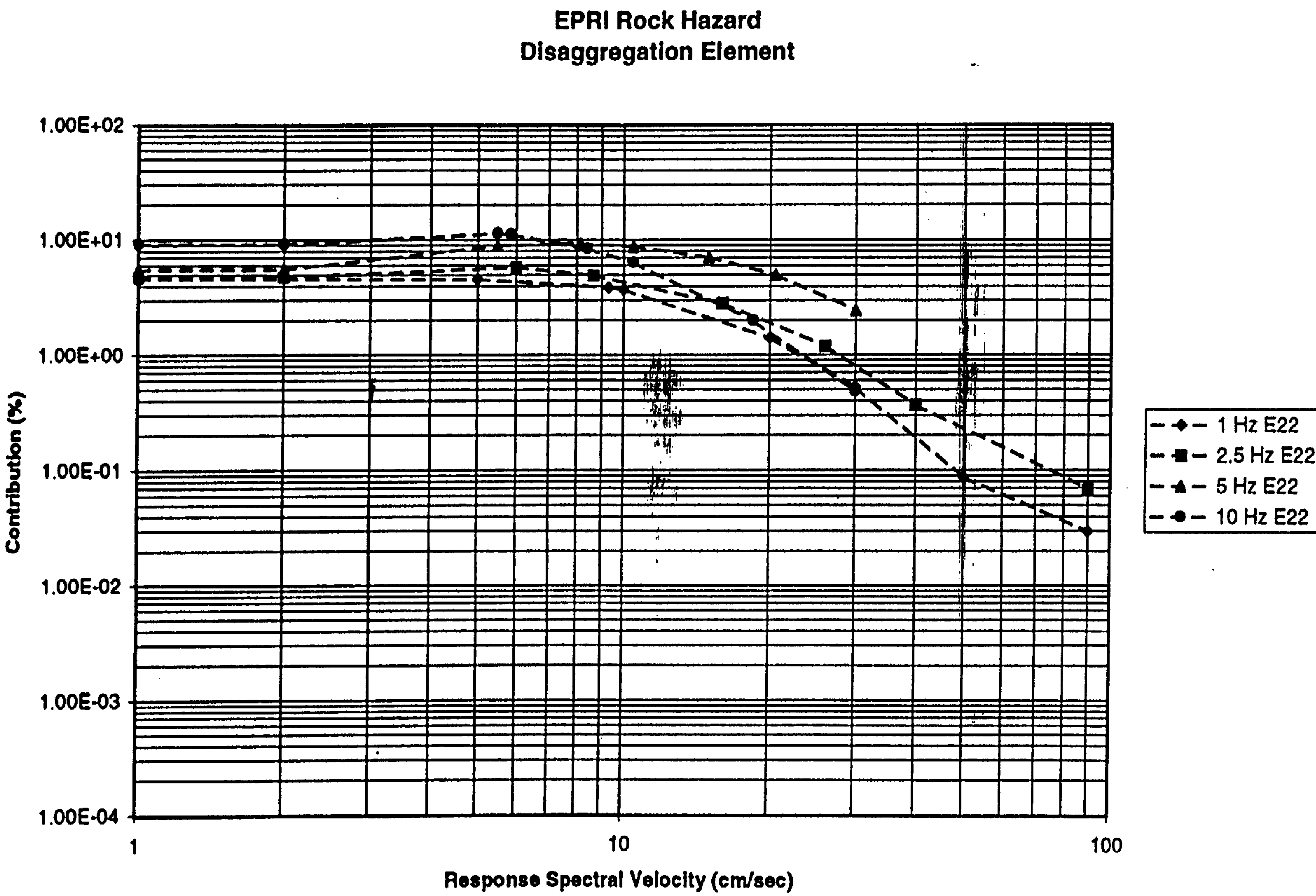

Figure E.7 - EPRI rock hazard disaggregation element 2,2 (Mw 5.25, 37.5 km) for the 1, 2.5, 5, and 10 Hz oscillator.

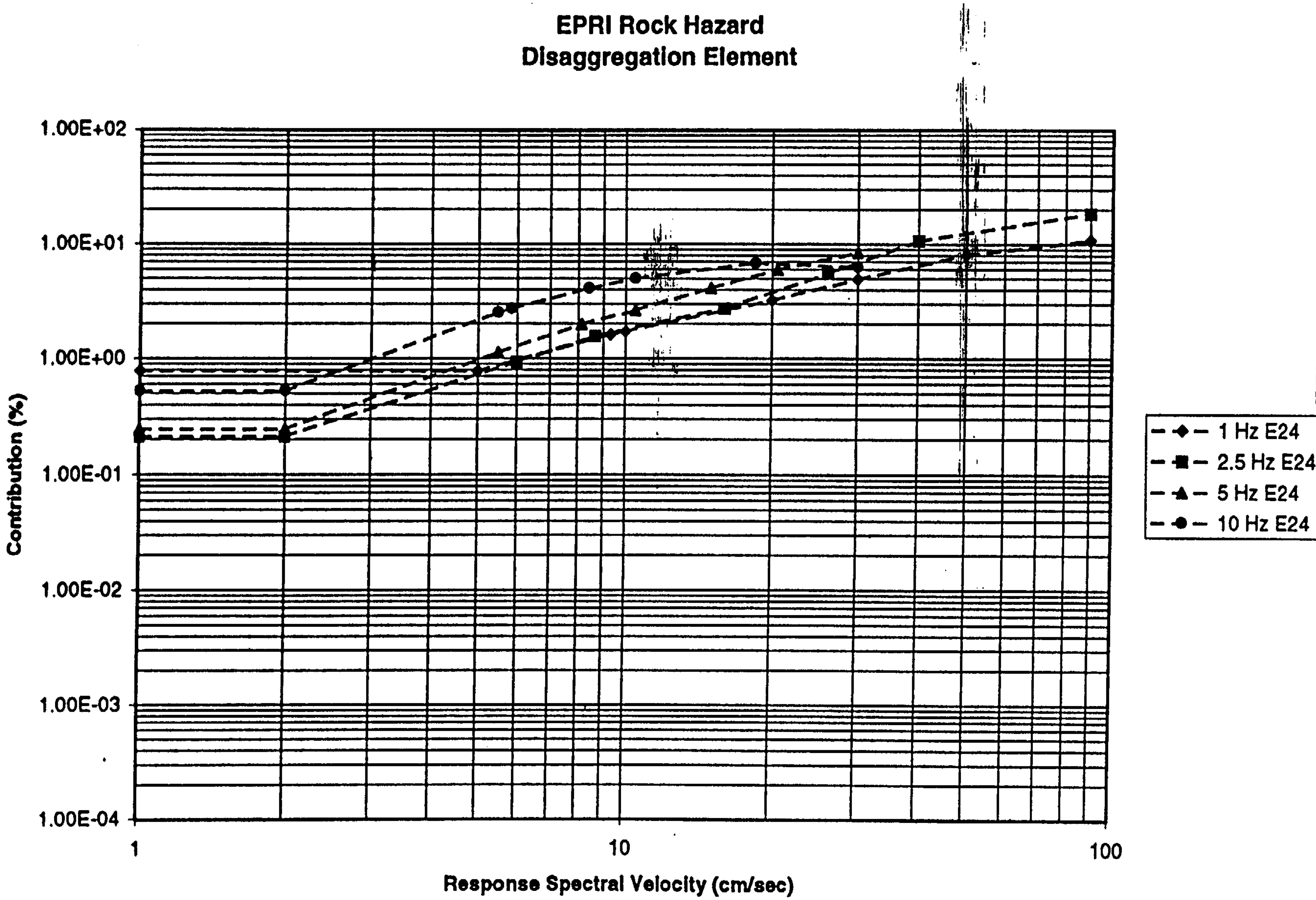

Figure E.9 - EPRI rock hazard disaggregation element 2,4 (Mw 6.7, 37.5 km) for the 1, 2.5, 5, and 10 Hz oscillator.

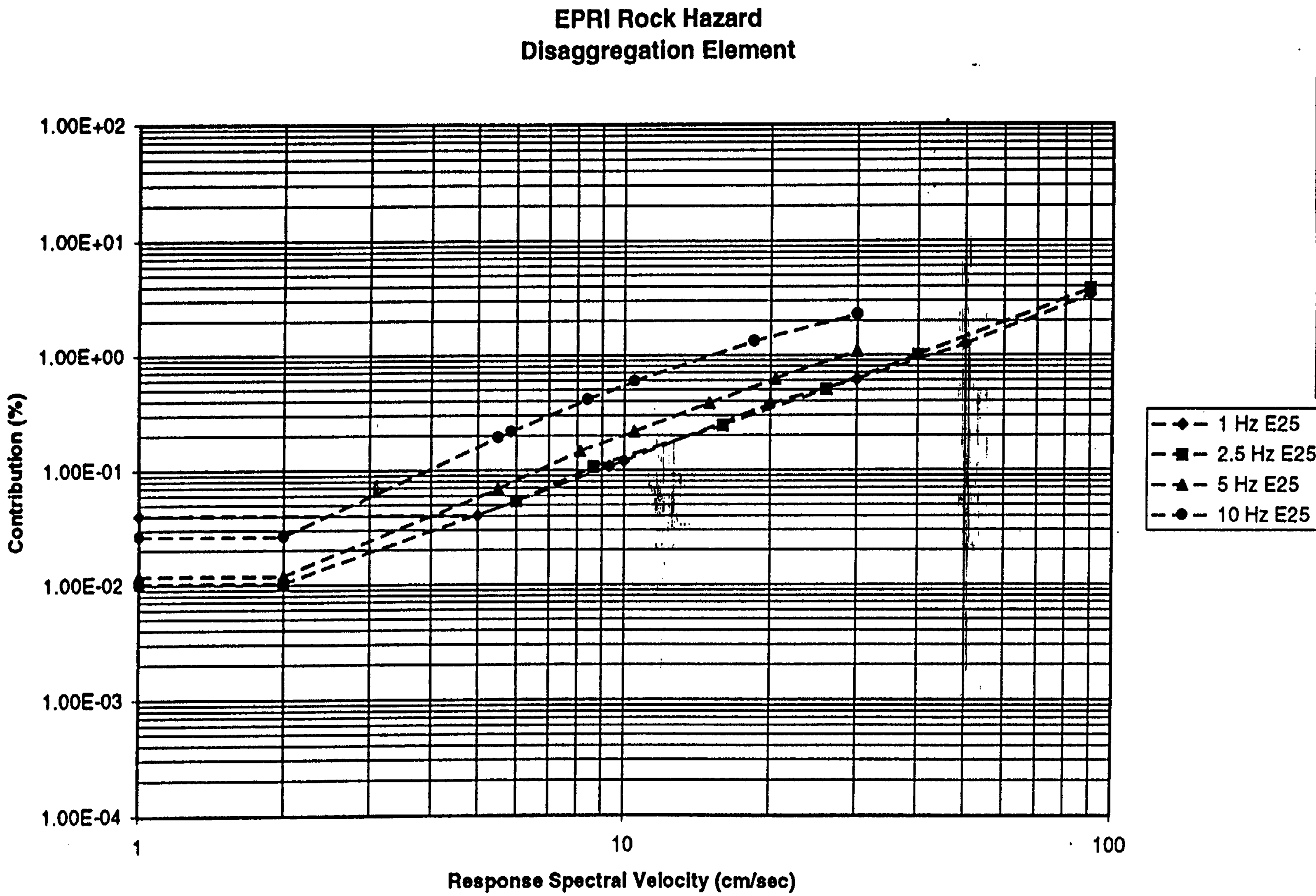

Figure E.10 - EPRI rock hazard disaggregation element 2,5 (Mw 7.8, 37.5 km) for the 1, 2.5, 5, and 10 Hz oscillator.

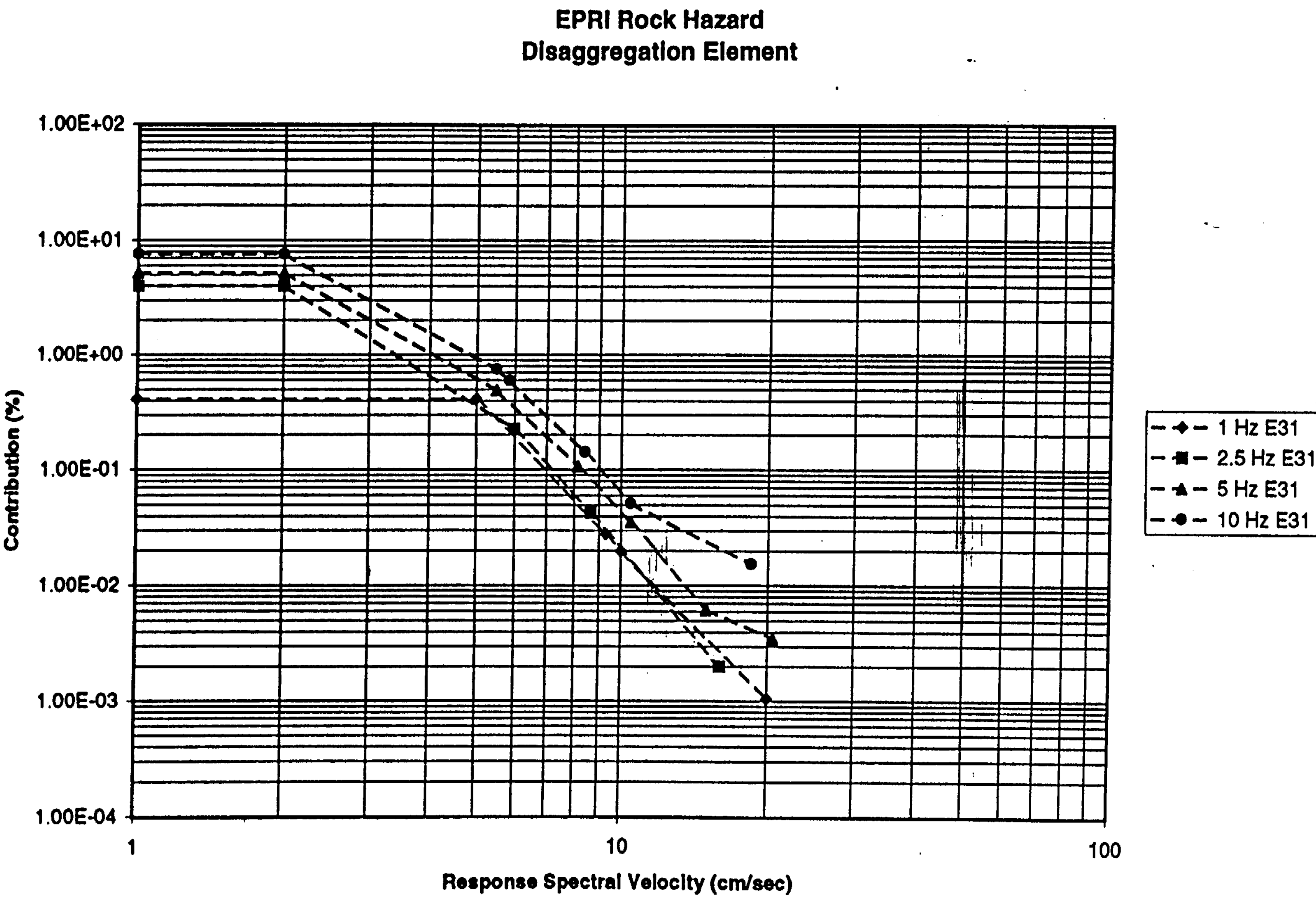

Figure E.11 - EPRI rock hazard disaggregation element 3,1 (Mw 4.75, 75. km) for the 1, 2.5, 5, and 10 Hz oscillator.

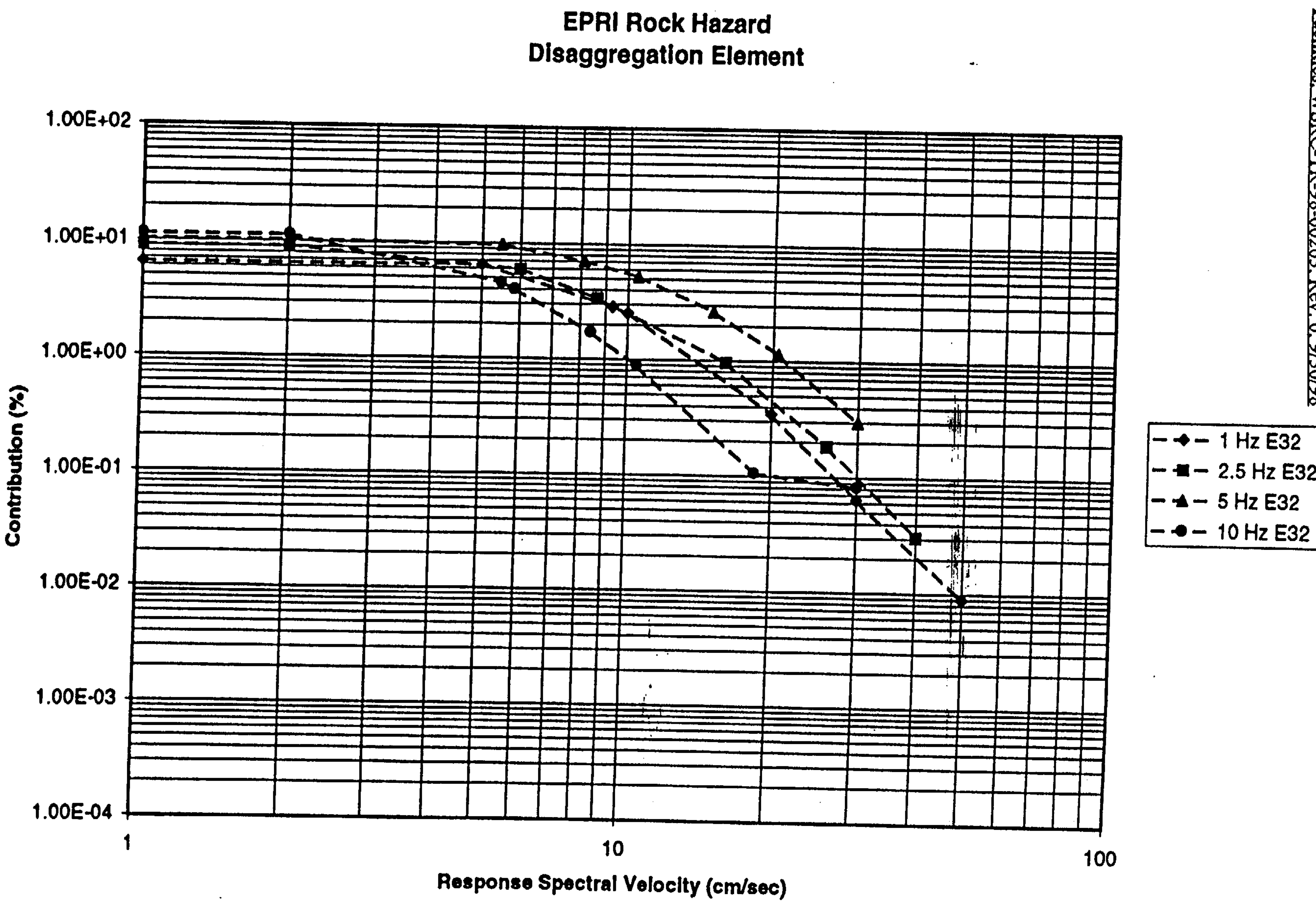

Figure E.12 - EPRI rock hazard disaggregation element 3,2 (Mw 5.25, 75. km) for the 1, 2.5, 5, and 10 Hz oscillator.

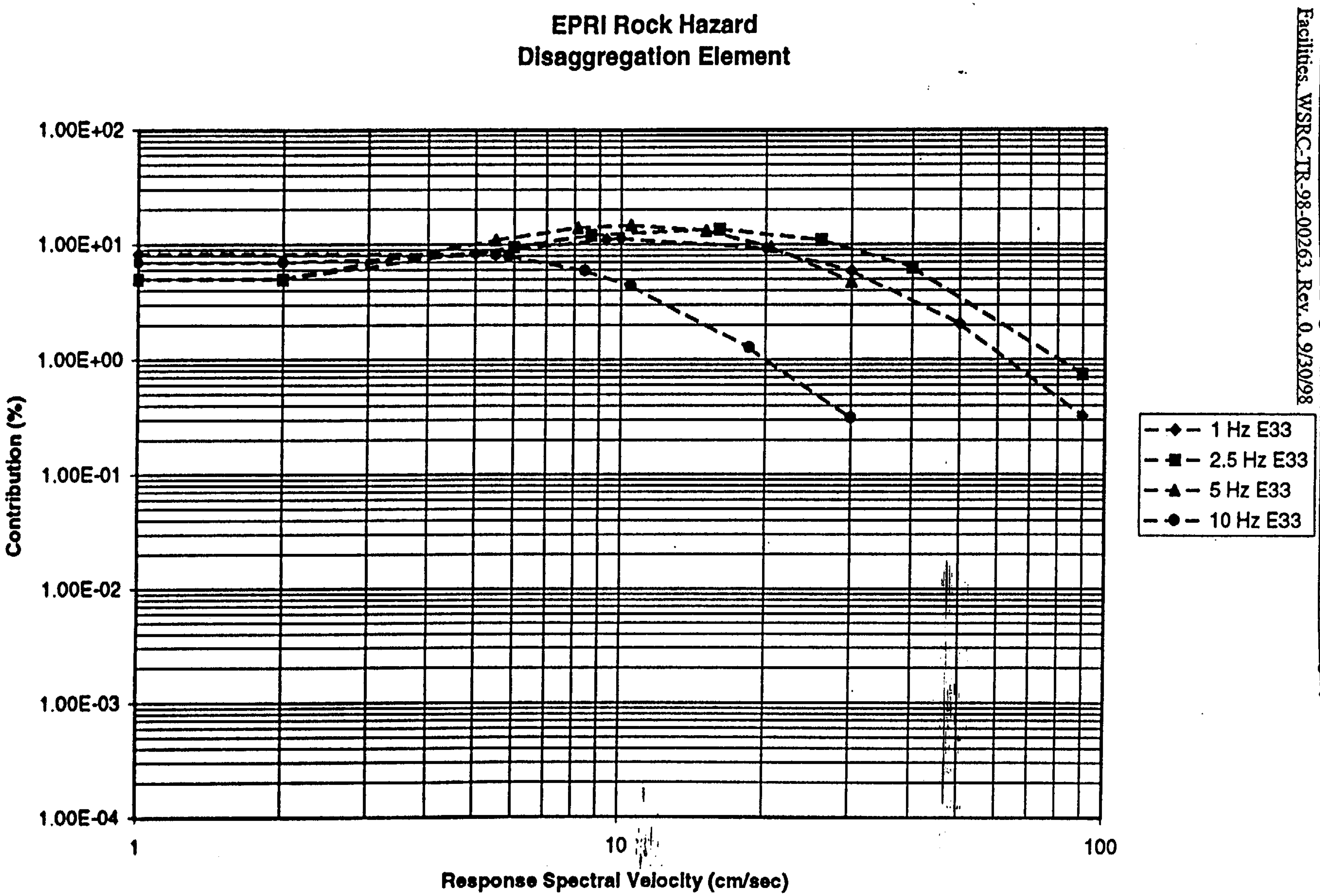

Figure E.13 - EPRI rock hazard disaggregation element 3,3 (Mw 5.9, 75. km) for the 1, 2.5, 5, and 10 Hz oscillator.

… element 3,4 (Mw 6.7, 75. km) for the 1, 2.5, 5, and 10 Hz oscillator.

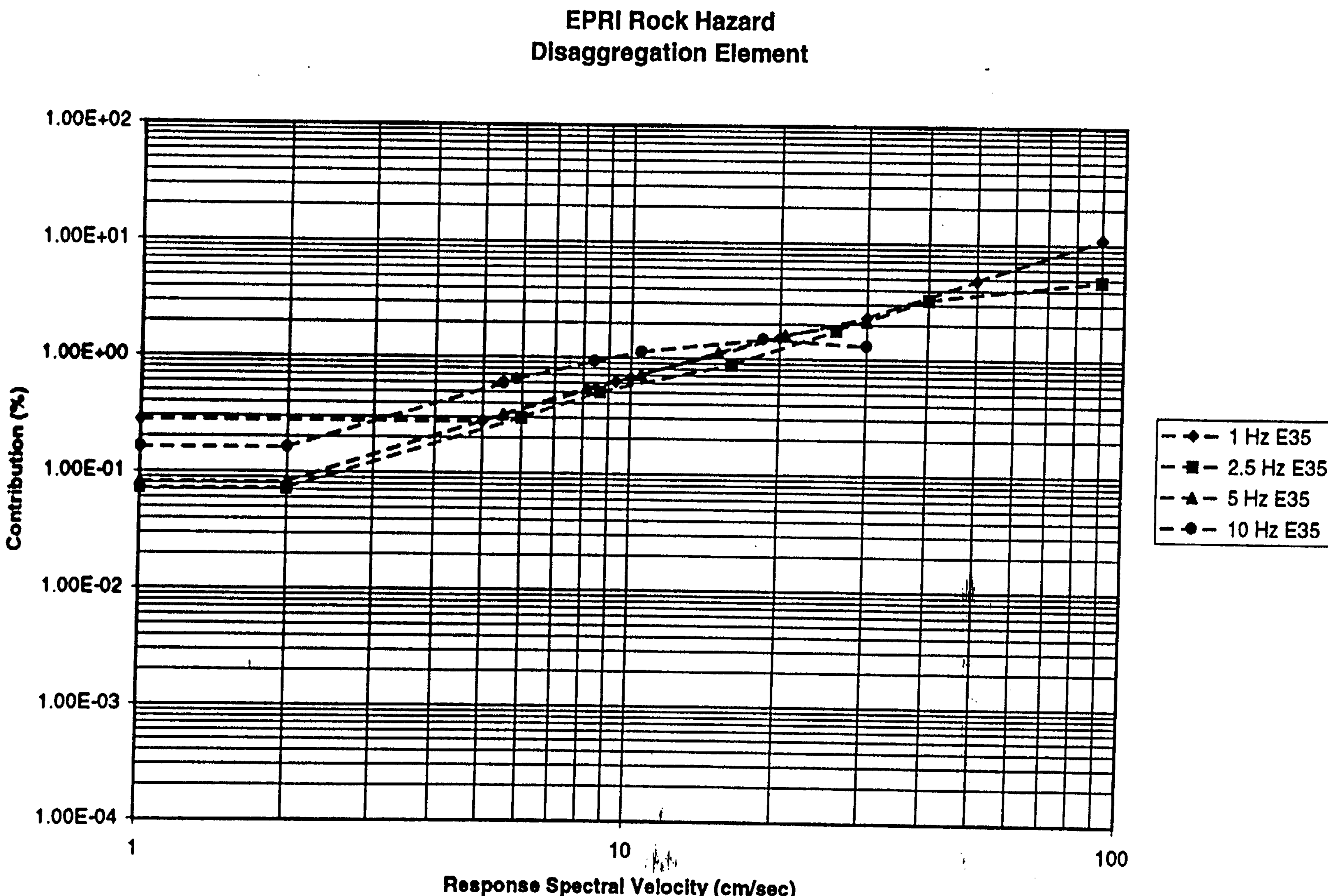

Figure E.15 - EPRI rock hazard disaggregation element 3,5 (Mw 7.8, 75. km) for the 1, 2.5, 5, and 10 Hz oscillator.

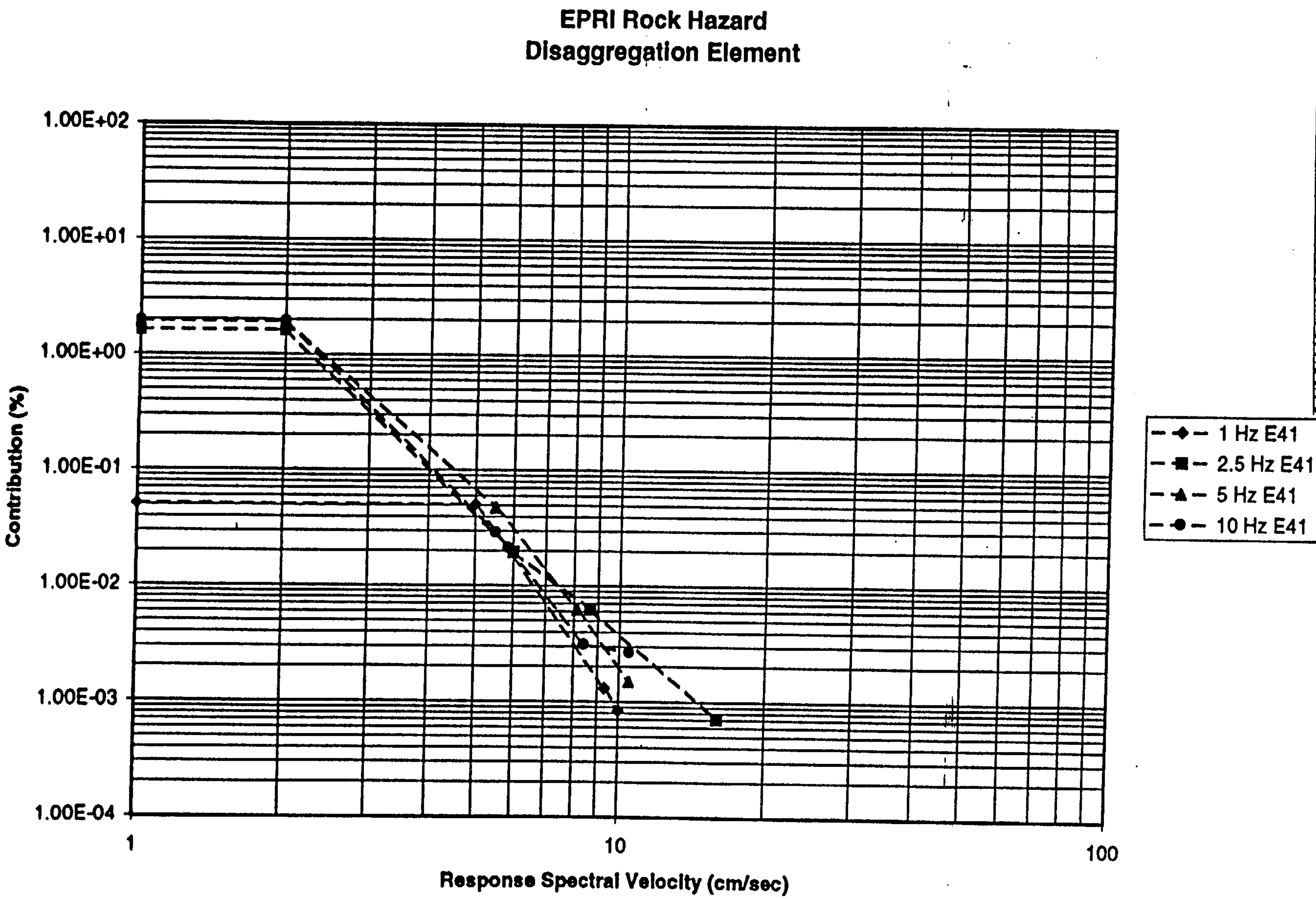

Figure E.16 - EPRI rock hazard disaggregation element 4,1 (Mw 4.75, 125. km) for the 1, 2.5, 5, and 10 Hz oscillator.

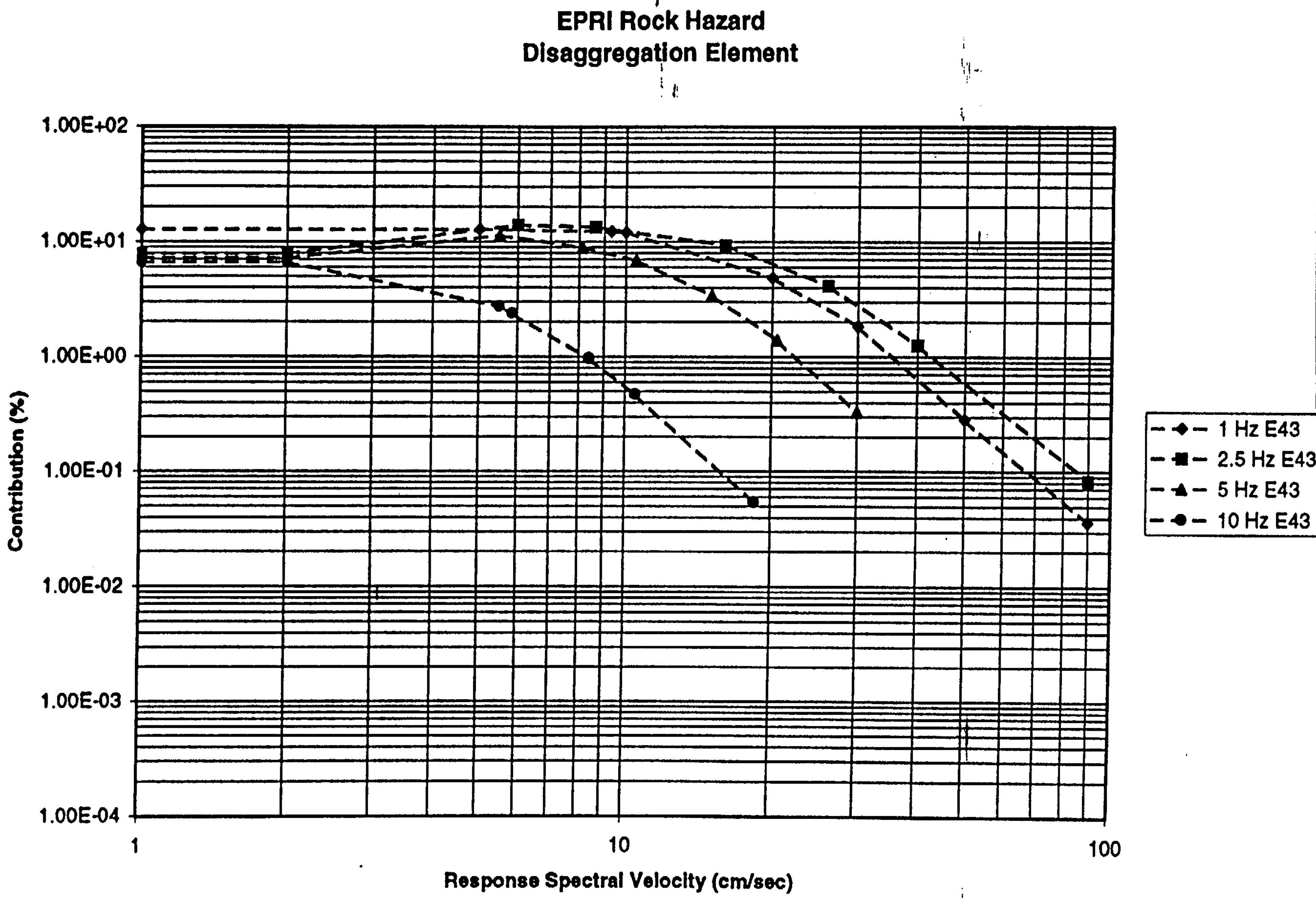

Figure E.18 - EPRI rock hazard disaggregation element 4,3 (Mw 5.9, 125. km) for the 1, 2.5, 5, and 10 Hz oscillator.

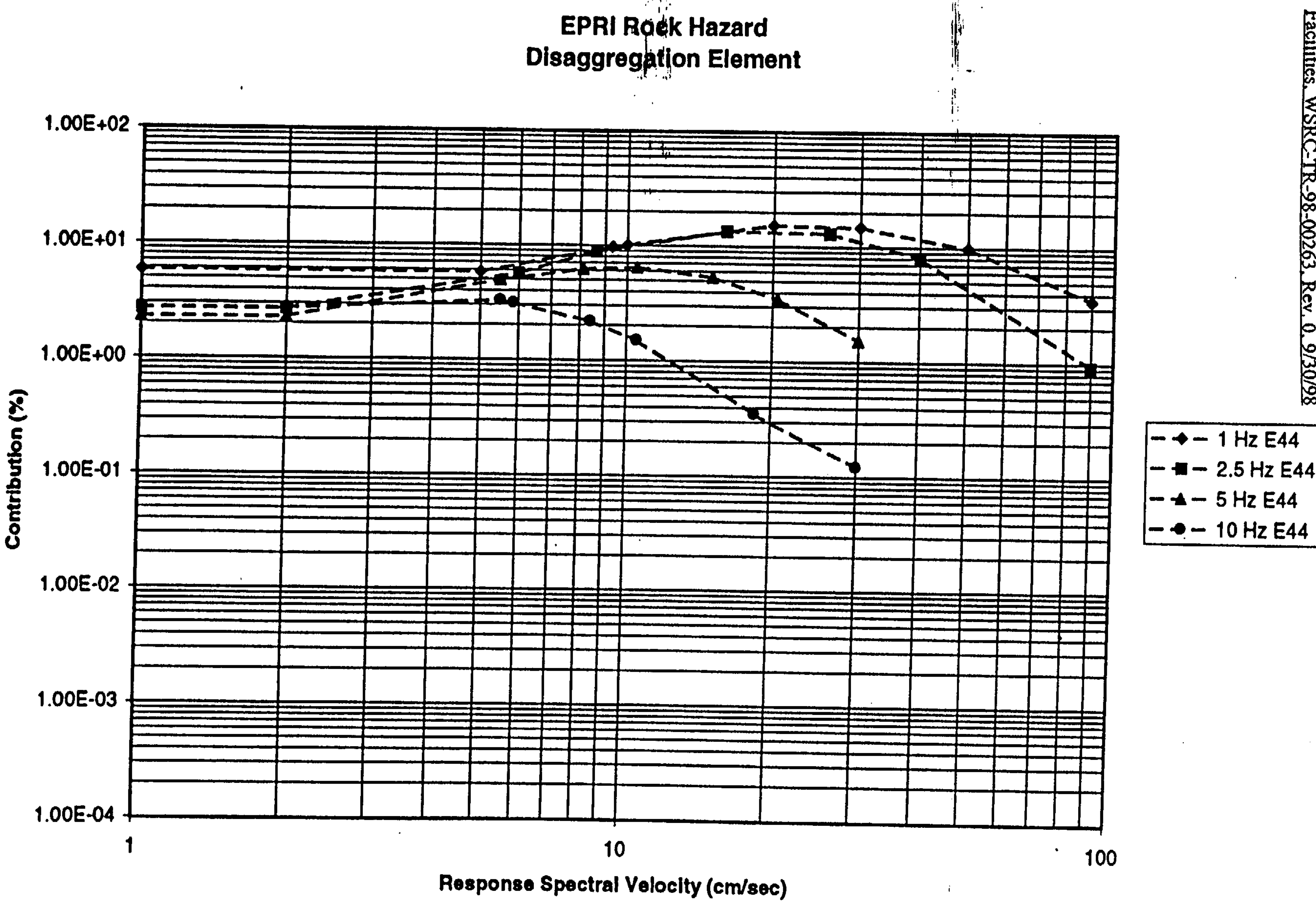

Figure E.19 - EPRI rock hazard disaggregation element 4,4 (Mw 6.7, 125. km) for the 1, 2.5, 5, and 10 Hz oscillator.

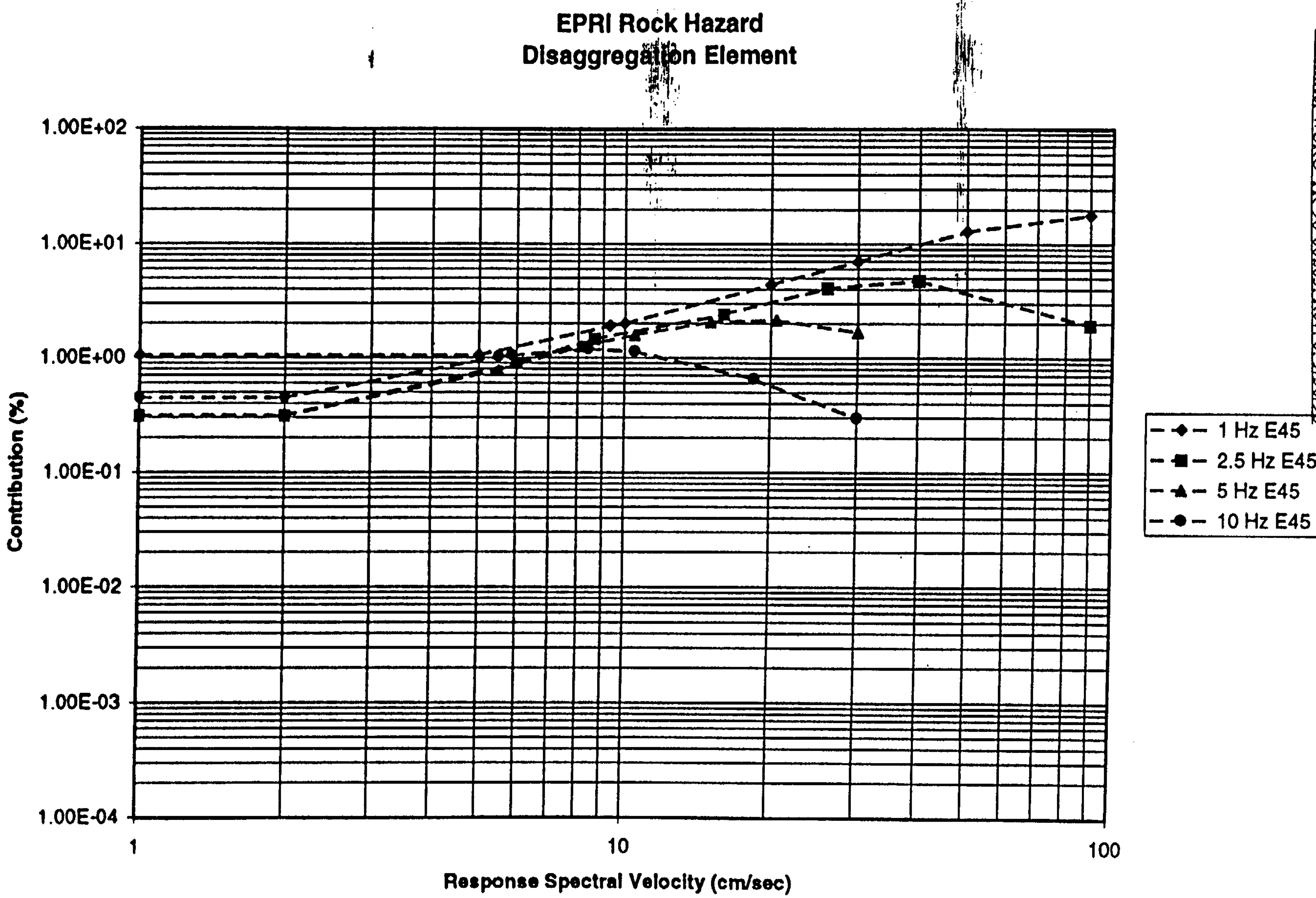

Figure E.20 - EPRI rock hazard disaggregation element 4,5 (Mw 7.8, 125. km) for the 1, 2.5, 5, and 10 Hz oscillator.

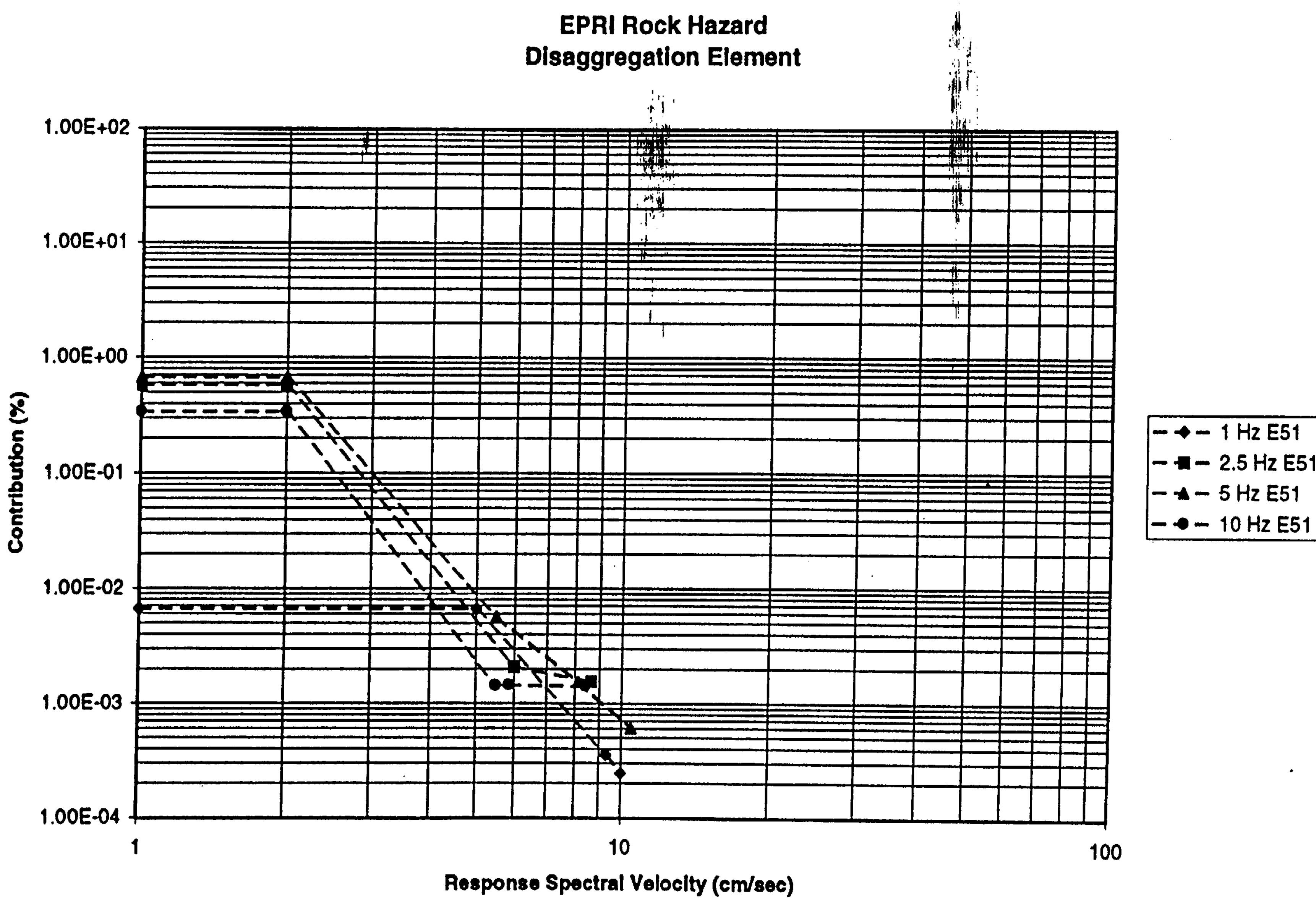

Figure E.21 - EPRI rock hazard disaggregation element 5,1 (Mw 4.75, 175. km) for the 1, 2.5, 5, and 10 Hz oscillator.

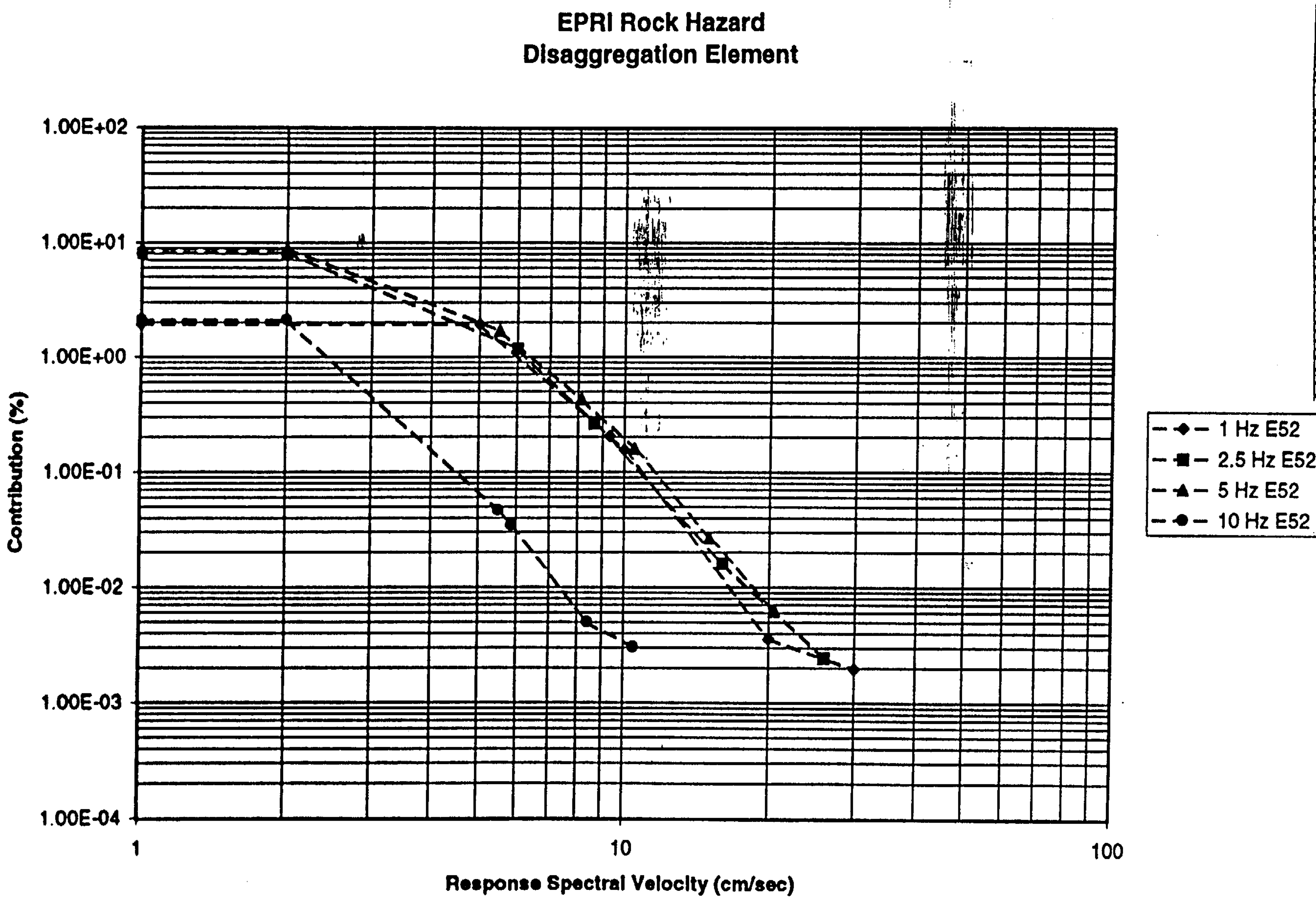

Figure E.22 - EPRI rock hazard disaggregation element 5,2 (Mw 5.25, 175. km) for the 1, 2.5, 5, and 10 Hz oscillator.

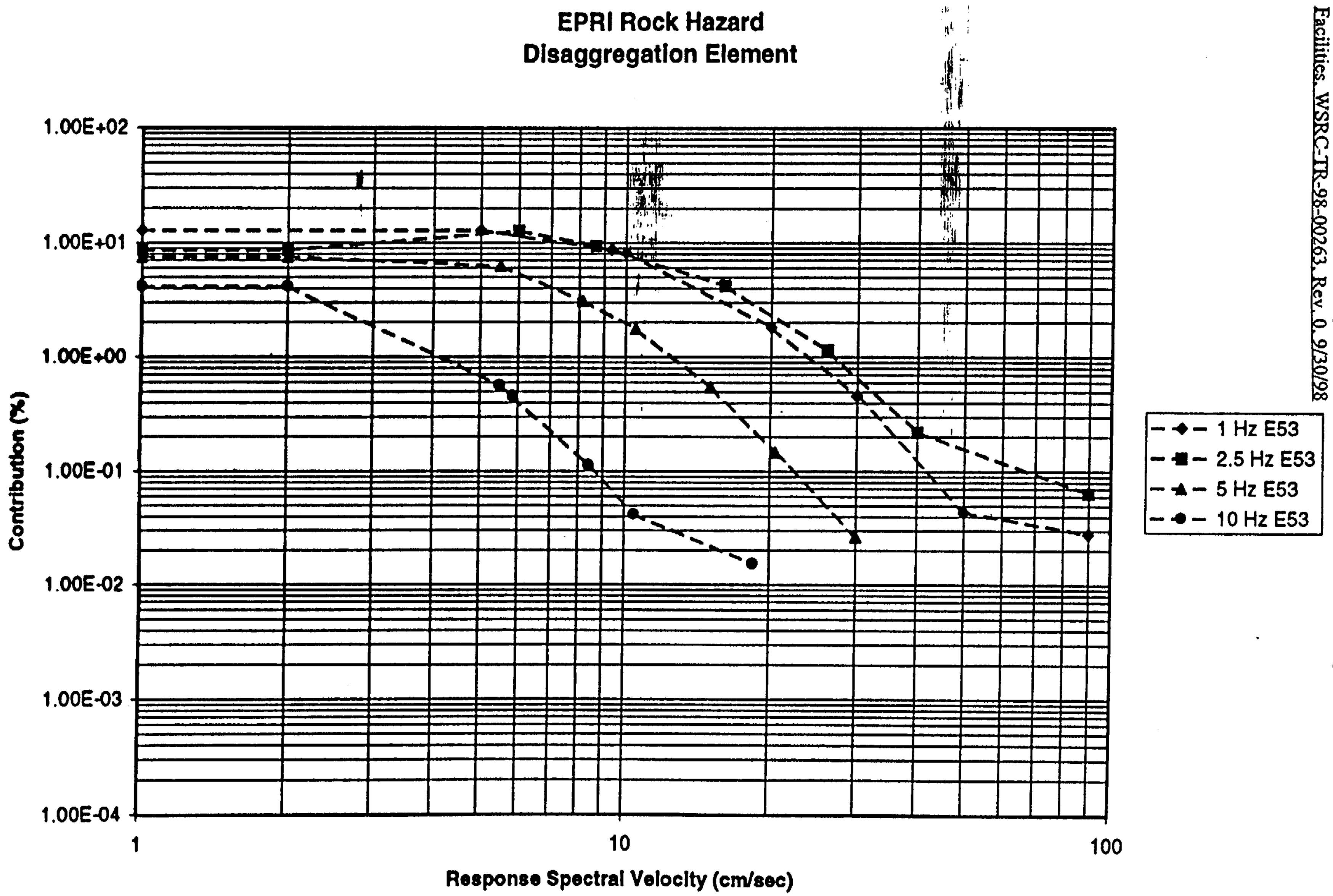

Figure E.23 - EPRI rock hazard disaggregation element 5,3 (Mw 5.9, 175. km) for the 1, 2.5, 5, and 10 Hz oscillator.

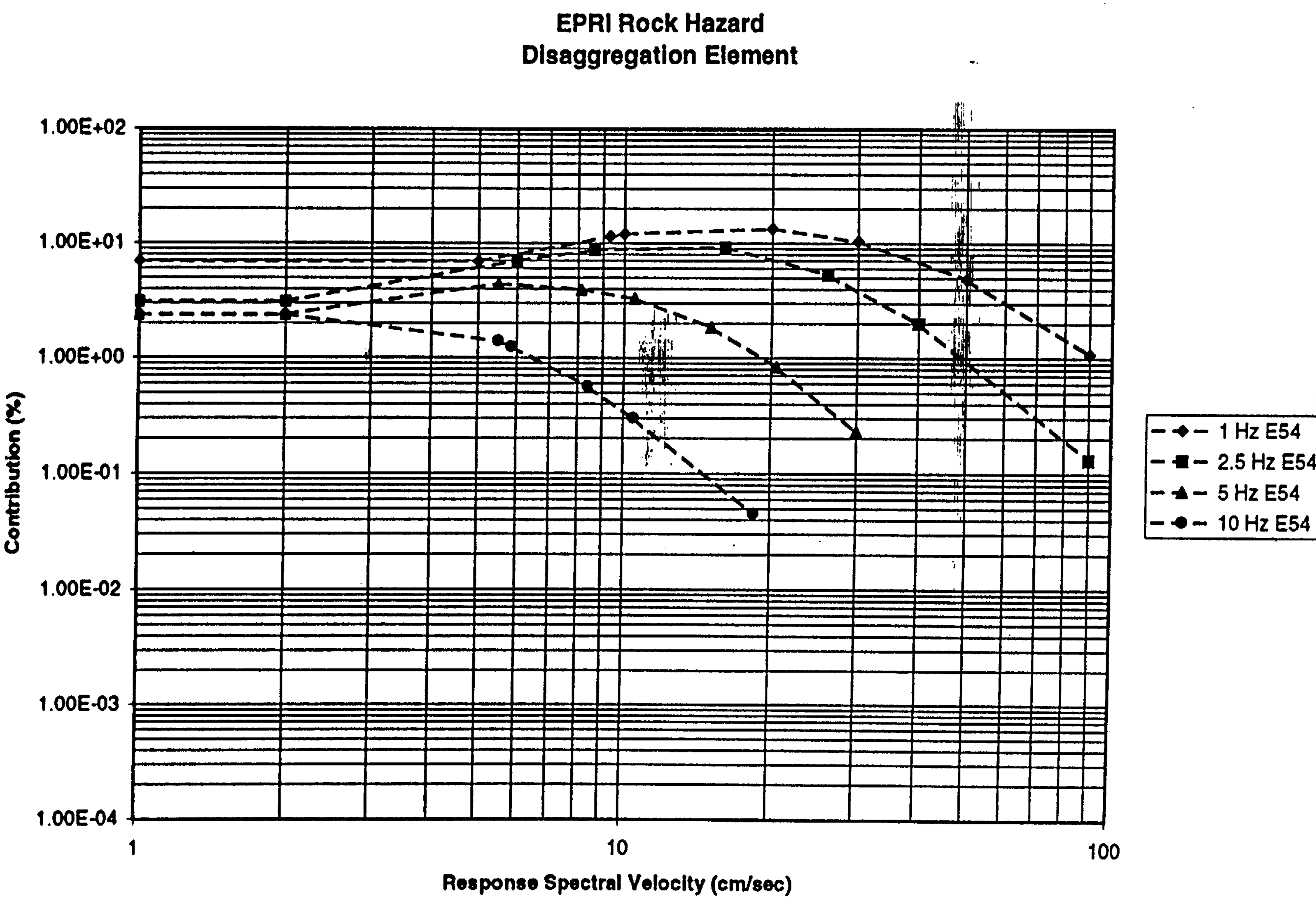

Figure E.24 - EPRI rock hazard disaggregation element 5,4 (Mw 6.7, 175. km) for the 1, 2.5; 5, and 10 Hz oscillator.

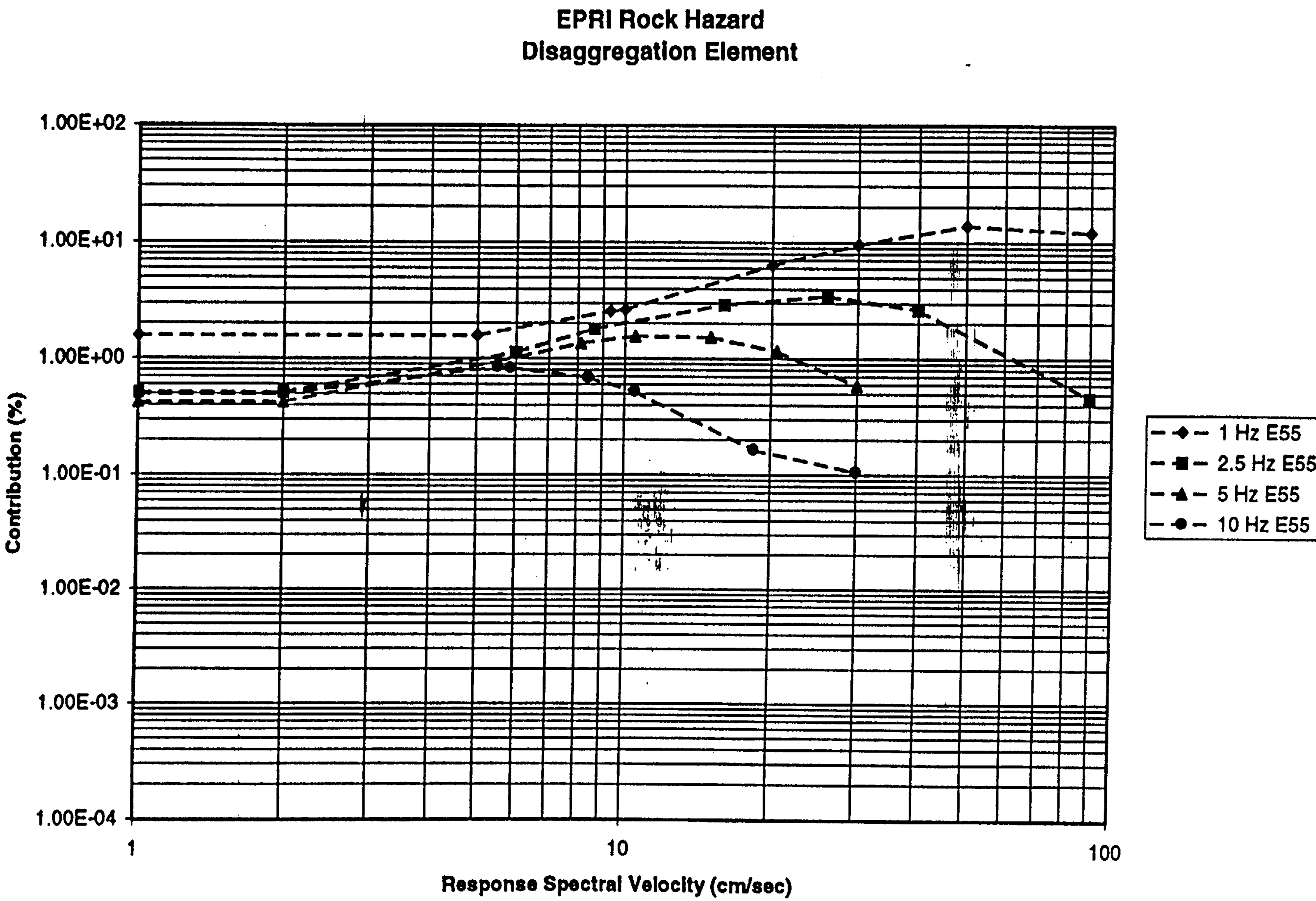

Figure E.25 - EPRI rock hazard disaggregation element 5,5 (Mw 7.8, 175. km) for the 1, 2.5, 5, and 10 Hz oscillator.

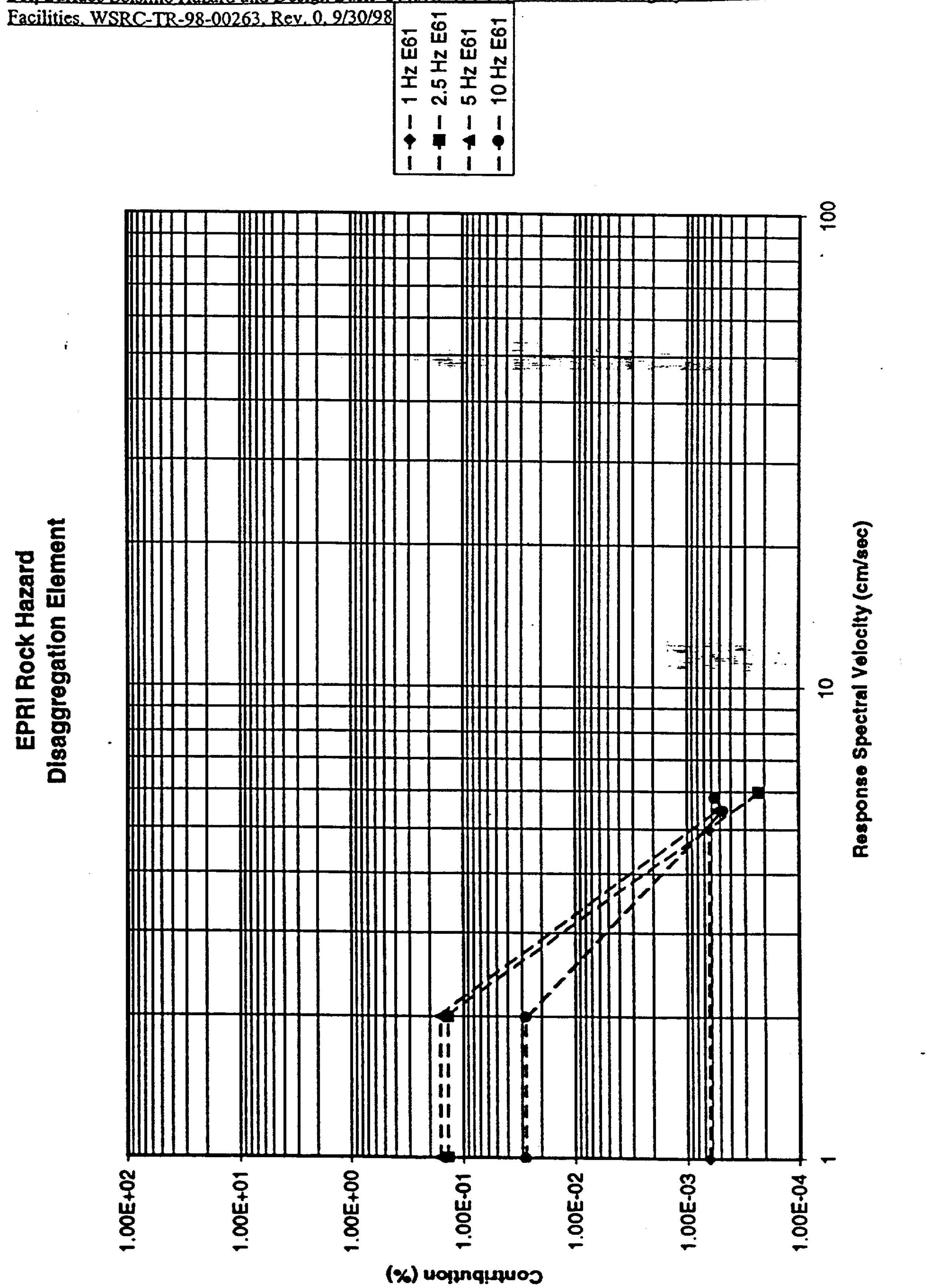

Figure E.26 - EPRI rock hazard disaggregation element 6,1 (Mw 4.75, 225. km) for the 1, 2.5, 5, and 10 Hz oscillator.

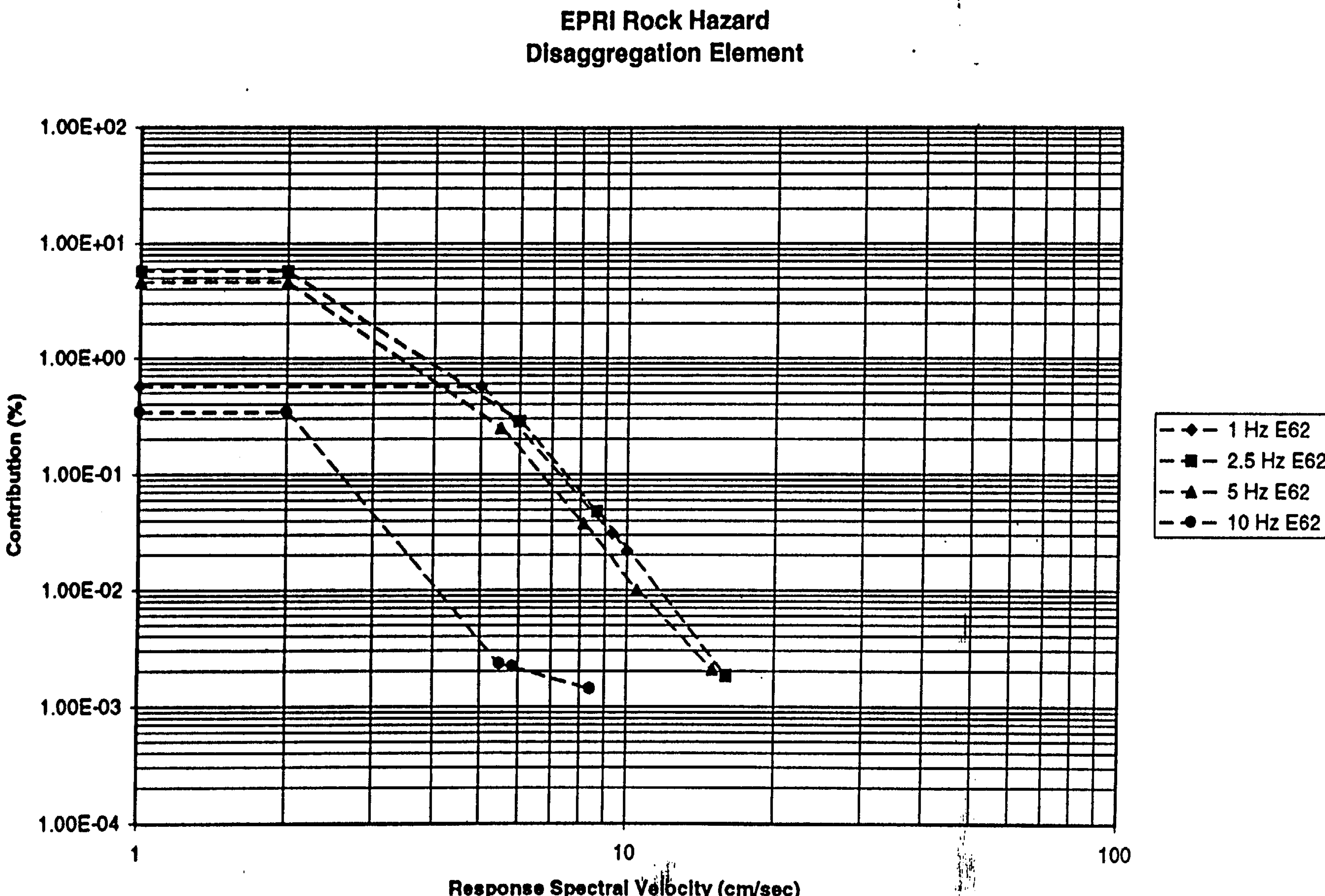

Figure E.27 - EPRI rock hazard disaggregation element 6,2 (Mw 5.25, 225. km) for the 1, 2.5, 5, and 10 Hz oscillator.

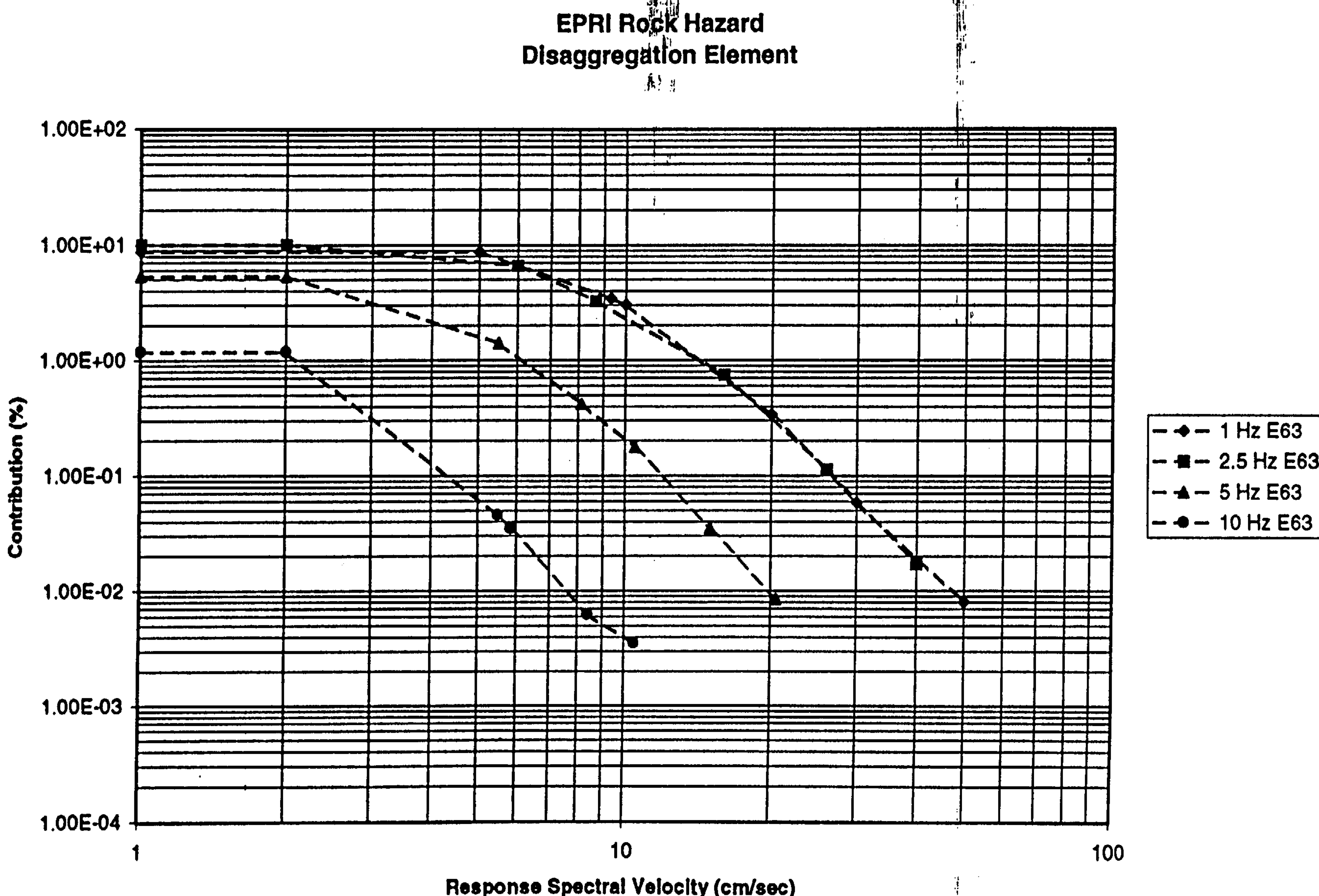

Figure E.28 - EPRI rock hazard disaggregation element 6,3 (Mw 5.9, 225. km) for the 1, 2.5, 5, and 10 Hz oscillator.

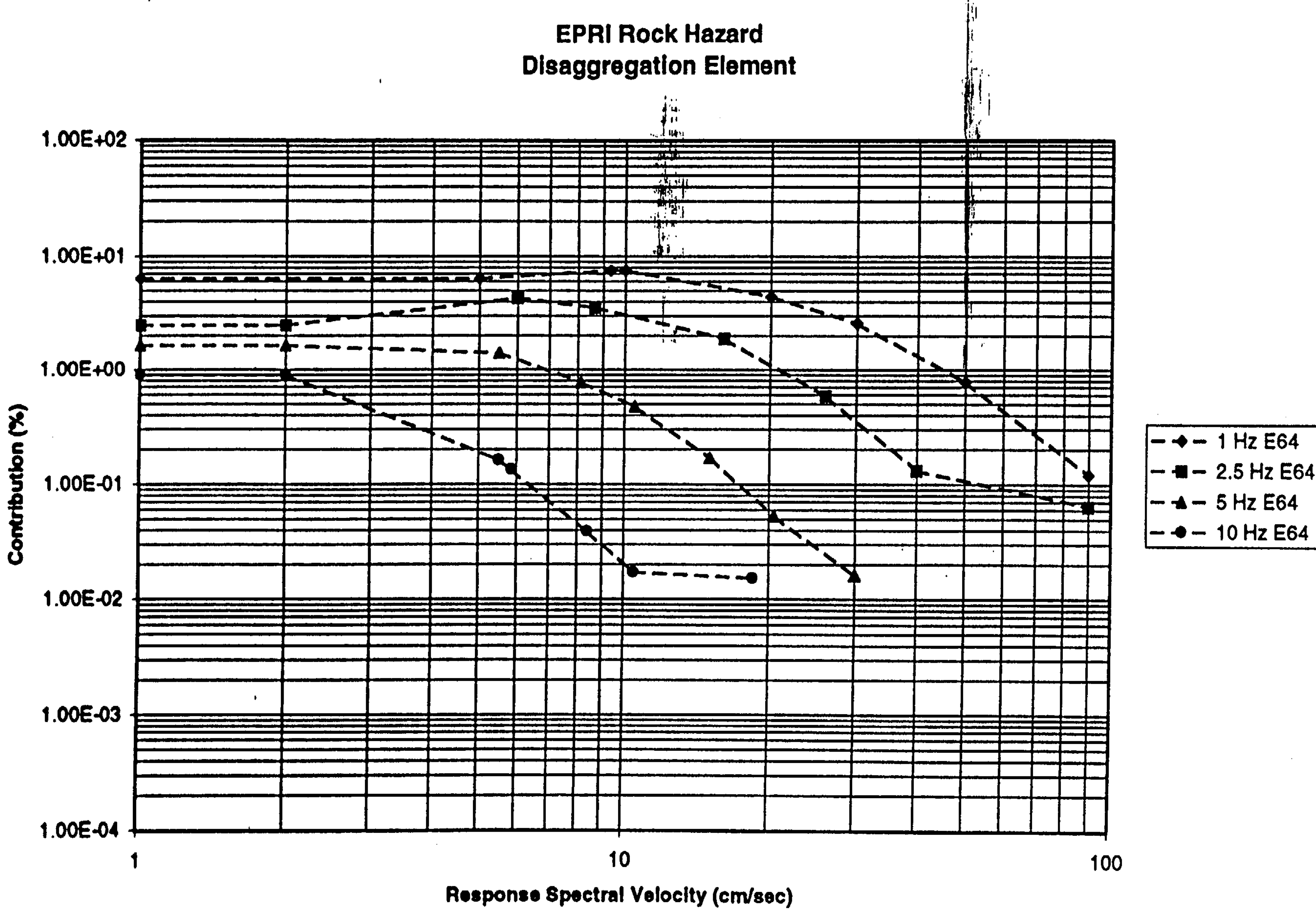

Figure E.29 - EPRI rock hazard disaggregation element 6,4 (Mw 6.7, 225. km) for the 1, 2.5, 5, and 10 Hz oscillator.

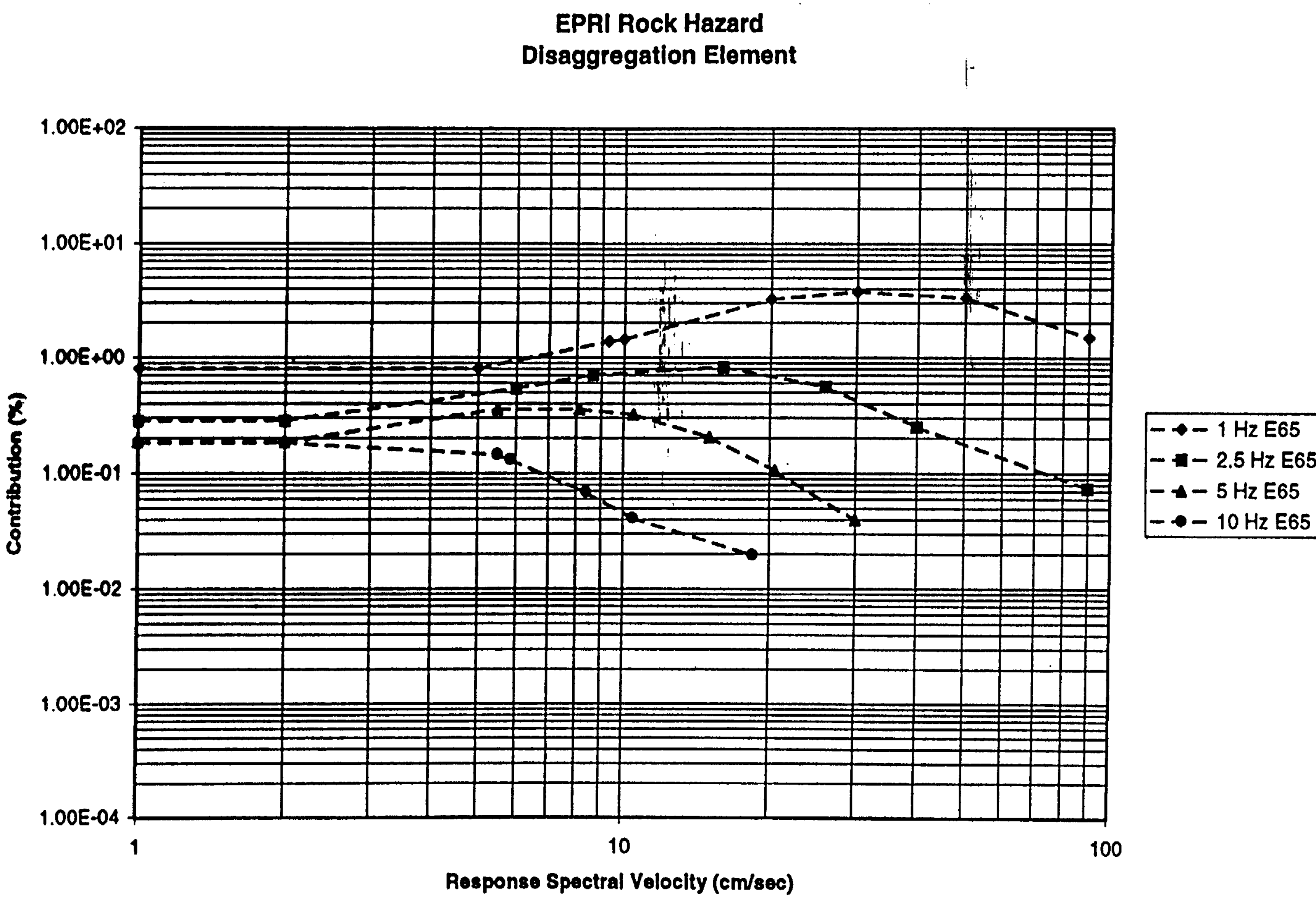

Figure E.30 - EPRI rock hazard disaggregation element 6,5 (Mw 7.8, 225. km) for the 1, 2.5, 5, and 10 Hz oscillator.

APPENDIX F

LLNL BEDROCK HAZARD DISAGGREGATION

This Appendix illustrates the LLNL hazard disaggregation.

The LLNL hazard disaggregation magnitude and distance bins are:

Magnitude (Mw): 5-5.5, 5.5-6.0, 6.0-6.5, 6.5-7, >7

Distance (km): 0-15, 15-25, 25-50, 50-100, 100-200, 200-300, >300

The LLNL disaggregation is comprised of nine (9) tables for frequencies of 1, 2.5, and 5 Hz having dimensions of 7(distance) x 5(magnitude), plus eight (8) tables for 10 Hz having dimensions of 7(distance) x 5(magnitude).

Figures F.1 to F.35 illustrate the 35 elements of the LLNL hazard disaggregation. For each element of the disaggregation, the percent contribution to the total hazard is shown as a function of response spectral velocity. Note that because the LLNL hazard disaggregation elements were given as percentiles ranging from 0-100, disaggregation elements with 0 percentile were not plotted. Thus, disaggregation element 7,1 (Mw 5.25, 350 km) were all zero for all four frequencies and all level of motions.

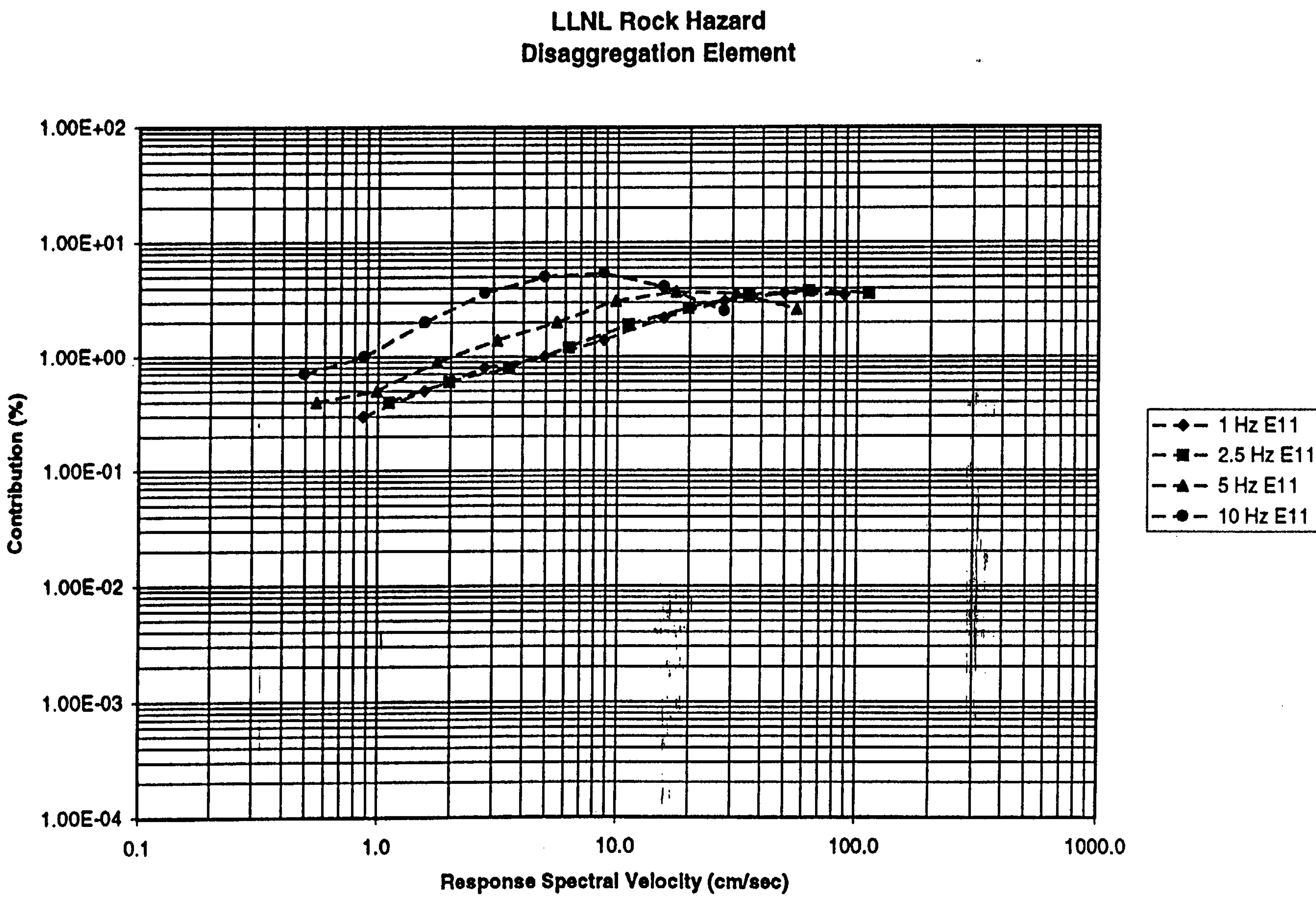

Figure F.1 - LLNL rock hazard disaggregation element 1,1 (Mw 5.25, 10. km) for the 1, 2.5, 5, and 10 Hz oscillator. Values less than 1% were identically 0 and not plotted.

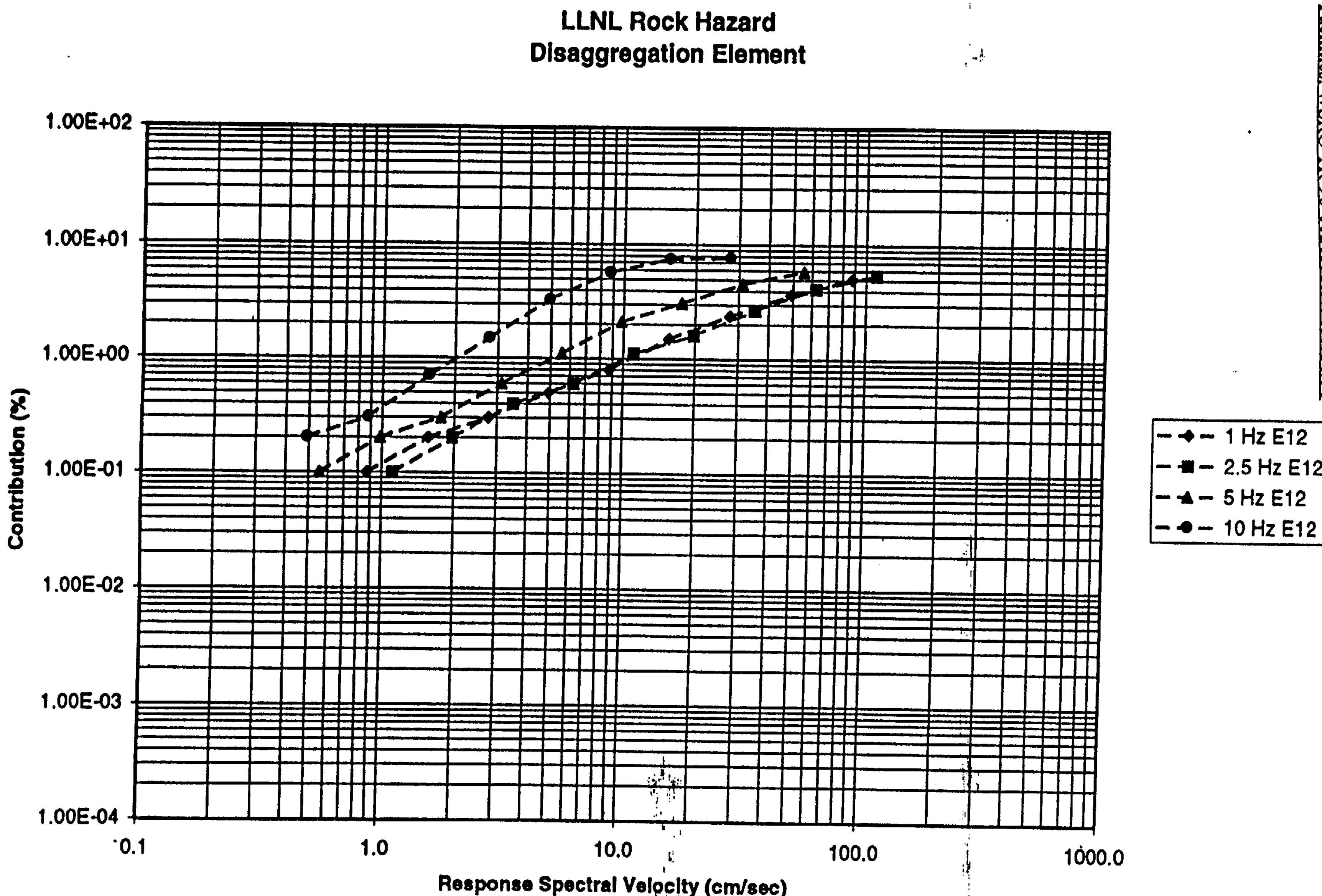

Figure F.2 - LLNL rock hazard disaggregation element 1,2 (Mw 5.75, 10. km) for the 1, 2.5, 5, and 10 Hz oscillator. Values less than 1% were identically 0 and not plotted.

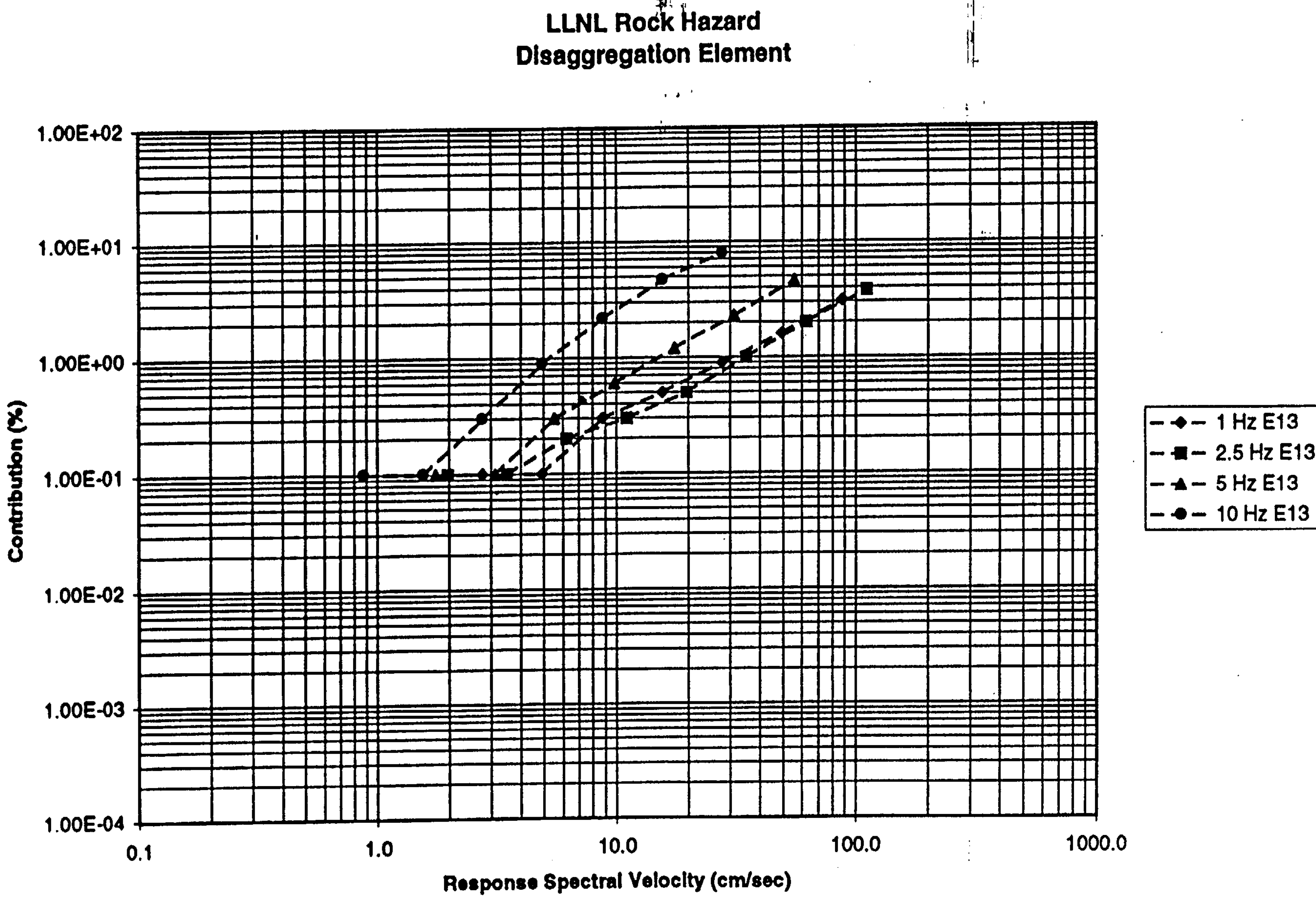

Figure F.3 - LLNL rock hazard disaggregation element 1,3 (Mw 6.25, 10. km) for the 1, 2.5, 5, and 10 Hz oscillator. Values less than 1% were identically 0 and not plotted.

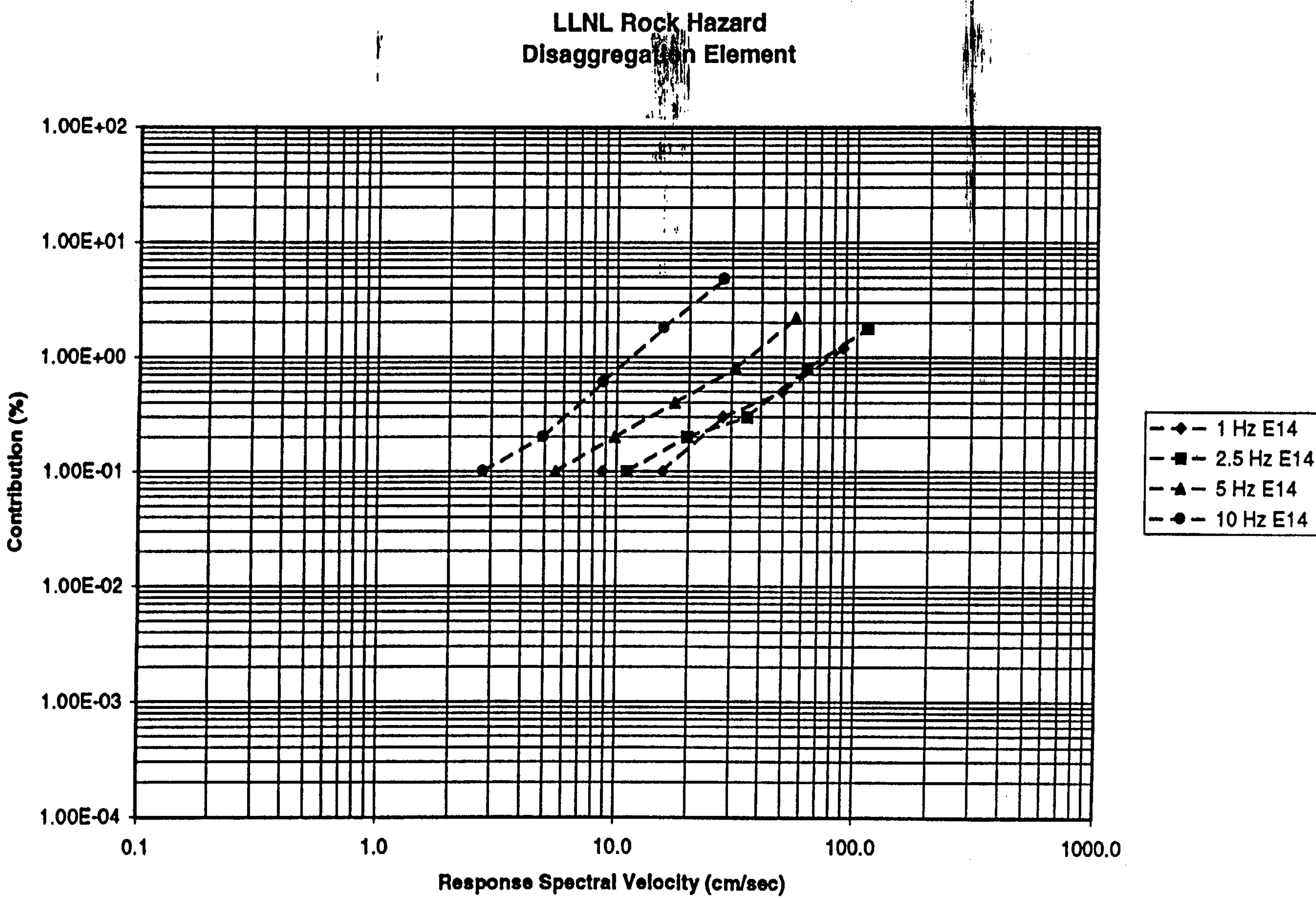

Figure F.4 - LLNL rock hazard disaggregation element 1,4 (Mw 6.75, 10. km) for the 1, 2.5, 5, and 10 Hz oscillator. Values less than 1% were identically 0 and not plotted.

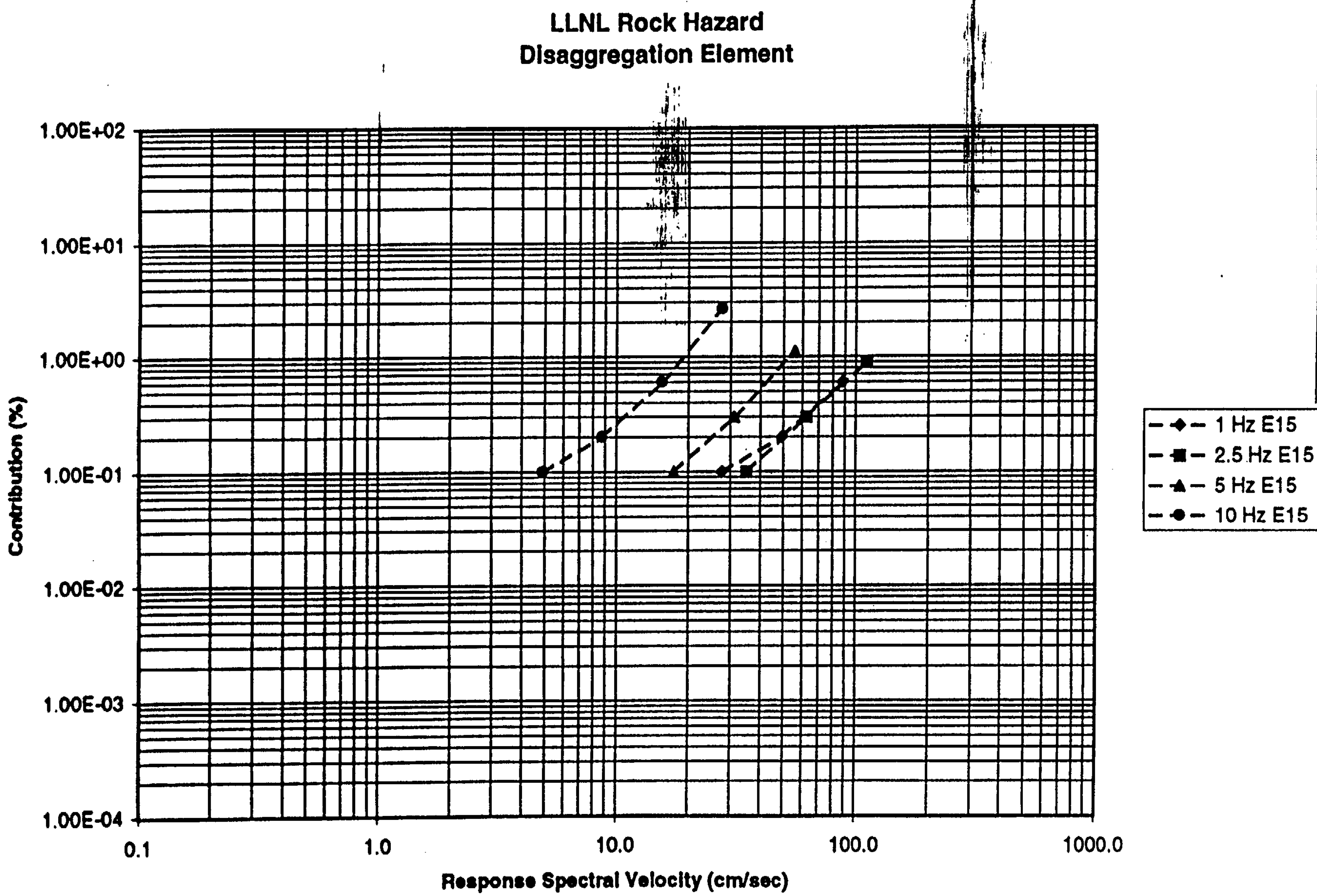

Figure F.5 - LLNL rock hazard disaggregation element 1,5 (Mw 7.5, 10. km) for the 1, 2.5, 5, and 10 Hz oscillator. Values less than 1% were identically 0 and not plotted.

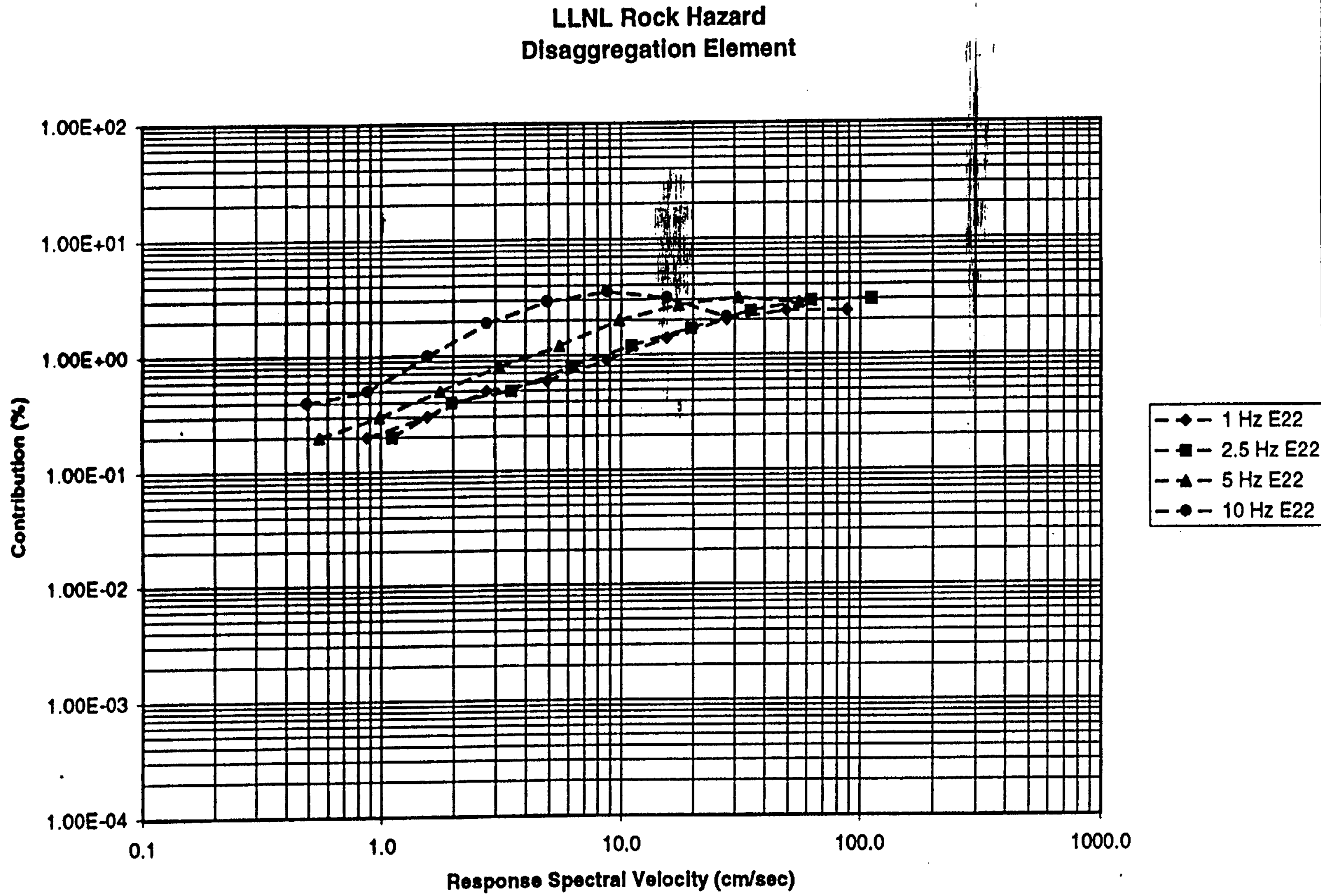

Figure F.7 - LLNL rock hazard disaggregation element 2,2 (Mw 5.75, 20.4 km) for the 1, 2.5, 5, and 10 Hz oscillator. Values less than 1% were identically 0 and not plotted.

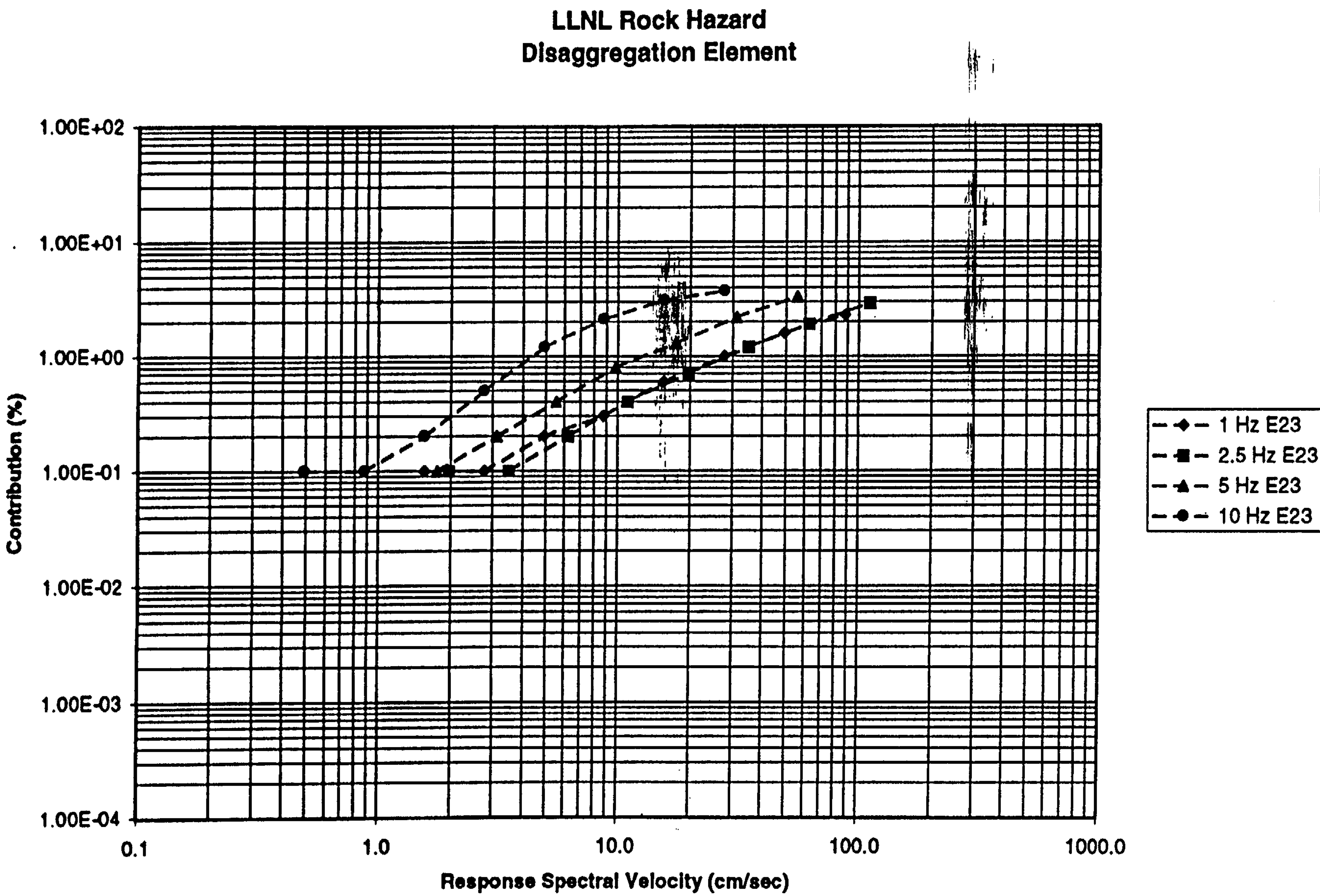

Figure F.8 - LLNL rock hazard disaggregation element 2,3 (Mw 6.25, 20.4 km) for the 1, 2.5, 5, and 10 Hz oscillator. Values less than 1% were identically 0 and not plotted.

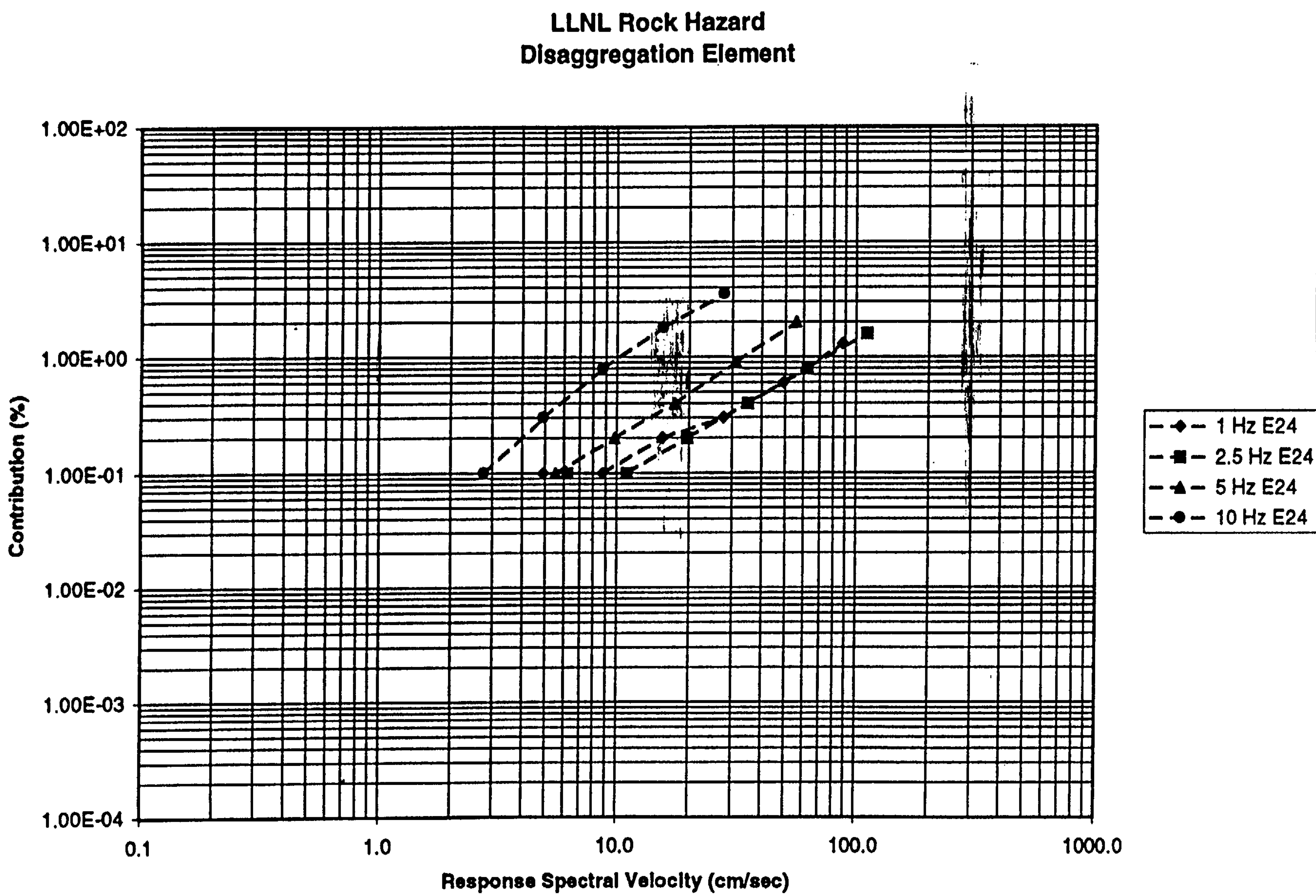

Figure F.9 - LLNL rock hazard disaggregation element 2,4 (Mw 6.75, 20.4 km) for the 1, 2.5, 5, and 10 Hz oscillator. Values less than 1% were identically 0 and not plotted.

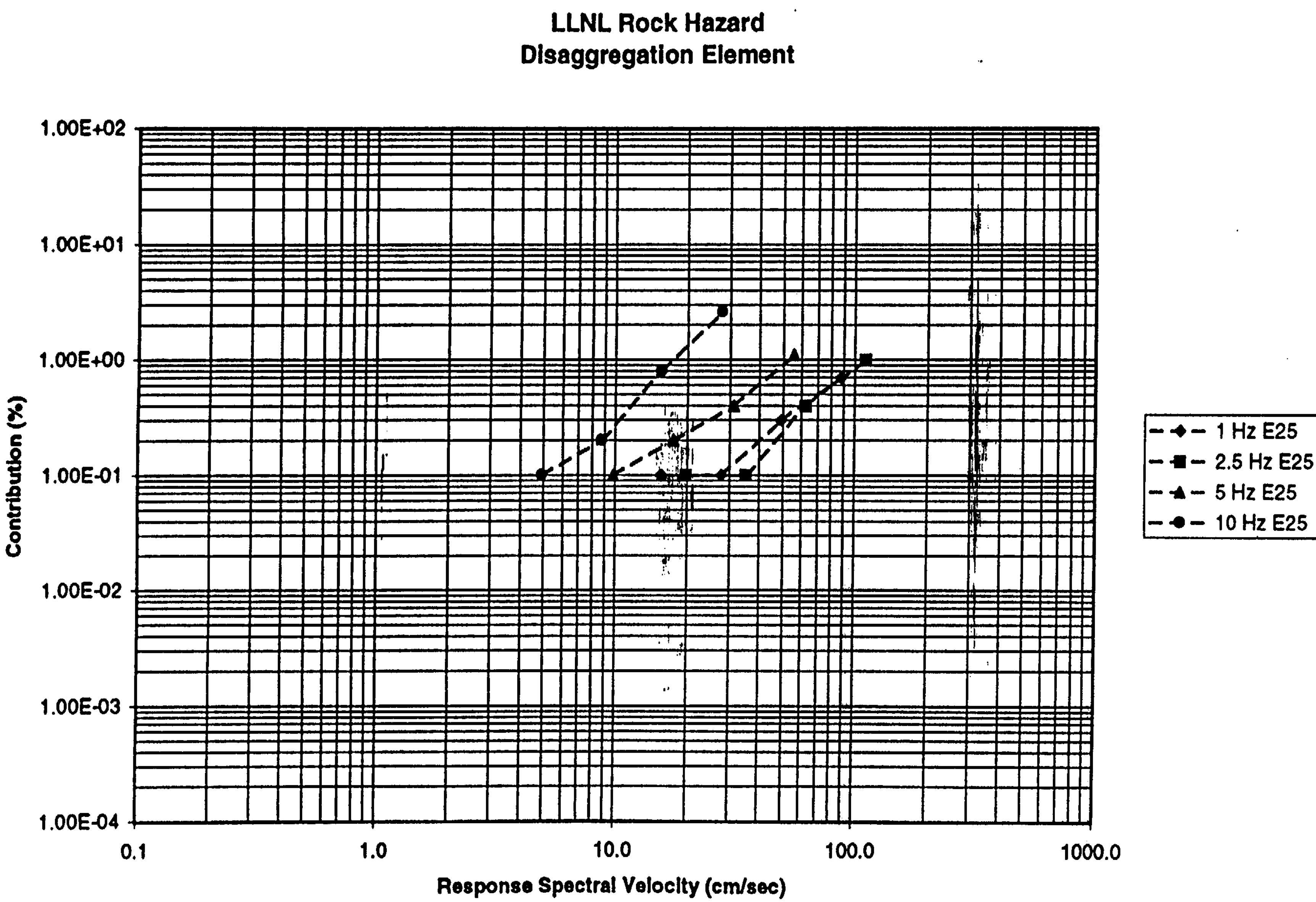

Figure F.10 - LLNL rock hazard disaggregation element 2,5 (Mw 7.5, 20.4 km) for the 1, 2.5, 5, and 10 Hz oscillator. Values less than 1% were identically 0 and not plotted.

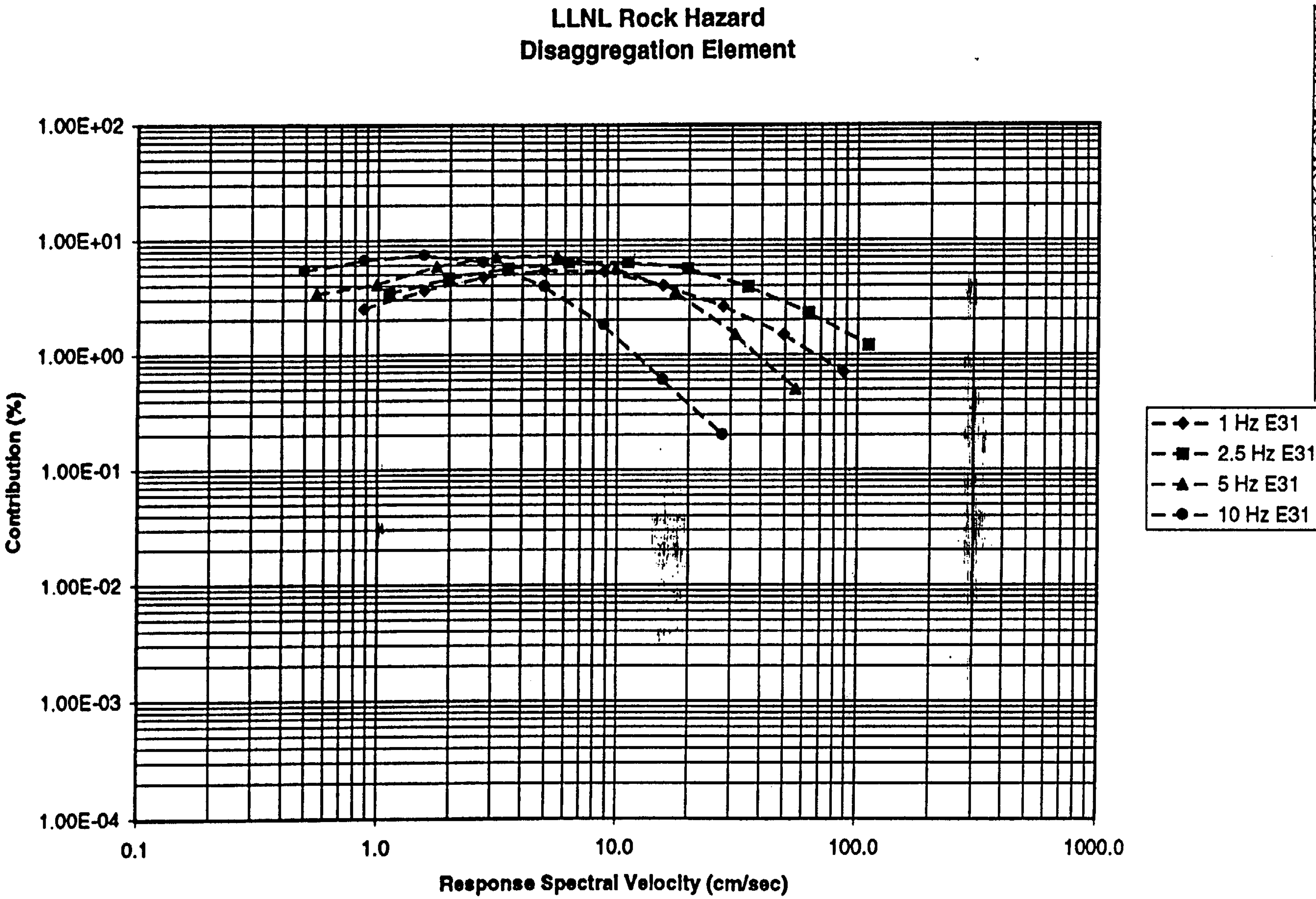

Figure F.11 - LLNL rock hazard disaggregation element 3,1 (Mw 5.25, 38.9 km) for the 1, 2.5, 5, and 10 Hz oscillator. Values less than 1% were identically 0 and not plotted.

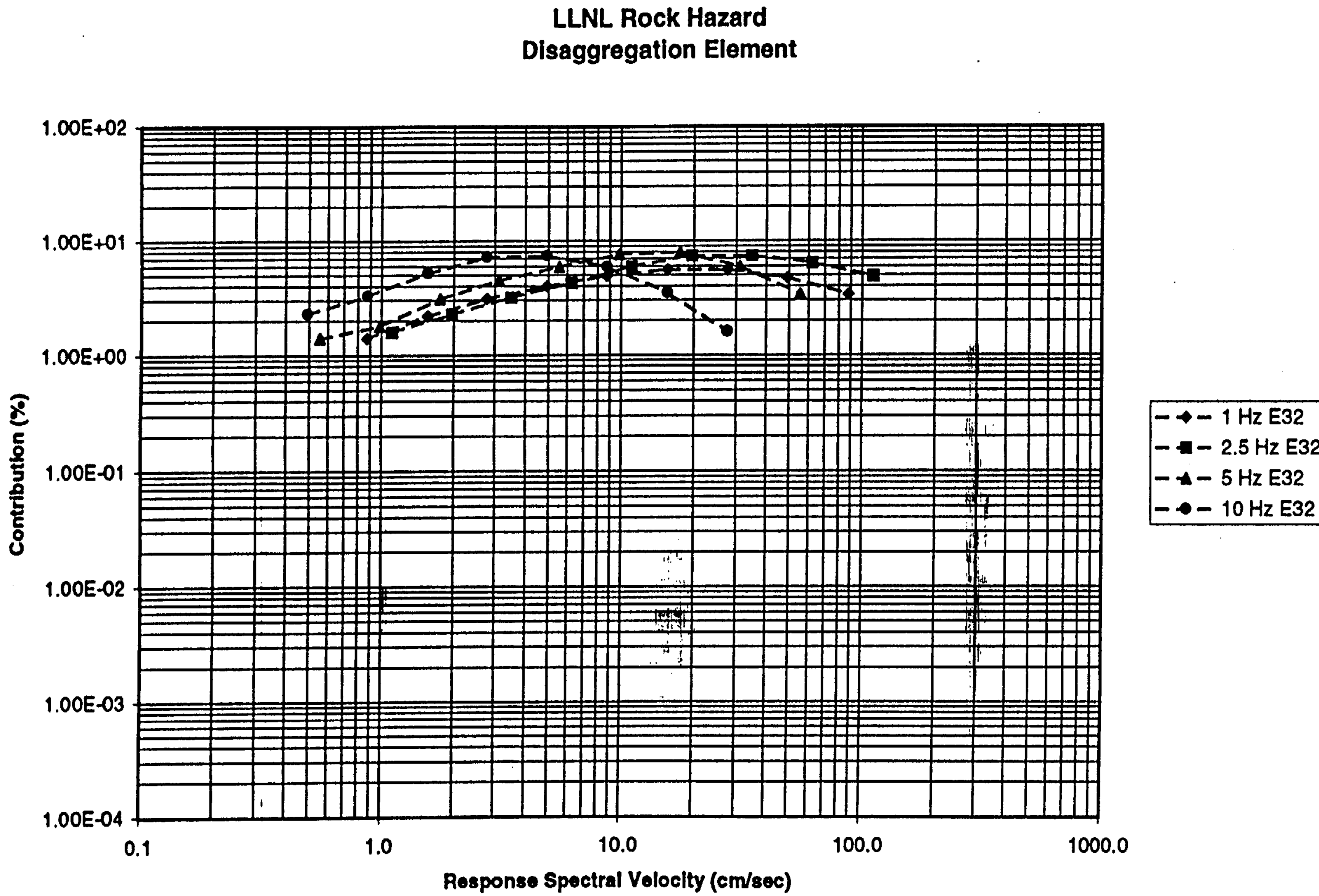

Figure F.12 - LLNL rock hazard disaggregation element 3,2 (Mw 5.75, 38.9 km) for the 1, 2.5, 5, and 10 Hz oscillator. Values less than 1% were identically 0 and not plotted.

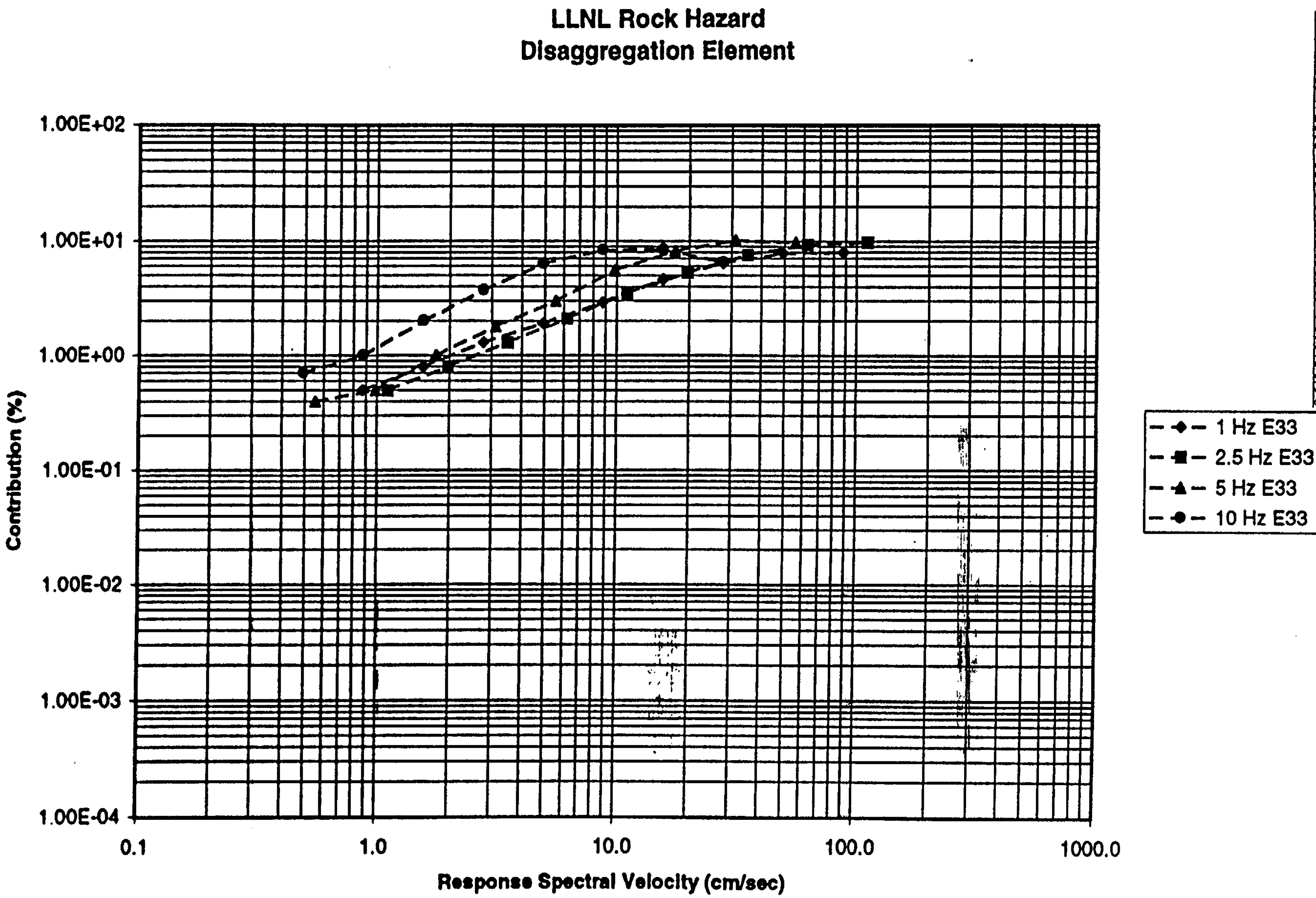

Figure F.13 - LLNL rock hazard disaggregation element 3,3 (Mw 6.25, 38.9 km) for the 1, 2.5, 5, and 10 Hz oscillator. Values less than 1% were identically 0 and not plotted.

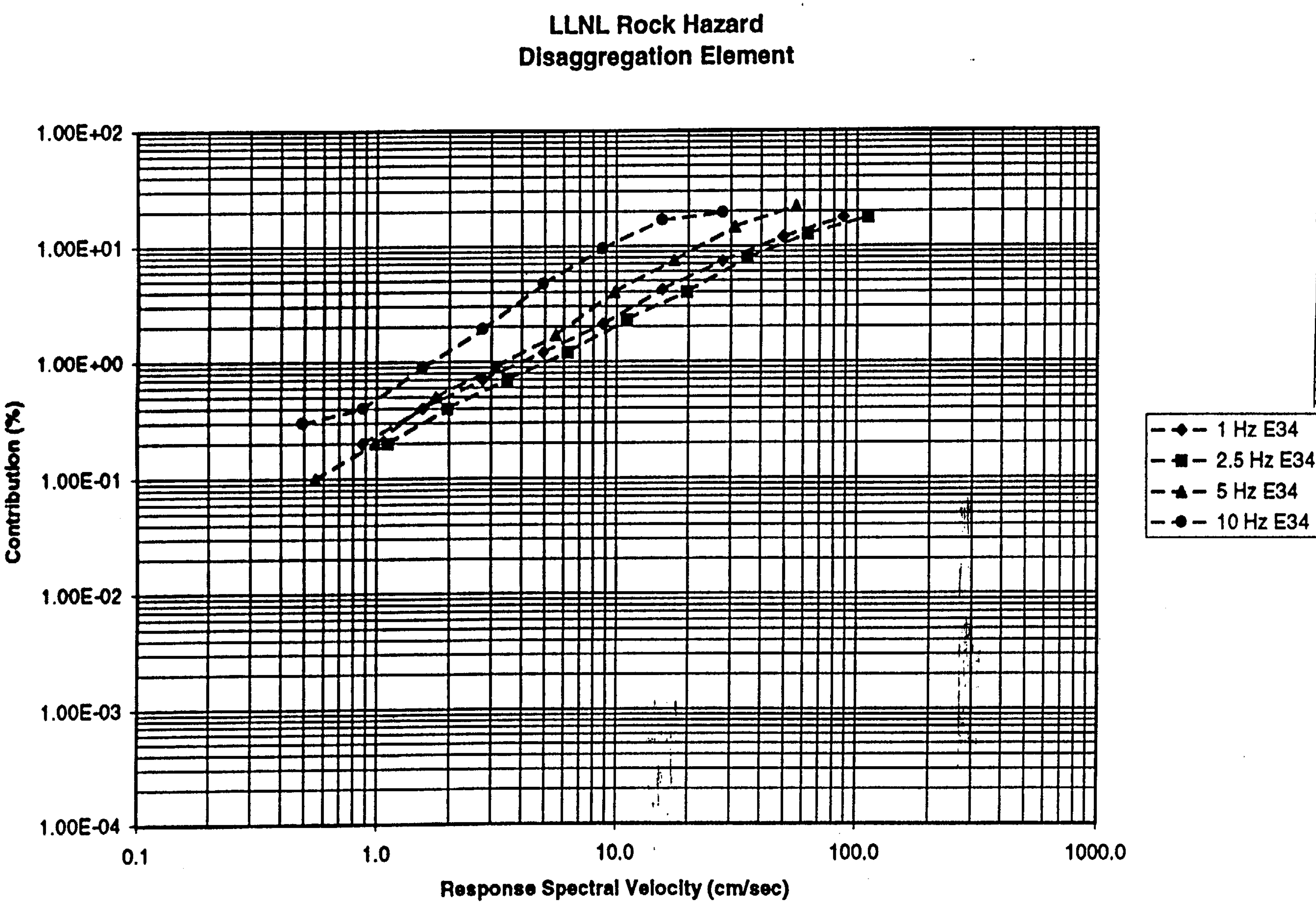

Figure F.14 - LLNL rock hazard disaggregation element 3,4 (Mw 6.75, 38.9 km) for the 1, 2.5, 5, and 10 Hz oscillator. Values less than 1% were identically 0 and not plotted.

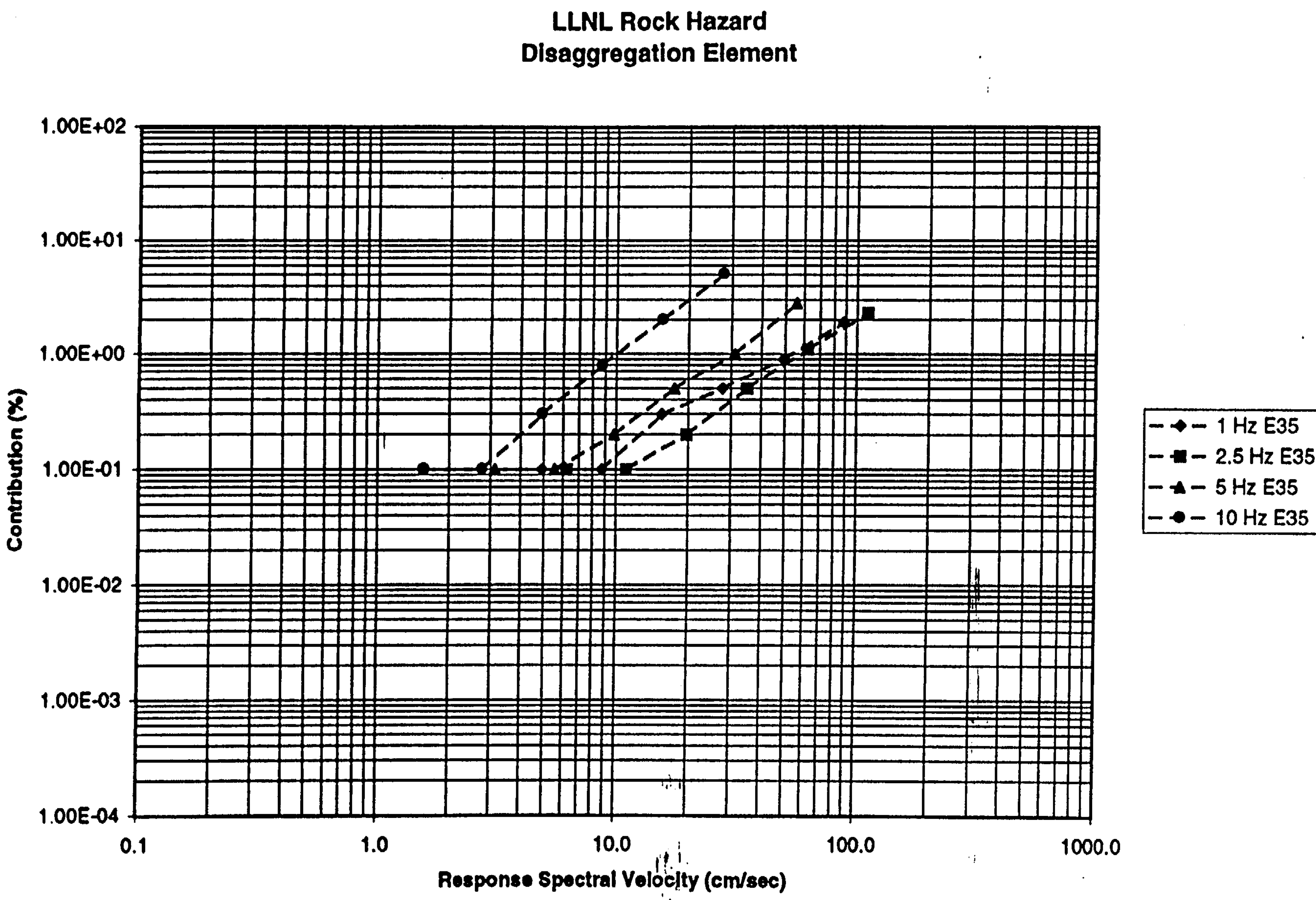

Figure F.15 - LLNL rock hazard disaggregation element 3,5 (Mw 7.5, 38.9 km) for the 1, 2.5, 5, and 10 Hz oscillator. Values less than 1% were identically 0 and not plotted.

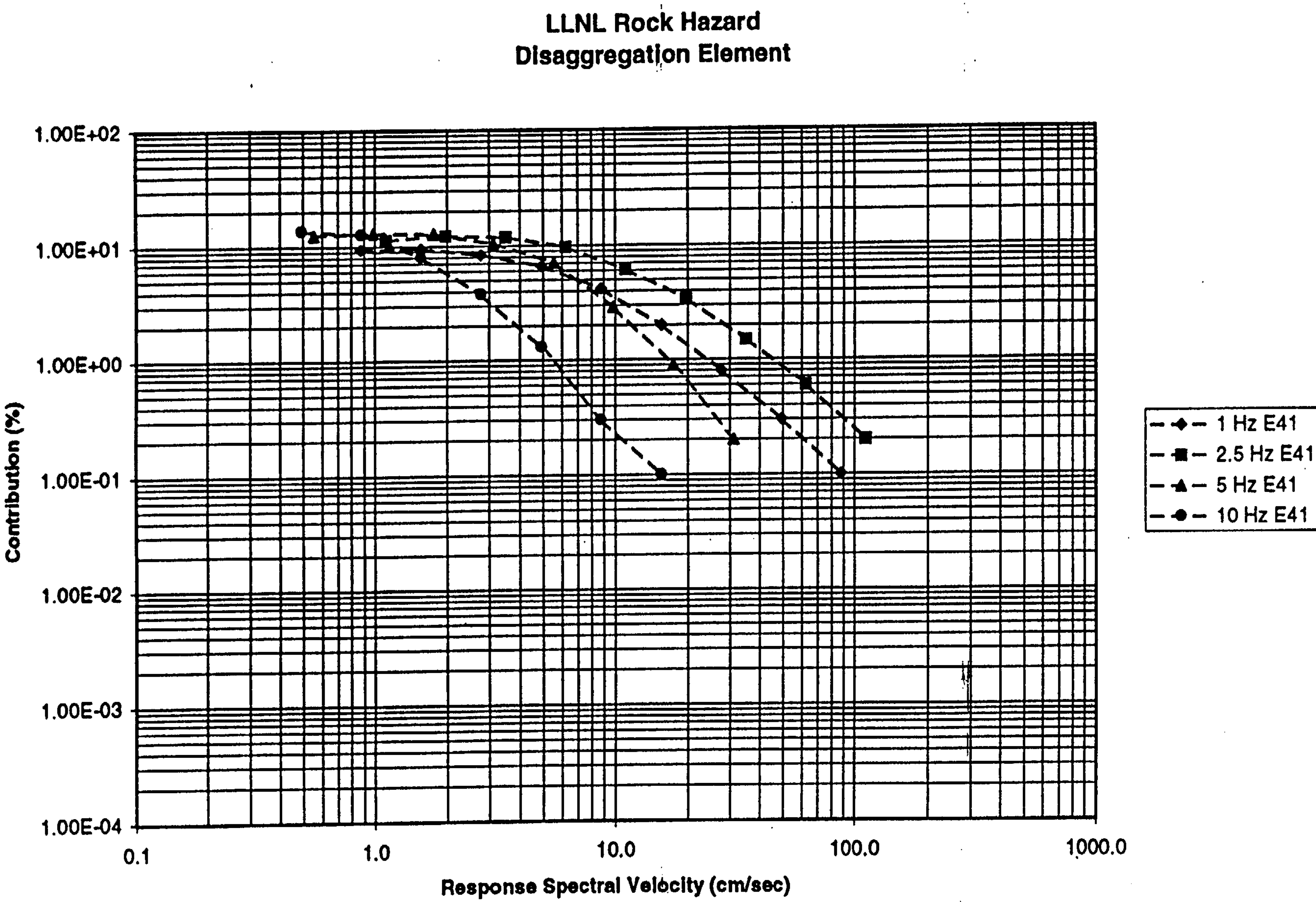

Figure F.16 - LLNL rock hazard disaggregation element 4,1 (Mw 5.25, 77.8 km) for the 1, 2.5, 5, and 10 Hz oscillator. Values less than 1% were identically 0 and not plotted.

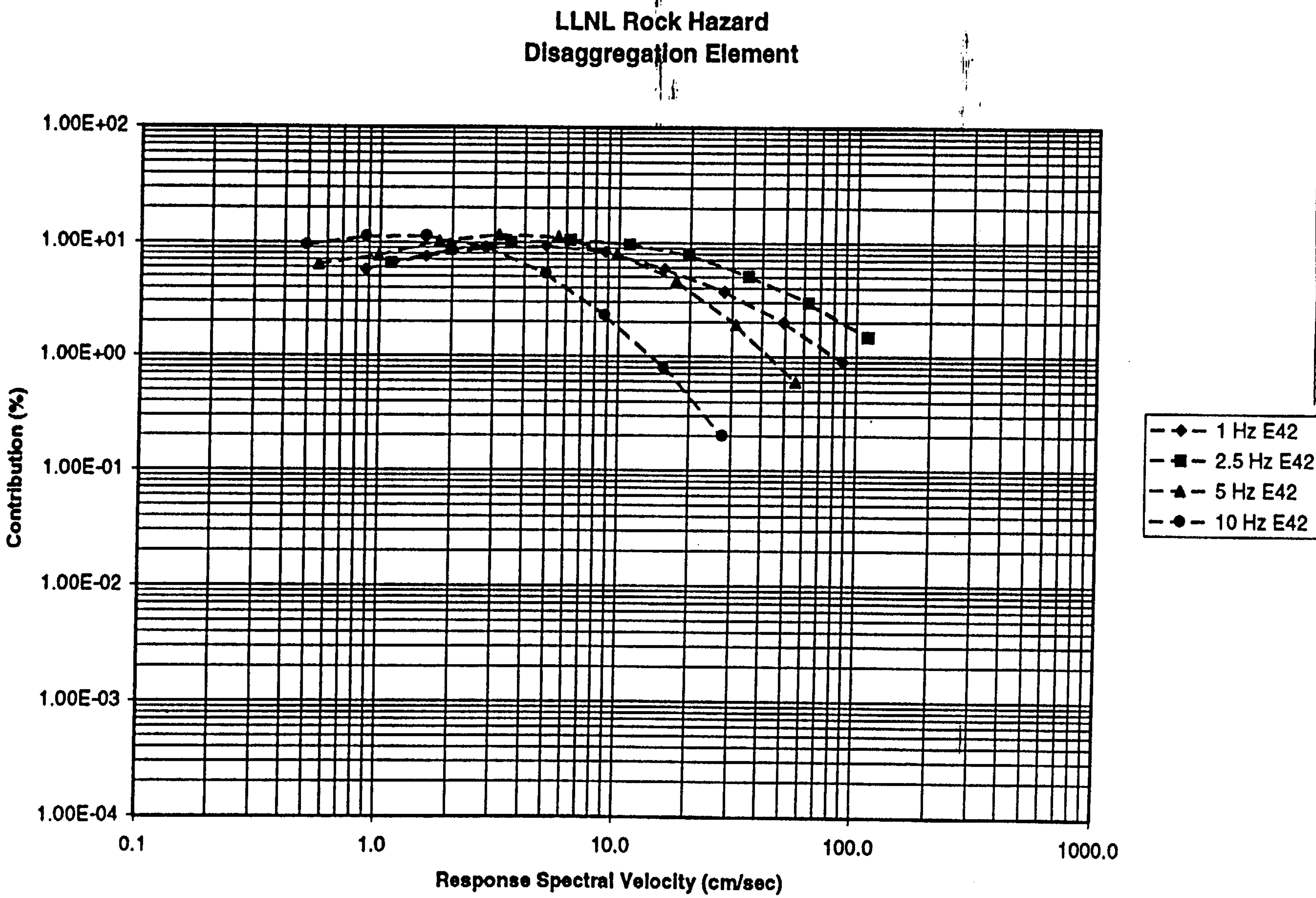

Figure F.17 - LLNL rock hazard disaggregation element 4,2 (Mw 5.75, 77.8 km) for the 1, 2.5, 5, and 10 Hz oscillator. Values less than 1% were identically 0 and not plotted.

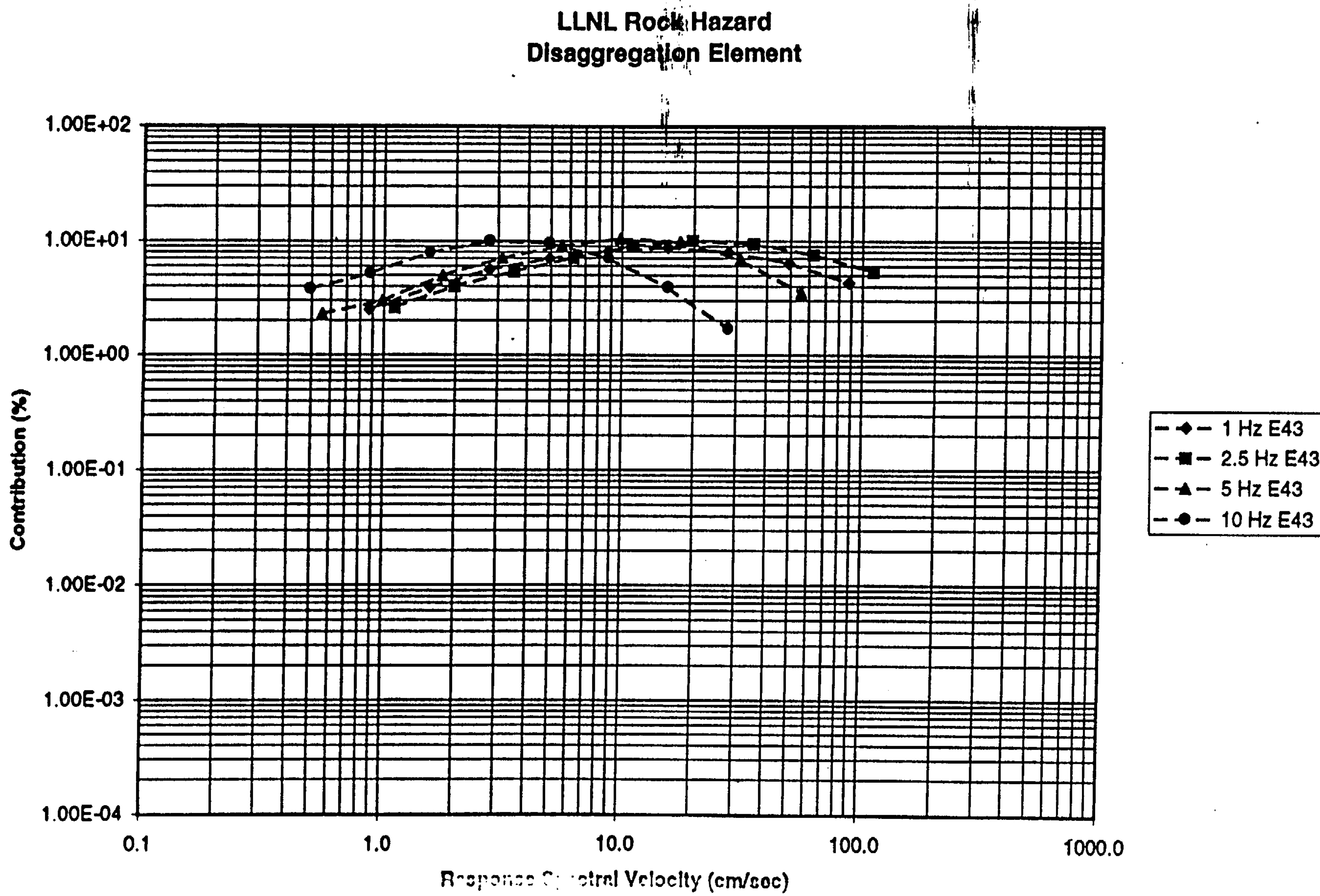
LLNL Rock Hazard
Disaggregation Element
Contribution (%)
1.00E+02
1.00E+01
1.00E+00
1.00E-01
1.00E-02
1.00E-03
1.00E-04
0.1
1.0
10.0
100.0
1000.0
1 Hz E43
2.5 Hz E43
5 Hz E43
10 Hz E43

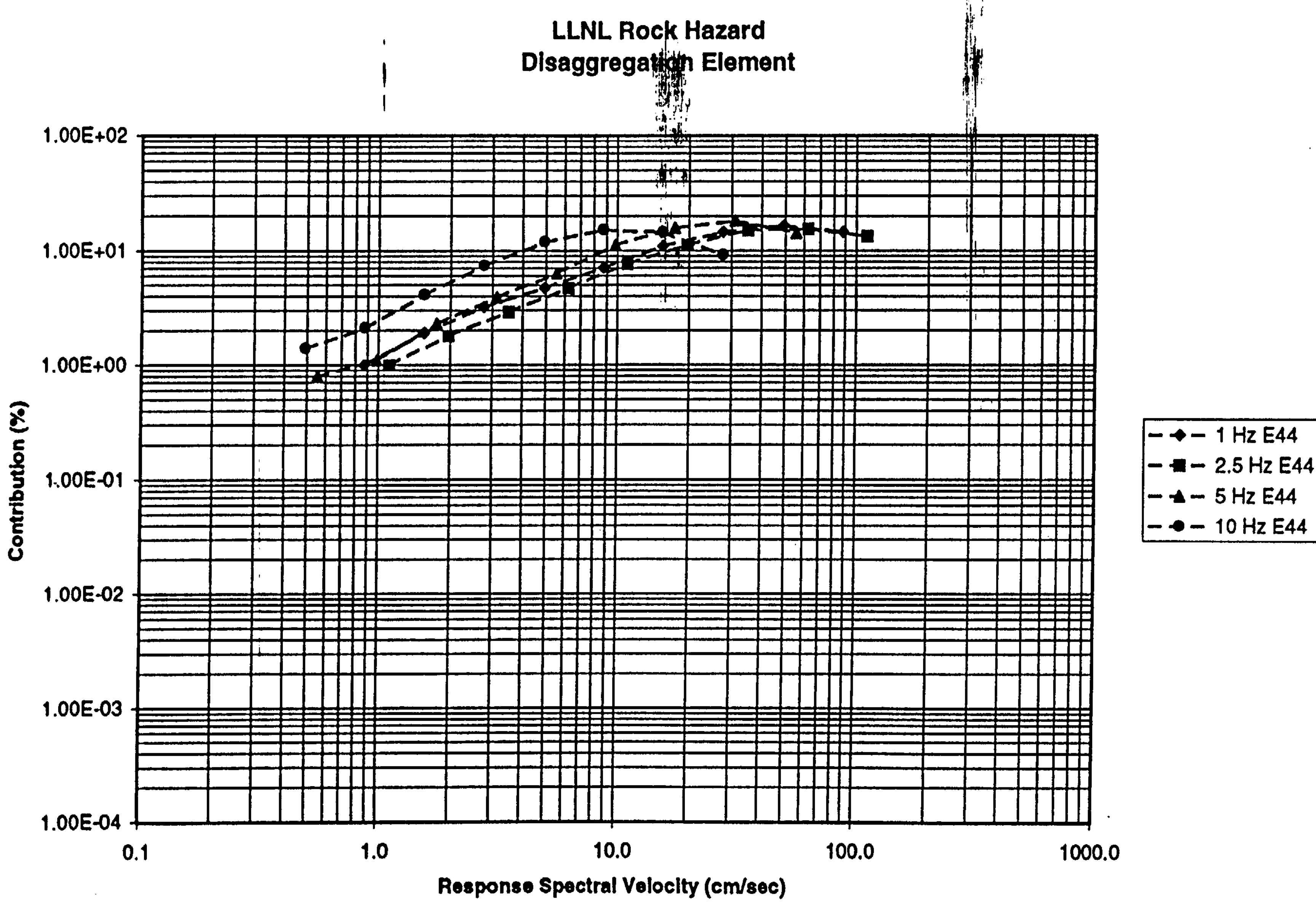

Figure F.19 - LLNL rock hazard disaggregation element 4,4 (Mw 6.75, 77.8 km) for the 1, 2.5, 5, and 10 Hz oscillator. Values less than 1% were identically 0 and not plotted.

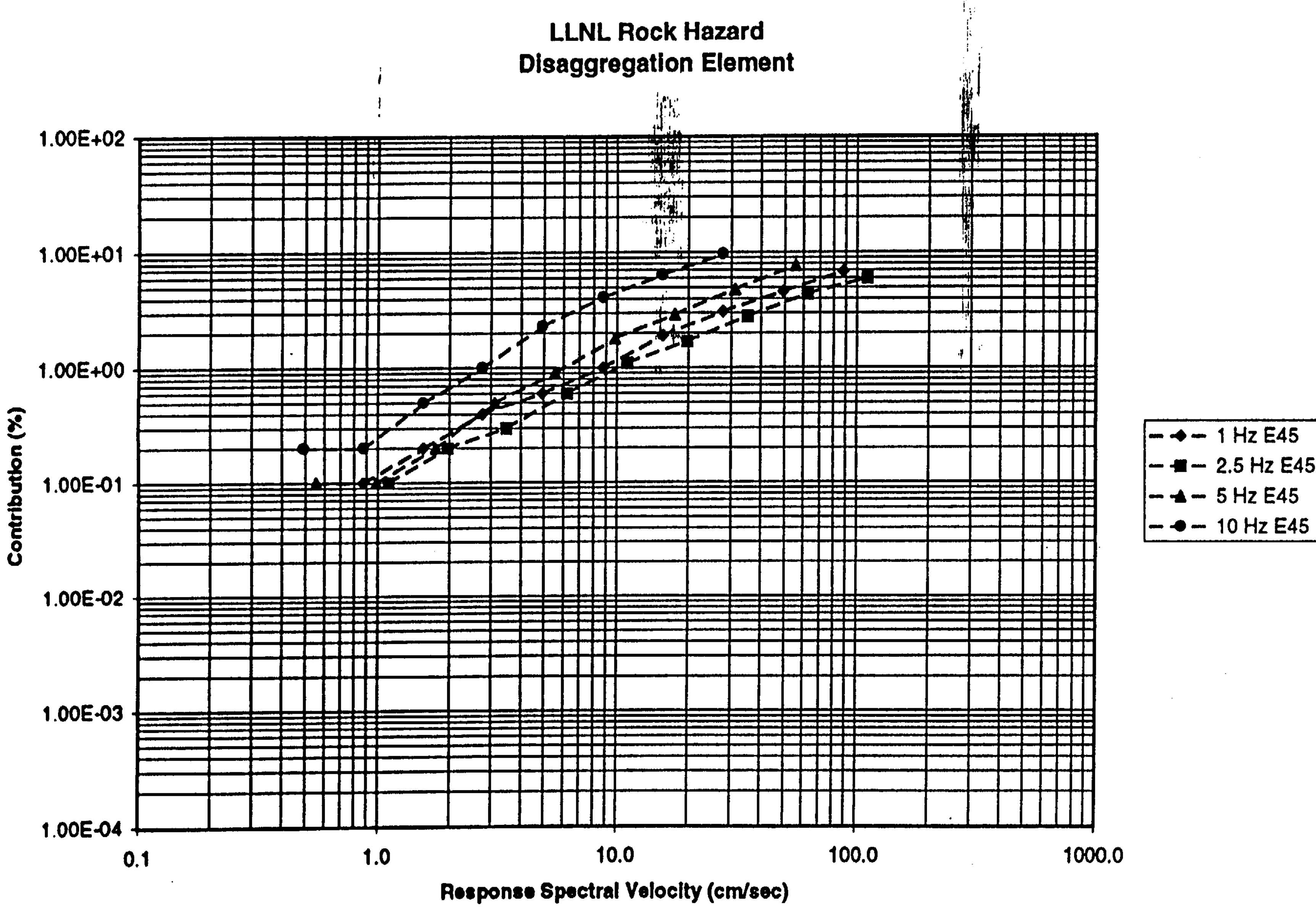

Figure F.20 - LLNL rock hazard disaggregation element 4,5 (Mw 7.5, 77.8 km) for the 1, 2.5, 5, and 10 Hz oscillator. Values less than 1% were identically 0 and not plotted.

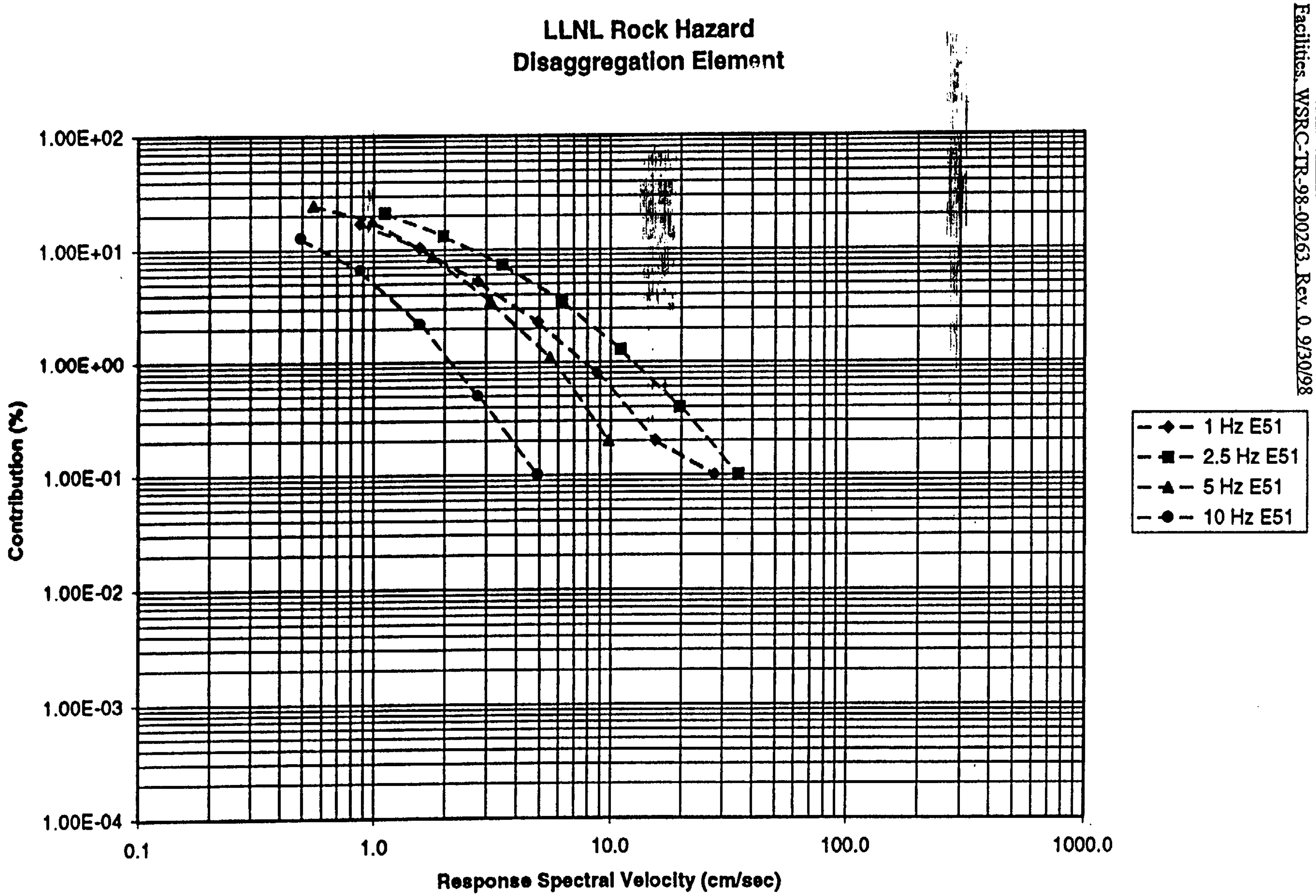

Figure F.21 - LLNL rock hazard disaggregation element 5,1 (Mw 5.25, 156. km) for the 1, 2.5, 5, and 10 Hz oscillator. Values less than 1% were identically 0 and not plotted.

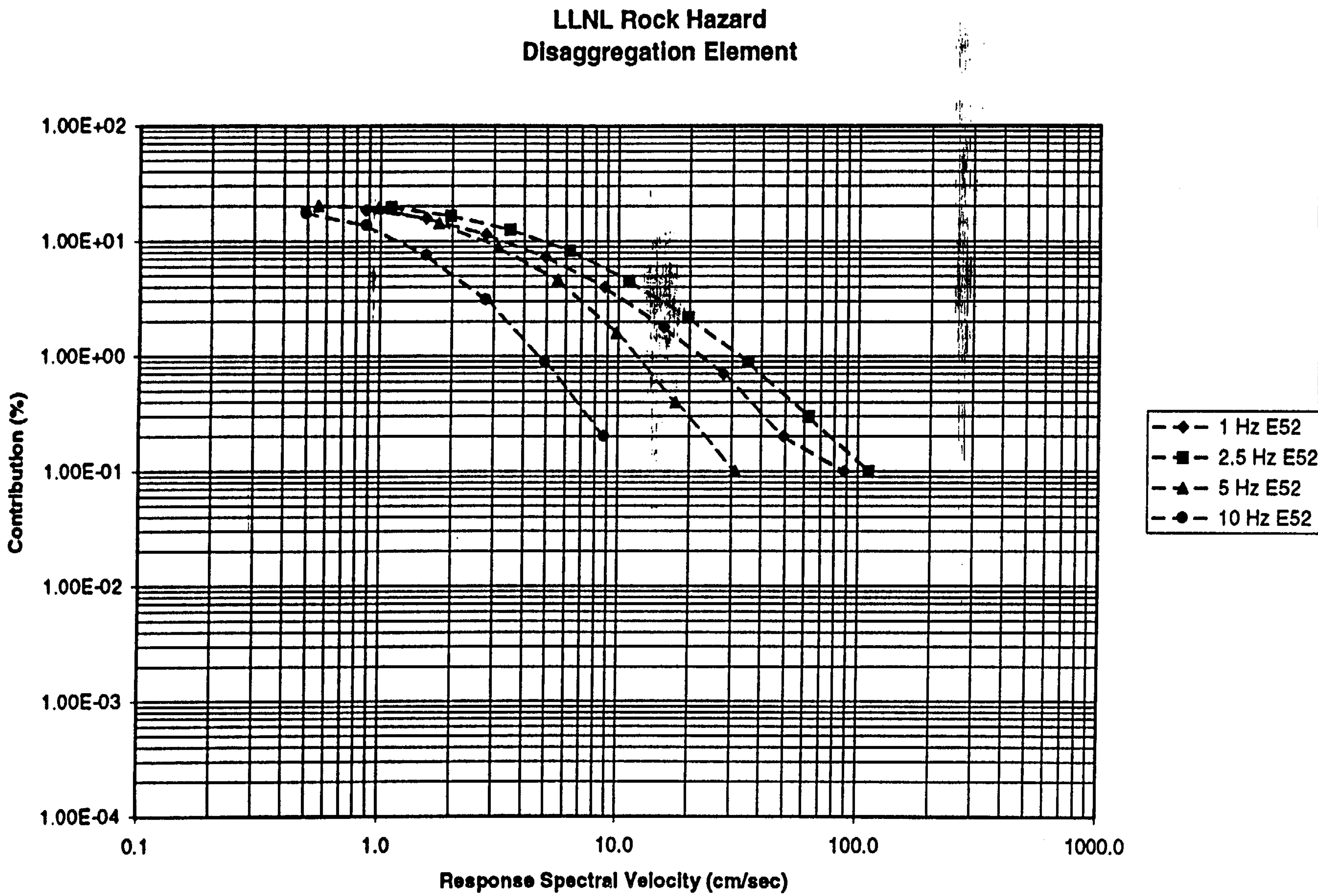

Figure F.22 - LLNL rock hazard disaggregation element 5,2 (Mw 5.75, 156. km) for the 1, 2.5, 5, and 10 Hz oscillator. Values less than 1% were identically 0 and not plotted.

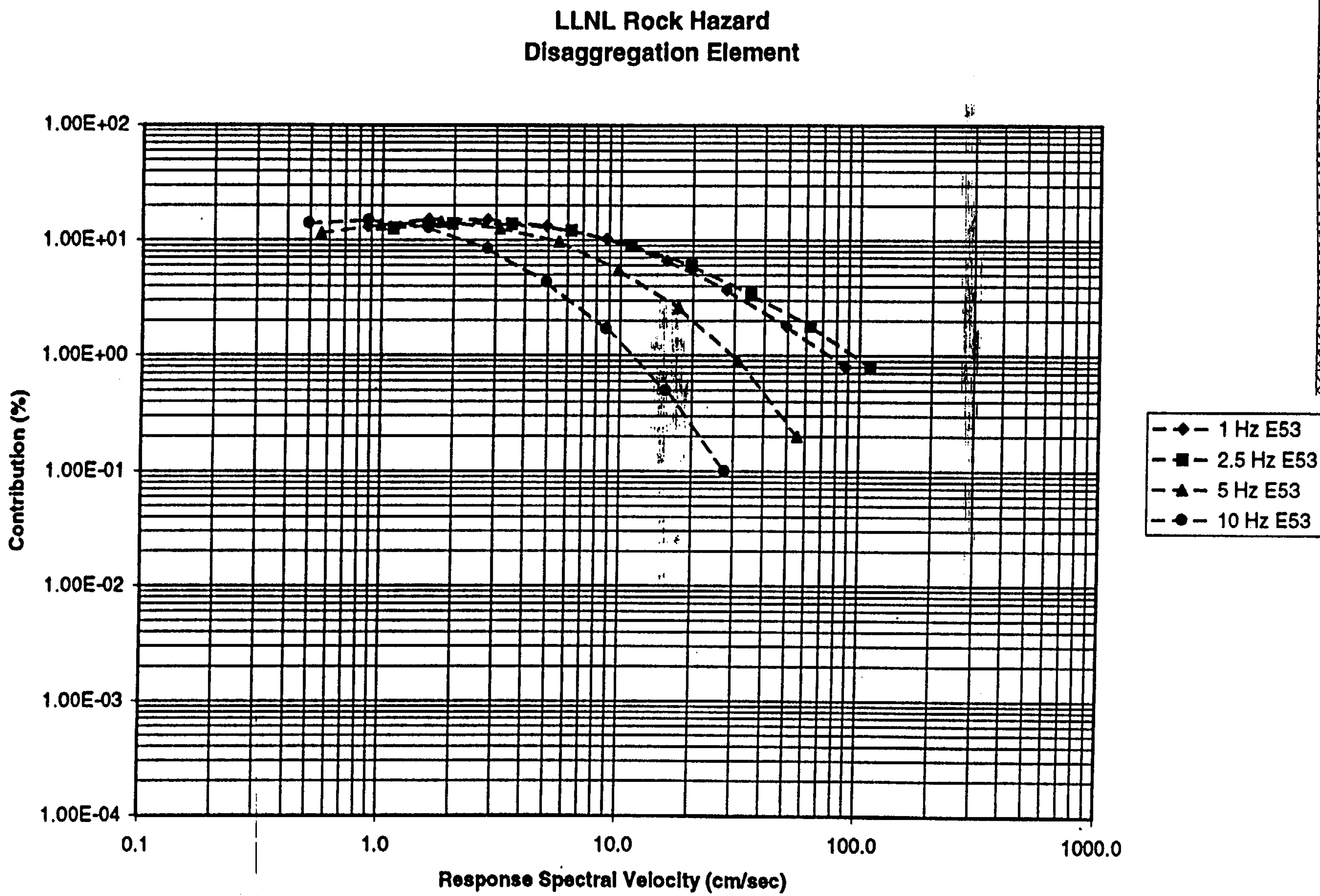

Figure F.23 - LLNL rock hazard disaggregation element 5,3 (Mw 6.25, 156. km) for the 1, 2.5, 5, and 10 Hz oscillator. Values less than 1% were identically 0 and not plotted.

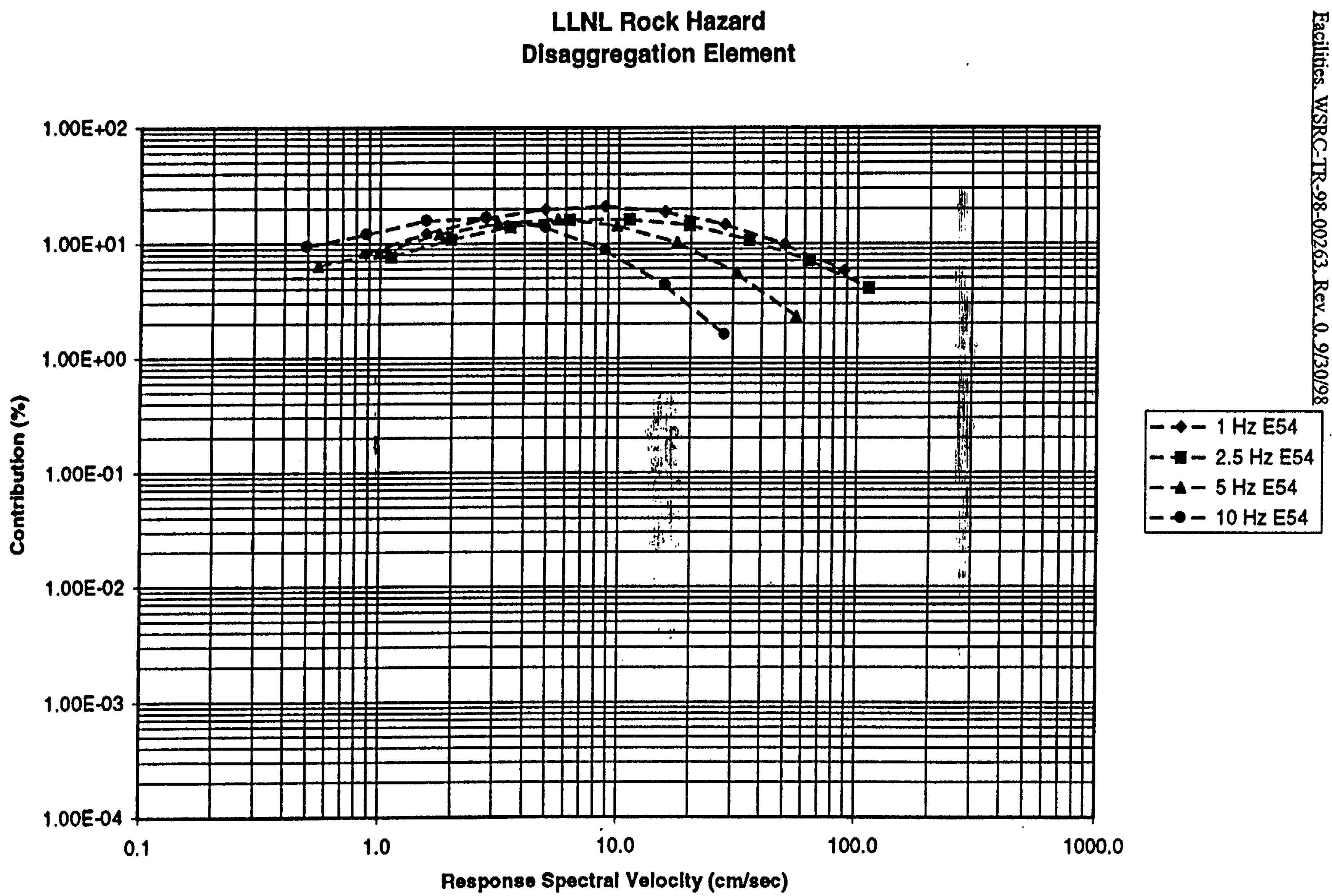

Figure F.24 - LLNL rock hazard disaggregation element 5,4 (Mw 6.75, 156. km) for the 1, 2.5, 5, and 10 Hz oscillator. Values less than 1% were identically 0 and not plotted.

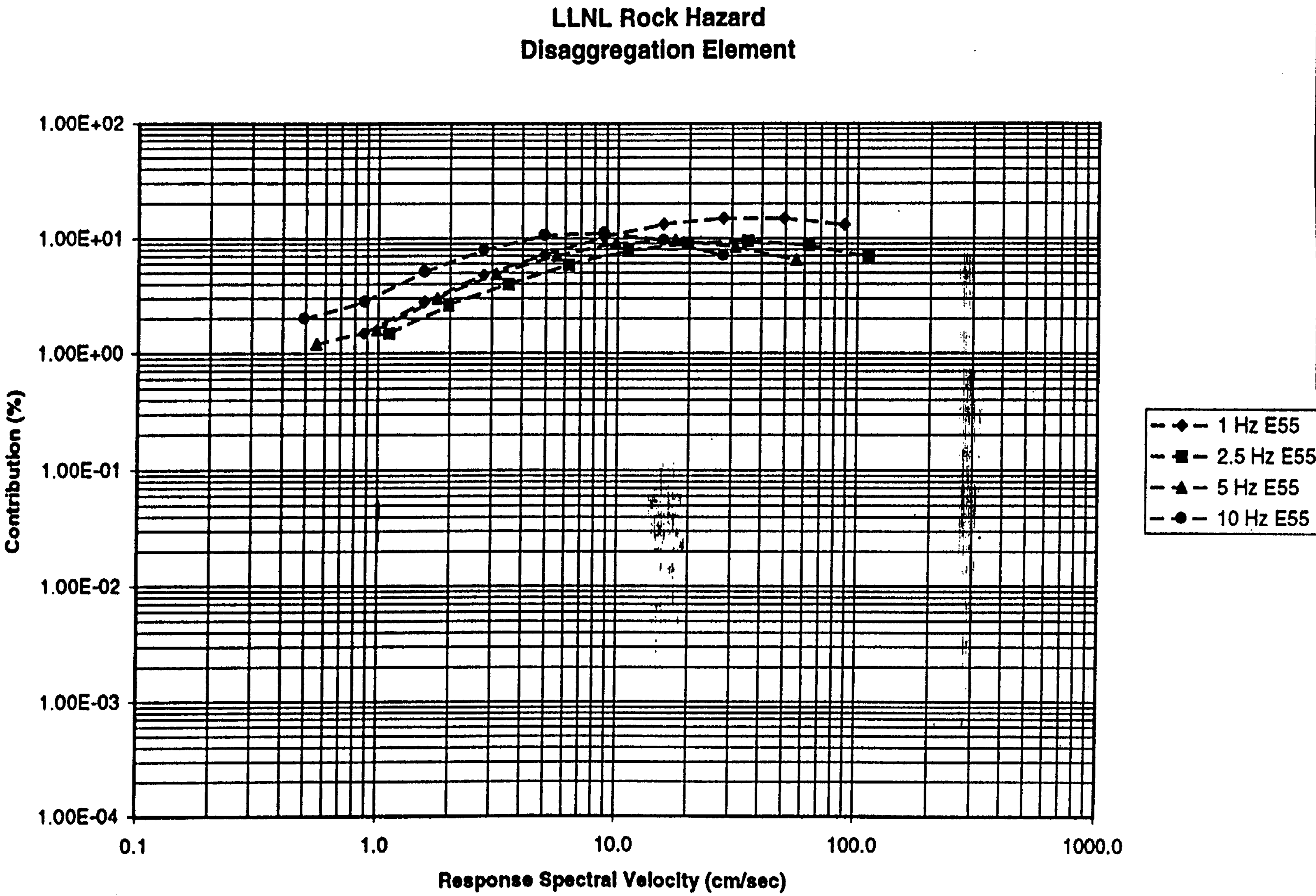

Figure F.25 - LLNL rock hazard disaggregation element 5,5 (Mw 7.5, 156. km) for the 1, 2.5, 5, and 10 Hz oscillator. Values less than 1% were identically 0 and not plotted.

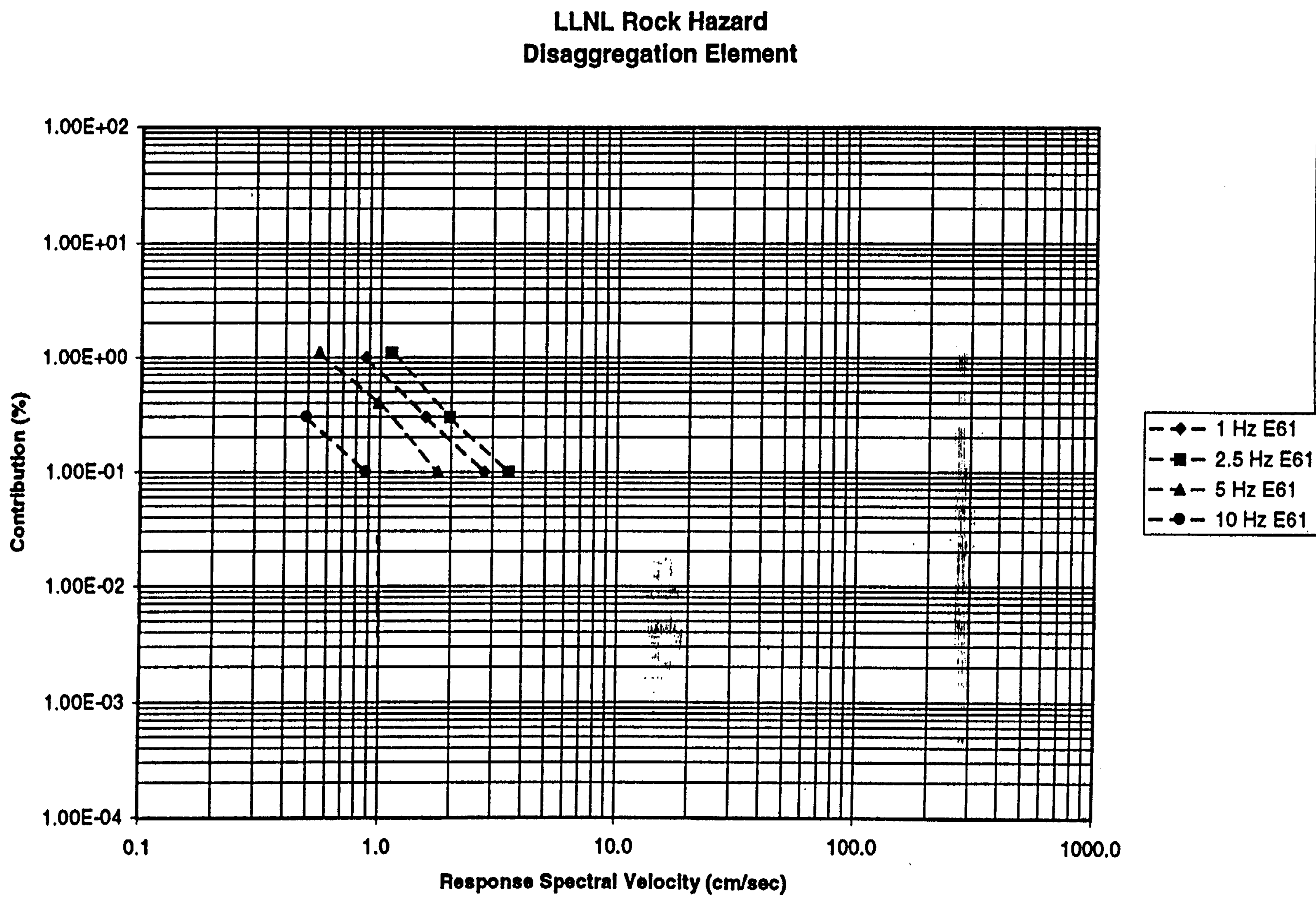

Figure F.26 - LLNL rock hazard disaggregation element 6,1 (Mw 5.25, 253. km) for the 1, 2.5, 5, and 10 Hz oscillator. Values less than 1% were identically 0 and not plotted.

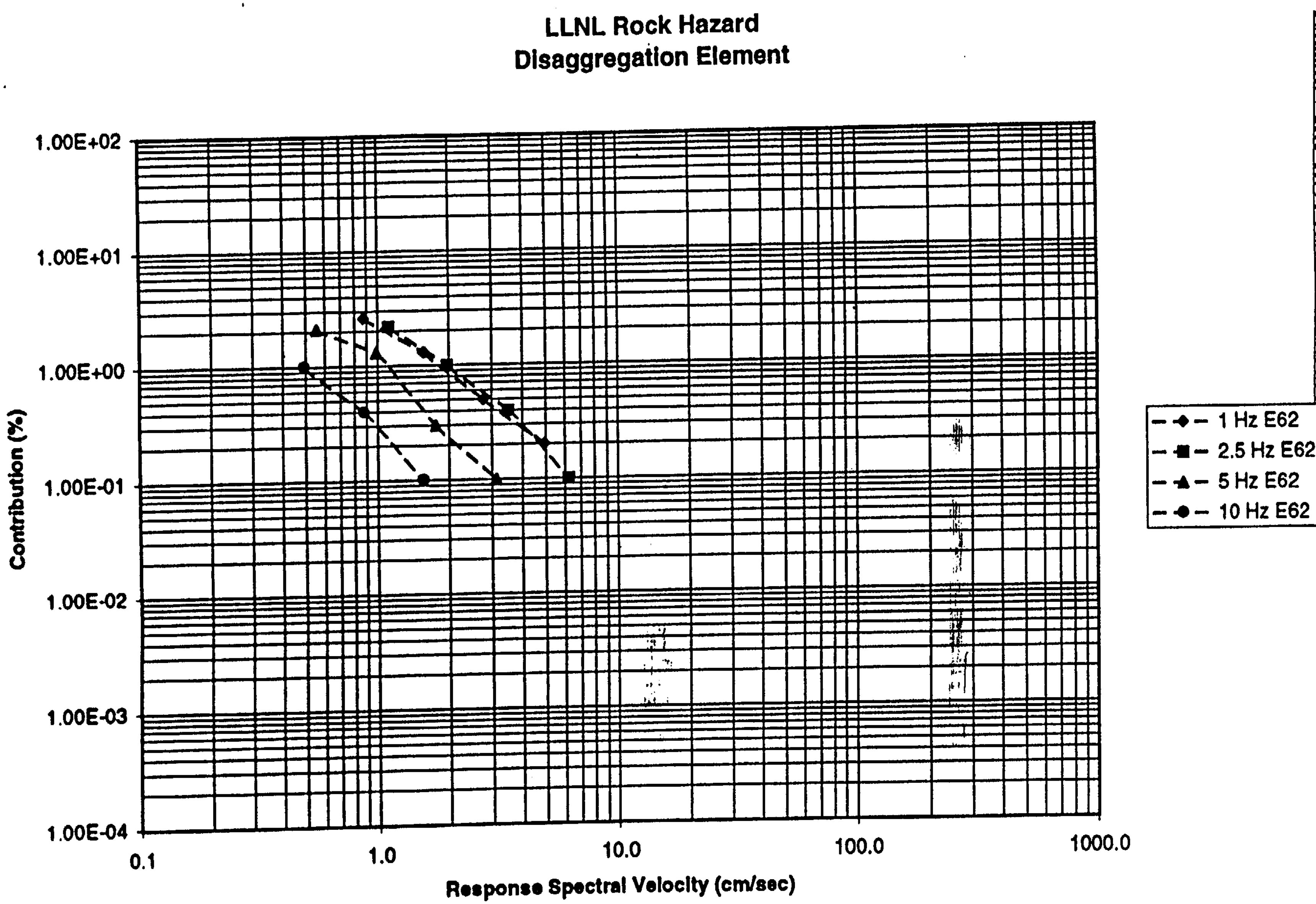

Figure F.27 - LLNL rock hazard disaggregation element 6,2 (Mw 5.75, 253. km) for the 1, 2.5, 5, and 10 Hz oscillator. Values less than 1% were identically 0 and not plotted.

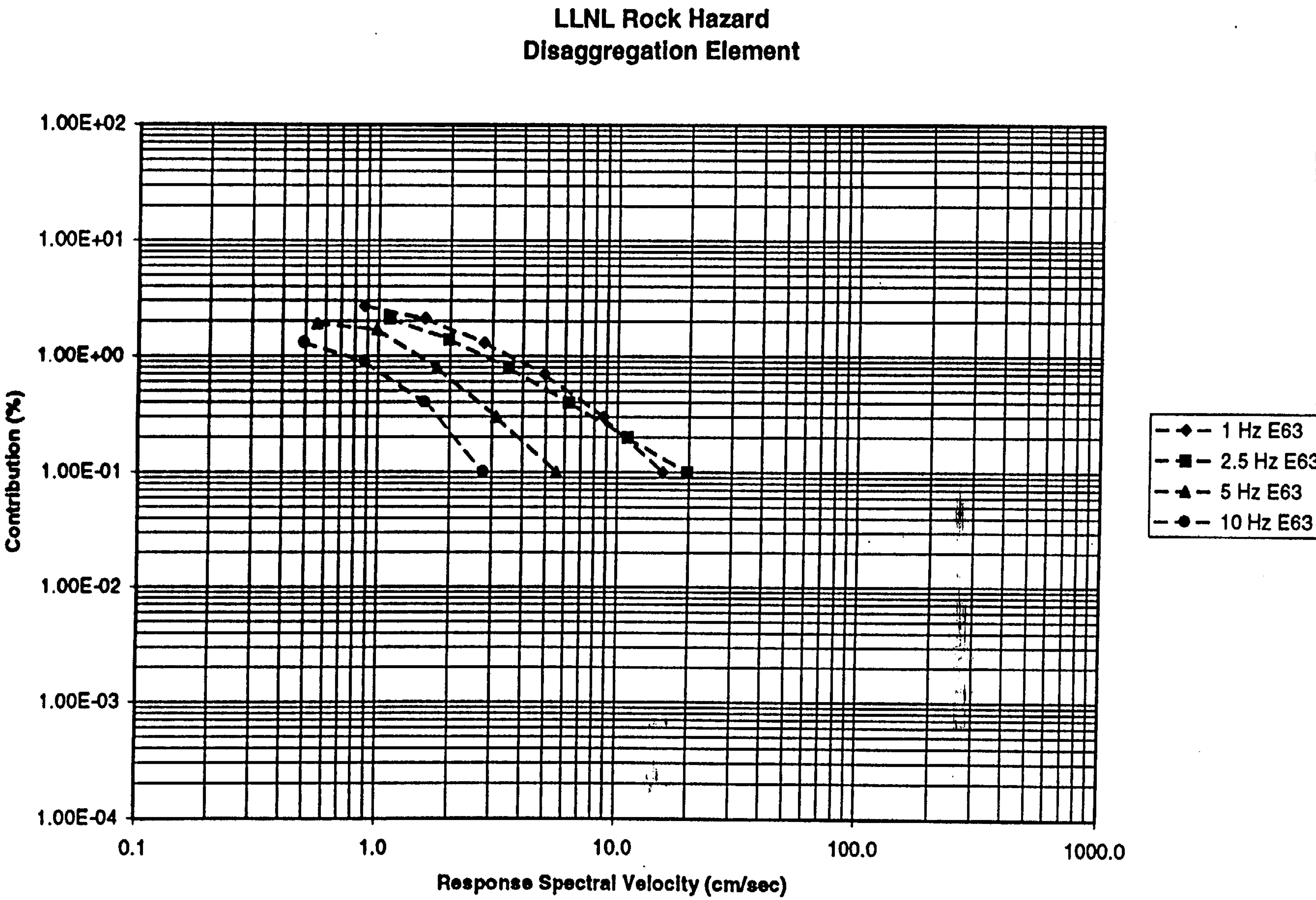

Figure F.28 - LLNL rock hazard disaggregation element 6,3 (Mw 6.25, 253. km) for the 1, 2.5, 5, and 10 Hz oscillator. Values less than 1% were identically 0 and not plotted.

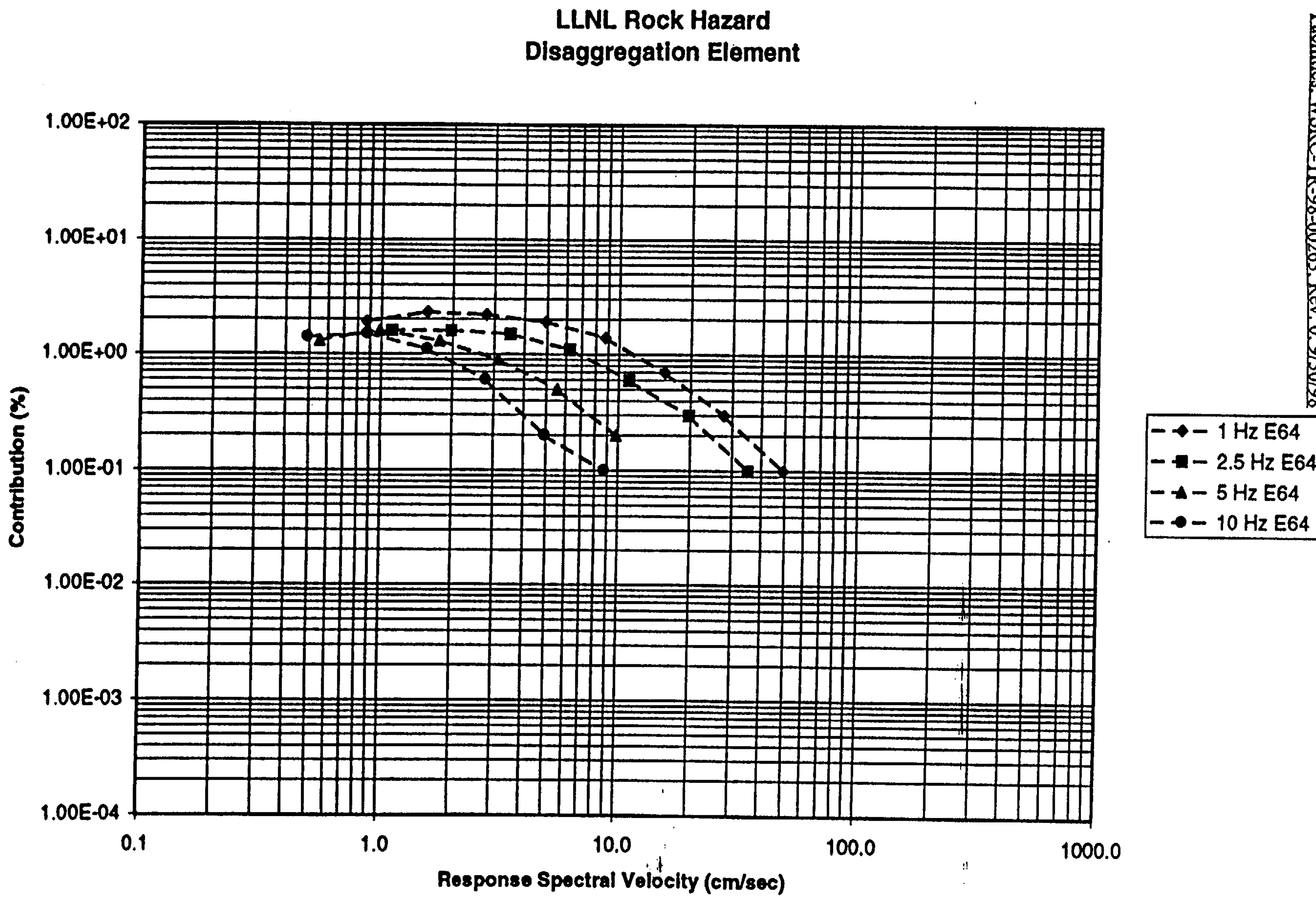

Figure F.29 - LLNL rock hazard disaggregation element 6,4 (Mw 6.75, 253. km) for the 1, 2.5, 5, and 10 Hz oscillator. Values less than 1% were identically 0 and not plotted.

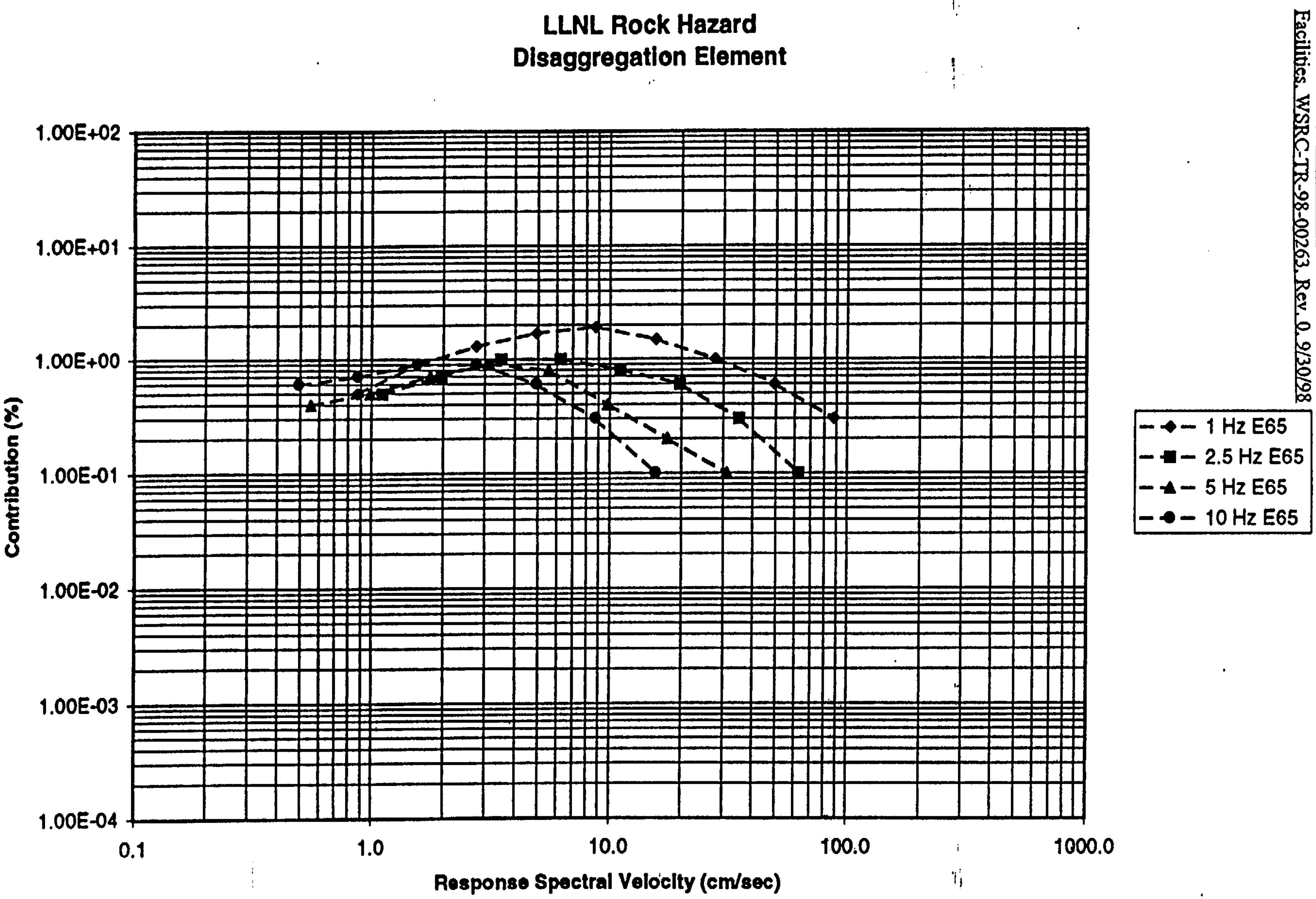

Figure F.30 - LLNL rock hazard disaggregation element 6,5 (Mw 7.5, 253. km) for the 1, 2.5, 5, and 10 Hz oscillator. Values less than 1% were identically 0 and not plotted.

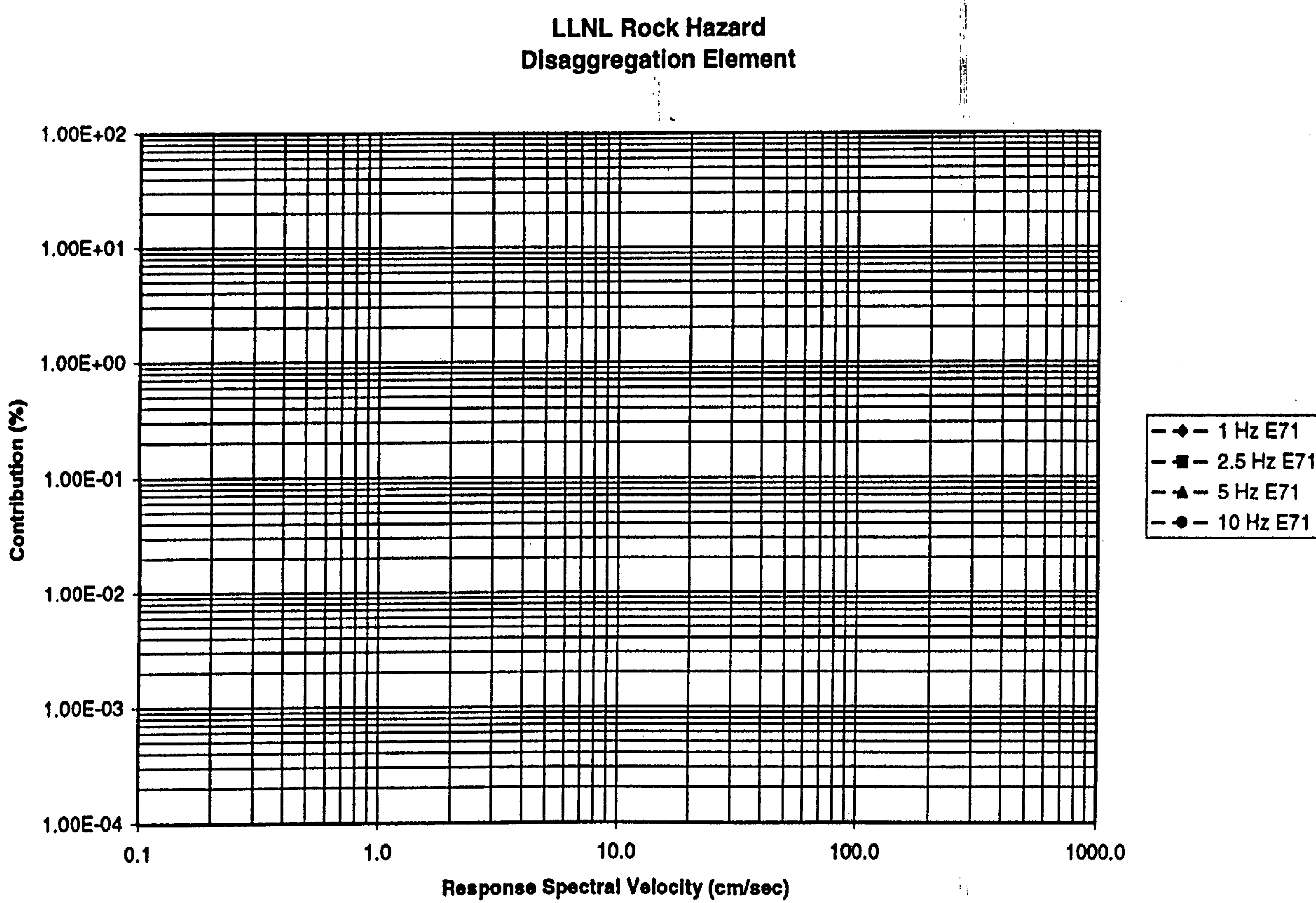

Figure F.31 - LLNL rock hazard disaggregation element 7,1 (Mw 5.25, 350. km) for the 1, 2.5, 5, and 10 Hz oscillator. Values less than 1% were identically 0 and not plotted.

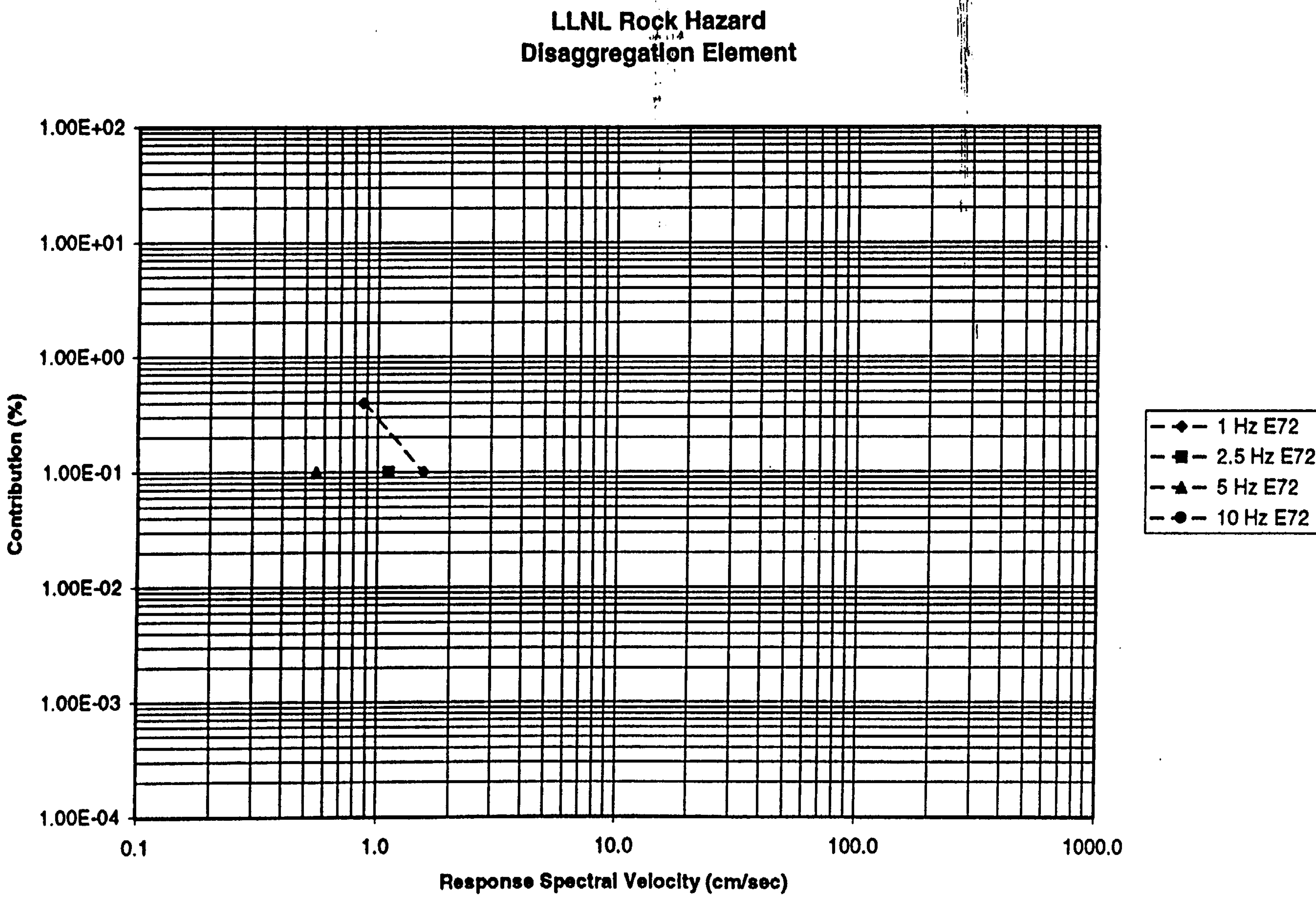

Figure F.32 - LLNL rock hazard disaggregation element 7,2 (Mw 5.75, 350. km) for the 1, 2.5, 5, and 10 Hz oscillator. Values less than 1% were identically 0 and not plotted.

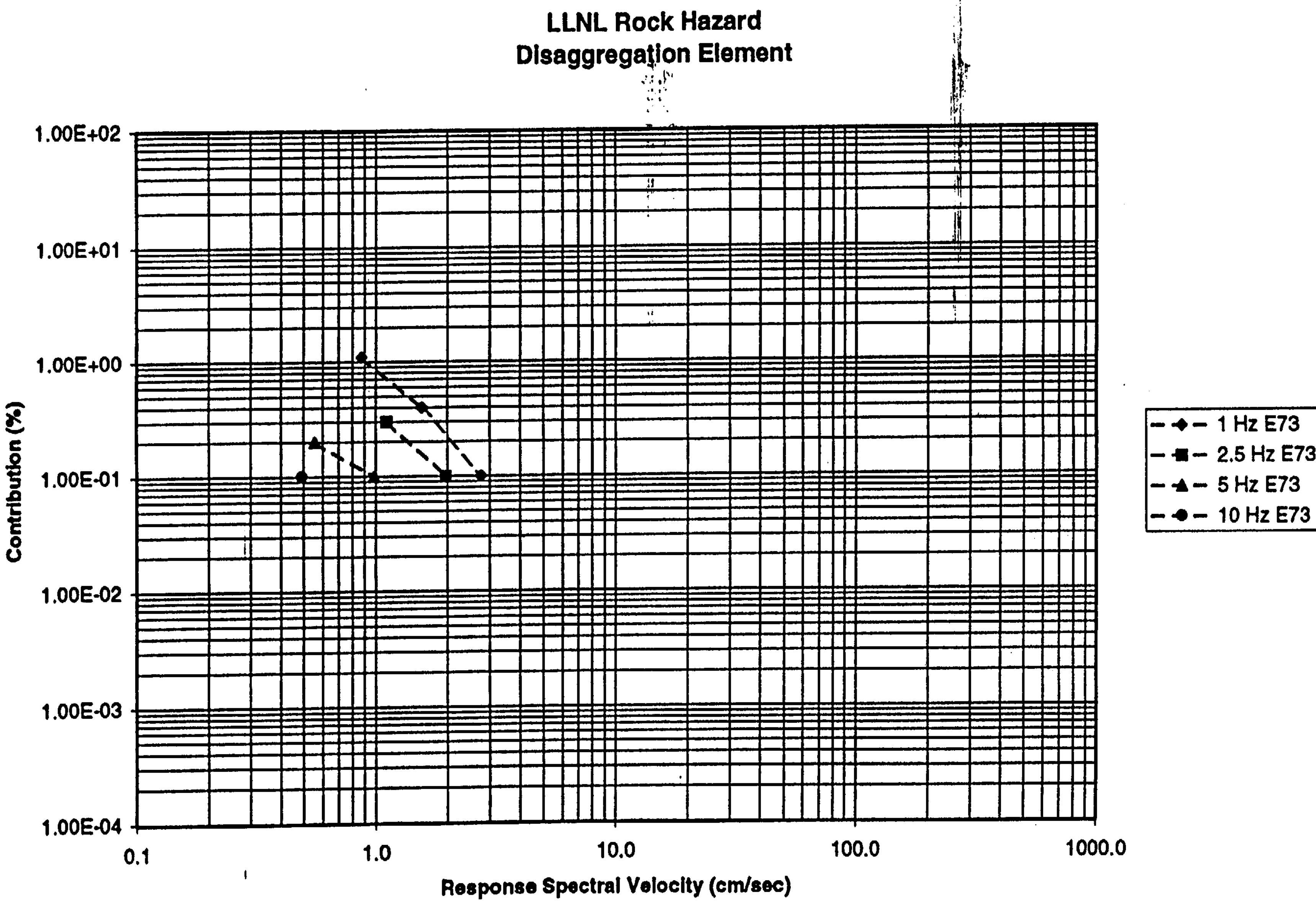

Figure F.33 - LLNL rock hazard disaggregation element 7,3 (Mw 6.25, 350. km) for the 1, 2.5, 5, and 10 Hz oscillator. Values less than 1% were identically 0 and not plotted.

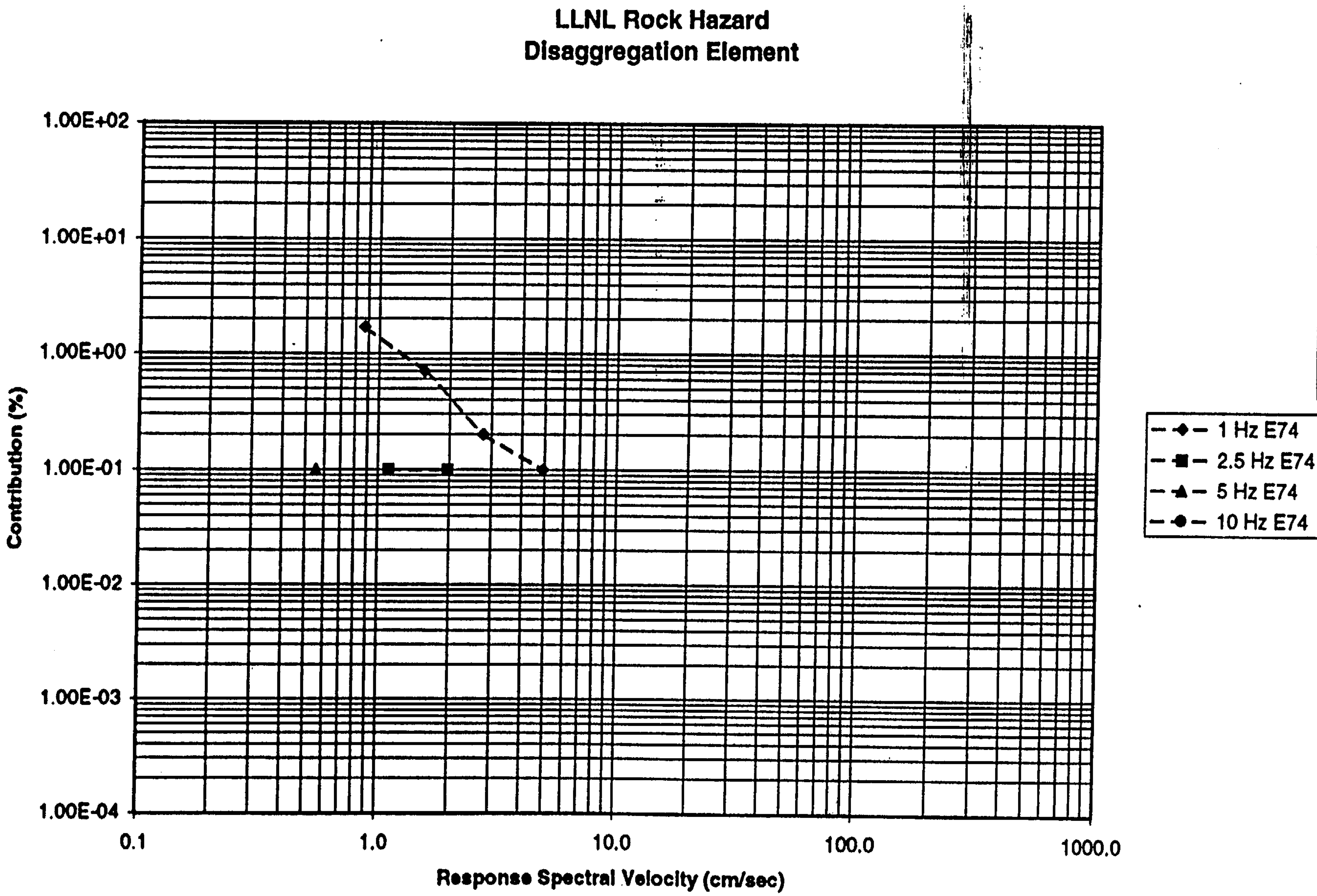

Figure F.34 - LLNL rock hazard disaggregation element 7,4 (Mw 6.75, 350. km) for the 1, 2.5, 5, and 10 Hz oscillator. Values less than 1% were identically 0 and not plotted.

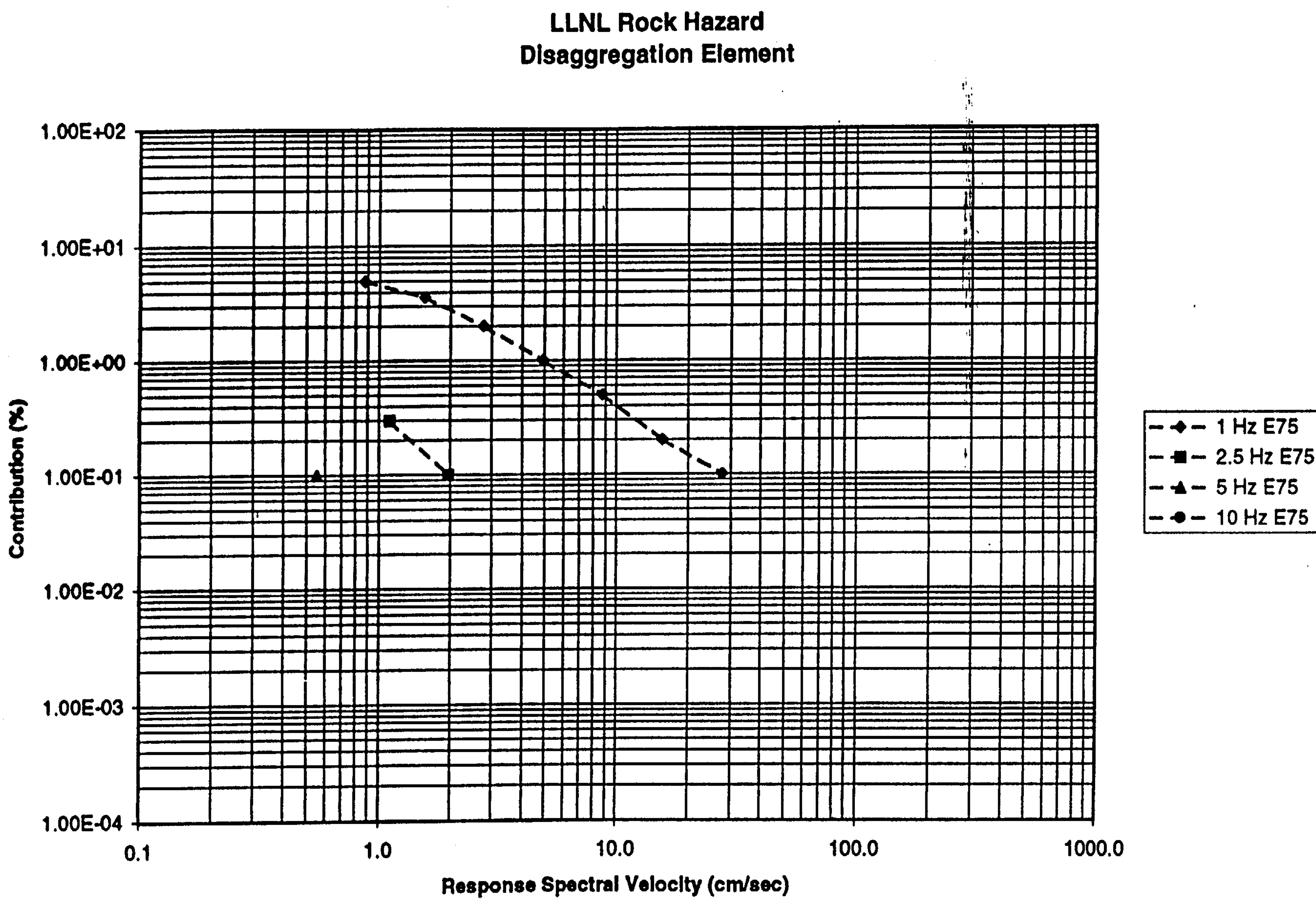

Figure F.35 - LLNL rock hazard disaggregation element 7,5 (Mw 7.5, 350. km) for the 1, 2.5, 5, and 10 Hz oscillator. Values less than 1% were identically 0 and not plotted.